

# **The Value of Concentrating Solar Power for a Sustainable Electricity Supply in Europe, Middle East and North Africa**

Von der Fakultät Energie-, Verfahrens- und Biotechnik  
der Universität Stuttgart zur Erlangung der Würde  
eines Doktor-Ingenieurs (Dr.-Ing.) genehmigte Abhandlung

**Vorgelegt von  
Denis Hess  
aus Stuttgart**

Hauptberichter: Prof. Dr. André Thess  
Mitberichter: Prof. Dr. Robert Pitz-Paal

Tag der mündlichen Prüfung: 09. April 2018

Institut für Energiespeicherung der Universität Stuttgart

2018

## Erklärung zur Dissertation:

Ich erkläre hiermit, dass die eingereichte Arbeit mit dem Titel:

**“The Value of Concentrating Solar Power for a Sustainable Electricity Supply in Europe, Middle East and North Africa”**

zur Erlangung der Würde eines Doktor-Ingenieurs (Dr.-Ing.) an der Universität Stuttgart selbständig erstellt worden ist. Hierbei habe ich nur die angegebenen Quellen verwendet.



Stuttgart, den 09.10.2017

Denis Hess

Basierend auf der Arbeit habe ich drei wissenschaftlich begutachtete Fachpublikationen im „peer-review“ Verfahren in den internationalen Fachmagazinen „Applied Energy“<sup>1</sup>, „Solar Energy“<sup>2</sup> und „Renewable Energy“<sup>3</sup> veröffentlicht.

---

<sup>1</sup> **D. Hess**, “The value of a dispatchable concentrating solar power transfer from Middle East and North Africa to Europe via point-to-point high voltage direct current lines”, *Applied Energy*, 2018.

<sup>2</sup> **D. Hess**, “The empirical probability of integrating CSP and its cost optimal configuration in a low carbon energy system of EUMENA”, *Solar Energy*, 2018.

<sup>3</sup> **D. Hess**, M. Wetzel, K.-K. Cao, “Representing node-internal transmission and distribution grids in energy system models”, *Renewable Energy*, 2017.

Wege verbinden Menschen

ممرات التواصل تربط الشعوب

Ways connect people

I saw eternity the other night,  
Like a great ring of pure and endless light,  
All calm, as it was bright;  
And round beneath it, time in hours, days, years,  
Driv'n by the spheres  
Like a vast shadow mov'd;  
In which the world and all her train were hurl'd.<sup>4</sup>

Ich sah die Ewigkeit jüngst in der Nacht,  
Gleich einem Ring, aus reinem endlosem Licht gemacht,  
Ganz still, ganz hell.  
Darunter, rund herum, bewegte sich die Zeit in Stunden, Tagen, Jahren,  
Getrieben von den Himmelsphären  
Als riesiger Schatten; dort hinein  
Geworfen war die Welt und all ihr Sein.

---

<sup>4</sup> Henry Vaughan (1621-1695), The Complete Poems. Hrsg. von Alan Rudrum. Harmondsworth, 1976

## Table of content

<b>Zusammenfassung / Abstract</b>	I-III
<b>1 Introduction</b>	<b>1</b>
1.1 Background	1
1.2 Research question	1
1.3 State of research, hypothesis, method and novelty	2
1.3.1 Energy system modelling	2
1.3.2 CSP modelling and value of CSP-HVDC	3
1.4 EUMENA region	4
1.5 Workflow	7
1.6 Statement of the chapter	8
<b>2 The concept of a CSP transfer to Europe</b>	<b>9</b>
2.1 CSP-HVDC power plant definition	9
2.1.1 CSP-HVDC power plant functionality, definition and configuration	9
2.2 Comparison of point-to-point interconnection, meshed overlay grid and their combination	10
2.3 Statement of the chapter	12
<b>3 Energy system modelling in REMix – methodology, assumptions and limits</b>	<b>13</b>
3.1 Energy system modelling	13
3.2 Energy supply and demand	15
3.2.1 Supply technologies	15
3.2.2 Modelling of CSP-HVDC in REMix	17
3.2.2.1 CSP-HVDC	17
3.2.2.2 CSP sites, HVDC point-to-point transmission corridors and offtaker points	18
3.2.3 Demand model	23
3.3 Basic modelling assumptions	24
3.3.1 Technological time series and electrical load curve	24
3.3.2 Demand Side Management	27
3.3.3 Storages	27
3.3.4 Security of supply	27

3.4	Uncertainty of cost and sensitivity analysis.....	28
3.5	Modelling mistakes and their consequences .....	28
3.6	Statement of the chapter .....	30
<b>4</b>	<b>Enhancement of the grid methodology in REMix .....</b>	<b>31</b>
4.1	Overlay grid modelling.....	31
4.2	Transmission and distribution grid modelling.....	31
4.2.1	Model description .....	32
4.2.2	Methodological overview, input data and validation .....	34
4.2.2.1	Specific investment cost for grid expansion .....	35
4.2.2.2	Starting point of grid expansion based on Wind and PV feed-in capacity.....	36
4.2.2.3	Excursion: Comparison of grid investment cost in European countries .....	38
4.2.2.4	Excursion: Annual basic grid cost in relation to peak load.....	39
4.2.3	Case study of the German energy system in 2050 and model calibration.....	40
4.2.3.1	Case study input values and modelling framework .....	40
4.2.3.2	Model calibration .....	42
4.2.3.3	Model validation.....	44
4.2.3.4	Derivation of specific grid expansion cost and starting point of grid expansion .....	44
4.2.3.5	Quality of calibration values and model results .....	44
4.2.3.6	Case study results of the German energy system.....	46
4.2.4	Conclusion and suggestion for improvements .....	49
<b>5</b>	<b>Assessing the value of CSP-HVDC applying REMix .....</b>	<b>51</b>
5.1	REMIX scenario analysis .....	51
5.1.1	Step 1: REMIX model – cost assumptions and results .....	54
5.1.1.1	Statement of the section .....	59
5.1.2	Step 2: REMIX model – Is spatial flexibility really needed? .....	59
5.1.2.1	Energy transmission according to power plant technology using an overlay grid .....	65
5.1.2.2	Statement of the section .....	66
5.1.3	Step 3: Regional integration probability and the role of CSP-HVDC and CSP for the energy system .....	67
5.1.3.1	Excursion: empirical probability of CCS and its value .....	71
5.1.3.2	The role of CSP-HVDC and CSP for the energy system.....	73

5.1.3.3	Statement of the section .....	76
5.1.4	Step 4: CSP-HVDC - direct comparison of CSP, nuclear energy and CCS ....	77
5.1.4.1	Comparison of evaluation criteria.....	77
5.1.4.2	Comparison of system cost deviation and annual full load hours .....	79
5.1.4.3	Statement of the section .....	80
5.1.5	Step 5: CSP-HVDC – value of CSP-HVDC with different capacity shares .....	81
5.1.5.1	Statement of the section .....	85
5.2	Value of CSP-HVDC – discussion of results.....	85
5.2.1	Power plant capacity .....	85
5.2.2	Electrical storage capacity.....	85
5.2.3	Curtailement.....	86
5.2.4	Power kilometre and utilisation of the overlay grid.....	87
5.2.4.1	Power kilometre .....	87
5.2.4.2	Utilisation of the overlay grid.....	91
5.2.5	System cost and annual cost.....	92
5.2.6	CO <sub>2</sub> emission .....	93
5.3	Used techno-economic data.....	93
<b>6</b>	<b>Perspective of a CSP transfer option.....</b>	<b>98</b>
6.1	Potential business case MEFID Solar Link .....	98
6.1.1	Need of a feasibility study .....	98
<b>7</b>	<b>Summary and outlook.....</b>	<b>102</b>
7.1	Résumé of evaluation criteria .....	103
7.2	Additional research results .....	106
7.3	Scientific contribution .....	108
7.4	Further research demand.....	108
7.4.1	Data .....	108
7.4.2	Multi-criteria consideration, optimization, simulation and evaluation .....	109
7.4.3	System configuration of CSP and conceptual technological alternatives .....	109
7.4.4	Feasibility study.....	110
7.5	Final conclusion .....	110
<b>8</b>	<b>Data Sets.....</b>	<b>111</b>

<b>9</b>	<b>References</b> .....	<b>111</b>
<b>10</b>	<b>Appendix</b> .....	<b>123</b>
10.1	Chapter 2 - The concept of a CSP transfer to Europe .....	123
10.1.1	CSP sites, HVDC point-to-point transmission lines and offtakers .....	123
10.1.1.1	Pathway lengths .....	123
10.2	Chapter 3 - Energy System Model .....	127
10.2.1	Energy supply and demand.....	127
10.2.1.1	Supply technologies and their resource potentials .....	127
10.2.1.2	Demand model .....	128
10.2.2	Basic modelling assumptions .....	131
10.2.2.1	Annual characteristic of load and renewable resources .....	131
10.2.2.2	Isopleth diagrams of electrical load and technological time series .....	131
10.2.2.3	Hourly time series profiles for EU of the year 2006 based on (Scholz, 2012) and for MENA of the year 2002 based on (Stetter, 2012).....	132
10.2.3	Grid method and validation .....	146
10.2.3.1	Overlay grid modelling .....	146
10.2.3.2	Transmission and distribution grid modelling .....	147
10.3	Chapter 4 – Scenario analysis .....	153
10.3.1	3 Step: CSP-HVDC, CSP, NUC, CCS sensitivity scenarios.....	153
10.3.2	4 Step: direct comparison of CSP-HVDC, CSP, NUC, CCS with same exogenous capacity.....	159
10.3.3	5 Step: exogenous scenarios handmade.....	160
10.3.4	Regional power kilometre .....	164
10.3.5	Model region radar charts as results of the scenario comparison without and with CSP-HVDC .....	165
<b>11</b>	<b>CV</b> .....	<b>174</b>



## List of figures

Figure 1: EUMENA geographical map.....	5
Figure 2: CSP-HVDC scheme transmitting dispatchable renewable energy over distance. The example shows a configuration of CSP in Morocco with a 2600km HVDC transmission line to Germany. ....	10
Figure 3: Model structure of REMix-EnDAT and REMix-OptiMo, input and output data based on (Gils, 2016).....	14
Figure 4: Line laying model based on (May, 2005) .....	19
Figure 5: Isotropic friction image based on (May, 2005) (OHL case) .....	20
Figure 6: Isotropic friction image based on (May, 2005) with addition of highest sea cost value (~40) to all land cost values allowing the algorithm to use predominantly offshore pathways (sea cable and UGC case) .....	20
Figure 7: Point-to-point CSP-HVDC with potential CSP hotspots in MENA and potential offtakers in Europe – predominant onshore line configuration (OHL case) .....	21
Figure 8: Point-to-point CSP-HVDC with potential CSP hotspots in MENA and potential offtakers in Europe – predominant offshore configuration (sea cable and UGC case) .....	21
Figure 9: Load and technological time series of model region G.....	26
Figure 10: Principle of the node-internal grid calculation model. Grid expansion is related to feed-in power of fluctuating energies depending on a starting point in relation to peak load.	34
Figure 11: Cost sensitivities MIN, MEAN and MAX investment costs of distribution grid expansion. Investment [bn €] based on (Rehtanz, et al., 2012), (Büchner, et al., 2014), trend curves based on (Cossent, et al., 2011). ....	36
Figure 12: Coefficient of determination ( $R^2$ ) of grid investment cost to peak load in Continental Europe ENTSO-e countries of the year 2013.....	38
Figure 13: Grid model in Germany with 491 nodes, AC (red) and DC (blue) transmission lines .....	40
Figure 14: Distribution of demand and capacities according to their potentials [% of total capacity].....	41
Figure 15: Grid cost of the 491 node model (blue dots from Table 11 and <i>C<sub>basic grid cost</sub></i> ) meeting cost bandwidths of the calibrated node-internal grid model (boxes). Green to red colours show the min to max cost deviation of the calibrated node-internal grid model to the 491 node model (boxes to dots). The x-axis shows the shares of fluctuating_dispatchable energy share (related to gross electricity consumption).....	45
Figure 16: Transmission line capacities, power kilometres under different shares of fluctuating and dispatchable energies.....	46
Figure 17: Bandwidths as results of cost assumption sensitivity analyses in the REMix model .....	47

Figure 18: Workflow of REMix scenario analysis .....	52
Figure 19: Used overlay grid and CSP-HVDC scheme in the stepwise analysis. The CSP power plants and P2P connections from MENA to EU are defined as CSP-HVDC.....	54
Figure 20: Use of REMix for three different cost assumptions and two transmission technologies. The results show the impact of a cost minimization. ....	57
Figure 21: Different CO <sub>2</sub> emission limits of 16g/kWh <sub>demand</sub> and 0g/kWh <sub>demand</sub> .....	58
Figure 22: Comparison of grid expansion in GW of overlay grid transmission lines and TWkm. A scenario with unlimited overlay grid interconnections (a) is compared to a scenario with isolated model regions with the exclusion of the overlay grid (b). The regional grid expansion possibility of transmission and distribution grid (nodal grid) and CSP-HVDC integration option is included in both scenarios. ....	61
Figure 23: Grid vs. Single. An unlimited grid expansion is a cost-efficient way but causes the need of many power km over EUMENA. Compared to the scenario without overlay grid there is only a cost reduction of about 7% but a power km increase of about 176%. Due to spatial flexibility using an overlay grid the energy system needs less power plant capacities, storages and causes less curtailment.....	61
Figure 24: Distribution of evaluation criteria in scenarios with unlimited overlay grid optimization and with isolated model regions (no overlay grid). ....	64
Figure 25: Probability of capacity integration of CSP-HVDC, CSP and nuclear power plants – no CCS allowed.....	70
Figure 26: Probability of capacity integration of CSP-HVDC, CSP, nuclear power plants, CCGT CCS, Coal CCS and the value of CCS .....	72
Figure 27: Solar Multiple (a, b) and Thermal Energy Storage full load hours (c, d) of CSP-HVDC (in MENA for EU) and CSP (in MENA and southern EU).....	74
Figure 28: Bandwidth of possible area use [km <sup>2</sup> ] of CSP and CSP-HVDC in EU and MENA	75
Figure 29: Comparison of CSP, nuclear energy, CCGT CCS and Coal CCS in multi criteria	78
Figure 30: Comparison of same exogenous capacities of CSP, nuclear energy, CCGT CCS and coal CCS in system cost deviation and annual full load hours .....	80
Figure 31: Radar charts showing the value of CSP-HVDC. Base scenario is shown in the left column in ochre, 50% reduction of CSP-HVDC capacity of base scenario in the right column in ochre. Grey radar charts show an energy system without CSP-HVDC as reference. Specific evaluation criteria per annual net electricity demand of each region are applied. ....	84
Figure 32: Regional grid and transmission line expansion measured in power km in scenarios with different CSP-HVDC capacity shares related to the base scenario .....	88
Figure 33: Different shares of CSP-HVDC capacity and resulting expansion of power kilometre according to transmission infrastructure categories.....	89

Figure 34: Trade-off of power kilometre between CSP-HVDC (P2P lines) and Transmission grid (nodal grid) in EUMENA .....	89
Figure 35: Trade-off of power kilometre between CSP-HVDC (P2P lines) and Transmission grid (nodal grid). In (a) of model region <b>T</b> , in (b) of model region <b>G</b> and in (c) of model region <b>NW</b> .....	90
Figure 36: Annual Energy of import (positive) and export (negative) in the scenarios “No CSP-HVDC” (a) and “With CSP-HVDC” (b). Energy is transmitted over the overlay grid.....	92
Figure 37: MEFID Solar Link – schematic bundling of common infrastructure .....	99
Figure 38: Picture of potential CSP-HVDC power plants for the Four Motors for Europe. In (a) for Catalunya, in (b) for Rhône-Alpes, in (c) for Lombardia and in (d) for Baden-Württemberg. In (e) the water pipeline infrastructure in Morocco reveals the use of water to supply the area around the CSP power plants for agricultural use, new living area and CSP itself with a small share. ....	101
Figure 39: Load and technological time series of model region I .....	132
Figure 40: Load and technological time series of model region E .....	133
Figure 41: Load and technological time series of model region ME .....	134
Figure 42: Load and technological time series of model region MES.....	135
Figure 43: Load and technological time series of model region N.....	136
Figure 44: Load and technological time series of model region NAE .....	137
Figure 45: Load and technological time series of model region NAW .....	138
Figure 46: Load and technological time series of model region NE .....	139
Figure 47: Load and technological time series of model region NW.....	140
Figure 48: Load and technological time series of model region S .....	141
Figure 49: Load and technological time series of model region SE.....	142
Figure 50: Load and technological time series of model region SW.....	143
Figure 51: Load and technological time series of model region T .....	144
Figure 52: Load and technological time series of model region W .....	145
Figure 53: Solar Multiple.....	154
Figure 54: Thermal energy storage full load hours.....	155
Figure 55: Electrical generation net of the CSP plant without transmission losses.....	156
Figure 56: Co-firing with natural gas.....	157
Figure 57: Solar field size – possible bandwidths of demand for land of CSP-HVDC and CSP .....	158
Figure 58: Regional power kilometre of the modelling framework in section 5.1.5. ....	164
Figure 59: Scenario with maximum set CSP-HVDC capacity (CSP-HVDC base scenario) .	167
Figure 60: Scenario with 25% reduction of CSP-HVDC capacity (-25% CSP-HVDC) .....	169
Figure 61: Scenario with 50% reduction of CSP-HVDC capacity (-50% CSP-HVDC) .....	171

Figure 62: Scenario with 75% reduction of CSP-HVDC capacity (-75% CSP-HVDC) .....173

## List of tables

Table 1: Population data in EUMENA and the world.....	5
Table 2: Aggregation of countries to 15 model regions in the examination area EUMENA ....	6
Table 3: Overview of point-to-point transmission lines and meshed overlay grid .....	11
Table 4: Classification and characteristic of used renewable energies for electricity generation based on (Scholz, 2012) – hydro reservoir is considered neither as fluctuating nor as dispatchable but as long term storage with additional natural inflow. ....	16
Table 5: CSP-HVDC transmission line lengths to model regions as potential offtakers.....	22
Table 6: Annual electrical demand of electricity, heat and mobility sector in 2010 and 2050	24
Table 7: Modelling simplification, mistake, consequence and suggestion of improvement....	29
Table 8: Methodological overview of the node internal grid model approach .....	35
Table 9: Distribution grid expansion cost sensitivity analysis with different expansion starting points .....	37
Table 10: Techno-economic parameters of AC and DC used in the case study .....	42
Table 11: Annual transmission grid cost in the 491 node model using different time resolution (values in bold represent the calibration data of the node-internal grid model) .....	43
Table 12: Model calibration points as critical grid hours.....	43
Table 13: Definition of cost sensitivity.....	55
Table 14: Analysed evaluation criteria.....	55
Table 15: Exemplary correlation of hourly time series from generation out of CSP, PV, Wind Onshore and Wind Offshore in NW and NAW with hourly time series of transmitted electricity .....	65
Table 16: Sensitivity analysis of a single technology in REMix using different technological cost relations.....	67
Table 17: Model region average integration probability considering the CO <sub>2</sub> emission limit reduction from 16 to 0 g CO <sub>2</sub> /kWh <sub>demand</sub> .....	68
Table 18: Results of cost and transmission infrastructure combination for the integration of CSP-HVDC capacity in Germany .....	69
Table 19: Comparing average empirical probability of CSP-HVDC, CSP and nuclear power plants in a scenario without CCS with a scenario allowing CCS .....	71
Table 20: CSP-HVDC and CSP configuration in sensitivity scenario of Figure 25 with small CO <sub>2</sub> emissions (16 g CO <sub>2</sub> /kWh <sub>demand</sub> ).....	76
Table 21: Sensitivity analysis of a single technology using different technological cost relations resulting in system cost.....	79
Table 22: Comparison of the overlay grid utilisation .....	91

Table 23: Correlation based on hourly time series of generation out of CSP, PV, Wind Onshore and Wind Offshore in NAW and transmitted electricity from selected regions to surrounding regions – scenario “No CSP-HVDC” .....	92
Table 24: Cost and technology parameters for power plants in the year 2050 based on expert assumptions .....	94
Table 25: Cost and technology parameters for storages in the year 2050 .....	95
Table 26: Cost and technology parameters for carbon emitting and nuclear technologies in the year 2050 .....	96
Table 27: Specific CO <sub>2</sub> emission .....	97
Table 28: CO <sub>2</sub> certificate cost representing environmental impact .....	97
Table 29: Techno-economic parameters of AC and DC infrastructure in the scenario analysis .....	97
Table 30: Learning curve approach of CSP solar field, thermal storage and power block based on installed capacity and progress ratio .....	97
Table 31: Approximation of CSP-HVDC configuration and cost for a parabolic trough with HVDC underground cables for the Four Motors for Europe .....	100
Table 32: Comparison of evaluation criteria of two energy systems in EUMENA without and with CSP-HVDC .....	102
Table 33: Selection of 124 pathway lengths from a potential CSP hot spot in MENA plant to potential offtaker in EU – grey rows show potential CSP hotspots and pathways for offtakers in Germany.....	123
Table 34: Link lengths of point-to-point hydro reservoir (not optimized) .....	126
Table 35: Limited resource potentials of used technologies.....	127
Table 36: GDP growth rate assumption and resulting annual electrical national demand following (Trieb, et al., 2006) .....	128
Table 37: Peak load and average resource full load hours of model regions .....	131
Table 38: Assumed overlay grid link length .....	146
Table 39: Capacity [GW] in Germany using the node-internal grid model (916 €/kW <sub>AC trans</sub> OHL and 1758 €/kW <sub>AC trans</sub> UGC). .....	147
Table 40: Capacity [GW] in Germany using the node-internal grid model (585 €/kW <sub>AC trans</sub> OHL and 900 €/kW <sub>AC trans</sub> UGC). .....	148
Table 41: Country specific grid values, peak load and cost of fluctuating feed-in power .....	149
Table 42: Regional exogenous capacity [MW] and solar multiple comparing technologies .....	159
Table 43: Exogenous capacities of CSP components .....	160
Table 44: Exogenous capacities of power plants [MW <sub>el</sub> ].....	161
Table 45: Exogenous capacities of hydro reservoir and pump storage plants [MW <sub>el</sub> ].....	161
Table 46: Exogenous link capacities.....	162

Table 47: Used parameters for distribution and transmission grid inside a model region ....163

## List of symbols

---

### Unit prefix

---

<i>k</i>	kilo
<i>M</i>	mega
<i>G</i>	giga
<i>T</i>	terra

---

### Unit

---

€	Euro
<i>g</i>	gram
<i>h</i>	hour
<i>m</i>	metre
<i>V</i>	volt
$W_{el}$	Watt electrical
$W_{th}$	Watt thermal
<i>y</i>	year



Parameter	Unit	Description
$C_{AC\ trans}$	[€/kW <sub>el</sub> ]	specific grid cost in AC configuration
$C_{basic\ grid\ cost}$	[€]	cost of existing / basic grid
$C_{cb,grid\ trans}$	[€/kW <sub>el</sub> ]	calibrated specific transmission grid cost
$C_{Emission}$	[k€/GWh]	specific emission cost
$C_{fluc, feed-in}$	[€/kW <sub>el</sub> ]	specific fluctuating capacity feed-in cost
$C_{Fuel}$	[k€/GWh]	specific fuel cost
$C_{O\&M\ Fix}$	[%/y]	annual specific operation and maintenance fix costs
$C_{grid\ cost}$	[€/kW <sub>el</sub> ]	specific grid cost
$C_{grid\ distr}$	[€/kW <sub>el</sub> ]	specific distribution grid cost
$C_{grid\ trans}$	[€/kW <sub>el</sub> ]	specific transmission grid cost
$C_{O\&M\ Variable}$	[k€/MWh]	specific operation and maintenance variable costs
$C_{specInv}$	[k€/MW]	specific investment cost
$epti_{18}$	[-]	relative empirical probability using 18 scenarios
$EPTI_{18}$	[-]	absolute empirical probability using 18 scenarios
$f_{annuity}$	[-]	Annuity factor
$f_{grid\ exp}$	[-]	Grid expansion factor
$\eta_{generator}$	[%]	Efficiency of the generator as product of the thermal and electrical efficiency
$\eta_{charge}$	[%]	Charging efficiency of the storage
$\eta_{discharge}$	[%]	Discharging efficiency of the storage
$\eta_{self}$	[%/h]	Self-discharging rate of the storage per hour
$i$	[%]	Interest and discount rate
$P_{existlines}$	[GW <sub>el</sub> ]	Net transfer capacity of exogenous power transmission lines
$P_{demand,peak}$	[GW <sub>el</sub> ]	Peak load
$P_{existCap}$	[GW <sub>el</sub> ]	Capacity of existing power plants
$P_{grid\ exp\ start}$	[kW <sub>el</sub> ]	Starting point of grid expansion
$P_{HVDC}$	[GW <sub>el</sub> ]	Capacity of the HVDC transmission line
$P_{PB, CSP}$	[GW <sub>el</sub> ]	Capacity of the CSP power block
$P_{SF, CSP}$	[GW <sub>th</sub> ]	Capacity of the CSP solar field
$P_{TES, CSP}$	[GWh <sub>th</sub> ]	Thermal energy storage capacity of the CSP
$R^2$	[-]	Coefficient of determination
$s_{gen}(t)$	[-]	Normalised generation time series of fluctuating energy
$SM$	[-]	Solar Multiple
$\Delta t$	[h]	Calculation time interval
$t_y$	[y]	Amortization time

<b>Variable</b>	<b>Unit</b>	<b>Description</b>
$C_{capital}$	[k€/y]	Annual depreciation of capital expenditure
$C_{operation}$	[k€/y]	Annual operation and maintenance costs
$C_{grid\ distr}$	[k€]	Investment cost of distribution grid expansion
$C_{grid\ trans}$	[k€]	Investment cost of transmission grid expansion
$C_{grid\ exp\ cost}$	[k€]	Investment cost of grid expansion
$P_{addedCap}$	[GW <sub>el</sub> ]	Capacity of additional power plants
$P_{addedlines}$	[GW <sub>el</sub> ]	Net transfer capacity of endogenous power transmission lines
$P_{curtail}(t)$	[GW <sub>el</sub> ]	Curtailed power generation
$P_{flow}(t)$	[GW <sub>el</sub> ]	Power flow over transmission lines
$P_{fluc\ feed-in,max}$	[GW <sub>el</sub> ]	maximum feed-in power of fluctuating power into the grid
$P_{gen}(t)$	[GW <sub>el</sub> ]	Power generation
$P_{grid}$	[GW <sub>el</sub> ]	Power of grid
$P_{grid\ distr}$	[GW <sub>el</sub> ]	Power of distribution grid
$P_{grid\ exp\ end}$	[GW <sub>el</sub> ]	End point of grid expansion
$P_{grid\ trans}$	[GW <sub>el</sub> ]	Power of transmission grid
$P_{used}(t)$	[GW <sub>el</sub> ]	Used power of Wind turbines and Photovoltaic
$P_{used,max}$	[GW <sub>el</sub> ]	Maximum used power of Wind turbines and Photovoltaic
$Q_{addedCap}(t)$	[GW <sub>th</sub> ]	Capacity of model endogenous CSP solar field
$Q_{BUS}(t)$	[GW <sub>th</sub> ]	Thermal output of the CSP co-firing system
$Q_{charge}(t)$	[GW <sub>th</sub> ]	Thermal energy storage input
$Q_{curtail}(t)$	[GW <sub>th</sub> ]	Thermal curtailment of the solar field
$Q_{discharge}(t)$	[GW <sub>th</sub> ]	Thermal energy storage output
$Q_{SF}(t)$	[GW <sub>th</sub> ]	Thermal output of the solar field
$U_{level}(t)$	[GWh <sub>th</sub> ]	Thermal energy storage level
$x_1$	[kW <sub>el, fluc feed-in</sub> ]	feed-in power of PV and Wind Onshore

## Abbreviations

AC	Alternating current
AUE	Arab Union of Electricity
BAU	Business as usual
CCGT	Combined-Cycle Gas Turbine
CCS	Carbon Capture and Storage
Coal	Coal fired steam turbine power plant
CSP	Concentrated Solar Power
CSP-HVDC	Concentrated Solar Power plant combined with a point-to-point high voltage direct current transmission line
DLR	Deutsches Zentrum für Luft- und Raumfahrt – German Aerospace Center
DNI	Direct Normal Irradiance
EGS	Enhanced geothermal system
EinsMan	Einspeisemanagement
EnDAT	Energy Data Analysis Tool
ENTSO-e	European Network of Transmission System Operators for Electricity
EPTI	Empirical probability of technological integration
ETH	Eidgenössische Technische Hochschule Zürich
EU	Geographical Europe
EUMENA	Europe, Middle East and North Africa
GDP	Gross Domestic Product
GHI	Global Horizontal Irradiance
FLUC FEED-IN	Power of Wind turbines and Photovoltaic which is feed into the grid.
HVDC	High voltage direct current
IEA	International Energy Agency
IER	Institut für Energiewirtschaft und Rationelle Energieanwendung - Institute of Energy Economics and Rational Energy Use
LCOE	Levelized cost of electricity

ME	Geographical Middle East
MEFID Solar Link	Bundling of CSP-HVDC power plants for the four Motors for Europe
MENA	Middle East and North Africa
NA	Geographical North Africa
NIGM	Node internal grid model
NPP	Net primary production
NREL	National Renewable Energy Laboratory
NUC	Nuclear steam turbine power plant
OECD	Organisation for Economic Co-operation and Development
OHL	Overhead line
O&M	Operation and Maintenance
P2G2P	Power-to-Gas-to-Power
P2P	Point-to-point
PEMFC	Proton exchange membrane fuel cell
PV	Photovoltaic
RAM	Random access memory
REMix	sustainable Renewable Energy Mix
SAM	System Advisor Model
UGC	Underground cable
UN	United Nation
USA	United States of America
UTC	Universal Time, Coordinated
VSC	Voltage Sourced Converter

<b>EUMENA model regions</b>	<b>Alias</b>	<b>Country or Region</b>
<b>G</b>	Germany	Germany
<b>N</b>	North	Denmark, Norway, Sweden, Finland, Lithuania, Latvia, Estonia
<b>E</b>	East	Poland, Czech Republic, Slovakia, Hungary
<b>S</b>	South	Switzerland, Austria, Liechtenstein, Italy, Slovenia
<b>W</b>	West	France, Belgium, Netherlands, Luxemburg
<b>NW</b>	North West	United Kingdom, Ireland, Iceland
<b>NE</b>	North East	Ukraine, Moldova, Belarus, Russia until Ural mountains, Azerbaijan, Armenia, Georgia
<b>SE</b>	South East	Greece, Croatia, Rumania, Serbia, Kosovo, Albania, Macedonia, Bulgaria, Bosnia-Herzegovina, Montenegro
<b>SW</b>	South West	Portugal, Spain
<b>T</b>	Turkey, Cyprus	Turkey, Cyprus
<b>MES</b>	Mesopotamia	Israel, Jordan, Palestine, Lebanon, Syria, Iraq
<b>I</b>	Iran	Iran
<b>ME</b>	Middle East	Djibouti, Yemen, Oman, Saudi Arabia, UAE, Qatar, Bahrain, Kuwait
<b>NAE</b>	North Africa East	Libya, Egypt
<b>NAW</b>	North Africa West	Morocco, Algeria, Tunisia

## Zusammenfassung

Solarthermische Kraftwerke (CSP) können in Kombination mit thermischen Energiespeichern und einer Zufeuerungsmöglichkeit bedarfsgerecht elektrischen Strom zur Verfügung stellen. Eine Übertragung von Strom aus solchen Kraftwerken in Wüstenregionen an entfernte Verbraucherzentren kann daher die regionalen oder heimischen Energiequellen ergänzen. Die Forschungsfrage nach dem Wert dieses Transfers wurde bereits in qualitativen Studien analysiert, die ein hohes Potential dieser Idee herausfanden. Eine detaillierte Energiesystemmodellierung, die den Wert von solarthermischen Kraftwerken aus dem Mittleren Osten und Nordafrika (MENA) für Europa (EU) zeigt, wurde jedoch noch nicht durchgeführt. Diese Arbeit schließt die wissenschaftliche Lücke unter Verwendung eines Energiesystemmodells mit minimalem Kosten-Ansatz und detaillierter Szenario-Analysen für das Jahr 2050. Die Dissertation beschreibt die Auswirkungen der Einbeziehung und des Ausschlusses eines Transfers von CSP aus MENA in die EU. Das Übertragungssystem besteht aus einem Kraftwerk und einer Hochspannungs-Gleichstrom-Übertragung (HVDC) und wird daher als CSP-HVDC-Kraftwerk bezeichnet. Die techno-ökonomischen Annahmen für diese zusammengesetzte Technologie werden konservativ gewählt, um eine Überbewertung zu vermeiden.

Bei der Prüfung von CSP-HVDC werden Bewertungskriterien von Energiesystemen berücksichtigt. Diese Multi-Kriterien zeigen die Auswirkungen von CSP-HVDC auf die Energieinfrastruktur, das Betriebsverhalten, die Kosten und die Emission des Energiesystems. Zur Bewertung des nationalen Netzausbaus wird eine neue Netzmethodik eingeführt, die sich aus Übertragungs- und Verteilnetz zusammensetzt. Dieses neue Modell reduziert die Komplexität des Netzausbaus und der Netzanalyse unter Berücksichtigung unterschiedlicher Kraftwerkspark-Portfolios.

Damit erweist sich CSP-HVDC als eine Anwendung, die einen zukünftigen nationalen Netzausbau in weit geringerem Umfang erfordert als ein Energiesystem mit einem hohen Anteil an Wind- und Photovoltaikenergie. Dies wird durch eine Validierung mit einem räumlich hochaufgelösten Modell belegt. Durch die Integration von CSP-HVDC in das nationale Stromnetz wird die Beanspruchung des Netzes gesenkt, da geringere Kapazitätsspitzen in den Übertragungsleitungen auftreten.

Kostensensitivitäten zeigen die Kostenunsicherheit eines zukünftigen Energiesystems. Die Untersuchung der Systemkostenunsicherheit zeigt, dass ein angemessener Anteil an regelbarer Energie, einschließlich CSP-HVDC, zu einer minimalen Unsicherheit der Systemkosten führt. Die Analyse der Kostenrelationen von CSP-HVDC zu allen anderen verwendeten Technologien (z. B. Nuklear- und CO<sub>2</sub>-Abscheidung und -Speicherung) zeigt, wie hoch die Häufigkeit einer Integration von CSP-HVDC ist. Innerhalb der EUMENA-Region

sind verschiedene Regionen unterteilt. Aufgrund der unterschiedlichen Charakteristika regionaler Energiesysteme hängt es von der Region ab, wie wahrscheinlich es ist, dass CSP-HVDC integriert wird. Für einige EU-Regionen kann eine Integrationswahrscheinlichkeit von bis zu 66% erreicht werden.

Das Ergebnis der Multi-Kriterien-Bewertung zeigt, dass Kraftwerks- und Speicherkapazität sowie Abregelungen geringere Auswirkungen haben, wenn CSP-HVDC zur Ergänzung des Energieportfolios eingesetzt wird. Die strengen Modellbedingungen für CSP-HVDC führen jedoch zu einer insgesamt höheren Übertragungsinfrastruktur, wenn CSP-HVDC aufgrund der langen Übertragungsdistanz in hohen Anteilen zum Einsatz kommt. Niedrigere CSP-HVDC-Anteile können die gesamte Übertragungsinfrastruktur einzelner Regionen reduzieren. Ein weiteres Ergebnis zeigt, dass die Systemkosten bei der Quantifizierung von CSP-HVDC nicht die wesentliche Rolle spielen, da die Systemkostenunterschiede gering sein können.

Der richtige Anteil an CSP-HVDC bietet mehr Freiheitsgrade, mehr Möglichkeiten und Kompromisse für die Auslegung eines kohlenstoffarmen Energiesystems anhand der genannten Bewertungskriterien. Ein technologisch vielfältiges Energiesystem mit geringen Kohlenstoffemissionen profitiert somit von CSP-HVDC.

## **Abstract**

Dispatchable solar power from concentrating solar thermal power plants (CSP) combined with thermal energy storage and co-firing option can provide energy according to demand. A transfer of such electricity from solar thermal power plants in desert regions to distant consumer centres may therefore complement regional or domestic energies. The research question of the value of this transfer was already analysed in qualitative studies that found out a high potential of this idea. However, a detailed energy system modelling showing the value of concentrating solar power plants from Middle East and North Africa (MENA) for Europe (EU) was not yet done. This thesis closes the scientific knowledge gap applying an energy system model with a least-cost approach and detailed scenario analysis for the year 2050. The thesis describes the effects of including and excluding a transfer of CSP from MENA to EU. The transfer-system consists of a power plant and a high voltage direct current transmission (HVDC) and is therefore called CSP-HVDC (concentrating solar power – high voltage direct current) power plant. The techno-economic assumptions for this composed technology are strictly chosen to avoid its overestimation.

The assessment of CSP-HVDC considers energy system evaluation criteria. These multi-criteria reveal the impact of CSP-HVDC on energy infrastructure, operational behaviour, cost and emission of the energy system. To evaluate national grid expansion, a new grid

methodology is introduced as composed of transmission and distribution grid. This new model reduces complexity of the grid and analyses grid expansion considering different power plant park portfolios.

As a result CSP-HVDC-application proves to require a future national grid expansion to a far lesser extent than a system with high shares of wind and photovoltaic energy. This is substantiated by a validation with a high-resolution grid model. Integrating CSP-HVDC into the national grid brings about reduction of grid stress due to lower capacity peaks in the transmission lines of the grid.

Cost sensitivity analyses indicate the cost uncertainty of the energy system. The examination of system cost uncertainty shows that an appropriate share of dispatchable energy including CSP-HVDC generates a minimal system cost uncertainty. Analysis of cost relations of CSP-HVDC to all other used technologies (e.g. nuclear and carbon capture and storage technologies) point out how high the probability of an integration of CSP-HVDC is. Inside the EUMENA region (Europe, Middle East and North Africa) various regions are subdivided. Due to different characteristics of regional energy systems, it depends on the model region in EU how probable it is that CSP-HVDC is integrated. For some EU regions up to 66% integration probability can be achieved.

The result of multi-criteria evaluation shows that power plant capacity, electrical storage expansion, and electrical curtailment cause a lower impact when CSP-HVDC is used to supplement the energy portfolio. However, the strict model conditions lead to a higher needed transmission infrastructure altogether, when CSP-HVDC is applied in high shares because of its long transfer distance. Lower CSP-HVDC shares can reduce the total transmission infrastructure of single regions. Another result demonstrates that system cost does not play the essential role in quantifying the value of CSP-HVDC because system cost differences may be small.

The right share of CSP-HVDC offers a higher degree of freedom, more options and compromises for the design of a low carbon energy system under the included evaluation criteria mentioned above. Thus, a technologically diverse energy system with low carbon emission rather benefits from CSP-HVDC.



# 1 Introduction

## 1.1 Background

Today's climate protection targets focus on a low global carbon emission. In the energy sector renewable energies, nuclear and CCS technologies are in the focus of global initiatives to reduce carbon emission. The use of diversified energy resources and technologies is a self-evident basis building up a sustainable energy supply system. However, many countries try to establish an energy system without strong cooperation between nations. A view beyond the horizon of national possibilities in order to profit mutually in an international alliance is often neglected.

A promising non-carbon emitting technology is concentrating solar power (CSP) in desert regions. Such a technology is available at the market and worldwide in use. Combined with thermal energy storage and a co-firing option, CSP can provide electricity according to demand and offers firm capacity. CSP is a steam cycle power plant such as nuclear and coal fired power plants but only with a very low or zero fuel demand. For the co-firing option e.g. renewable biomass can be used in very low shares. CSP has a high global potential especially in the MENA region (DLR, 2006). Making such a potential accessible, it is necessary to implement this technology and to transmit the CSP generated electricity to consumers.

In MENA the electricity demand is increasing and sustainable technological solutions are needed. Thus, CSP might be one technology among others supplying electricity for MENA. Furthermore, the EU searches for sustainable ways to cover its electricity demand. Cooperation between MENA and EU in the electricity sector might be a useful option to supply both regions with dispatchable energy. Supplementing EU's electricity demand with CSP from MENA could be a cost-efficient alternative element compared to purely national energy transition plans for a medium and long-term perspective until the year 2050. The EUMENA region could therefore be a prospective opportunity working closer together for climate protection targets and a sustainable energy supply. In advance of such cooperation, scepticism can arise on political level due to potential political influences. This thesis therefore works on factual level and provides scientific findings with the focus on a techno-economic system analysis.

## 1.2 Research question

Cooperation in the field of energy between MENA and EU can be an exchange of electricity and a specific transfer of energy to supplement the power plant park portfolio of a region. Such a transfer from MENA to EU might be suitable for electricity generated by CSP as a business case because the EU has not many available renewable dispatchable energy

resources on the own territory at its disposal (Scholz, 2012). This inaugurates to the research question of the value of a transmission of dispatchable energy in terms of CSP from MENA to EU:

**Is a transmission of dispatchable energy of CSP from MENA to EU beneficial for the composition of a sustainable energy system in the year 2050?**

What benefits and drawbacks in terms of: cost, uncertainty, infrastructural need, operational behaviour such as curtailment and grid stress and also carbon emission result from an energy system that includes such a CSP transfer compared to an energy system that excludes this technological option? Are there tangible alternatives that lead to similar benefits?

### 1.3 State of research, hypothesis, method and novelty

Research activities of the DLR and other institutions depict the potential use of CSP in MENA and the transmission of CSP to Europe (DLR, 2005), (DLR, 2006), (Trieb, et al., 2012), (BETTER, 2015). They found out that the use of CSP from MENA via specific high voltage direct current transmission lines (HVDC) can supplement the energy mix e.g. by reducing power plant expansion compared to a scenario that uses the same share of renewable energy without this option. The combined and enclosed use of CSP and HVDC is defined as CSP-HVDC power plant in the following.

Based on former studies, it seems that the energy system in the EU can profit from CSP-HVDC. However, other energy system criteria such as cost, infrastructure like the grid and storage, operational behaviour and emission have not precisely been analysed with an energy system model so far. To answer the research question of the value of CSP-HVDC in the thesis, an energy system model with a least-cost approach is applied. This model is a bottom-up model which includes today's available technologies. Assessing the value of CSP-HVDC, suitable model frameworks are analysed which consider potential alternatives to such a transfer. Finally, two energy systems in EUMENA are compared which include and exclude this CSP transfer option. The value is shown applying energy system evaluation criteria such as resulting system cost, required infrastructure, operational behaviour and emission. Especially, the electrical grid is analysed in more detail revealing the impact of CSP-HVDC on this energy infrastructure.

The state of research and novelty of the thesis in energy system modelling and assessing the value CSP-HVDC are discussed separately in the following sections.

#### 1.3.1 Energy system modelling

Energy system models are today's methods to approximate optimal future energy systems. Often they follow the target function of minimal system cost, perfect foresight and linear programming (REMIX, PLEXOS, TIMES, ReEDS, etc. (IRENA, 2017)). These numerical

models are bottom-up models using detailed technology modules building up a simulation of an energy system. A review of energy system models for energy policy applications is available from (Pfenninger, et al., 2015). The author emphasized the needed improvement in energy system modelling:

- Higher temporal and spatial resolution which increase the complexity and thus the computing capacity and calculation time
- Consideration of uncertainty, especially in modelling future energy system with sensitivity of cost assumptions
- Multi-criteria analysis improving the perception of different criteria (e.g. more than just cost)

In this thesis an insight for the reader is provided for each of the above listed suggestions. The innovation of the thesis is based on a high temporal (hourly) and spatial resolution for the grid model. Cost sensitivity analyses show the probability or uncertainty of an integration of a technology in the year 2050. Multi-criteria analyses evaluate the energy system for a holistic examination leading to sustainability. In this context sustainability means that the impact of the energy system should be minimal for its carbon emission, cost, infrastructure and operation. An analysis of the operation behaviour of the grid and the power plant park considers the peaks in the grid and the curtailment of power plants and reveals the possible differences with the use of CSP-HVDC. Possible competitive technologies such as nuclear power plants and CCS are contrasted with CSP-HVDC exposing their advantages for the energy system.

### **1.3.2 CSP modelling and value of CSP-HVDC**

In the field of CSP modelling there are techno-economic models such as SAM (System Advisor Model) for the dimensioning of renewable energies and CSP configurations. System analyses consider such basic spatiotemporal and techno-economic models e.g. by NREL using ReEDS (Denholm, et al., 2012), DLR using REMix (Fichter, et al., 2014), (Gils, et al., 2017), Stellenbosch University using an own model without long-term perfect foresight (Gauché, 2016), IER using TIMES (Tomaschek, et al., 2013) or in single technological models by ETH (Pfenninger, et al., 2014). The authors found out that CSP is able to provide dispatchable renewable energy complementing fluctuating PV and Wind energy in a low carbon energy scenario for the south west of the USA, Jordan, and South Africa. However, the value of CSP in MENA for Europe was only described in a qualitative way in (May, 2005), (DLR, 2006), (Trieb, et al., 2012), (Hess, 2013), (BETTER, 2015) and in Europe as well as in North Africa in (Brand, 2015). An energy system analysis with numerical models considering CSP in MENA with electrical interconnections to Europe was only done until now in combination with a so-called “overlay grid” environment (Haller, et al., 2012), (Stetter, 2012),

(Boie, et al., 2016). Such an overlay grid is comparable to a transmission grid which represents the possibility to transmit energy over a large spatial area.

The novelty of the present thesis considering CSP for Europe is the use of CSP-HVDC power plants. This infrastructure can be specified exactly using point-to-point (P2P) transmission lines from a CSP power plant to an offtaker. This allows a possible business case (Hess, 2013). CSP-HVDC is also opposed to an overlay grid comparing both infrastructures. This allows assessing the value of a transfer of CSP from MENA to Europe. CSP inside Europe is also an important option and considered in the study. However, the economic potential and average utilisation in southern Europe is lower than in MENA countries and the sites in Europe have often a conflict of use by agricultural activities (Scholz, 2012). In this thesis the value of CSP is assessed for EU, MENA and EUMENA separately using the same evaluation criteria and paying regard to where CSP technology is located. Thus, not only EU is considered as geographical examination area, but EU and MENA, that is EUMENA.

#### 1.4 EUMENA region

The used examination area assessing the value of CSP-HVDC is EUMENA (Figure 1). This geographical region consists of geographical sub-regions: Europe, Middle East and North Africa (Knies, et al., 1997). Having an impression of the global significance of EUMENA, the population in the year 2015 and 2050 is compared in EU, ME and NA using population data from the UN medium population scenario in Table 1.

In the year 2015 the region was inhabited by 1.26bn people and had a global population share of 17.2%. While population of Europe will decrease till 2050 the MENA region will grow strongly according to (United Nations, 2015). Thus, energy demand of MENA countries will rise intensively (DLR, 2005). However, MENA cannot grow enough to compensate the loss in Europe and the declining global population share of EUMENA with 15.2% in the year 2050. Nevertheless, Europe would even lose more global influence without the MENA region considering its population decline in global population share from 10.3% to 7.5%. Thus, cooperation could be a WIN-WIN for all EUMENA sub-regions stabilising the region in social issues but also profiting from environmental, economic and institutional affairs. An exchange potential rises therefore also in other fields beyond energy.

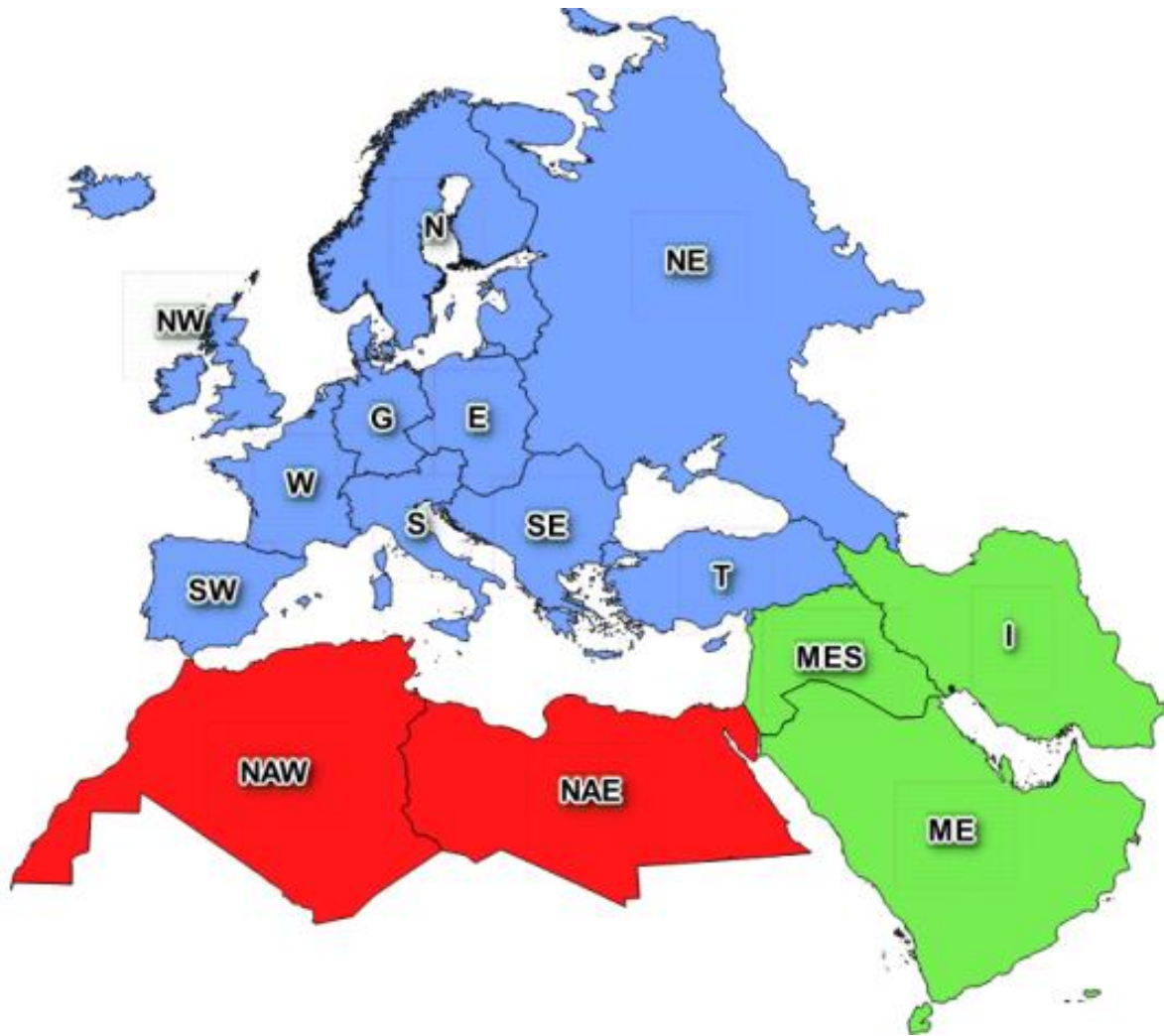


Figure 1: EUMENA geographical map

Table 1: Population data in EUMENA and the world

<b>Population data</b> (United Nations, 2015)				
<b>Region</b>	<b>Population [bn]</b>		<b>Global population share</b>	
	2015	2050	2015	2050
<b>World</b>	7.35	9.73	100%	100%
<b>EUMENA</b>	1.26	1.47	17.2%	15.2%
<b>EU*</b>	0.76	0.73	10.3%	7.5%
<b>ME</b>	0.32	0.47	4.3%	4.8%
<b>NA</b>	0.18	0.27	2.5%	2.8%

\*Russia until Ural Mountains is assumed with 75% of population in Russian Federation (Russian Federal State, 2010)

In Figure 1 the 15 analysed regions inside EUMENA are illustrated. An aggregation inside such regions is made due to computational constraints of the used energy system model. In the following Table 2 the spatial aggregation for the model regions of Figure 1 is shown. The spatial focus of the analysis is not only on the entire EUMENA region but also on sub-regions and nations, wherefore Germany is used as a national example.

An aggregation of separate nations can lead to a smoothing of their demand and resource characteristic. To reduce such falsification an aggregation is at first made according to a similar distribution of demand. Secondly the aggregation is made to limit the east-west expansion of a region avoiding an excessive smoothing of solar resources. Depending on the spatial proximity of a model region to Germany, the model regions close to Germany have a smaller spatial area than the distant model regions. This allows a better model framework to cope with a higher influence of the surrounding regions for Germany.

Table 2: Aggregation of countries to 15 model regions in the examination area EUMENA

<b>Model region</b>	<b>Alias</b>	<b>Country or region</b>
<b>G</b>	Germany	Germany
<b>N</b>	North	Denmark, Norway, Sweden, Finland, Lithuania, Latvia, Estonia
<b>E</b>	East	Poland, Czech Republic, Slovakia, Hungary
<b>S</b>	South	Switzerland, Austria, Liechtenstein, Italy, Slovenia
<b>W</b>	West	France, Belgium, Netherlands, Luxemburg
<b>NW</b>	North West	United Kingdom, Ireland, Iceland
<b>NE</b>	North East	Ukraine, Moldova, Belarus, Russia until Ural mountains, Azerbaijan, Armenia, Georgia
<b>SE</b>	South East	Greece, Croatia, Rumania, Serbia, Kosovo, Albania, Macedonia, Bulgaria, Bosnia-Herzegovina, Montenegro
<b>SW</b>	South West	Portugal, Spain
<b>T</b>	Turkey, Cyprus	Turkey, Cyprus
<b>MES</b>	Mesopotamia	Israel, Jordan, Palestine, Lebanon, Syria, Iraq
<b>I</b>	Iran	Iran
<b>ME</b>	Middle East	Djibouti, Yemen, Oman, Saudi Arabia, UAE, Qatar, Bahrain, Kuwait
<b>NAE</b>	North Africa East	Libya, Egypt
<b>NAW</b>	North Africa West	Morocco, Algeria, Tunisia

## 1.5 Workflow

Figure 1 illustrates the workflow of the thesis. Chapter 1 shows the background, literature review, research question and novelty of the thesis. The concept of CSP-HVDC is explained in Chapter 2. The research is based on a system analytic approach which analyses techno-economic values of energy under a least cost optimization defined in chapter 3. For robust results of a holistic energy system analysis a new grid methodology is introduced in chapter 4 and validated. In chapter 5 scenarios with broad sensitivity analyses quantify the value of CSP and contrast other dispatchable technologies considering climate targets for a long-term energy system in the year 2050. Finally, an exemplary perspective of a practical concept and its future manageability is outlined in chapter 6. Chapter 7 summarizes the results and gives an outlook of further research demand.

Chapter 1	Research question	Background, literature review and novelty
Chapter 2	How does the concept of a CSP transfer look like?	Comprehensibility of a CSP transfer
Chapter 3	What are the model assumptions?	Energy system modelling in REMix – assumptions and limits
Chapter 4	How can the electrical grid be represented?	Grid methodology
Chapter 5	What is the value of transferring CSP to Europe?	Assessing the value of CSP-HVDC
Chapter 6	How can the concept be manageable?	Perspective of a CSP transfer option
Chapter 7	Summary and outlook	Conclusion and further research demand

Figure 1: Structure of the thesis - chapters in red build the core of the work

## 1.6 Statement of the chapter

Energy system modelling approximates possible energy systems near to reality. A model can only deal with complex relations showing interdependencies of elements in a system.

As shown in former studies, CSP can provide dispatchable power according to demand. Only a few system analysis studies consider CSP and its use for Europe. However, the value of a CSP transfer from MENA to Europe is not yet quantified in detail. The reason for this is, that former studies use an overlay grid topology (no definite use of CSP over point-to-point connections) and no or sparsely sensitivity analyses in cost or other energy relevant criteria. To date the EUMENA region is hardly considered as an energy cooperation area. The population development in EUMENA shows a growth in MENA and a decrease in EU. As a region with about 15% of global population in 2050, EUMENA still influences global climate targets significantly and therefore needs careful considerations on the composition of its future energy systems.



## 2 The concept of a CSP transfer to Europe

A CSP-HVDC power plant is an option to supply centres of demand with dispatchable solar power from distance. In this chapter the characteristic of CSP-HVDC is explained, how it works and how it is modelled in REMix. An overview of different transmission line and grid topologies is given to show the relative merits of the concept of CSP-HVDC compared to the overlay grid concept. Finally, these concepts are combined in the study (in section 5.1.5) to use the advantages of both.

### 2.1 CSP-HVDC power plant definition

#### 2.1.1 CSP-HVDC power plant functionality, definition and configuration

A dispatchable renewable CSP power plant uses direct normal irradiance (DNI) as resource. The components to convert DNI into electricity are shown in Figure 2 and consist of a solar field (orange), a thermal storage (red) and a power block (grey - steam turbine with co-firing option and a generator). Solar fields can be realised for such a configuration as parabolic trough, linear Fresnel or single heliostats for a solar tower. These solar fields can be used in combination with a thermal storage either sensible or latent (phase change) providing dispatchable electricity on demand with a power block. To quantify the value of CSP a representing CSP technology is used. A parabolic trough system with sensible heat storage is chosen which today is the most implemented CSP technology (SACM, 2017). The steam turbine converts thermal energy (either from the solar field, the thermal storage or from the co-firing by fuels of all kind) into electricity via a generator. Alternating current from the power block is then transformed into direct current. To connect a CSP power plant in MENA with an offtaker in Europe, point-to-point HVDC transmission lines with AC/DC converters are needed (Figure 2 – light blue). This infrastructure can transmit dispatchable renewable energy keeping transmission losses low over distance. The power plant and transmission infrastructure is defined as a CSP-HVDC power plant including the point-to-point transmission line within the power plant. At the destination point in Europe, DC is transformed back into AC which is then fed into the transmission grid for a consumer's electricity supply.

Covering its relative small water consumption due to dry cooling, the power plant can use desalinated sea water from a water pipeline. Additionally, this sustainable water supply can provide surrounding desert regions with water for workers (~1 job per MW) and for new living space or agriculture (DLR, 2006), (BETTER, 2015). An exemplary CSP-HVDC configuration is shown in Figure 2, bringing with  $2200 \text{ MW}_{\text{el,gross}}$  ( $1500 \text{ MW}_{\text{el,net}}$ ) about 10 TWh/y dispatchable energy from a CSP plant in Morocco to a 2600km distant offtaker in southern Germany (Hess, 2013).

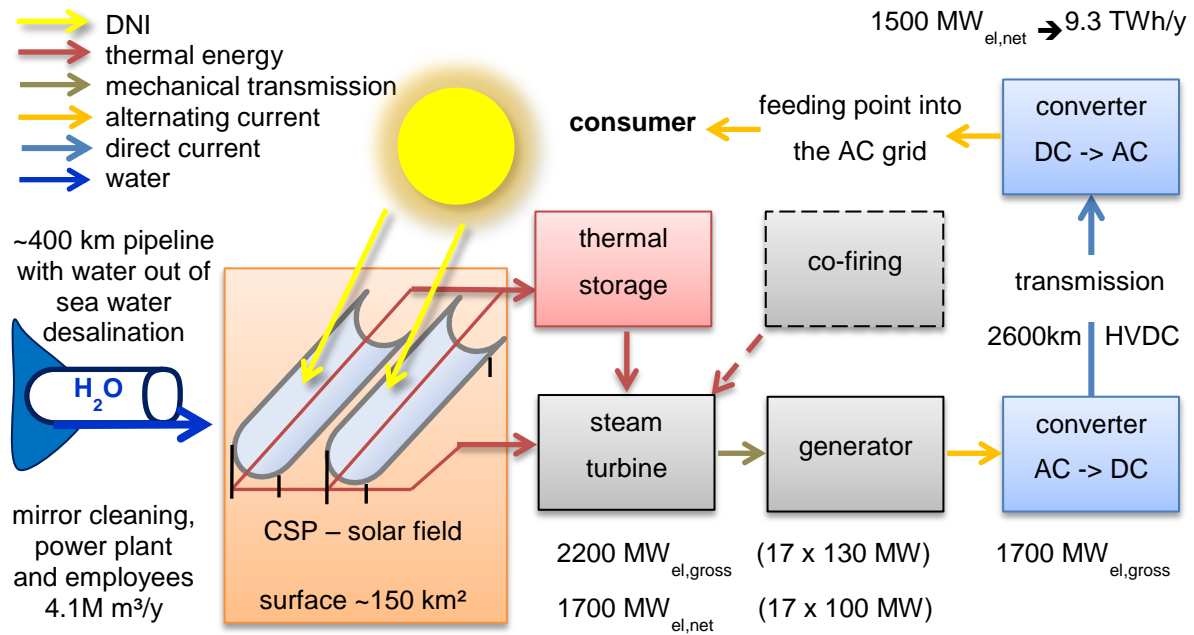


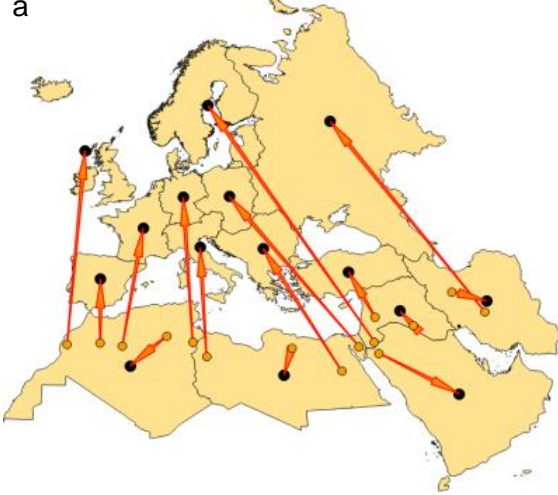
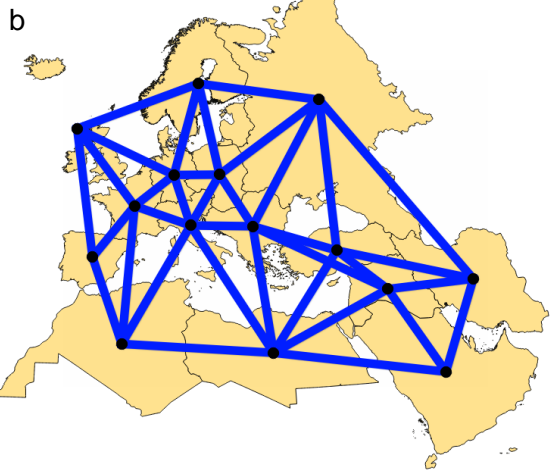
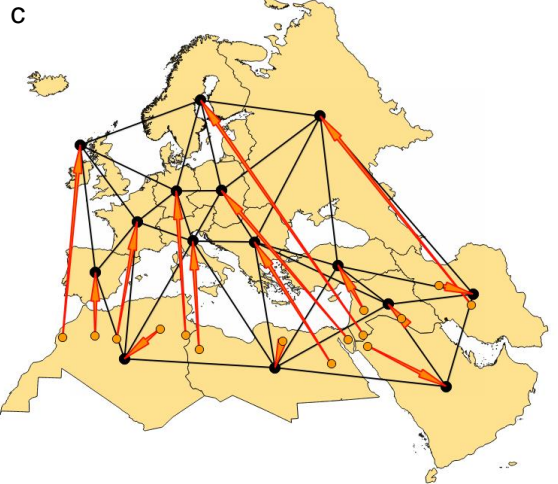
Figure 2: CSP-HVDC scheme transmitting dispatchable renewable energy over distance. The example shows a configuration of CSP in Morocco with a 2600km HVDC transmission line to Germany.

## 2.2 Comparison of point-to-point interconnection, meshed overlay grid and their combination

Point-to-point interconnection and a meshed overlay grid differ in their topology, financing and operational behaviour. A point-to-point interconnection is an infrastructure which connects two precise points of a system. This can be a power plant and an offtaker, two grid nodes or two grids. A meshed overlay grid can be compared to a transmission grid. However, an overlay grid is often used in a context of a large spatial area such as Europe (Cole, et al., 2011). An overlay grid is a possible future energy infrastructure which can transmit a high energy amount over a large distance without specific destination.

Former studies combined the use of renewable energies in EUMENA with the use of a meshed overlay grid (Haller, et al., 2012), (Boie, et al., 2016). In the context of CSP, point-to-point transmission infrastructures have not yet been analysed in EUMENA with an energy system optimisation model. Table 3a and b highlight the advantages and disadvantages of the point-to-point and overlay grid infrastructure. Table 3c indicates their combination. Good planning ability and high spatial flexibility of the energy supply might be the optimum of an energy transmission infrastructure. However, transmission line infrastructures are difficult to implement already nationally due to low social acceptance (Steinbach, 2013). Thus, the effort in building new transmission capacity should remain low, using as many advantages of point-to-point and overlay grid infrastructure as possible which is only feasible of course in a combination.

Table 3: Overview of point-to-point transmission lines and meshed overlay grid

Relative merits of transmission line and grid topology	Legend
<p><b>Point-to-point transmission lines</b></p> <p>Advantage</p> <ul style="list-style-type: none"> <li>• Projectable with specific producers and offtakers thus a clear business case is possible (BETTER, 2015).</li> <li>• Bundling of transmission lines can allow common infrastructure corridors.</li> </ul> <p>Disadvantage</p> <ul style="list-style-type: none"> <li>• Transmission line expansion is needed inside a multi-national structure.</li> </ul>	<p>a</p> 
<p><b>Meshed overlay grid</b></p> <p>Advantage (Cole, et al., 2011)</p> <ul style="list-style-type: none"> <li>• Can increase the overall reliability.</li> <li>• Can balance renewable energy due to a large spatial expansion.</li> <li>• International trade possibility.</li> </ul> <p>Disadvantage</p> <ul style="list-style-type: none"> <li>• Huge planning effort over a large area with a multitude of different authorities.</li> <li>• Unclear financing and operation.</li> </ul>	<p>b</p> 
<p><b>Expansion of existing grid and meshed overlay grid with point-to-point transmission lines</b></p> <p>Advantage</p> <ul style="list-style-type: none"> <li>• Combination of limited overlay grid (similar to existing transmission grid) and focussed use of dispatchable renewable energy.</li> </ul> <p>Disadvantage</p> <ul style="list-style-type: none"> <li>• New grid, existing grid and single transmission line expansion is needed.</li> </ul>	<p>c</p> 

### 2.3 Statement of the chapter

A CSP-HVDC power plant is technologically ready for use and its elements are in operation worldwide for many years so far. The important point of view is that such a power plant includes the HVDC transmission line. Therefore, it has to be considered as a power plant in distance, just with a longer line from the generator to the feed-in point into the grid. An expansion of point-to-point transmission lines and the existing grid is better projectable and more concrete than just outlining a meshed overlay grid. In the future a reinforcement of the transmission grid with additional point-to-point lines can be implemented at first and then an enforcement of both infrastructures might take place leading to a meshed overlay grid still including point-to-point transmission lines.

### **3 Energy system modelling in REMix – methodology, assumptions and limits**

Modelling near to reality is often the major aim of a modeller in energy systems. Yet, the dynamic of an energy system is hard to capture due to simplifications of a model and the resulting mistakes. This critical point often leads to misinterpretation of scientific results and should be regarded very critically when policy recommendations are made.

In this chapter the basic assumptions of the modelling environment are shown and the used methodology with the model REMix is explained. Finally the potential drawbacks are discussed. The basic modelling approach is a relative conservative consideration of CSP-HVDC to prove if this technology can be neglected or if it has a positive system influence using relative strict assumptions.

#### **3.1 Energy system modelling**

As a numerical energy system model REMix (sustainable Renewable Energy Mix) (Scholz, 2012), (Stetter, 2012) and (Gils, et al., 2017) is applied. This bottom-up model has the target function of minimizing system cost (total cost) using linear programming under perfect foresight. System cost include the annuities of investment and the cost of operation and maintenance (O&M), fuel and emission cost for energy relevant technologies (power plants, storage and grid) shown in Eq. (1). REMix consists of two models: REMix-EnDAT (Energy Data Analysis Tool) and REMix-OptiMo (Energy System Optimization). REMix-EnDAT uses climate and weather data to calculate potentials and technological time series of PV, Wind, CSP and hydro power plants. By regarding the cost of technologies, REMix-OptiMo can decide upon configuration and operation of the energy system. This means a quantitative decision about which capacity is built and which dispatch is used. Such an optimization can be performed based on a “greenfield” (model endogenous optimization), a “partial greenfield” (model endogenous optimization under exogenously given capacities) or just a dispatch optimization with only exogenously given capacities. REMix-OptiMo performs the following output data: capacity, generation, system operation, cost as well as emission data. The model structure is illustrated in Figure 3.

REMix is built in the algebraic language GAMS using the CPLEX solver. A detailed overview of the model methods is available in the references (Scholz, 2012), (Stetter, 2012) and (Gils, et al., 2017). Due to worldwide available meteorological data, calculated and compiled by the German Aerospace Centre, REMix is worldwide applicable.

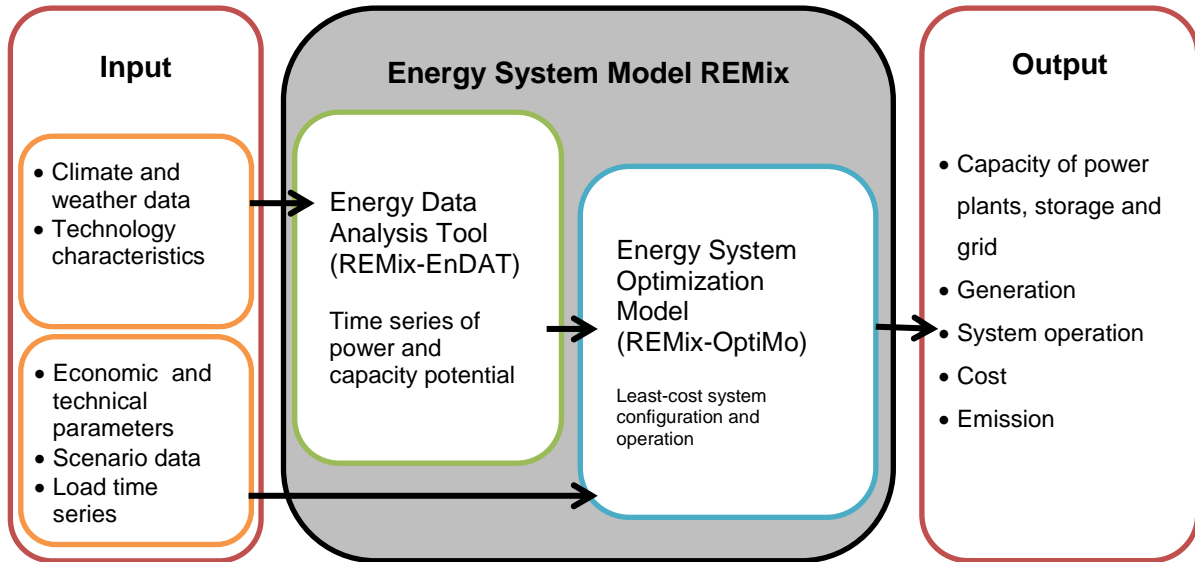


Figure 3: Model structure of REMix-EnDAT and REMix-OptiMo, input and output data based on (Gils, 2016)

Objective function in the linear program framework to be minimized:

$$\sum \text{System cost [k€]} \rightarrow \text{minimize} \quad (1)$$

The following equations concretise the system cost and calculation method. REMix, can optimize the variables which are written in bold. System cost is the sum of capital cost  $C_{capital}$  and operation cost  $C_{operation}$  described in Eq. (2). For the calculation of capital cost the annuity method is used including endogenous capacity  $P_{addedCap}$  and exogenous capacity  $P_{existCap}$  according to Eq. (3) and (4) which are multiplied with specific cost  $c_{specInv} \left[ \frac{\% \text{ of investment}}{\text{year}} \right]$ . The operation cost of the power plant park is calculated using fix and variable O&M as well as fuels and emission cost according to Eq. (5). All cost assumptions in the thesis are given in constant monetary value of the year 2015.

$$\text{System Cost [k€]} = C_{capital} + C_{operation} \quad (2)$$

$$= \text{Capital Cost} + \text{Fix O\&M Cost} + \text{Variable O\&M Cost} + \text{Fuel Cost} + \text{Emission Cost}$$

$$C_{capital} = (P_{addedCap} + P_{existCap}) \cdot c_{specInv} \cdot f_{annuity} \quad (3)$$

$$f_{annuity} = \frac{i \cdot (1 + i)^{ty}}{(1 + i)^{ty} - 1} \quad (4)$$

$$C_{operation} = (P_{addedCap} + P_{existCap}) \cdot c_{specInv} \cdot C_{O\&M \text{ Fix}} \quad (5)$$

$$+ \sum_t P_{gen}(t) \cdot (C_{O\&M \text{ Variable}} + C_{Fuel} + C_{Emission})$$

The used parameters of Eq. (2) - (5) are available in section 5.3.

## 3.2 Energy supply and demand

### 3.2.1 Supply technologies

The REMix model includes weather dependent technologies such as photovoltaic, wind onshore, wind offshore and hydro run-of-river so-called fluctuating renewable energies and non-weather dependent technologies such as biomass, geothermal energy, nuclear, gas, coal fired power plants (also CCS) and CSP with co-firing so-called dispatchable energies. Biomass, geothermal and CSP with thermal energy storage and co-firing are defined as renewable dispatchable technologies. Dispatchable energies can provide electricity according to the demand and offer firm capacity. The electricity generating renewable technologies applied in the thesis are listed in Table 4. These technologies are available today and they are functioning. Contrarily, technologies with a low technological readiness level such as nuclear fusion or a hydrogen turbine are not considered. This allows a pragmatic and robust energy system analysis without speculation of technological breakthroughs from today's point of view. Non-renewable technologies such as nuclear, gas, coal fired power plants (also CCS) are characterised in Table 26 on page 96. Defining the characteristic of a technology, a representative example out of a technology group is selected, but not the whole bandwidth of all specific occurrences of one technology is examined. The examples are representative for the general characteristic of a chosen technology. However, a simplification makes sense comparing only the technology groups in competition to each other. Other applied technologies defined as flexibility options such as electrical storages and the electrical grid. Potentials of pump storage, hydro run-of-river, hydro reservoir, geothermal energy, solid biomass and CSP are limited and are made available in the appendix Table 35.

Table 4: Classification and characteristic of used renewable energies for electricity generation based on (Scholz, 2012) – hydro reservoir is considered neither as fluctuating nor as dispatchable but as long term storage with additional natural inflow.

	<b>Technology class of electricity generating power plants</b>	<b>Characteristics</b>	<b>Range of validity</b>
Fluctuating renewable energies	Photovoltaic	Silicon cells with a module efficiency of 18%	Standard test conditions: 25 °C module temperature, 1000 W/m <sup>2</sup> irradiance
	Wind Onshore	Rotor diameter: 130 m Hub height: 132 m	Start-up wind speed: 2 m/s, nominal power output is reached at 12 m/s. Cut-off was set to start at 25 m/s and to end at 35 m/s.
	Wind Offshore	Rotor diameter: 140 m Hub height: 192 m	
	Hydro run-of-river (here fluctuating because of fluctuating water level and no co-firing option)	No power plant model – analysis is based on empirical time series	Power plants in operation, annual generation and generation potentials in Germany
Dispatchable renewable energies (with co-firing option)	Biomass	Power plant with steam turbine - 35% electric efficiency - using forest wood, waste wood, straw and energy crops	Domestic share of net primary production potential, yields and competing use scenarios per country for forestry, agriculture and other sectors - agricultural statistics.
	Geothermal power	Enhanced geothermal system (EGS)	Depth range 2000 - 5000 m
	Concentrating Solar power	Parabolic trough power plant with molten salt storage - 37% power block efficiency and 95% storage efficiency -	Reference irradiance - direct normal irradiance (DNI) - with 800 W/m <sup>2</sup> , tracking the sun along the north south axis

Other characteristic of power plant and storage are available with technological and economic data in Table 24 to Table 28.



### 3.2.2 Modelling of CSP-HVDC in REMix

#### 3.2.2.1 CSP-HVDC

As described in section 2.1.1, a CSP-HVDC power plant is modelled with a solar field (SF), thermal energy storage (TES), power block (PB) with co-firing system (BUS), two HVDC converters and a HVDC transmission. Each of these components has its own techno-economic characteristics which are listed in Table 24 and Table 29 and are considered by REMix. The following description is based on (Gils, et al., 2017) and reveals the functioning of the CSP model with thermal storage and co-firing option in REMix.

The total solar field thermal capacity is composed of the exogenous capacity  $Q_{existCap}$  and the model endogenous capacity  $Q_{addedCap}$  and is limited to the total potential calculated by REMix-EnDAT. The solar field thermal output  $Q_{SF}(t)$  arises from the overall capacity  $(Q_{addedCap} + Q_{existCap})$  and the normalised hourly availability of the solar resource  $s_{gen}(t)$  as thermal time series. This is described in Eq. (6).

$$Q_{SF}(t) \stackrel{!}{=} (Q_{addedCap} + Q_{existCap}) \cdot s_{gen}(t) \quad \forall t \quad (6)$$

(Gils, et al., 2017)

The thermal balance of CSP plants includes the thermal output of a solar field  $Q_{SF}(t)$ , backup unit  $Q_{BUS}(t)$ , TES charging  $Q_{charge}(t)$  and discharging  $Q_{discharge}(t)$ , the thermal curtailment of the solar field  $Q_{curtail}(t)$ , the power generation of the power block  $P_{gen}(t)$  according to Eq. (7) and the efficiency of the power block  $\eta_{generator}$ . The efficiency of the power block  $\eta_{generator}$  is the product of the thermal and electrical efficiency.

$$Q_{SF}(t) + Q_{BUS}(t) + (Q_{discharge}(t) - Q_{charge}(t)) - Q_{curtail}(t) \stackrel{!}{=} \frac{P_{gen}(t)}{\eta_{generator}} \quad \forall t \quad (7)$$

Hourly changes in TES energy level  $U_{level}(t)$  are described by the storage balance, which accounts for charging, discharging, and self-discharging in Eq.(8). An additional equation sets the storage level in the first and last time step to the same value, assuring that no energy is produced in the storage (Gils, et al., 2017).

$$U_{level}(t) \stackrel{!}{=} U_{level}(t-1) + \left( Q_{charge}(t) \cdot \eta_{charge} - \frac{Q_{discharge}(t)}{\eta_{discharge}} \right) \cdot \Delta t - \frac{1}{2} \cdot (U_{level}(t) + U_{level}(t-1)) \cdot \eta_{self} \quad \forall t \quad (8)$$

(Gils, et al., 2017)

The hourly output of the power block  $P_{gen}(t)$  is limited by the available capacity. The storage level  $U_{level}(t)$  must be in all time steps lower than the overall TES capacity (Gils, et al., 2017).

The novelty of modelling does not consist in the CSP model - developed by (Scholz, 2012), (Fichter, 2017) and (Gils, et al., 2017) - but in the method of implementing CSP-HVDC in REMix. A CSP-HVDC power plant transmits electricity via HVDC point-to-point transmission line directly to one offtaker in Europe. Thus, for this offtaker CSP is available apparently locally like home-grown renewable energies. Therefore CSP-HVDC is modelled as a power plant which has the solar resource of a MENA country and HVDC transmission losses - occurring with the transmission of CSP generated electricity to the consumer - but CSP from MENA is placed virtually in a European region. The gross capacity of the HVDC line  $P_{HVDC,gross}$  is the same as the net capacity of the CSP power block  $P_{PB,CSP,net}$  as described in Eq. (9).

$$P_{PB,CSP,net} = P_{HVDC,gross} \quad (9)$$

Transmission losses are assumed to increase linearly with an increasing distance.

### 3.2.2.2 CSP sites, HVDC point-to-point transmission corridors and offtaker points

The basis for the CSP-HVDC power plant modelling is built by an exemplary identification of 15 CSP sites (hotspots) in MENA and 82 potential offtakers in geographical Europe (Figure 7 and Figure 8). These production and offtaker centres define the starting and end point of a CSP-HVDC power plant in the model. CSP hotspots are chosen selecting good solar resource (Trieb, et al., 2012), short distance to Europe and diversified placement in different MENA countries. The CSP resource is taken within a 30km radius of the hotspot. Offtakers are bigger EU cities that represent centres of demand.

The pathways of HVDC between these CSP hotspots and offtaker are calculated using a line laying algorithm (May, 2005). This algorithm considers the geographical terrain with cost and minimizes cost to find a cost optimal pathway. Its spatial resolution is 1km x 1km.

The transmission pathway is calculated according to excluded areas (highest cost), preferred and unprivileged areas (lower or higher cost). Here two geographical categories are essential: The first category is independent from the direction of a pathway which is called isotropic friction image. The second category is dependant from the direction of the pathway and called anisotropic friction image (such as slope). With both categories cost-distance images of the CSP hotspots are calculated. Including the offtaker (demand centre) in the analysis a cost optimal pathway can be calculated with the cost-distance image.

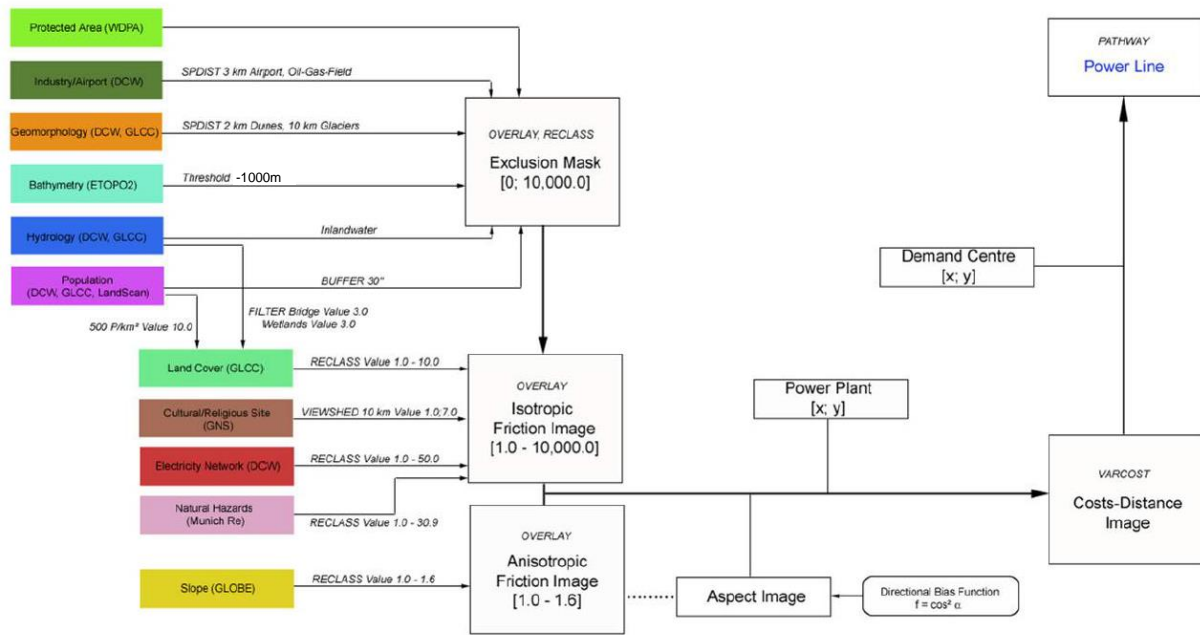


Figure 4: Line laying model based on (May, 2005)

The used isotropic friction images are exhibited in Figure 5 and Figure 6 showing two cost sensitivities:

- In Figure 5 a business as usual cost assumption is assumed which leads to predominant onshore pathways as shown in (May, 2005) and (Trieb, et al., 2012).
- In Figure 6 a dominant use of offshore pathways results. Here the isotropic friction image was calculated like in Figure 5 but with an addition of its highest sea cost value (~40) to the existing cost assumption of the land area.

Out of all possible combinations with 15 CSP sites and 82 potential off-takers (1230 possibilities) those CSP-HVDC plants are chosen which have a short distance to the consumer and at the same time a diversified solar resource from different CSP sites. The 124 chosen lines are shown in Figure 7 and Figure 8 and are listed in appendix Table 33. Both figures illustrate the same connections between CSP hotspot and off-taker with different pathways. Evaluating CSP-HVDC in this thesis with an energy system model presumes a reduction of this high-resolution infrastructure due to computational limits. Thus, average transmission lengths and average solar resource from selected CSP-HVDC are used each for one model region. The total average length to one model region is between 1200km and 3800km and is listed in Table 5. The average solar resource is shown by full load hours of the solar field in the appendix in Table 37. These solar resources of the CSP hotspots are assumed as relative conservative compared to the spatial average solar resources of a model region.

Figure 7 and Figure 8 illustrate a possible topology of CSP-HVDC. It is visible that in Figure 8 more straight pathways occur than in Figure 7 due to total higher cost. Thus, it can be assumed that Figure 8 represents sea cable and also underground cable. The CSP power plant sites and off-takers are exemplary and do neither represent real projects nor feasibility studies.

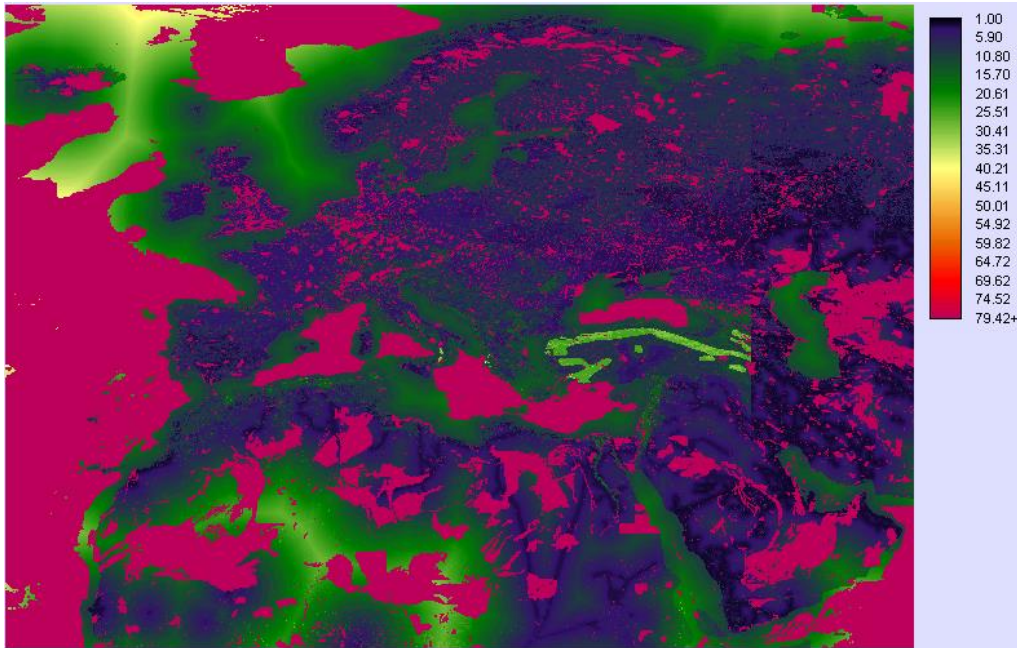


Figure 5: Isotropic friction image based on (May, 2005) (OHL case)

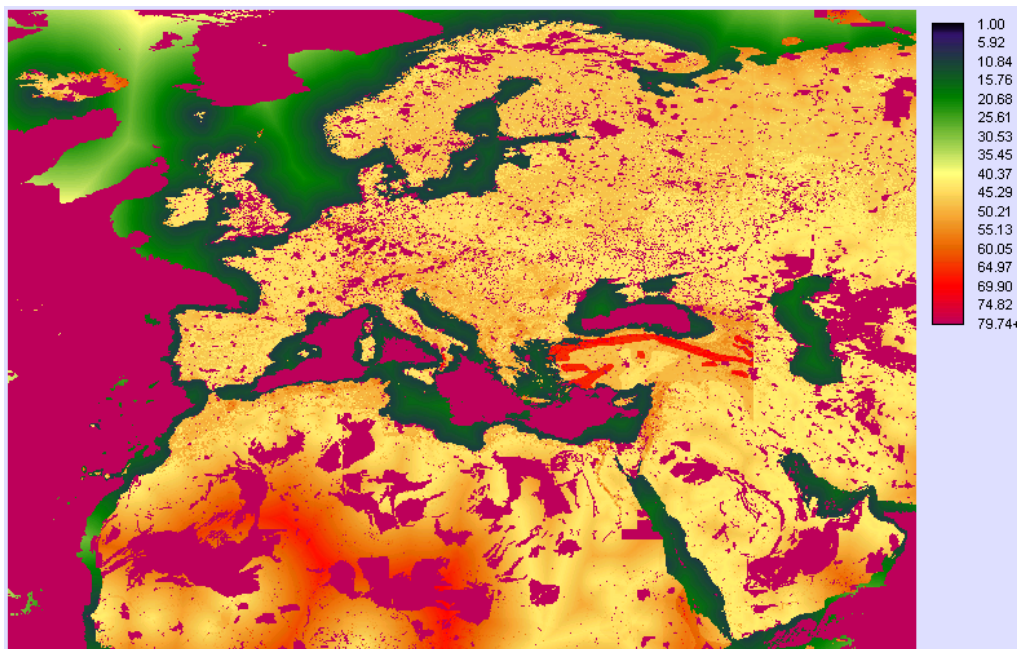


Figure 6: Isotropic friction image based on (May, 2005) with addition of highest sea cost value (~40) to all land cost values allowing the algorithm to use predominantly offshore pathways (sea cable and UGC case)

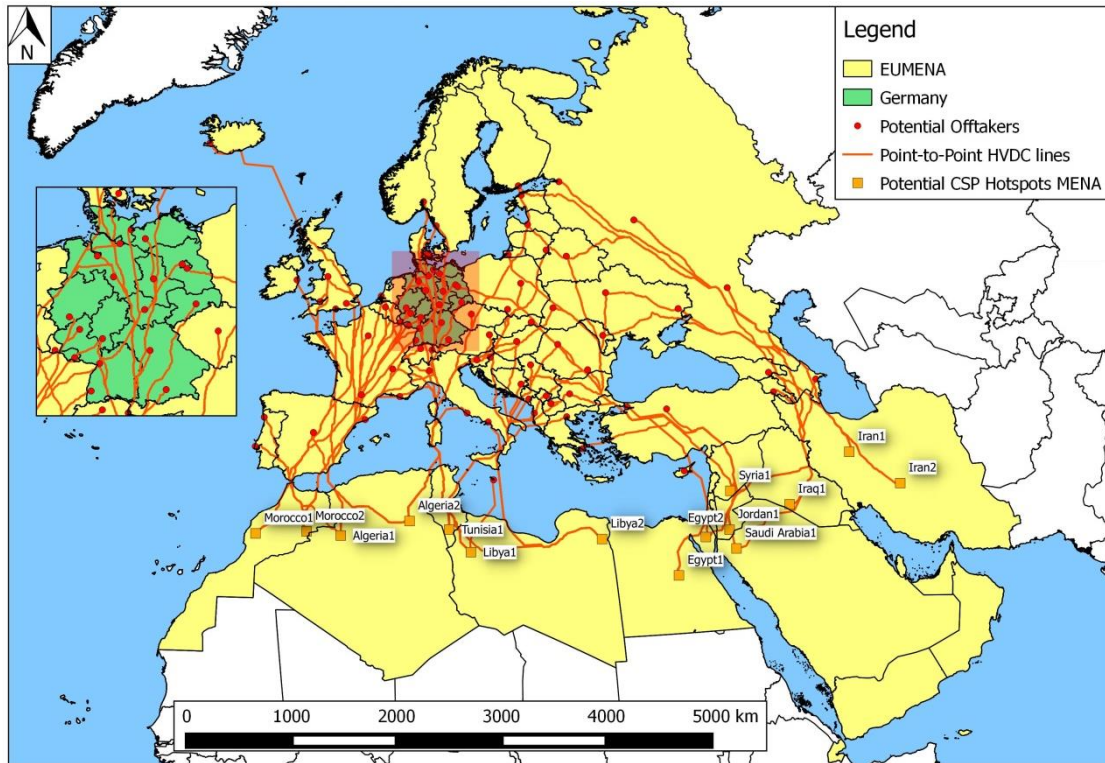


Figure 7: Point-to-point CSP-HVDC with potential CSP hotspots in MENA and potential off-takers in Europe – predominant onshore line configuration (OHL case)

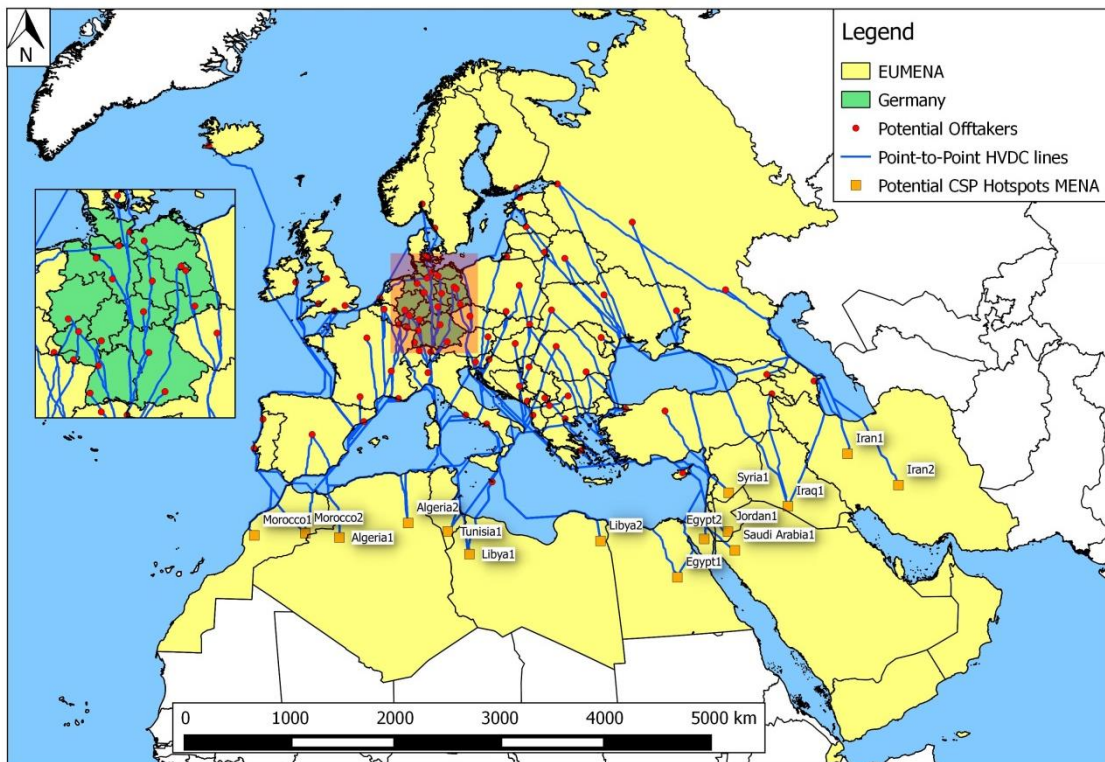


Figure 8: Point-to-point CSP-HVDC with potential CSP hotspots in MENA and potential off-takers in Europe – predominant offshore configuration (sea cable and UGC case)

For Germany a relatively high number of offtakers is included to identify precisely the average length of a specific point-to-point line.

Table 5: CSP-HVDC transmission line lengths to model regions as potential offtakers

Model region	Predominant OHL configuration		Predominant sea and UGC configuration		Total average length of point-to-point line
	Length line	Length line	Length line	Length line	
	land	sea	land	sea	
<b>G</b>	2343	249	1212	1403	2604
<b>N</b>	3461	331	1675	1915	3691
<b>E</b>	2549	356	1104	1626	2818
<b>S</b>	1540	366	568	1321	1898
<b>W</b>	2178	214	1012	1318	2361
<b>NW</b>	2747	930	645	3291	3807
<b>NE</b>	2502	109	1342	1129	2541
<b>SE</b>	1928	441	587	1604	2280
<b>NAE</b>	0	0	0	0	0
<b>NAW</b>	0	0	0	0	0
<b>SW</b>	1206	88	521	846	1331
<b>T</b>	899	255	406	838	1199
<b>MES</b>	0	0	0	0	0
<b>I</b>	0	0	0	0	0
<b>ME</b>	0	0	0	0	0

By analogy point-to-point transmission lines for hydro reservoir power plants are determined which are going from model region **N** in Figure 1 to the nearest surrounding model regions **G**, **E** and **NW** in Figure 1. Due to the high potential in model region **N** and current initiatives using hydro reservoir from Norway for some European countries, this technological option is included as one European home-grown energy resource. Pathway length and the assumed distribution of hydro reservoir capacity to the model region **G**, **E** and **NW** are shown in the appendix Table 34. The model regions of Table 5 are defined in Table 2.

### 3.2.3 Demand model

The analysis considers only the electricity demand. However, the demand model includes an electricity share of heat and mobility. The occurring electricity demand of these two sectors is added to the conventional electricity demand. In the following the assumptions of the demand until the year 2050 are explained showing the data that build the basis of the assumption in the demand model. The historical data of electricity, heat and mobility in the used model start in the year 2010 and are taken from IEA database (IEA, 2017).

- Electricity: net electricity demand (electricity, final consumption)
- Heat: residential and commercial heat demand (from coal, oil and gas)
- Mobility: transport demand (from oil)

The development of the electricity sector is derived from the GDP according to DLR (Trieb, et al., 2006). This reference uses a scenario for the development of the GDP per capita growth rate. The used GDP per capita growth rate in the scenario “closing the gap” assumes to reduce the difference of GDP per capita of a given country to 50% compared with the GDP per capita of the USA in the year 2050. National GDP growth rate and resulting electrical demand are shown in appendix Table 36. Population data are taken from the UN medium scenario (United Nations, 2015). For the development of the electricity share of the heat sector a 60% electricity share of global buildings final energy demand until 2050 is used and a demand reduction per capita and year (2010 to 2050) of 0.65% in OECD, 0.39% in Middle East and Africa and 0.28% in Eastern Europe and Russia is assumed (IPCC, 2014). The conversion factor using final energy of heat from oil, gas or coal is 90%. For the development of the electricity share of the mobility sector outgoing from 2020 a 15% electricity share of final energy demand until 2050 is used and a demand reduction per capita and year (2010 to 2050) of 1.08% in OECD, -0.45% in Middle East and Africa and -0.82% in reforming countries is assumed (IPCC, 2014), (IIASA, 2013). The conversion factor using final energy from oil for mobility is 30%. For heat and mobility there is still a higher share of carbon resource than in the electricity sector in 2050. However, the assumption considers low carbon emission trying to reach the 2°C target (Rogelj, et al., 2015).

The resulting electricity demand in Table 6 of heat and mobility is added to the electrical load curve with the same profile because today’s load curve already includes heat and mobility shares. The hourly profile of the electrical load curve is taken from ENTSO-e in 2006, Arab Union of Electricity (AUE) in 2012 and a synthetic load profile from (Gruber, 2012), (Pleißmann, et al., 2014) and thus represent historical demand curve. It is assumed that these load curves do not have another characteristic than in the year 2050.

Table 6: Annual electrical demand of electricity, heat and mobility sector in 2010 and 2050

Model region	Electricity demand [TWh]		Electrical heat demand [TWh]*	Electrical mobility demand [TWh]*	Total electrical demand [TWh]	
	2010	2050	2050	2050	2010	2050
G	532	510	173	22	532	706
N	382	541	13	17	382	571
E	235	337	82	11	235	429
S	436	522	141	27	436	689
W	641	673	205	42	641	920
NW	370	552	201	32	370	785
NE	608	839	170	27	608	1037
SE	195	298	15	8	195	321
NAE	151	1127	19	31	151	1178
NAW	71	582	74	19	71	674
SW	295	315	9	18	295	342
T	175	509	90	14	175	613
MES	150	796	99	56	150	950
I	186	484	362	28	186	874
ME	393	869	18	87	393	974
<b>Sum</b>	<b>4819</b>	<b>8953</b>	<b>1672</b>	<b>439</b>	<b>4819</b>	<b>11064</b>

\*Additional electrical heat and mobility demand are assumed to be 0 in the year 2010.

The rising electrical demand in EUMENA, which more than doubles from 4819 TWh in 2010 to 11064 TWh in 2050, leads to a capacity expansion and higher demand of resources. Thus, in Europe dispatchable renewable energies such as biomass and geothermal energy can reach their techno-economic limit. Solving this lack, Wind, PV, storage and CSP inside Europe and from MENA can provide renewable energy. It can be expected that a rising electrical demand may lead to a rising demand of renewable dispatchable energy and therefore to a rising demand of a transfer of CSP generated electricity from MENA to Europe.

### 3.3 Basic modelling assumptions

#### 3.3.1 Technological time series and electrical load curve

The time series of CSP, photovoltaic, wind onshore, wind offshore, hydro run-of-river power plants and hydro reservoir natural inflow are country-wide averages calculated with REMix-EnDAT based on bottom-up power plant models (see Table 4) (Scholz, 2012), (Stetter, 2012). This calculation includes exclusion areas for renewable energies which define with technology parameters the potential of each renewable energy technology. For each grid box, the approach yields hourly power generation based on technology parameters and



resource availability. The hourly time series are available of the years 1984-2004 on global level (resolution  $0.045^\circ \times 0.045^\circ$  or  $\sim 50\text{km} \times 50\text{km}$  at equator) (Stetter, 2012) and of the years 2006 - today on European level (resolution  $0.083^\circ \times 0.083^\circ$ ,  $\sim 10\text{km} \times 10\text{km}$ ) (Scholz, 2012). For the analysis a typical meteorological year is considered, which is the year 2006 in Europe (Scholz, 2012) and the year 2002 in MENA (Stetter, 2012). Two different years can be chosen due to relative low meteorological differences. On European level the output of the time series deviate in the available years of about 15% max. (Kühnel, 2013). Possible changes of the renewable resource availability due to climate change are an uncertainty which is not considered in the analysis. Peak load of demand and average resource full load hours of the model regions are available in the appendix Table 37. These input data are important for a reproducibility of the results showing key characteristics of annual input values as well as temporal intensity and temporal availability. Figure 9 serves as an example of the electrical load and technological time series of one year for Germany (country average). Here isopleth diagrams are used to illustrate such time series over the day of the year (y-axis) and over the hour of the day series (x-axis). They show in (a) the electrical load as share of peak load, in (b) the normalised availability of generated electricity by PV capacity, in (c) by wind turbines offshore, in (d) by wind turbines onshore, in (e) by hydro run of river power plants, in (f) the normalised availability of natural inflow by hydro reservoir power plants, in (g) by imports of hydro reservoir power plants from Norway, in (h) the normalised availability of generated thermal energy by the solar field of CSP in MENA for Germany and are related to the design point of  $800 \text{ W/m}^2$ . The hydro reservoir time series are derived from hydro run of river (Scholz, 2012). The CSP time series is an average of selected CSP hotspots (see appendix Table 33 for the origin of the CSP hotspots for one model region and Table 37 for average full load hours of the solar field).

The temporal profiles reveal the intensity and availability of the demand and the resources. Characteristic for the time series is the time period of regularly and unregularly low and high availability. For example the wind resources show irregular monthly and seasonal lacks (green colour Figure 9c, d) of wind compared to solar resources (black in Figure 9b,h). Solar resources are more periodical available during a year than wind or hydro resources. The availability of the solar resources PV (GHI) is smoother than the scattered resource of CSP (DNI). Comparing PV in Germany and CSP in MENA, it is visible that in winter PV drops in Germany while CSP in MENA stays in its availability nearly constant. Hydro time series are seasonally less fluctuating than wind or solar but not always such intensively available. The load curve shows a peak demand in winter which is typical in northern European regions. All isopleth diagrams of the used model regions refer to one year, start in the lower left corner (0,0) on January 1<sup>st</sup> and are shown in the appendix in Figure 39 to Figure 52.

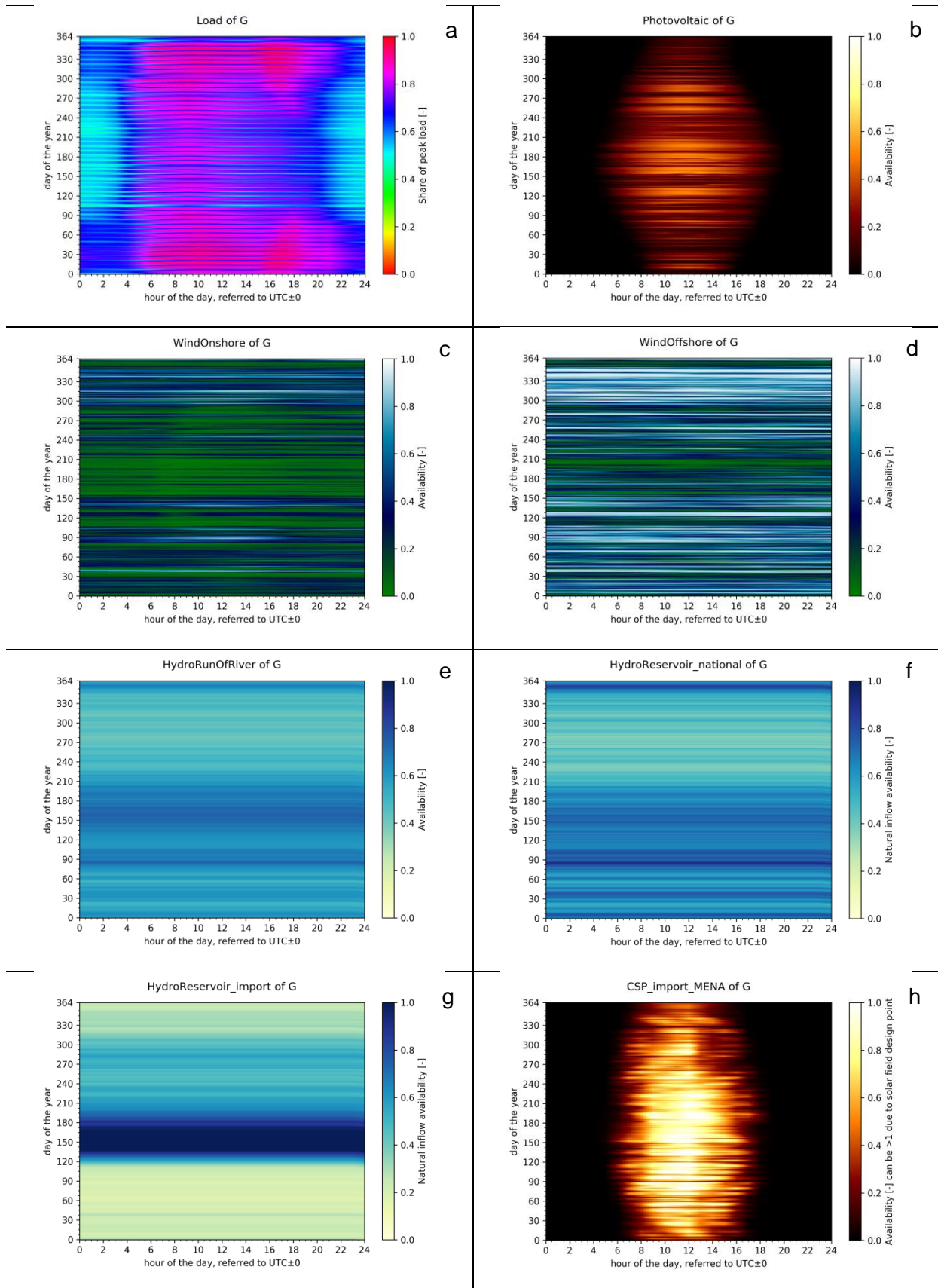


Figure 9: Load and technological time series of model region G

### **3.3.2 Demand Side Management**

Regarding Demand Side Management (DSM), former studies have shown that the economic potential of DSM in Germany is approximately 10 GW (Gils, 2016) (Gils, 2014). DSM substitutes short time storages (e.g. lithium ion batteries) and cost-efficient gas turbines (Gils, 2016) (Gils, 2014). Thus, DSM has only a small influence on system cost and operating behaviour of the power plant park in Germany (Gils, 2016) (Gils, 2014). Therefore DSM is neglected in the analysis.

### **3.3.3 Storages**

The model uses different types of storage: short-term (e.g. battery type, represented by parameters for lithium ion batteries), medium-term (e.g. compressed air and pump storages) and long-term storages (e.g. hydrogen storages). The representatives are chosen due to the optimization method with the target function of minimizing system cost. When modelling technologies with about the same cost, the optimizer always uses the cheapest technology. Other technologies with about the same characteristics are therefore excluded by the optimizer. Thus, only the used three types of storage are considered due to their different temporal commitment.

Power-to-Gas-to-Power (P2G2P) is modelled with an electrolysis (alkali in maximum cost sensitivity, PEMFC in minimum cost sensitivity), methanation, compressed and stored in a salt cavern or in the gas distribution grid and burned in gas turbines. Power capacity of electrolyser and turbine can be optimized separately.

### **3.3.4 Security of supply**

To ensure security of supply, the capacity credit is introduced (see Table 24). The capacity credit defines revision and outage of the installed capacity of each technology as an empirical value. For security and reserve reasons, the total firm capacity (product of capacity credits and related power plant capacities) must be 100%. So the total firm capacity is calculated referred to peak load at about 105%. To ensure firm national capacity in Germany, gas turbines are installed to cover the total peak demand together with other national dispatchable capacities in case of any failure. Installation of back-up capacities raise new financing questions if these capacities were not used (e.g. apportionment financing). CSP-HVDC is assumed with a capacity credit of 0% to model a possible total outage based on non-technical reasons. However, this dispatchable technology is able to ensure firm capacity due to its co-firing option. Thus, CSP-HVDC could substitute national gas turbines and reduce system cost if firm capacity abroad is accepted as such.

### 3.4 Uncertainty of cost and sensitivity analysis

Considering uncertainty in future energy systems, there are possible future changes (or even disruptions) like new technological developments which cannot all be presented and foreseen in this thesis. The focus in the thesis is on today's available technologies having a detailed look on uncertainty of the target function: the cost of annuity, O&M and fuels cost. They are varied in a sensitivity analysis. In this analysis maximal, mean and minimal assumptions for cost and lifetime are considered in section 5.3 in Table 24 to Table 29 showing the total spectrum of cost deviations from expert assumptions. Because CSP has different specific cost components, CSP learning curves are modelled using different installed capacities with different progress ratios for each component in Table 29 on page 97. A detailed technological cost sensitivity analysis in section 5.1.3 shows the integration probability of technologies (e.g. CSP-HVDC) varying the cost of only one technology compared to the cost of all other technologies.

### 3.5 Modelling mistakes and their consequences

As described at the beginning of this chapter, it is important to know about the modelling assumptions, mistakes and consequences. Table 7 shows a qualitative listing of resulting mistakes made by the used REMix model and makes suggestions of improvement for further research analyses. The made simplifications are related to methodology and assumption. The major barriers of a rapid improvement are today's computational constraints such as calculation time and unavailable random access memory. Despite the explained drawbacks, the model is able to show interdependencies of technologies in a possible energy system. Thus, assessing the value of CSP-HVDC is still possible but needs to consider the drawbacks of the model.

The methodological simplifications are linear modelling, perfect foresight and the cost optimization on macroeconomic scale. The simplifications of the assumptions of model input parameters are the spatio-temporal resolution, the exemplary examination year, the used techno-economic characteristic of technologies, the assumed node-internal grid characteristic (in the following chapter) and the assumption of the inflexible load curve.

Such barriers can be overcome using sensitivity scenarios with more criteria and by implementing characteristics of models which analyse more details. In other words: reducing complexity by integrating certain key characteristics. The last proposal depends on the research question and the possibility to reduce complexity of a certain characteristic without a major increase of mistakes. In the next chapter such a complexity reduction is made for the electrical grid (node-internal grid model).

Table 7: Modelling simplification, mistake, consequence and suggestion of improvement

<b>Simplification in</b>	<b>Simplification type</b>	<b>Mistake, consequence (→) and suggestion of improvement (+)</b>
Methodology	Linear modelling	<p><i>Smoothing non-linear to linear modelling</i></p> <p>→ No consideration of non-linear effects e.g. grid losses or change in efficiency of power plants during partial load</p> <p>+ Using mixed integer* or non-linear programming</p>
Methodology	Perfect foresight	<p><i>The model knows at the beginning of the calculation already the entire time period</i></p> <p>→ Storages are optimally dimensioned for the system but in reality the storage size might be not optimal due to missing perfect foresight. Thus, storage capacity can be too small or too much for a storage operator.</p> <p>+ Model exogenous placement of storage capacity</p>
Methodology	Cost optimization on macroeconomic scale (view of a social planner)	<p><i>Focus on minimal cost and no consideration of social, operational or other energy economic values</i></p> <p>→ The view of a power plant or grid operator - e.g. managing curtailment - is neglected.</p> <p>→ Unrealistic optimization based on lowest system cost and negligence of other sustainability criteria.</p> <p>+ Multi-criteria optimization</p>
Assumption	Temporal and spatial resolution	<p><i>Low resolution</i></p> <p>→ Sub-spatiotemporal resolution leads to missing information with unknown characteristic inside a region or between two time steps. Here an hourly resolution is used which leads to an overestimation of fluctuating energies and to missing information of primary or secondary system service. This indicates a higher need of power plant flexibility. Different topography inside a region could be problematic for a site placement.</p>
Assumption	Exemplary year	<p><i>Consideration of one year (e.g. 2050) without pathway optimization including previous years</i></p> <p>→ today's existing power plant park is neglected which may be already decommissioned in the year 2050. The consideration of the power plant park in the 2030 or 2040 is neglected. Thus, the way or possible dead</p>

		ends until 2050 are uncertain. + pathway optimization
Assumption	Technologies	<i>Representative technologies</i> → variation of specific technological details such as different height of a wind turbine or different compass direction of solar technologies are neglected → uncertainty in technological development (disruption) such as efficiency gains or material change + technological sensitivity analysis
Assumption	Transmission and distribution grid inside a node or model region	<i>Calibration of model with grid critical hour, no hourly consideration of each transmission line over one year</i> → negligence of grid losses over one year and Thus, overestimation of the grid performance + more and detailed calibration values
Assumption	Load curve	<i>Inflexible electrical load curve</i> → integration of fluctuating energy may be underestimated + consideration of more flexibility such as demand-side management and electrical demand curves of heat and mobility sector

\*Mixed integer linear modelling can adjust to non-linear effect but is not used in the thesis due to computational constraints.

A certain barrier of REMix assessing the value of CSP-HVDC is according to Table 7 the temporal resolution. A sub-hourly modelling does not consider system stability criteria such as primary and secondary reserve. CSP-HVDC with thermal storage, co-firing option and voltage sourced converter (VSC) can contribute to system stability criteria while other technologies might need addition features. Thus, CSP-HVDC is underestimated.

### 3.6 Statement of the chapter

The displayed modelling framework and assumptions of this chapter show that the analysis is based on a broad approach and on a critical view of REMix and CSP-HVDC. Moreover profound details of technologies are considered to quantify the value of CSP-HVDC. The used model can show possible future energy systems and technological interdependencies despite the drawbacks of the used methodology and assumptions.

## 4 Enhancement of the grid methodology in REMix

In this chapter a novel grid expansion model is presented. It characterizes the electricity grid expansion by the feed-in capacity of PV and Wind. Therefore a case study of the German transmission and distribution grid is used. The grid model is divided into two parts. The first part is the grid between model regions in EUMENA (overlay grid) and the second part is the grid inside a model region (transmission and distribution grid) of which the latter is explained and validated in detail within the case study. The grid inside a model region represents a major novelty for the modelling framework in REMix. Both grid models are important to show the grid utilisation and the needed grid expansion to assess the value of CSP-HVDC.

### 4.1 Overlay grid modelling

As described in section 2.2, an overlay grid is used for an electricity exchange in EUMENA. The topology is shown in Table 3b. This overlay grid model uses a DC flow approximation which calculates the power displacement of two regions for overhead line, underground cable and sea cable. Thus, the model can make conclusions of grid expansion and grid utilization. Each model region has for each connection one converter station.

The power flow  $P_{flow}(t)$  between model regions is limited by the overall capacity of the available lines ( $P_{addedlines} + P_{existlines}$ ). Eq. (10) describes the power flow in both directions between the model regions.

$$P_{flow}(t) \stackrel{!}{\leq} P_{addedlines} + P_{existlines} \quad \forall t \text{ (Gils, et al., 2017)} \quad (10)$$

Power transmission losses are calculated according to distances between the model regions and increase linearly with the power transmission. Such a simple transport model is described in (Hitchcock, 1941). The used overlay grid infrastructure with its length and capacity is listed in the appendix Table 38.

### 4.2 Transmission and distribution grid modelling

One important research question considering the value of CSP-HVDC and the grid is: How much transmission and distribution grid is necessary with different shares of Wind, PV and CSP in a scenario with high shares of renewable energies?

Former research quantified an overlay grid using different energy scenarios or varying the shares of Wind and PV (Haller, et al., 2012), (Schaber, et al., 2012). They found out that an overlay grid is efficient due to the reduction of power plant capacity and cost. However, the

grid inside a model region is totally neglected. Hence, the grid performance to integrate Wind and PV is overestimated in such unlimited regions or so called “copper plates”.

In a novel approach the region internal grid is modelled respecting the main grid expansion drivers: Wind and PV feed-in power into the grid. Grid expansion related to a rising demand is considered additionally and independently. The model is capable of making conclusions of grid expansion and curtailment of PV and wind energy in an optimized energy system.

This section engages in the question how to reduce the grid in its complexity keeping key characteristics of its expansion in an energy system model. The development of such a grid model is described systematically and tested in the following structure:

In the first part (section 4.2.1 and 4.2.2) the hypothesis and functionality of the model is explained. The used input data and their derivation are clarified. The two model parameters are specific cost for grid expansion  $c_{grid\ cost}$  of transmission and distribution grid and the grid expansion starting point  $P_{grid\ exp\ start}$ . They are determined in a first step and calibrated for the transmission grid in the second part of this section. Excursions show  $c_{grid\ cost}$  in other European countries and model independent basic grid cost  $C_{basic\ grid\ cost}$  according to demand.

In the second part (section 4.2.3) the model is calibrated and validated. For this purpose a case study of the German transmission grid is used. The modelling framework is explained for a calibration of the model. The calibration approach leads to a derivation of the specific cost for grid expansion  $c_{grid\ cost}$  and  $P_{grid\ exp\ start}$  of the transmission grid. With the new model data a validation of the hypothesis of the model is made. The results of the case study show the major differences between a model without node-internal model and the new node-internal model in cost, structure of the power plant park and curtailment.

#### 4.2.1 Model description

The fundamental idea of the model consists of the following: fluctuating renewable energy generates surpluses which lead to grid expansion. Figure 10 and in Eq. (11) - (18) illustrates the general functionality of the new “node-internal”<sup>5</sup> grid model with a simplified power dispatch. Variables are listed in bold. Eq. (11) describes the generated power  $\mathbf{P}_{gen}(t)$  and curtailed power  $\mathbf{P}_{curt}(t)$  dependent on the existing capacity  $P_{existCap}$  and added capacity  $\mathbf{P}_{addedCap}$  multiplied with a time series of a specific electricity yield  $s_{gen}(t)$  from REMix-EnDAT (Gils, et al., 2017).

---

<sup>5</sup> Node means a reduction of an area into one point – here a region is defined as a node which includes transmission and distribution grid of this region.



$$P_{used}(t) + P_{curtail}(t) \stackrel{!}{=} (P_{addedCap} + P_{existCap}) \cdot s_{gen}(t) \quad \forall t \text{ (Gils, et al., 2017)} \quad (11)$$

$$P_{gen}(t) = P_{used}(t) + P_{curtail}(t) \quad \forall t \quad (12)$$

$$P_{used}(t) \leq P_{fluc\ feed-in,max} \quad \forall t \quad (13)$$

While the existing grid is able to handle a certain amount of PV and Wind, a starting point of grid expansion  $P_{grid\ exp\ start}$  arises (Eq. (14)). The end of maximum grid expansion  $P_{grid\ exp\ end}$  is reached when maximum feed-in of fluctuating power  $P_{fluc\ feed-in,max}$  is used (Eq. (15), (16)).

$$P_{grid\ exp\ start} = P_{demand,peak} \cdot f_{grid\ exp} \quad (14)$$

$$P_{grid\ exp\ end} \geq P_{demand,peak} \cdot f_{grid\ exp} \quad (15)$$

$$P_{grid\ exp\ end} = P_{fluc\ feed-in,max} = P_{used,max} \quad (16)$$

Due to the uncertainty of meeting the starting point exactly, the starting point is varied subsequently in section 4.2.2.2 and calibrated in the case study 4.2.3. The model uses a feed-in power of PV and Wind  $P_{fluc\ feed-in}$  into the grid and a starting point of grid expansion which is in relation to peak load. The starting point is the product of peak load  $P_{demand,peak}$  and a grid expansion factor  $f_{grid\ exp}$ . When the start point  $P_{grid\ exp\ start}$  is passed by feed-in power, grid is expanded according to the difference of highest used feed-in power  $P_{used,max}$  and the start point - see Eq. (17) and red double arrow in Figure 10.

$$P_{grid\ exp} = P_{used,max} - P_{grid\ exp\ start} \quad (17)$$

The resulting maximum delta  $P_{grid\ exp}$  in the examined year is multiplied with a grid specific cost  $c_{grid\ cost}$  value, respectively - Eq. (18).

$$C_{grid\ exp\ cost} = P_{grid\ exp} \cdot c_{grid\ cost} \quad (18)$$

Grid specific cost values represent the cost for the expansion of the transmission and distribution grid. This grid specific cost  $c_{grid\ cost}$  can also be interpreted as additional cost of fluctuating feed-in power  $c_{fluc,feed-in}$  - Eq. (19).

$$c_{grid\ cost} = c_{fluc,feed-in} \quad (19)$$

Distribution and transmission grid have different characteristics. They differ in the use of feed-in power of technologies, cost and the starting point of grid expansion. The distribution

grid can use feed-in power of PV and Wind Onshore while the transmission grid can use feed-in power of PV, Wind Onshore and Wind Offshore. When grid expansion is too expensive, the model can decide to use other available technologies or curtail the feed-in power  $P_{curtail}$ . A linear expansion of the grid in relation to fluctuating feed-in power is assumed.

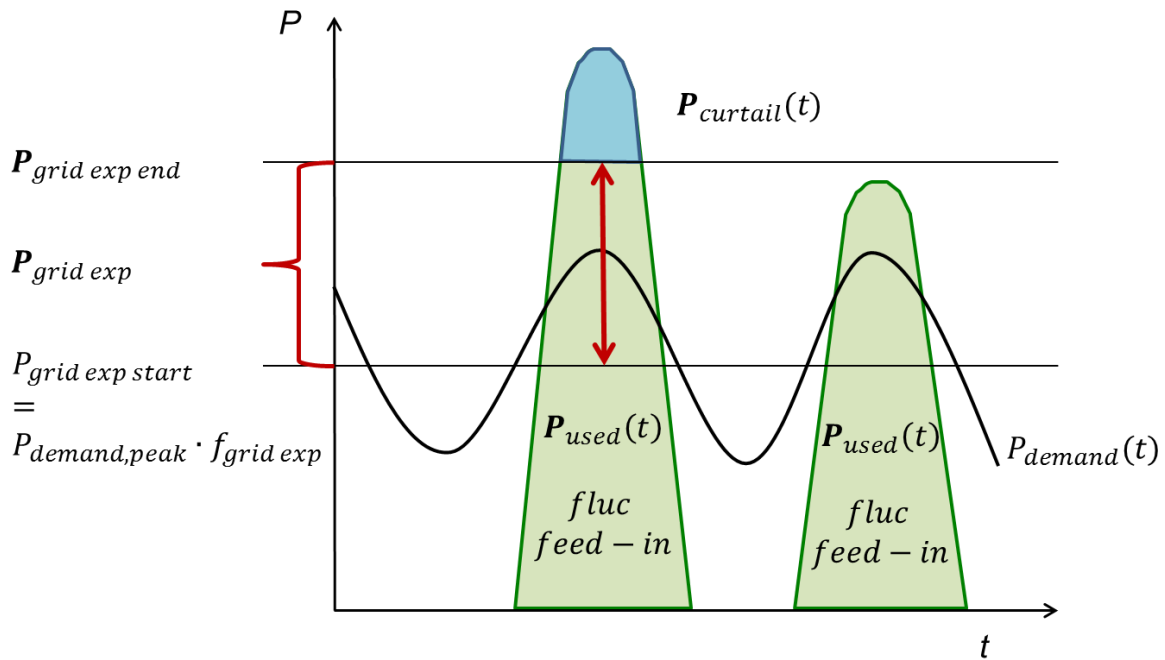


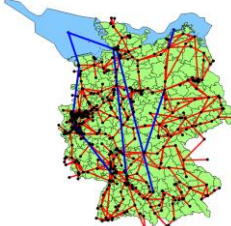



Figure 10: Principle of the node-internal grid calculation model. Grid expansion is related to feed-in power of fluctuating energies depending on a starting point in relation to peak load.

#### 4.2.2 Methodological overview, input data and validation

Grid specific cost  $c_{grid\ cost}$  is assumed in the first step with existing grid cost per grid power of the transmission grid in section 4.2.2.1, Eq. (20). This cost assumption is essential to determine the power plant park as a result of a greenfield optimization. Later in the case study (section 4.2.3), where this power plant park is used,  $c_{grid\ cost}$  is fitted with a high resolution transmission grid model. For  $c_{grid\ cost}$  of the distribution grid and the starting point of grid expansion  $P_{grid\ exp\ start}$  data from literature are used for a meta-analysis in section 4.2.2.2. The overall methodological approach is shown in Table 8.

Table 8: Methodological overview of the node internal grid model approach

Description	First node internal model	Distribution grid (meta-analysis)	Transmission grid (case study)	Final node-internal grid model
Modelling characteristic ↑ result	Determination of $c_{grid\ cost}$ as a first approximation → power plant park	Meta-analysis → determination of $P_{grid\ exp\ start}$ and $c_{grid\ distr}$	Use of power plant park of the first node internal model → validating $c_{grid\ trans}$ and $P_{grid\ exp\ start, trans}$	Use of iterated $c_{grid\ cost}$ and $P_{grid\ exp\ start}$ → representing transmission and distribution grid
Symbol				

As an excursion in section 4.2.2.3,  $c_{grid\ cost}$  is compared with ENTSO-e countries. Having in mind that the model only measures the grid expansion related to fluctuating feed-in capacity, the grid expansion related to the rising demand is shown in section 4.2.2.4.

#### 4.2.2.1 Specific investment cost for grid expansion

Cost of the existing grid is calculated with the circuit lengths from (ENTSO-e, 2016) and a specific cost value per km (400.000 €<sub>2015</sub>/km (220 kV), 500.000 €<sub>2015</sub>/km (380kV)). With these values, cost of the existing German transmission grid in 2013 is calculated. The resulting cost are 15.85 bn €<sub>2015</sub>. To measure the internal grid capacity roughly, the sum of the border transfer capacities from Germany with about 17 GW (ENTSO-e, 2010) is used because these values are also available for other countries. The result is nearly in the same range when calculating the quotient of existing power kilometres with about 28 TWkm in Germany and the maximum average grid length with assumed 1400 km (North-South and East-West spatial extent) which leads to maximum about 20 GW. Thus, 17 GW<sub>AC trans</sub> seem reasonable as minimum capacity value for the German transmission grid. According to Eq. (20) the grid investment cost per grid capacity in Germany for overhead line configuration are Thus, assumed minimal about 916 €/ kW<sub>AC trans</sub> for OHL and 1758 €/ kW<sub>AC trans</sub> for UGC (UGC = 1.92 x OHL (Hess, 2013)). For the distribution grid data from literature (Rehtanz, et al., 2012) and (Büchner, et al., 2014) are used with 375 to 500 €/kW<sub>grid distr</sub> which are described later in

Table 9. The grid power [kW] either for transmission or distribution grid describes the power which is necessary to include, transmit and distribute fluctuating feed-in power.

$$c_{AC\ trans} = \frac{\text{Cost of grid in Germany}}{\text{Maximum export capacity}} \quad (20)$$

Example: Germany:  $c_{AC\ trans} = \frac{\sim 15.85\ \text{bn}\ \text{€}}{\sim 17\ \text{GW}_{AC\ trans}} \approx 916\ \frac{\text{€}}{\text{kW}_{AC\ trans}}$

#### 4.2.2.2 Starting point of grid expansion based on Wind and PV feed-in capacity

In this section the derivation of the starting point of grid expansion is explained. Figure 11 shows the grid investment cost as a function of feed-in capacity of PV and Wind Onshore. The dots represent data from former analysis in literature based on (Rehtanz, et al., 2012), (Büchner, et al., 2014). An extrapolation of the regression curve is done to find the starting point of grid expansion  $P_{grid\ exp\ start}$ . When the regression curves intersect the x-axis  $P_{grid\ exp\ start}$  is met. Due to the fact that the six data points from literature are based on a peak load with  $\sim 91\text{GW}$  and the present study uses  $\sim 111\text{GW}$  peak load for Germany,  $P_{grid\ exp\ start}$  are shifted proportionally to the right.

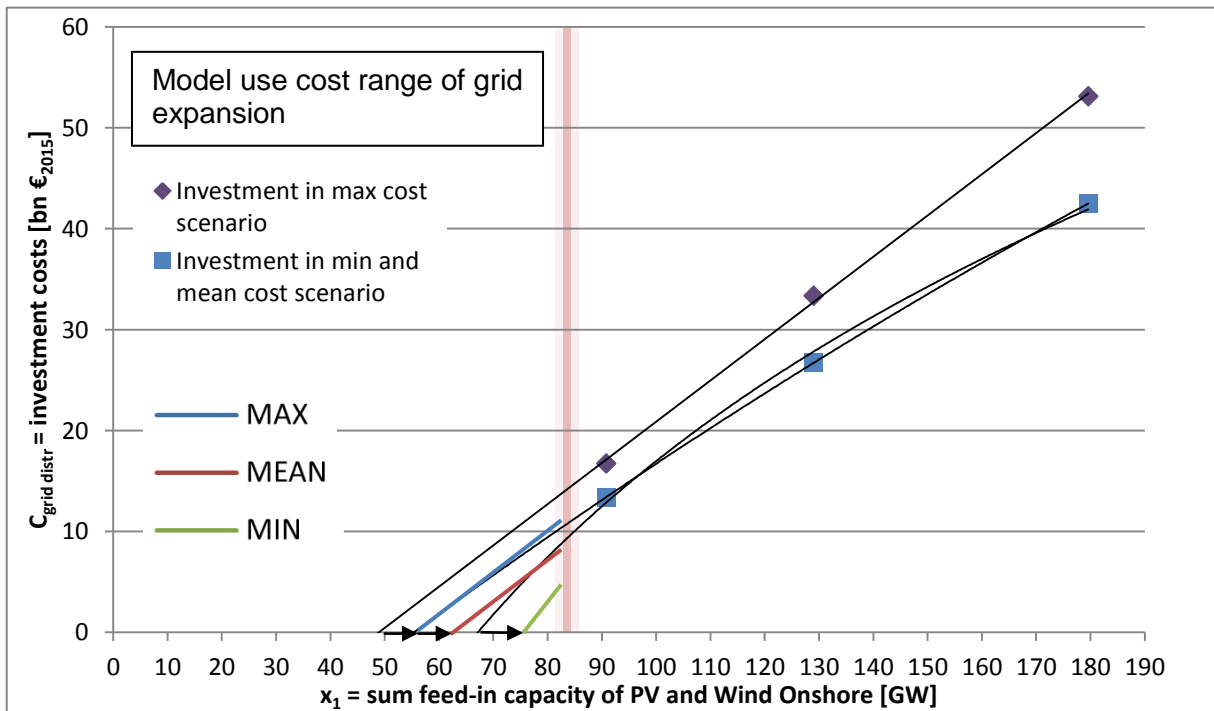


Figure 11: Cost sensitivities MIN, MEAN and MAX investment costs of distribution grid expansion. Investment [bn €] based on (Rehtanz, et al., 2012), (Büchner, et al., 2014), trend curves based on (Cossent, et al., 2011).

For the regression curves of distribution grid expansion cost of former studies, a logarithmic (min), a polynomial (mean) and a linear (max) trend line curves are used that are based on reference (Cossent, et al., 2011). Grid expansion in the distribution grid starts at 67.15 GW (min), at 55.31 GW (mean) and at 48.90 GW (max) of PV and wind onshore capacity. This equates to  $f_{grid\ exp}$  with 73.4% (min), 60.5% (mean) and 53.5% (max). To implement the regression curves in the new model, a linearization of the regression curves is done to fulfil the linear model environment (see Table 9).

Table 9: Distribution grid expansion cost sensitivity analysis with different expansion starting points

Cost sensitivity	$C_{grid\ distr,max}$	$C_{grid\ distr,mean}$	$C_{grid\ distr,min}$
Function from (Cossent, et al., 2011) adjusted to cost values of (Rehtanz, et al., 2012), (Büchner, et al., 2014)	$0.4086x_1 - 19.983$ [M€] (with UGC in the 110kV level)	(21) - $0.0004x_1^2 + 0.4371x_1 - 22.951$ [M€]	(22) (23) $42.625\ln(x_1) - 179.28$ [M€]
Linearized function in relation to fluctuating feed-in power ( $x_1$ ) used in the model	$0.4086x_1$	(24) $0.375x_1$	(25) (26) $0.500x_1$
Start point of grid expansion in relation to peak load	$f_{grid\ exp} = 0.535$	$f_{grid\ exp} = 0.605$	$f_{grid\ exp} = 0.734$
Specific grid cost	$\rightarrow C_{grid\ distr,max}$ = 408.6 €/kW <sub>grid distr</sub>	$\rightarrow C_{grid\ distr,mean}$ = 375 €/kW <sub>grid distr</sub>	$\rightarrow C_{grid\ distr,min}$ = 500 €/kW <sub>grid distr</sub>

The results of the calculation in REMix show with the red beam in Figure 11 that the sum of feed-in capacity of PV and Wind Onshore is less than 82 GW. Thus, the linearization of the regression curves is still in the range of validity. Table 9 shows the linear approximation in Eq. (24), (25) and (26) of the non-linear Eq. (21), (22) and (23). However, the used distribution grid studies (Rehtanz, et al., 2012), (Büchner, et al., 2014) are based on a more detailed analysis, so that the distribution grid cost may be undervalued in the new model due to uncertain distribution of Wind and PV power plants. Effects based on intentions to reinforce the distribution grid, due to already placed wind turbines and photovoltaic, are not included in the distribution grid model.

#### 4.2.2.3 Excursion: Comparison of grid investment cost in European countries

For a view beyond the horizon of the German electricity grid, grid cost, peak load and the comparability to the approach in Germany are compared on European level. As shown in Figure 12, the coefficient of determination of peak loads and grid costs is 85.88 % which is relatively high and thus shows a high correlation. Grid cost is modelled with a typical cost value per transmission circuit length and this determination can be also interpreted as peak load to grid length determination.

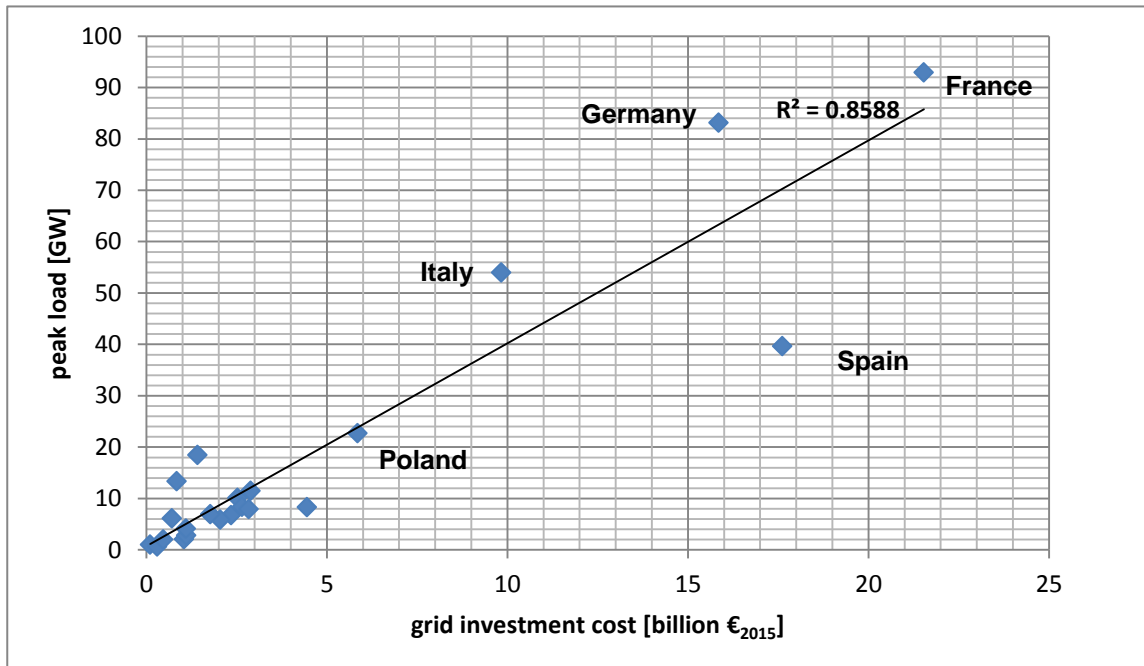


Figure 12: Coefficient of determination ( $R^2$ ) of grid investment cost to peak load in Continental Europe ENTSO-e countries of the year 2013.

Due to missing grid data in EUMENA, it is assumed that the existing grid in other countries has the same ability (ratio of peak load to grid capacity) like in Germany. The above mentioned correlation of grid investment cost and peak load and the previous assumption allows to the use of country specific grid cost with the same peak load to grid capacity ratio. Cost for reaching this grid status like in Germany is neglected in the analysis. Germany has a ratio of 5 with its peak load of  $83 \text{ GW}_{\text{peak load}}$  and grid capacity of  $\sim 17 \text{ GW}_{\text{AC trans}}$ . With this ratio France has a grid capacity of about  $18.5 \text{ GW}_{\text{AC trans}}$  ( $92.9 \text{ GW}_{\text{peak load}} / 5$ ) and Spain of  $8 \text{ GW}_{\text{AC trans}}$  ( $39.6 \text{ GW}_{\text{peak load}} / 5$ ). With 17.6 bn. € especially Spain has relative high grid cost in relation to its 40 GW peak load. In the present approach, Spain has relative high cost of grid in relation to grid capacity ( $\sim 2135 \text{ €/kW}_{\text{AC trans}}$ ) according to Eq. (20) compared to Germany ( $\sim 916 \text{ €/kW}_{\text{AC trans}}$ ), France ( $\sim 1113 \text{ €/kW}_{\text{AC trans}}$ ), Italy ( $\sim 874 \text{ €/kW}_{\text{AC trans}}$ ) and Poland ( $\sim 1237 \text{ €/kW}_{\text{AC trans}}$ ). These investment costs are iterated with the case study in section 4.2.3. The iterated costs for all considered countries in EUMENA are listed in the appendix Table 41.

#### 4.2.2.4 Excursion: Annual basic grid cost in relation to peak load

Since grid expansion can be assumed as linear (high correlation of peak load to grid cost in Figure 12) with a rising demand, Eq. (27) determines basic grid cost values for Germany. For the subsequent calculation of cost using the annuity method, annual cost of transmission grid in Germany are regarded. They can be calculated according to the existing annual grid expenditures (average of the years 2007-2013) (Klobasa, et al., 2014):

$$C_{basic\ grid\ cost} = \frac{Annual\ grid\ expenditures}{peak\ load} \left[ \frac{\frac{\text{€}}{y}}{GW_{peak\ load}} \right] \quad (27)$$

Transmission grid:  $0.95\ \text{bn}\ \text{€}/y / 91\ \text{GW}_{peak\ load} = 10.4\ \text{mio}\ \text{€}/y / \text{GW}_{peak\ load}$

Distribution grid:  $5.96\ \text{bn}\ \text{€}/y / 91\ \text{GW}_{peak\ load} = 65.5\ \text{mio}\ \text{€}/y / \text{GW}_{peak\ load}$

With the used scenario peak load of Germany in the year 2050 of  $111\ \text{GW}_{peak\ load}$  (705 TWh/y electricity demand) the annual cost of the transmission grid is 1.15 bn. €/y and for the distribution grid 7.27 bn. €/y. These specific basic grid cost are assumed also for other regions due to currently missing detailed data.

### 4.2.3 Case study of the German energy system in 2050 and model calibration

To validate the input data assumptions of section 4.2.2.1 and 4.2.2.2 and the model itself, the transmission grid is calculated in a high resolution grid model (491 regions) inside Germany with a model endogenous power plant park and a determined grid topology in a 100% renewable energy scenario (reaching maximum grid expansion). For the grid expansion quantification different shares of fluctuating and dispatchable energy (combination of 10% to 90% share) are used related to gross electricity consumption.

#### 4.2.3.1 Case study input values and modelling framework

For a computational feasible determination of the power plant park, at first a one node model for Germany is used in which all capacities are endogenously optimized (with cost sensitivities, OHL/UGC configuration and fluctuating/dispatchable energy share combination) with the grid model assumptions of section 4.2.2. The resulting capacities are shown in the appendix Table 39. Secondly the capacity and demand for Germany are regionally distributed to the 491 regions according to their potentials (appendix Figure 14). REMix data for AC and DC technologies (see Table 10) are included. The transmission grid is represented by 491 model nodes (Figure 13). The transmission

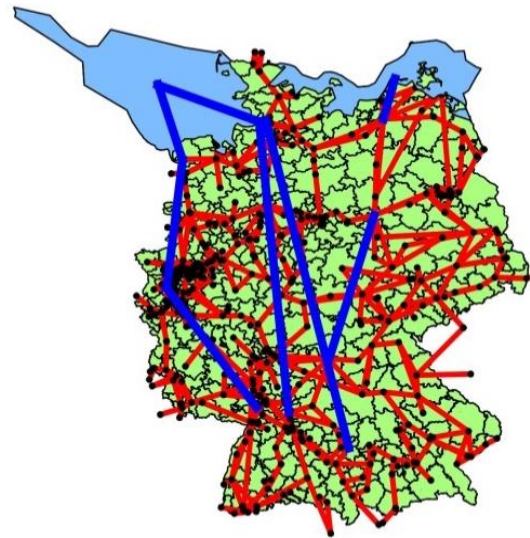


Figure 13: Grid model in Germany with 491 nodes, AC (red) and DC (blue) transmission lines

line topology with the modelled transmission connections is based on today's AC connections and the recently planned DC connections (Medjroubi, et al., 2015), (Bundesnetzagentur, 2015). The 491 node model includes all details in lengths and nodes of the existing transmission grid in Germany. The areas around the 491 grid nodes are formed by an aggregation of postal codes surrounding the nearest grid node (Metzdorf, 2016). Thus, one model node represents an agglomeration of postal code areas.

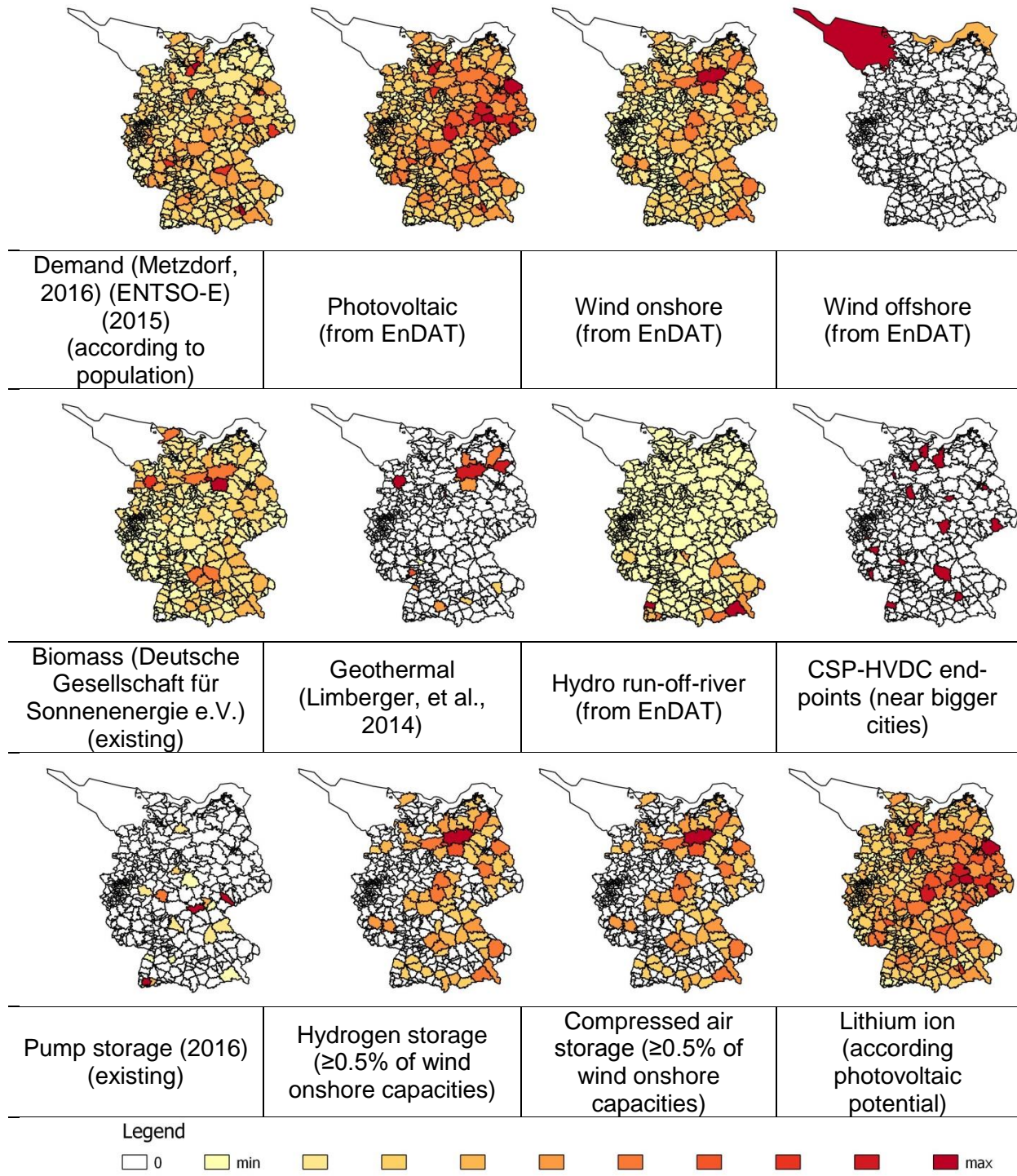
In the case study hydro reservoir power plants are excluded. This technology is defined neither fluctuating nor dispatchable. Also nuclear, gas, coal and CCS are excluded due to their non-renewable property. This leads to a 100% renewable energy scenario. Such a scenario is important to show the grid expansion in its possible full extent.

In Figure 14 the capacity distribution with qualitative potential maps of Germany with 491 regions (grid node model) is shown. Regional potential is either based on EnDAT, existing



power plants, correlations of interdependent technologies (storages) or on manually selected sites (CSP-HVDC offtakers).

Figure 14: Distribution of demand and capacities according to their potentials [% of total capacity].



On the technological side, hydrogen, adiabatic compressed air and lithium ion are distributed according to renewable potentials due to their high charging and operational correlation (Cebulla, 2017).

Table 10: Techno-economic parameters of AC and DC used in the case study

		AC	AC substation	DC	DC converter
Specific	Cost	500.000 €/km	24.790.000 €	786.000 €/km	148.730.000 €
	OHL		per station		per station
Specific	Cost	962.000 €/km	24.790.000 €	2.271.350 €/km	148.730.000 €
	UGC		per station		per station
Specific		1005 MW	1005 MW	1500 MW	1500 MW
	Capacity				
Specific	Voltage	380 kV		600 kV	

Sources: (Brakelmann, 2004), (Trieb, et al., 2012), (Hess, 2013), (Bundesnetzagentur, 2015)

#### 4.2.3.2 Model calibration

In the following the specific transmission grid expansion assumptions of Eq. (20) are calibrated. The analysis has the aim to calibrate the model using maximum grid expansion results under a least cost optimization. The calculation of a 491 node model in hourly resolution over one year would be a suitable environment to calibrate the model but causes a disproportionately high calculation effort. Therefore, average hours (24h over one year) and critical hours (one hour in a year) are used in Table 11 to determine grid cost. The power plant park capacity, identified by pre-optimization, is distributed to the 491 regions. The grid capacity is endogenously optimized in the predefined grid topology (Medjroubi, et al., 2015).

Fluctuating energy causes energy supply peaks. Hence, critical grid hours show relevant grid cost in scenarios with high share of fluctuating energy. In scenarios with low fluctuating energy share (or higher dispatchable share) a 24h time resolution over one year can determine the grid expansion. This is shown in Table 11 with the combination of the used time resolutions. Higher grid cost with higher share of fluctuating energy confirms the assumption that grid is expanded with higher share of fluctuating energy. As a measurement of uncertainty of the resulting annual transmission grid cost (Table 11 – values in bold) the sum of maximum cost of each transmission line within a scenario is considered. Table 11 shows these values in the last column. The average deviation is 15% above the used values in bold. Thus, transmission grid cost is calibrated conservatively.

Table 11: Annual transmission grid cost in the 491 node model using different time resolution (values in bold represent the calibration data of the node-internal grid model)

Characteristic of time resolution and <i>time interval</i>	24h average		High load with high feed-in of Wind		Low load with high feed-in of Wind		<i>Sum of maximum cost of each transmission line of the scenarios to the left</i>	
	<b>one year</b>		<b>one hour</b>		<b>one hour</b>			
	[bn. €/y]		[bn. €/y]		[bn. €/y]		[bn. €/y]	
Cost scenario with a defined energy share fluctuating_dispatchable	Max UGC	Min OHL	Max UGC	Min OHL	Max UGC	Min OHL	Max UGC	Min OHL
10_90	<b>1.93</b>	<b>0.80</b>	0.01	0.3	0.24	0.50	1.93	0.92
30_70	<b>4.63</b>	<b>1.58</b>	3.10	1.01	3.73	1.22	5.27	1.71
50_50	<b>6.30</b>	<b>1.74</b>	5.13	1.64	5.80	1.55	7.91	2.05
70_30	7.58	2.12	8.05	2.10	<b>9.14</b>	<b>2.48</b>	11.53	3.07
90_10	8.07	2.70	<b>11.57</b>	<b>3.28</b>	8.31	2.69	13.11	3.76

The calibration points, defined as critical grid hours, are hour 7963 and hour 8706 out of 8760 hours. Their resulting characteristics in wind feed-in capacity are shown in Table 12.

Table 12: Model calibration points as critical grid hours

Criteria	calibration point A	calibration point B
Load	high load: 102 GW	low load: 89 GW
Hour	High feed-in of Wind (hour 7963)	High feed-in of Wind (hour 8706)
% of installed wind capacity	31.6% wind onshore 85.0% wind offshore	37.4% wind onshore 82.5% wind offshore

Other combinations of high/low load, wind-feed-in, PV feed-in do not lead to higher grid cost.

Using grid critical hours means that the grid is not represented with each needed maximum transmission line capacity but with the entire maximum transmission capacity of the whole transmission grid. To prove that grid critical hours (hour 7963 and 8706) are found, the curtailment in these hours is considered. In these hours no or an infinitesimal curtailment occurs. Thus, it seems provable that the grid is maximal expanded in these hours as long as all produced electricity is transmitted or used (no curtailment). None of other selected hours

in high-low combination of load, wind and photovoltaic feed-in do show higher grid cost (not listed in the analysis).

#### 4.2.3.3 Model validation

The model assumption is that a rising share of fluctuating energy leads to a rising grid expansion in a cost optimized framework. The use of the 491 node model with different power plant parks has proven this hypothesis. Thus, the model can represent a grid expansion according to fluctuating energy share and is therefore considered as valid.

#### 4.2.3.4 Derivation of specific grid expansion cost and starting point of grid expansion

Based on the results in Table 11 with the 491 node model, it is clear that transmission grid expansion does not start relatively late like that of the distribution grid, but early at about 20-30% of fluctuating feed-in power. This starting point (compared to grid expansion and today's fluctuating energy share in Germany) occurs when comparing the annual grid cost of the model with the current annual grid cost in reality. The resulting grid expansion cost of  $c_{cb,grid\ trans}$  with 585 €/kW<sub>grid trans</sub> (OHL) and 900 €/kW<sub>grid trans</sub> (UGC) is lower than the former assumed cost  $c_{grid\ trans}$  in section 4.2.2.1. Thus, a cost reduction is achieved in the OHL case with 35% (from 916 €/kW<sub>grid trans</sub> to 585 €/kW<sub>grid trans</sub>) and in the UGC case with 52% (from 1728 €/kW<sub>grid trans</sub> to 900 €/kW<sub>grid trans</sub>). Consequently, the lower grid expansion cost and earlier grid expansion starting point are considered and taken for calculation.

#### 4.2.3.5 Quality of calibration values and model results

A quality control should prove if the node-internal grid model can confirm the grid cost which are given by the calibration values in Table 11. For this comparison a "greenfield" approach with six cost sensitivity scenarios is used. The sensitivity scenarios consist of a combination of OHL/UGC and "all max", "all mean" and "all min" technological cost assumptions in Table 24 to Table 30. The examination area is Germany as a one node energy model. The node-internal grid model is applied with the calibrated specific grid cost  $c_{cb,grid\ trans}$ . Figure 15 illustrate the calibration values of Table 11 and the results of the application of the node-internal grid model. As shown in Table 11, annual grid investment cost rises in a linear manner together with an increasing fluctuating energy share of Wind power and PV. This linear correlation is depicted in Figure 15 with model calibration values of Table 11. It is visible that the coefficient of determination is 99.52% (UGC max) and 96.73% (OHL min).

The cost bandwidth of Table 11 can be met by the calibrated node-internal grid model in Figure 15. Comparing the results of cost bandwidths of Table 11 (linear interpolated dots) and the calibrated node-internal grid model (bars), a medium deviation of 4.53% is determined. In other words:  $C_{grid\ trans}$  match.

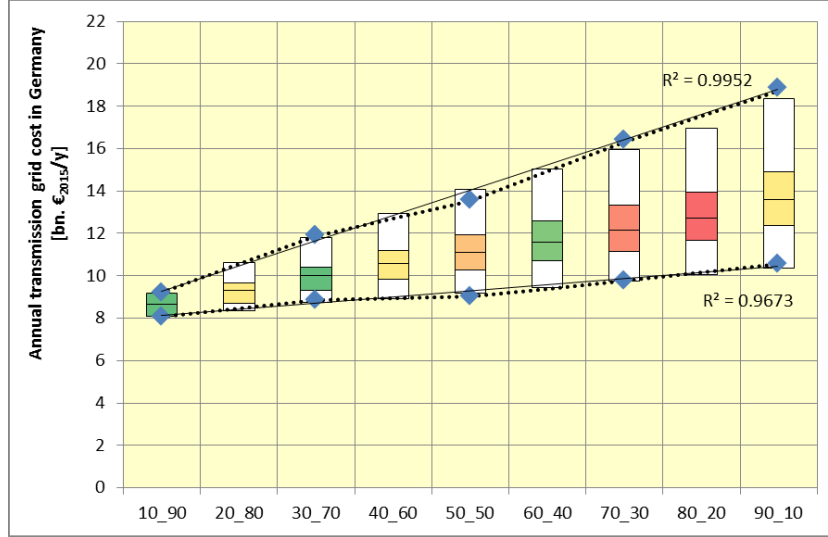


Figure 15: Grid cost of the 491 node model (blue dots from Table 11 and  $C_{basic\ grid\ cost}$ ) meeting cost bandwidths of the calibrated node-internal grid model (boxes). Green to red colours show the min to max cost deviation of the calibrated node-internal grid model to the 491 node model (boxes to dots). The x-axis shows the shares of fluctuating\_dispatchable energy share (related to gross electricity consumption).

As assumed in section 4.2.2.1,  $c_{grid\ trans}$  can also be calculated for other countries like for Germany. This statement is based on the calibrated results and cost reductions for Germany (see appendix Table 41). Detailed grid analyses should prove the cost ranges of the different national grids in future analyses when more technical calculation performance and more detailed data are available. Figure 16 shows exemplified detailed results of the 491 node model representing the German transmission grid. The used transmission line topology represents the installed link capacities in a case specific grid. These case specific grid configurations indicate the maximum cost of the grid. It is obvious that some transmission lines are missing (light blue – no capacity expansion) especially in Figure 16a and in Figure 16f.

With regard to Eq. (28) the power kilometres in Germany are calculated to quantify the dimension of the grid in addition to the cost. Power kilometres can show how much power is transmitted over what distance. In Figure 16 they triple to quadruple from the 10\_90 to 90\_10 scenario while the major impact arises from the HVDC North-South transmission lines. This effect is visible in Figure 16c and f regarding the red lines. Especially Wind offshore causes a high transmission expansion due to the high transmission capacity starting at the North Sea.

$$TWkm := \sum_{transmission\ line} TW \cdot km \quad (28)$$

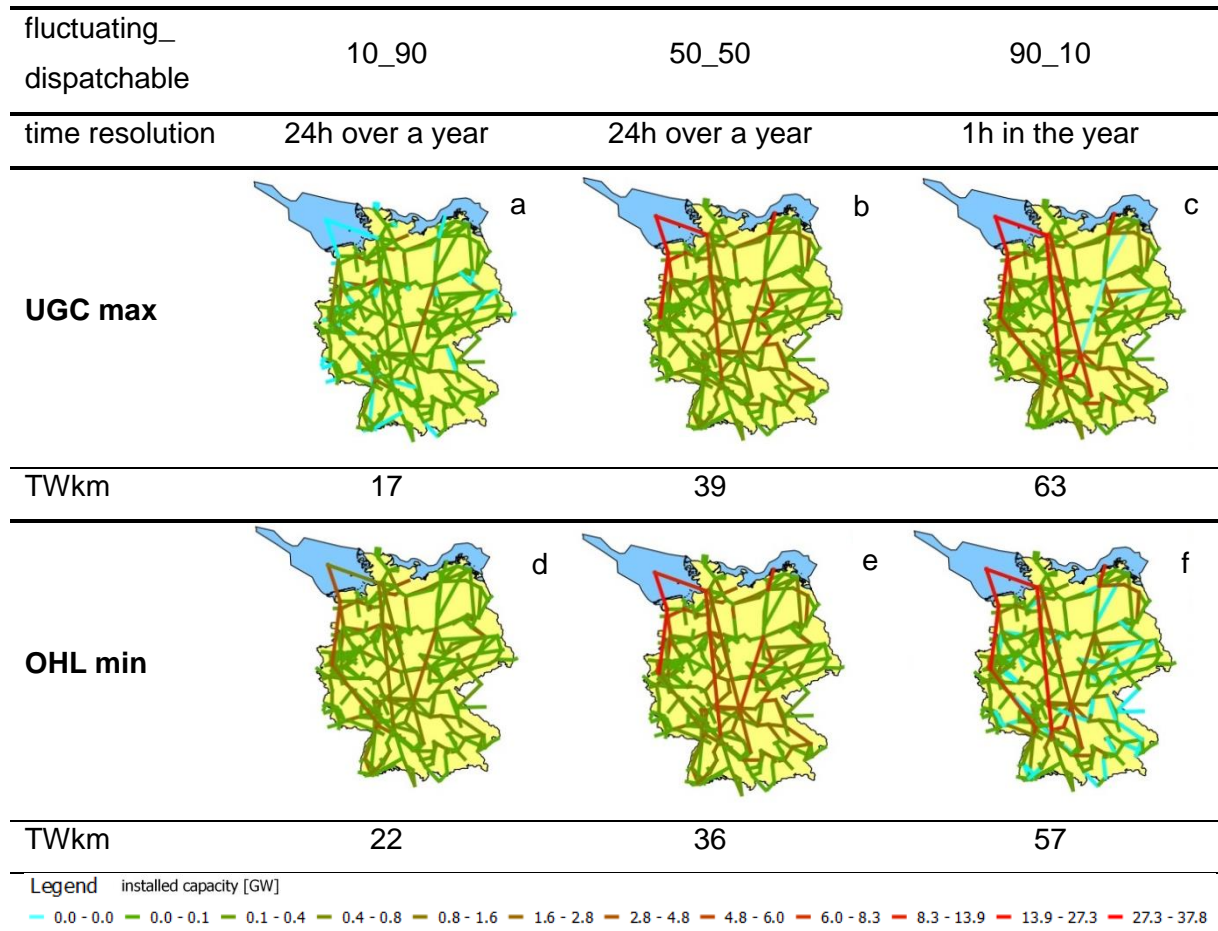


Figure 16: Transmission line capacities, power kilometres under different shares of fluctuating and dispatchable energies

For calculation of TWkm by grid cost values of the node-internal grid model, the following cost assumptions are used: 1.01 k€/MWkm for transmission grid (Bundesnetzagentur, 2015) and 5.21 k€/MWkm for distribution grid (Rehtanz, et al., 2012), (Büchner, et al., 2014).

#### 4.2.3.6 Case study results of the German energy system

This section discusses the used case study of Germany with the REMix calculations of the approaches without the grid (business as usual) and with the calibrated grid model. The research question of the case study is: How is the energy system influenced neglecting and including the transmission and distribution grid? The results in Figure 17 show the resulting bandwidths (uncertainties) as output data of grid cost, system cost, capacity and curtailment. The range of ‘fluctuating\_dispatchable’ in the figures of Figure 17 extends from a high dispatchable energy share (left) to a high fluctuating energy share (right) showing the smallest system cost bandwidth in green and its largest in red. In Figure 17 a-d (left column) the business as usual (BAU) case is shown neglecting the node-internal grid. In Figure 17 e-h (left column) the node-internal grid model (NIGM) is shown integrating transmission and distribution grid.

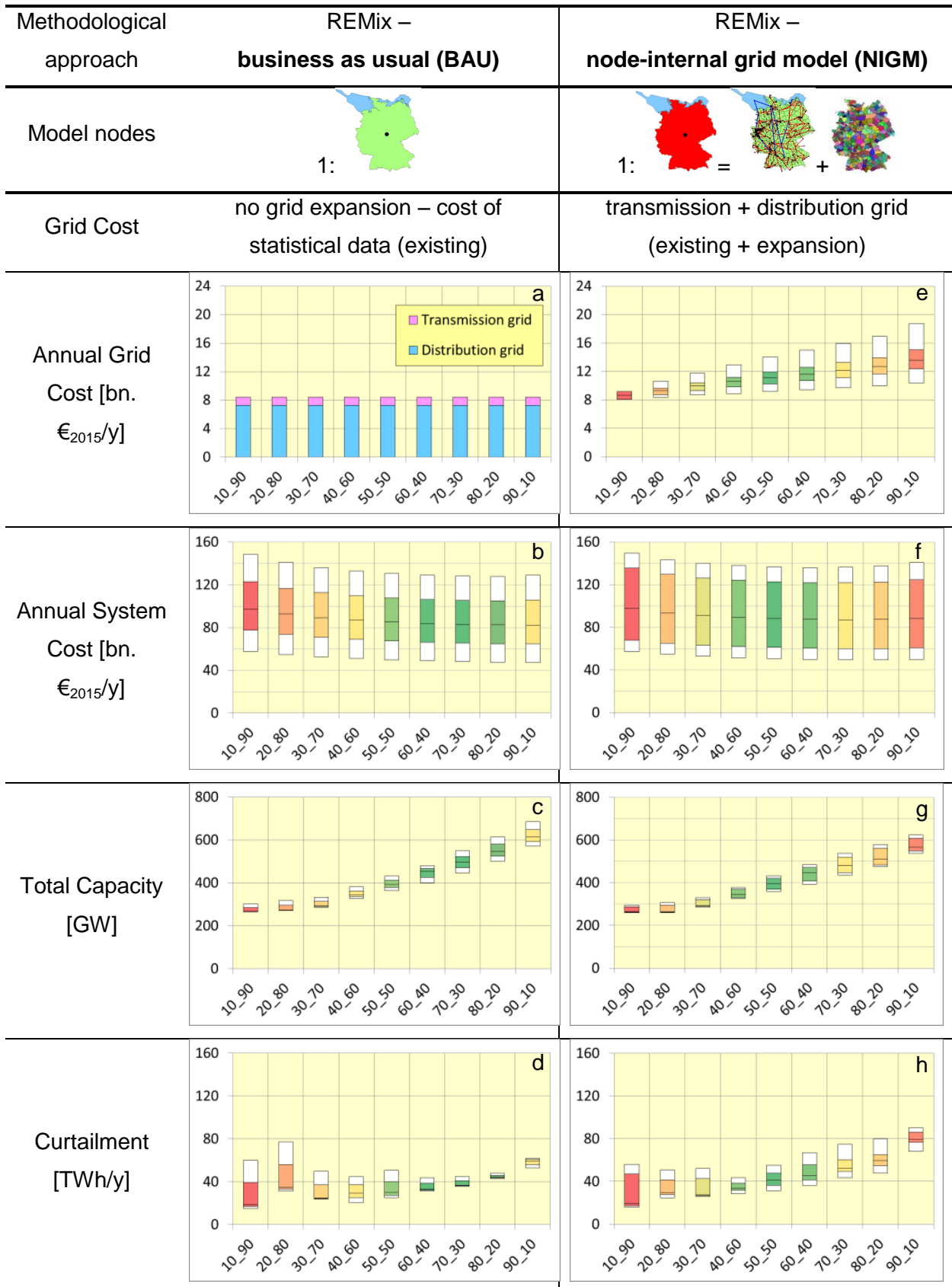


Figure 17: Bandwidths as results of cost assumption sensitivity analyses in the REMix model

**Grid cost:**

Annual grid cost consists of grid expansion cost  $C_{grid\ exp\ cost}$  and base grid cost  $C_{basic\ grid\ cost}$ . Figure 17a shows the BAU case with  $C_{basic\ grid\ cost}$  of 8.4 bn. €/y as a fix value in each scenario. Figure 17e shows the NIGM case with the same  $C_{basic\ grid\ cost}$  and additionally  $C_{grid\ exp\ cost}$  of 1-12 bn. €/y (up to 11.7% of system cost). Grid expansion cost has also an effect on the expanded capacity and thus the curtailment. Such cost can't be neglected in a robust energy system analysis that claims to consider a broad spectrum of technological characteristics.

Considering the grid cost ranges, it is obvious that uncertainty of grid cost rises with an increasing share of fluctuating renewable energy.

**System cost:**

Annual system cost includes cost of annual operation and maintenance (O&M), fuel cost and annuity capital expenditures. In Figure 17b and f the system cost and its uncertainty is shown. The BAU case has the minimal system cost uncertainty (green) in a higher fluctuating share (scenario 60\_40) while the absolute system cost minimum results from the highest fluctuating share (scenario 90\_10). This relation is shifted towards higher dispatchable share (scenario 50\_50) when calculating with the grid expansion cost (Figure 17f). System cost uncertainty referred to minimal median value in Figure 17f is -46% to +59%. *A well-balanced renewable energy mix of dispatchable and fluctuating can reduce system cost uncertainty up to 7% of maximum system cost bandwidth. This equates to less system cost deviation of 6 bn. €/y.* However, system cost minimum does not distinguish strongly and system cost bandwidths overlap in all scenarios consequently as a result of these system cost bandwidths. Thus, system cost doesn't play a major role in deciding between more fluctuating or more dispatchable energy shares from today's point of view. However, when calculating with determined and well known cost (no bandwidths), the right mixture of fluctuating and dispatchable share might save up to double-digit billions of € per year. The unknown future cost development of fluctuating and dispatchable energy will therefor show a cost-efficient energy mixture.

**Power plant and storage capacity:**

Total capacity includes all capacities of power plant, electrical storage charge and electrical storage discharge units. A higher share of fluctuating energy leads to higher installed capacity. In the highest fluctuating energy share, capacity expansion is up to 6 times of peak load (up to 700 GW). In the highest dispatchable energy share, capacity expansion is about 3 times of peak load (300 GW). Comparing the BAU case in Figure 17c and the NIGM case in Figure 17g it is evident that in the NIGM case less capacity is integrated towards high shares of fluctuating energy. These capacities are listed in detail in the appendix in Table 40.



The assumption for cheap fluctuating energies and electrical storage is that much capacity is installed to reduce their cost by a learning curve approach. However, the more capacity is installed, the more probable are material bottlenecks or the use of other (perhaps more costly or less efficient) materials. Therefore, the cost development of these technologies should be considered critically.

#### **Curtailment:**

Curtailment predominantly occurs depending on the following factors: the model endogenous optimized capacities, the variable O&M cost and the share of fluctuating and dispatchable energy. The approaches show the trend of increasing curtailment (up to 13% of annual demand) with increasing share of fluctuating energy. Comparing the BAU case in Figure 17d and the NIGM case in Figure 17h it can be seen that in the NIGM case towards high shares of fluctuating energy curtailment is higher than in the BAU case. Curtailment occurs also in a high share of dispatchable energy due to a high renewable energy share. This curtailment might be reduced if the model considers not only the optimal system cost perspective but an appropriate operation perspective.

#### **Full load hours:**

Considering the results of power plant capacity and curtailment, the average full load hours of the power plant park can be evaluated. A high curtailment leads to low full load hours of the power plant park. The highest differences of curtailment between BAU and NIGM occur in a high share of fluctuating energy. In the BAU case power plant capacity is relatively high and curtailment low. So, full load hours are relatively high. In the NIGM case power plant capacity is lower and curtailment higher. So, full load hours are lower. Including the grid leads to lower full load hours of power plants. While curtailment is only considered for fluctuating renewable energies like Wind turbines and photovoltaic, the consideration of the grid reduces their full load hours compared to a model which does not include the grid.

#### **4.2.4 Conclusion and suggestion for improvements**

The new node-internal grid model facilitates the consideration of the transmission and distribution grid with two parameters. The grid expansion cost depends on fluctuating feed-in capacity and the starting point. Here a validation approach is applied. However, the node-internal grid model is validated in a 100% renewable energy mix with fluctuating and dispatchable energy shares. While renewable dispatchable energies might have different cost characteristics from coal, gas or nuclear power plants, the grid model assumptions could also be different in low renewable energy share scenarios – but probably quite similar due to fundamental grid expansion with a rising share of fluctuating energy. New calibration approaches with higher spatio-temporal resolution can still improve the precision of the node-internal grid model.

The major achievement of the model is that it can represent the grid in cost and power system interdependencies such as the use of fluctuating and dispatchable power plants. Grid relevant integration cost of fluctuating renewable energies is thus better represented. Furthermore, curtailment behaviour can be modelled. However, the grid model cannot calculate each transmission line, its bottleneck and transmission loss due to the unknown direction of power flows of each transmission line. Thus, the model might still overestimate the ability of the electrical grid.

## 5 Assessing the value of CSP-HVDC applying REMix

In this chapter a broad range of scenario analyses is exhibited with the REMix model considering the barriers of the model and tangible technological alternatives of CSP-HVDC critically. A scenario points out how a future may be from today's point of view. Therefore several cost assumptions are used in sensitivity analyses to include future uncertainty of the year 2050. Multi-criteria analyses are represented by the use of different evaluation criteria which show scenarios from various perspectives. This leads to a quantification of the system influence of local CSP in MENA and southern EU and CSP-HVDC power plants in MENA for the use in EU. In the first section of this chapter the analyses are described and the results are shown. In the second section a discussion of the results is carried out assessing the value of CSP-HVDC according to cost, infrastructure, operational behaviour and emission of the energy system.

### 5.1 REMix scenario analysis

This section reveals five different systematic steps to show the reader the most important interactions of the input data and the modelling framework in different foci (Figure 18).

The foci of the approaches are:

1. The influence of cost assumption and the resulting energy system evaluation criteria.
2. The use of an overly grid, its exclusion and the consequences for the energy system.
3. The empirical probability of an integration of low carbon dispatchable technologies.
4. The role and comparability of such technologies.
5. The value of CSP-HVDC including and excluding this option.

The stepwise approaches are built upon each another. This structure is essential to find a suitable modelling framework assessing the value of CSP-HVDC.

⇒ ***The consequence of each modelling step for the following steps is shown.***

Following sections describe the five approaches:

- 5.1.1 – In this section a cost sensitivity analysis shows the influence of cost and the results in energy system evaluation criteria such as CO<sub>2</sub> emission. This approach indicates the bandwidth of possible modelling results without any exogenous limit. An exogenous limit of CO<sub>2</sub> emission is therefore implemented.
- 5.1.2 – Avoiding CO<sub>2</sub> using high shares of renewable energies leads to a demand of flexibility in spatial and temporal shift. This flexibility is represented by the grid and storages. Here the reader gets an impression which influence the use of an overlay grid has on system cost and other evaluation criteria.
- 5.1.3 – As intermediate result of the previous steps it is visible that the cost relation of technologies plays the major role for the integration of a specific technology. This section analyses therefore the empirical probability of the integration of CSP-HVDC and other technologies.
- 5.1.4 – Competitive technologies of CSP may be nuclear power plants and CCS technologies due to their dispatchability and low carbon emission. The comparison between these technologies and their system influence is analysed. This shows the value of these technologies with respect to the applied evaluation criteria.
- 5.1.5 – Considering all previous analysis steps for a suitable modelling framework, this section reveals the value of CSP-HVDC. A systematic reduction of the share of CSP-HVDC capacity is performed. For this purpose a “partial greenfield” is used in a modelling environment with exogenous limited overly grid and carbon emission limit.

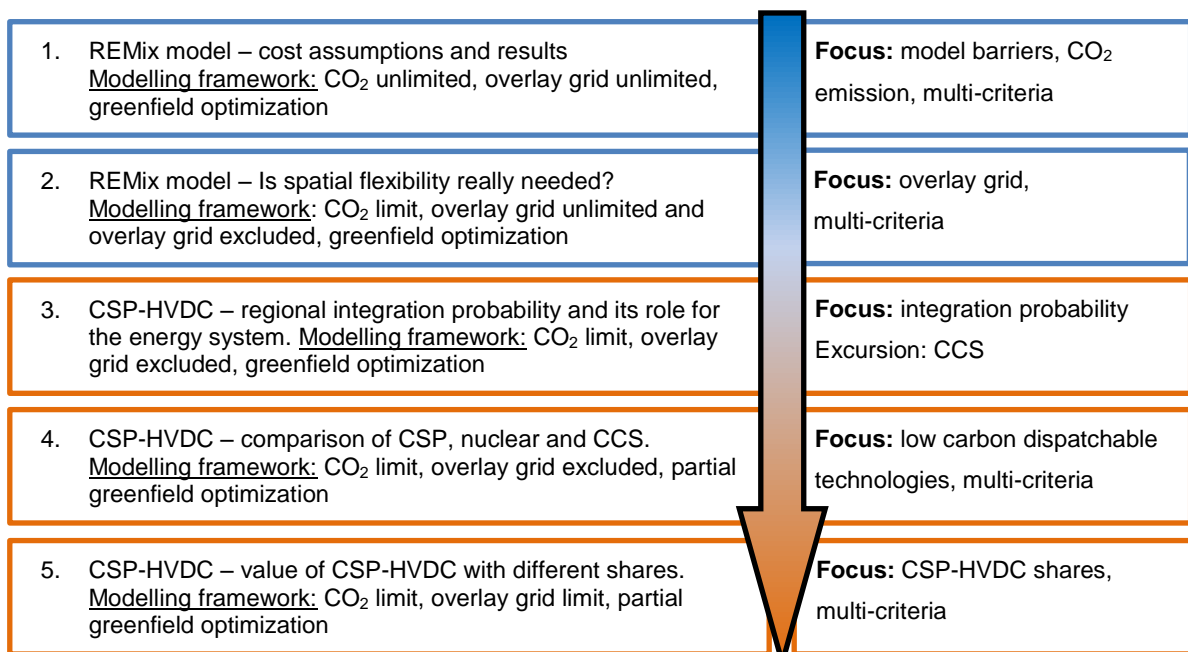


Figure 18: Workflow of REMix scenario analysis

Research questions assessing the model results and CSP-HVDC are analysed in this section. These research questions surround the main objective evaluating CSP-HVDC.

*REMix model – fundamental questions of a sustainable energy scenario (blue boxes in Figure 18):*

- Can CO<sub>2</sub> emission be cost efficiently avoided or completely eliminated?
- What are the consequences of using a cost optimizer for modelling energy systems?
- What impacts can be expected from an overlay grid?

*CSP-HVDC – questions concerning the value of this technology (orange boxes in Figure 18):*

- Which differences occur using an overlay grid or CSP-HVDC?
- How probable is an integration of CSP, CSP-HVDC, nuclear energy and CCS?
- Can nuclear energy and CCS be competitive technologies to CSP and CSP-HVDC?
- What is the value of CSP-HVDC comparing scenarios with different CSP-HVDC shares?

These research questions are systematically assessed in accordance with the workflow described in Figure 18.

The used overlay grid and CSP-HVDC scheme is illustrated in Figure 19. In Step 1 an unlimited overlay grid is used (Figure 19a), in Step 2 the unlimited overlay grid with its exclusion is compared (Figure 19a and b), in Step 3 and in Step 4 the examination approach uses isolated model regions (Figure 19b) and Step 5 is based on a limited overlay grid. Here the system influence of a reduction of CSP-HVDC is analysed (Figure 19c and d).

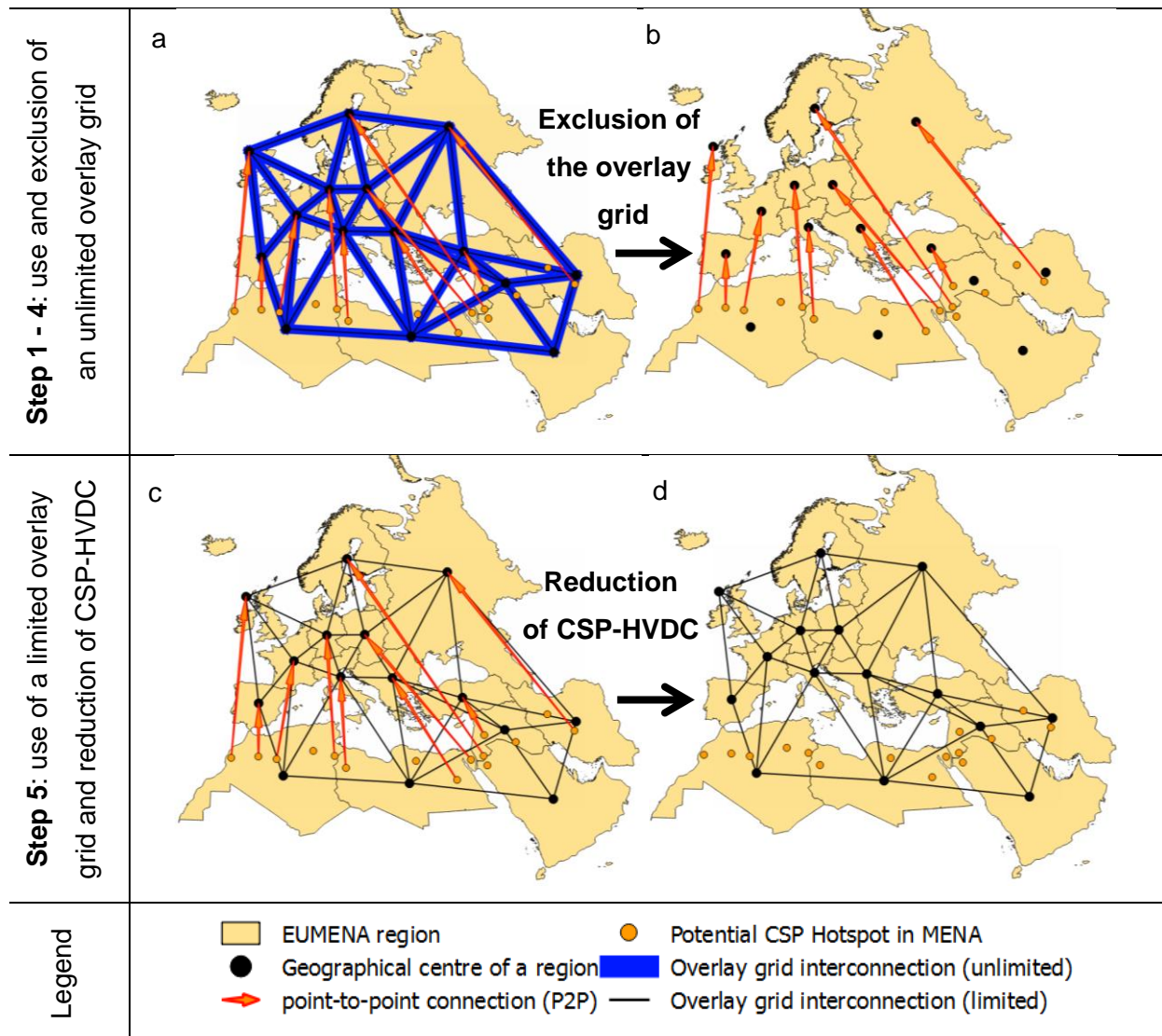


Figure 19: Used overlay grid and CSP-HVDC scheme in the stepwise analysis. The CSP power plants and P2P connections from MENA to EU are defined as CSP-HVDC.

### 5.1.1 Step 1: REMix model – cost assumptions and results

REMix uses a cost minimization as objective function for energy system optimization. Due to small cost difference among technologies, some technologies can be excluded automatically by the optimization model due to a small cost difference. This so-called “penny flip” effect is a major barrier in optimizing energy systems because it leads to unrealistic results. To solve this barrier a comprehensive cost sensitivity analysis is applied. Cost sensitivities are defined in this section according to Table 13. The used cost assumptions show different cost relations of technologies among each other and lead to different power plant park portfolios. The results in Figure 20 demonstrate the resulting power plant park capacity its annual energy balance and the bandwidth of cost and other energy systemic criteria as a measure

of uncertainty. CO<sub>2</sub> emission is not limited in this step showing which different results can be achieved considering only a system cost minimum.

Table 13: Definition of cost sensitivity

<b>Cost sensitivity</b>	<b>Description</b>
“max”	combination of all maximum cost input data
“mean”	combination of all mean cost input data
“min”	combination of all minimum cost input data

Evaluation criteria are chosen in Table 14 to clarify other relevant energy systemic criteria beside cost that have an impact of the energy system regarding infrastructure, operational behaviour, cost and emission. These evaluation criteria build the basis of this chapter to assess scenarios. To compare the criteria among regions, the data are specific per annual electricity net demand

Table 14: Analysed evaluation criteria

<b>Evaluation criteria</b>	<b>Unit</b>	<b>Description</b>
Power Plant Capacity	[GW/TWh]	All power plants plus the electrical discharge capacity of P2G2P and hydro reservoir
Electrical Storage Capacity	[GW/TWh]	Electrical storage charge capacities
Curtailement	[TWh/TWh]	Electrical curtailment of photovoltaic, wind turbines, hydro run off river and hydro reservoir
Power Kilometre	[TWkm/TWh]*	Capacity of a power line multiplied with its length. Power km of grid, node internal transmission and distribution grid and point-to-point infrastructure – the power km of the grid connections between model regions are divided equally between these regions.
System Cost	[€/kWh]	Capital cost, fix and variable O&M cost, fuel cost and emission cost
Carbon Emission	[g/kWh]	Carbon emission of coal, lignite and natural gas during fuel conversion into electricity

\*Capacity of power kilometre (TWkm) and annual electricity demand (TWh) can't be reduced in a fraction due to their different characteristic!

In addition to the three cost sensitivities of Table 13 two different transmission infrastructures (overhead line and underground cable) are used. This leads to a modelling of overall six

scenarios. The examination year is 2050 and the examination is EUMENA with unlimited interconnected sub-regions (overlay grid of Figure 19a). The optimization is made under a “greenfield approach”. The scenarios reveal which energy system is preferred. The results delineate in Figure 20 the power plant park capacity (a, d, g) its annual energy balance (b, e, h) and in radar chart (c, f, i) energy system evaluation criteria according to Table 14.

In the case of all “max” cost assumption only high carbon emitting energies (predominantly lignite steam turbines) are used, whereas in the case of all “min” cost assumption a high share of low carbon emitting energies (renewable energies) is preferred. A low CO<sub>2</sub> emission scenario (~16 g CO<sub>2</sub>/kWh<sub>demand</sub>) can therefore be reached automatically when cost assumptions of renewable energies are minimal. This carbon emission is in the range trying to reach the 2°C goal (Rogelj, et al., 2015). The preferred use of lignite and coal power plants in the “max” cost assumption scenario results in low power km expansion, low curtailment, low storage need and low power plant capacity. The integration of high shares of PV, CSP and wind turbines with “min” cost assumptions leads to high power km expansion, high curtailment, high electrical storage need and high power plant capacity. The “mean” cost assumption scenario causes a more equilibrated energy system however still with too high carbon emission (>100 g CO<sub>2</sub>/kWh<sub>demand</sub>).

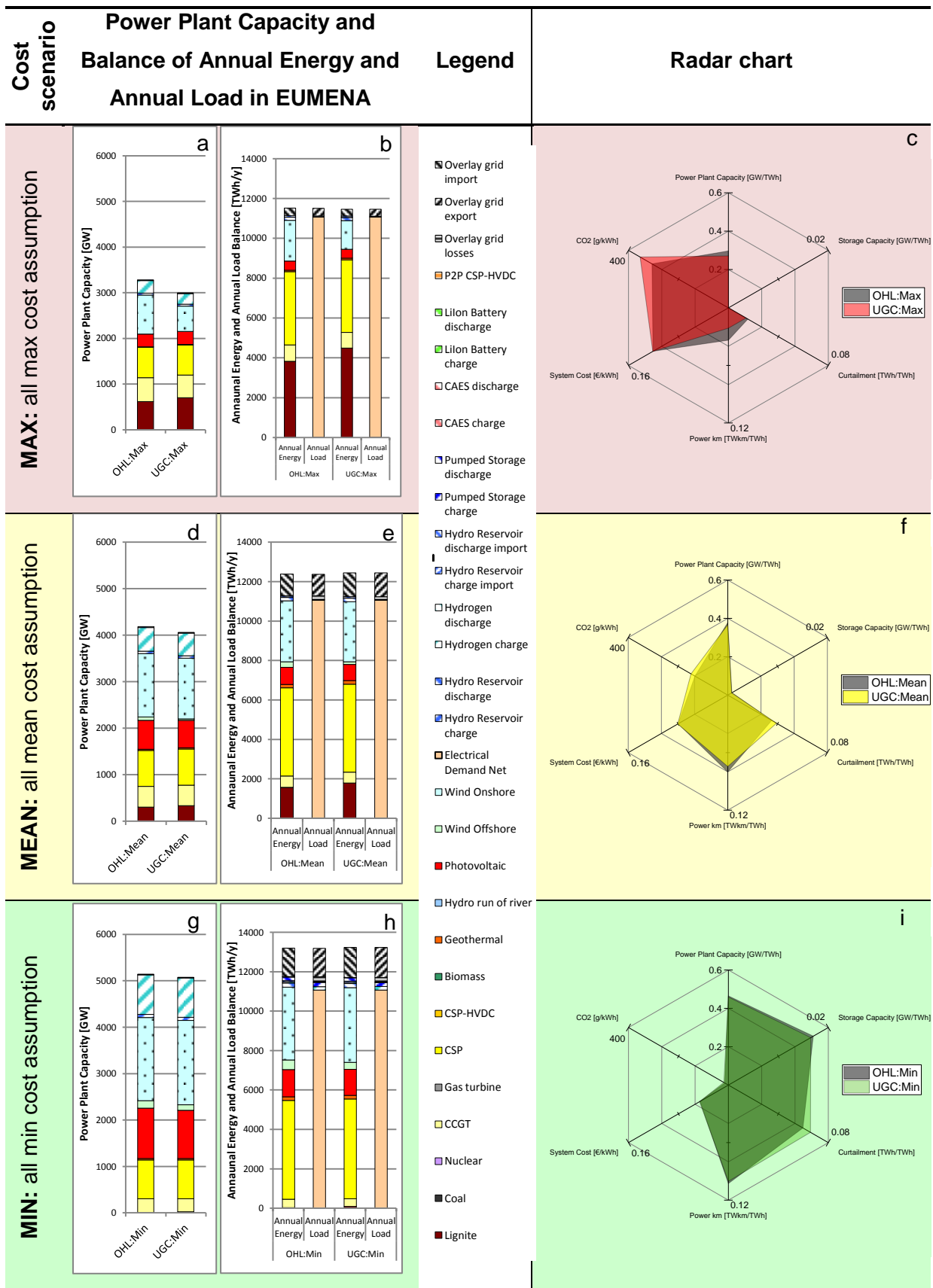
The influence of choosing overhead line or underground cable is almost insignificant. Compared to overhead lines the use of underground cable increases curtailment and carbon emission and decreases power kilometre and power plant capacity only in a small scale however.

⇒ ***Thus, only overhead lines are used as exemplary reference technology for electricity transmission.***

The resulting energy systems may have a high impact either on carbon emissions, power plant capacity, storage, curtailment or power kilometre expansion. This effect is called Pareto optimality which leads to an aggravation of a value when another value improves. Minimizing all values may lead to a more sustainable energy system. The results show that using the optimization model regarding cost exclusively, will not necessarily lead to a sustainable energy system.

Minimizing the evaluation criteria leads to a small area of the radar chart optically. To minimize the evaluation criteria of Table 14, the model needs to be restricted wisely. Such model restrictions lead subsequently to a simplified multi-criteria analysis. Further research minimizing the evaluation criteria - in an acceptable boundary framework - with an optimizer can show a more objectively optimized energy system if needed.





Reducing carbon emission to 0 g CO<sub>2</sub>/kWh<sub>demand</sub> is also possible but increases all other evaluation criteria. This is confirmed in Figure 21a that diagrams the energy system in EUMENA with a limit of 16 g CO<sub>2</sub>/kWh<sub>demand</sub> and in Figure 21b that illustrates the energy system limited to 0 g CO<sub>2</sub>/kWh<sub>demand</sub>. Avoiding completely CO<sub>2</sub> emission may therefore not be the ultimate goal.

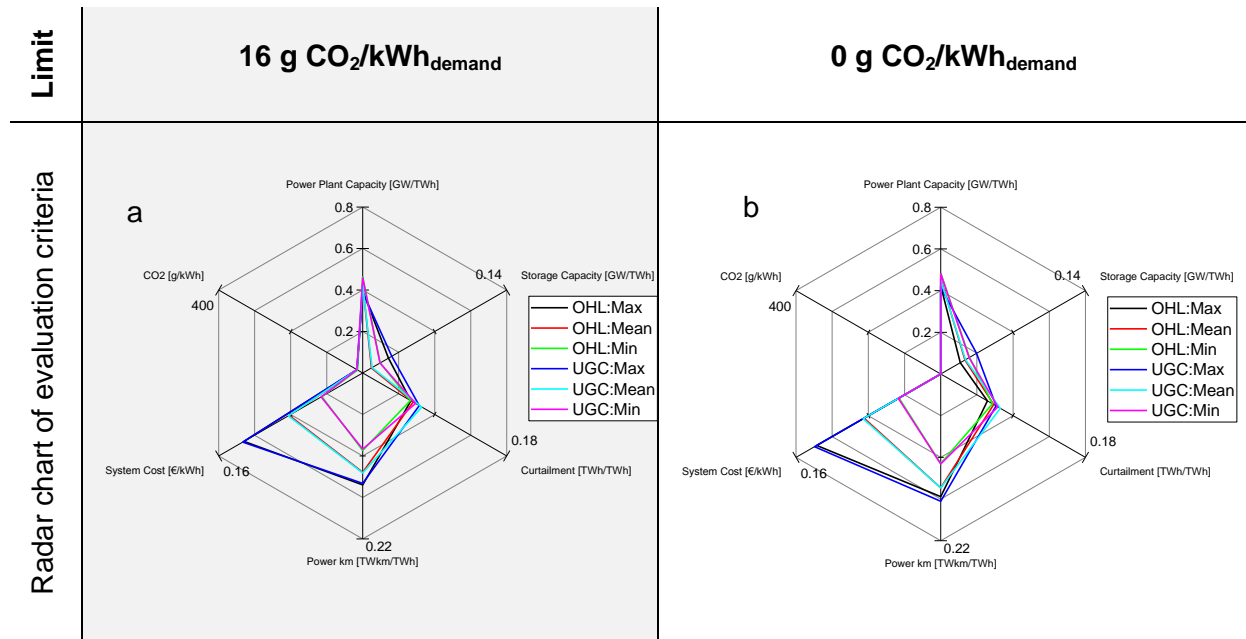


Figure 21: Different CO<sub>2</sub> emission limits of 16g/kWh<sub>demand</sub> and 0g/kWh<sub>demand</sub>

⇒ ***Thus a CO<sub>2</sub> emission limit is set to ~16 g/kWh<sub>demand</sub> for the entire examination area. This normative approach is helpful to exclude all other high carbon emitting scenarios trying to reach the 2°C target.***

The next scenario analysis step considers the power kilometre and storage capacity expansion because the use of renewable energies requires spatial and temporal flexibility options.

The evaluation criteria - used in Table 14 - can evaluate the energy system and also reflect the impact of a technology on the system. Thus, the research question of the value of CSP-HVDC can also be answered with the interdependencies of these evaluation criteria, exerting or excluding this technology. Impacts regarding infrastructure, operational behaviour, cost and emission can be analysed. This is shown in the last step of the systematic approach in section 5.1.5, learning at first about the optimization model itself and the resulting evaluation criteria.

#### 5.1.1.1 Statement of the section

In this section cost sensitivities are analysed using evaluation criteria of an energy system. Cost input data cause different CO<sub>2</sub> emission. The used minimum cost assumption “min” results in minimum CO<sub>2</sub> emission too. It can therefore be concluded that CO<sub>2</sub> emission can be avoided cost efficiently due to low cost of renewable energies. However, an optimization based on cost exclusively may not lead to a holistic optimal or sustainable energy system. A multi-criteria analysis should therefore be conducted in order to evaluate energy scenarios.

#### 5.1.2 Step 2: REMix model – Is spatial flexibility really needed?

An important consideration of flexibility in energy systems is the application of grid and storage capacity. A mixture of both flexibility options may be suitable for an energy system to use their advantages dealing with a higher share of renewable energy. Such advantages can be a possible cost advantage of the grid, possible higher acceptance of storage, less curtailment and less power plant capacities using both flexibility options. An exclusion of one flexibility option would lead to a probable higher effort for a low carbon energy system.

In this analysis the focus is on the overlay grid as spatial flexibility in the EUMENA region. Therefore two scenarios are applied. The scenario “Grid OHL” is based on the unlimited expansion of an overlay grid that connects regions in EUMENA. Such a scenario implies a strong collaboration inside EUMENA. The other scenario “Single OHL” excludes this overlay grid but still uses grid expansion inside the regions (nodal grid expansion). This scenario shows an uncooperative EUMENA in that the regions are independent. Both scenarios apply a “greenfield approach” with an integration option of all technological options of the thesis including CSP-HVDC, nuclear power plants and CCS, with the same carbon emission limit of 16 g/kWh<sub>demand</sub>, cost input parameters “mean” and an overhead line (OHL) transmission infrastructure. The scenarios help to detect the influence of an overlay grid under a least-cost optimization and an evaluation of multi-criteria (of Table 14) for an energy system.

Figure 22 shows the results with the integration of the overlay grid (Figure 22a) as well as its exclusion (Figure 22b). Figure 22a illustrates with the blue lines an expansion of transmission lines of the overlay grid. Up to 85GW from model node **NW** to model node **W** can occur. Transmission lines are expanded more in north-south direction than in east-west direction. Interconnections between **NAW**, **NAE** and **ME** are assessed as insignificant by the model. Both figures also show the grid expansion inside the model regions. This so-called node-internal grid expansion of the transmission and distribution grid in Figure 22a shows a high expansion in some regions and in Figure 22a an almost equally distributed expansion in every model region.

The power kilometre subdivision in Figure 22a shows that CSP-HVDC is not integrated using an overlay grid. The exclusion of the overlay grid leads to the integration of CSP-HVDC. Thus, for the scenario “Grid OHL” it can be questioned if CSP is built in MENA and then transmitted using the overlay grid? This question is examined in the following section 5.1.2.1.

Having a look on the evaluation criteria in Figure 23, it is remarkable that the two scenarios do not distinguish much in system cost but in almost every other criterion. The use of the overlay grid is about 7% more cost-efficient. Compared to the scenario “Single OHL” the scenario “Grid OHL” reduces power plant capacity to about 13%, storage capacity to about 272% and curtailment to about 34%. However, it causes a significant increase of power kilometre with about 176%.

Thus, *small cost changes can lead to a recognizable change in all other parameters of an energy system.* A least-cost approach can therefore be helpful comparing scenarios with other evaluation criteria on the same least-cost level. As shown in this analysis, alternatives are essential for a comparison of scenarios. Otherwise a least-cost approach can also lead to misinterpretations if comparable alternatives and sensitivities are missing!

The option of the overlay grid is chosen in the scenario because it is more cost-efficient to balance energy over a spatial area than building electrical storages or curtail power plants. However, the need of such a large capacity expansion of power lines is arguable due to social, political and organisational barriers.

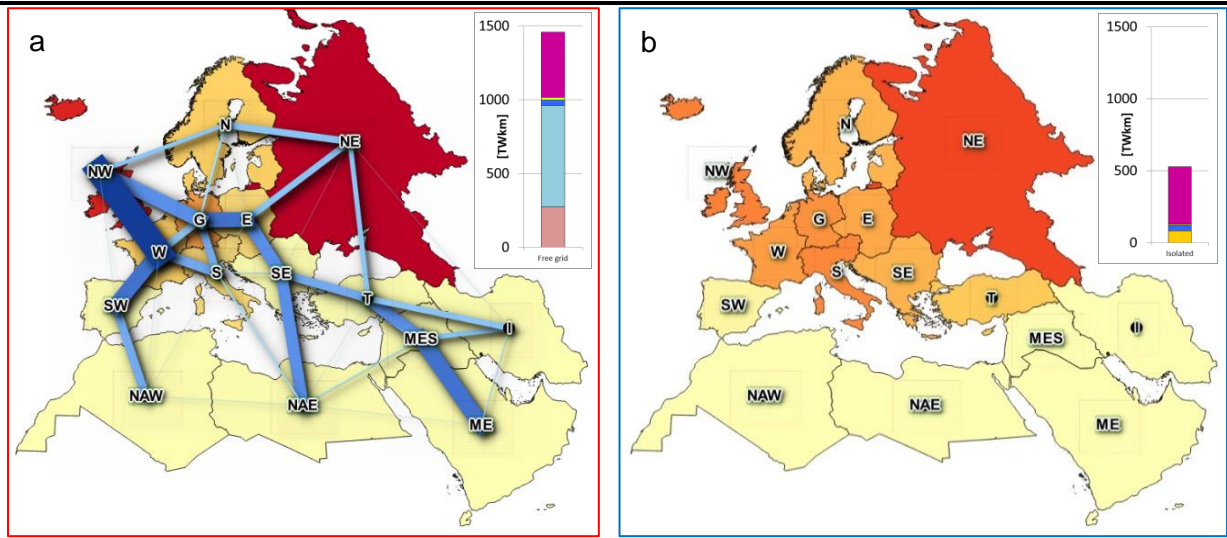
As mentioned before, an unequal spatial distribution effect of nodal grid expansion arises including the overlay grid. This effect also appears with power plant capacities. The model places the capacities in those regions where it is the most cost-efficient, thus some regions have a giant capacity of only few technologies while in other regions some of today’s already installed technologies (e.g. PV) are totally missing. The consequence is a strong interdependency of model regions. This result is achieved due to the optimization of minimizing cost and using an overlay grid in a so-called “greenfield approach”. Figure 24 illustrates detailed regional distribution of such parameters.

Free grid interconnections (Grid OHL):

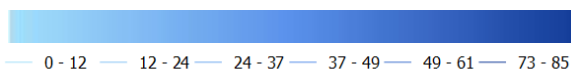
sum 1457 TWkm

Isolated model regions (Single OHL):

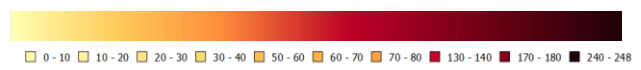
sum 528 TWkm



Overlay grid capacity expansion [GW]



Regional grid and point-to-point transmission line expansion (related to the destination region) [TWkm]



■ Transmission Grid ■ Distribution Grid ■ Hydro Reservoir Import ■ CSP-HVDC ■ HVDC 600kV OHL ■ AC 380kV OHL

Figure 22: Comparison of grid expansion in GW of overlay grid transmission lines and TWkm. A scenario with unlimited overlay grid interconnections (a) is compared to a scenario with isolated model regions with the exclusion of the overlay grid (b). The regional grid expansion possibility of transmission and distribution grid (nodal grid) and CSP-HVDC integration option is included in both scenarios.

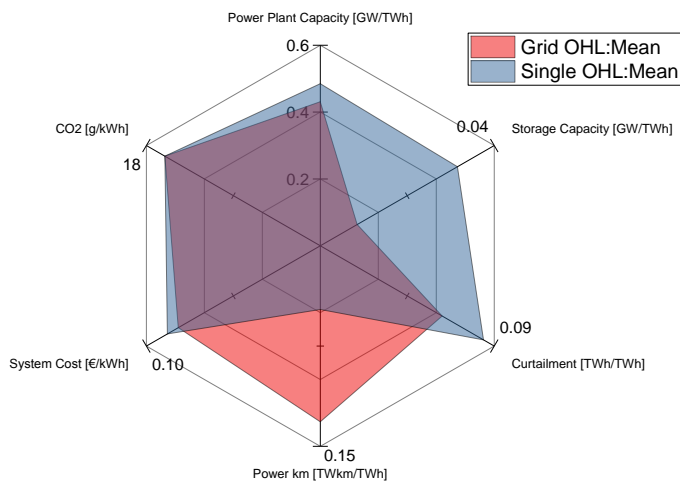
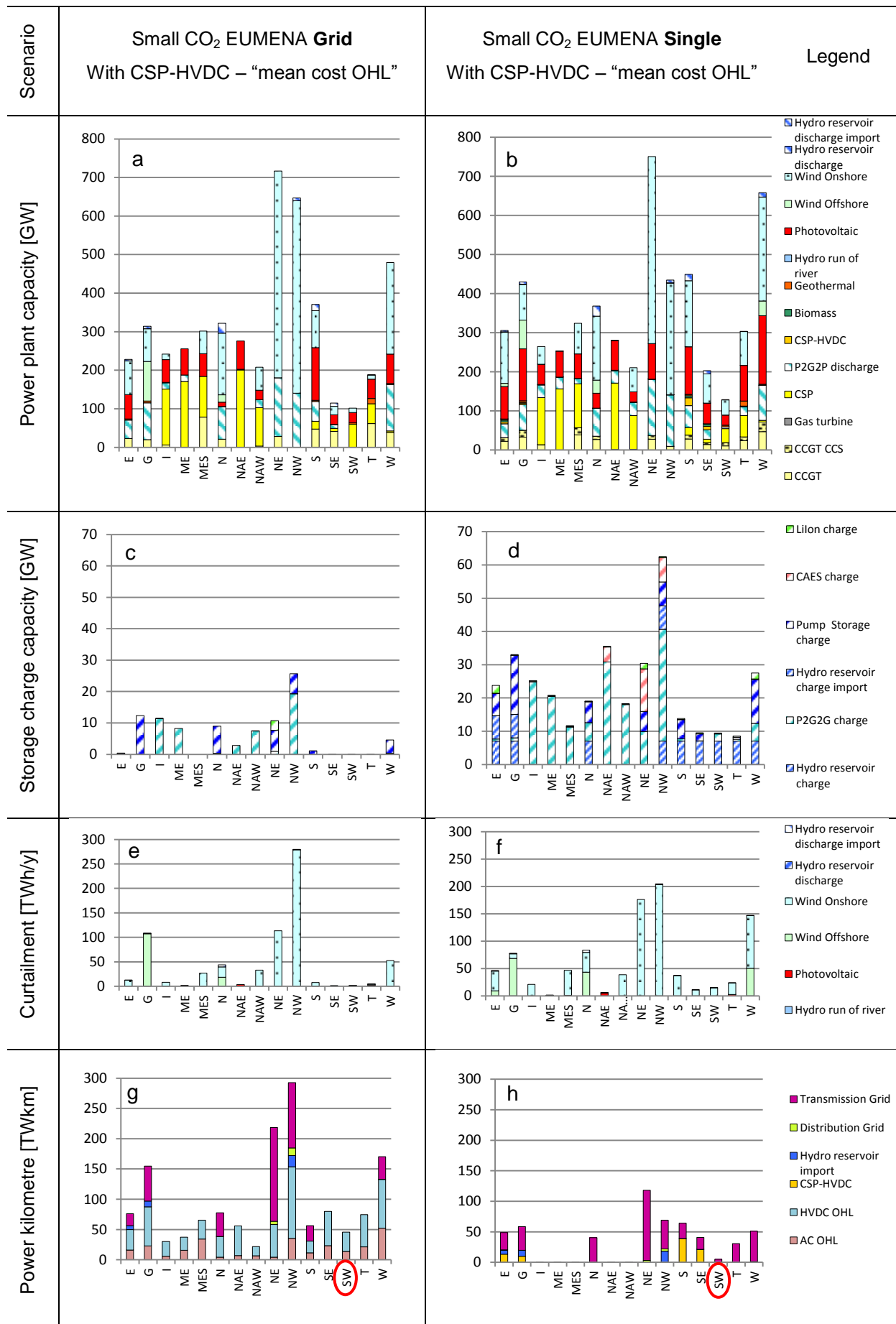


Figure 23: Grid vs. Single. An unlimited grid expansion is a cost-efficient way but causes the need of many power km over EUMENA. Compared to the scenario without overly grid there is only a cost reduction of about 7% but a power km increase of about 176%. Due to spatial flexibility using an overlay grid the energy system needs less power plant capacities, storages and causes less curtailment.

Figure 24 shows the regional shift of technologies and related values considering a scenario with an overlay grid with unlimited capacity expansion possibility (left column in Figure 24) and a scenario of isolated model regions (right column in Figure 24) both with 16 g CO<sub>2</sub>/kWh<sub>demand</sub>. It appears that the “**Grid OHL**” scenario has less regional diversified technologies. Thus, a concentration of regional capacities of power plant (a,b), storages (c,d), curtailment (e,f), power km (g,h), cost (i,j) and CO<sub>2</sub> emission (k,l) can be seen. Figure 24a shows for example that there is much wind capacity e.g. in **NE** or **NW**. However, no more photovoltaic capacity in **G**, no wind offshore capacity in **W** or no biomass power plants in EUMENA. Also CCS capacity is not built in the “Grid OHL” scenario. In the scenario “**Single OHL**”, there is a more regional and more diversified energy portfolio (Figure 24b). An integration of CSP-HVDC is only achieved in the single scenario in the regions **E**, **G**, **SE** and **SE**. However, in the “**Grid OHL**” scenario more CSP capacity is installed in MENA regions than in the “**Single OHL**” scenario without overlay grid. This additional CSP capacity is probably used for export to EU (see analysis in section 5.1.2.1). Figure 24c shows that the electrical storage charge capacity consists of pump storage, P2G2P and in small amount of lithium ion batteries. Figure 24d uses also these technologies but include additionally hydro reservoir and CAES. Thus, more storage technologies are needed in this scenario. Figure 24e reveals that the curtailment of wind onshore is predominant in **NW**. Figure 24f illustrates a more regional distributed curtailment but in sum a higher curtailment. The power kilometre in Figure 24g and h are divided in three sections: overlay grid (HVDC OHL and AC OHL), point-to-point lines (CSP-HVDC and Hydro reservoir import) and nodal grid (internal transmission grid and distribution grid). Figure 24g demonstrates high power kilometre with the use of the overlay grid. Here it is recognizable that no CSP-HVDC is integrated. Figure 24h shows lower power kilometre and an integration of CSP-HVDC. Figure 24i and j illustrate the annual cost (sum of capital, fix and variable O&M, fuel and emission cost) per region and technology. The majority of the cost built the capacities of the power plant park while storage and grid have a lower contribution to the total cost. Figure 24i illustrates that some regions e.g. **NW** and **W** have relative high cost while other regions e.g. **E** and **SE** have lower cost. Compared to Figure 24j these regions reduce or increase their cost drastically while total system cost of the EUMENA region does only change of about 7%. Some regions of the MENA region (**I**, **ME**, **NAE** and **NAW**) and the regions **N** and **SW** do not change their cost much under the influence of the overly grid. Thus, cost savings due to the use of an overlay grid is rather insignificant for these regions. *Especially the region **SW** would not profit much of such cost savings but would have much power kilometre in its area to transmit energy from NA to northern EU regions.* Figure 24k illustrates that CO<sub>2</sub> emission only occurs by the use of CCGT and that the regions **ME**, **NW** and **SW** can reduce their CO<sub>2</sub> emission to 0. In Figure 24l it is visible that also CCS and CSP co-firing lead to CO<sub>2</sub> emission.



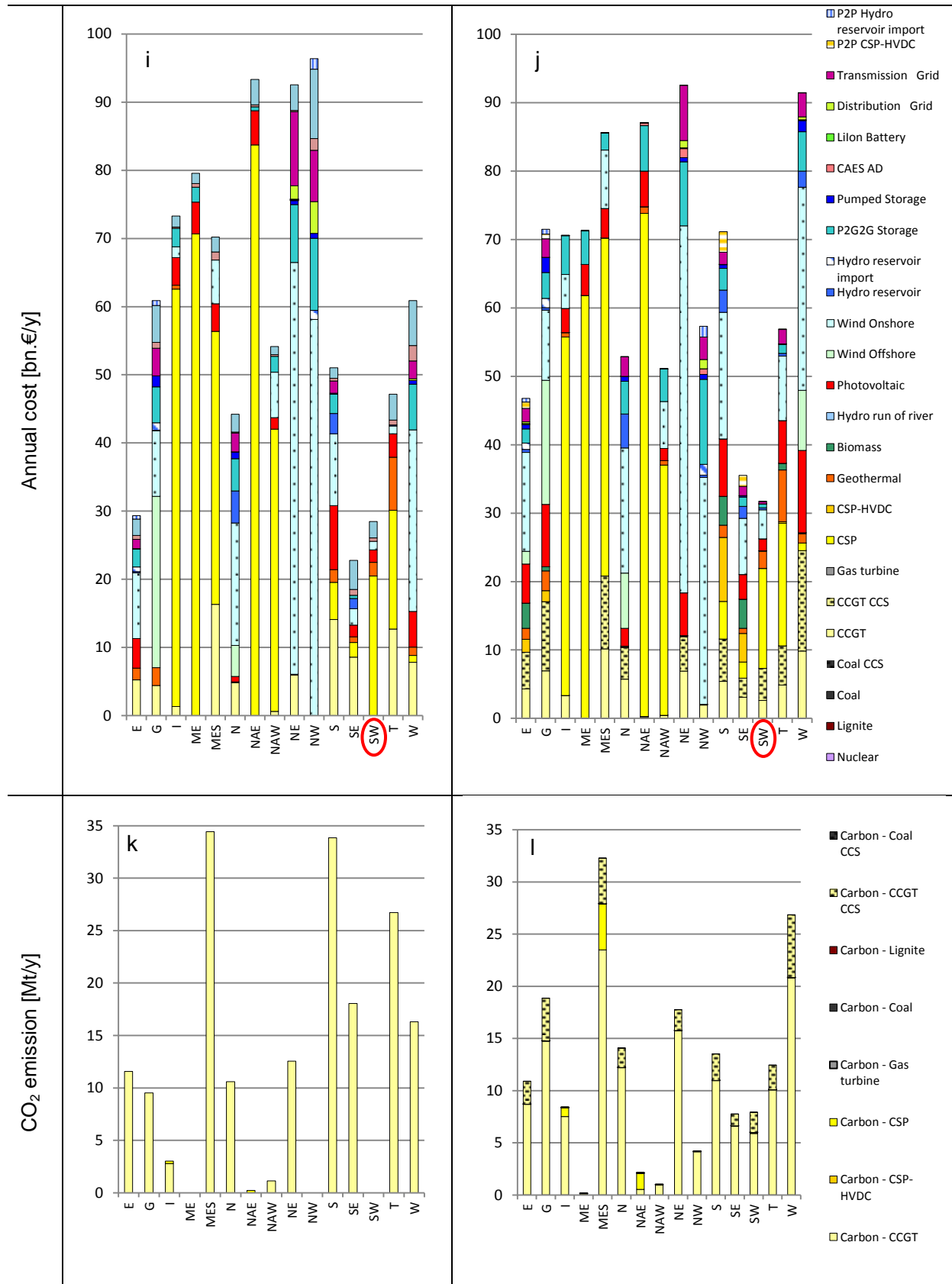


Figure 24: Distribution of evaluation criteria in scenarios with unlimited overlay grid optimization and with isolated model regions (no overlay grid).



### 5.1.2.1 Energy transmission according to power plant technology using an overlay grid

As seen in the previous section, the CSP-HVDC power plants are not expanded using an overlay grid model environment. The reason therefore is a more cost-efficient use of the overlay grid. The overlay grid allows an energy transmission of all technologies compared to the CSP-HVDC infrastructure which can just transmit energy from CSP.

The interesting question is which technology provides its energy for transmission? Therefore a correlation analysis is done comparing power generation of different renewable energy technologies and the transmission line usage between selected model regions. This correlation analysis investigates the probability of the hourly energy production of a power technology and the hourly use of a selected transmission line of the overlay grid. Positive values near to 100% mean a high correlation (export), negative values indicate an anti-correlation (import).

Table 15 shows the results of the correlation analysis. The time series of CSP generated electricity in model region **NAW** and the transmission from **NAW** to western EU offer a high correlation of an export form this technology to the model regions **SW**, **W** and **NW**. The correlation of Wind Onshore electricity in model region **NW** and the transmission from **NW** to western EU and North Africa feature a high correlation of an export from this technology to the model regions **W**, **SW** and **NAW**. Other correlations do not show a comparable extent. The results show that CSP is highly suitable for an export from North Africa to Western Europe using an overlay grid.

Table 15: Exemplary correlation of hourly time series from generation out of CSP, PV, Wind Onshore and Wind Offshore in NW and NAW with hourly time series of transmitted electricity

Electricity generation in	Transmission line / export from - to	Transmission				
		CSP	PV	Wind Onshore	Wind Offshore	Sum PV and Wind
NW	NW-W	-	-43%	90%	28%	90%
NW	W-SW	-	-37%	54%	27%	54%
NW	SW-NAW	-	-26%	37%	11%	37%
NAW	NAW-SW	76%	12%	-1%	1%	9%
NAW	SW-W	72%	22%	-10%	-9%	9%
NAW	W-NW	49%	22%	-14%	-6%	5%

Green colours reveal a high correlation, red colours show an anti-correlation. Yellow colours indicate no correlation.

### 5.1.2.2 Statement of the section

It can be concluded that the expansion of the grid leads to a reduction of cost, curtailment and a reduction of capacity of power plants and storage. However, a high capacity expansion of an overlay grid among regions in EU and MENA may have high difficulties to be realised due to acceptance barriers but also of unsolved financial and operational questions. Some regions profit from the overlay grid with a reduction of cost and other evaluation criteria whereas other regions don't profit much and need a relative high transmission infrastructure on their territory to transfer energy to other regions. A limited grid expansion might be therefore more suitable.

⇒ ***Thus, in the last step of the scenario analysis (Step 5 in section 5.1.5) an overlay grid with exogenous fixed and appropriate transmission line capacities is used.***

The missing integration of CSP-HVDC in the overlay grid scenario has made evident that the use of the overlay grid is more efficient. Transmitting electricity produced by CSP exclusively over a dedicated transmission line is therefore not the absolute cost-efficient way. However, the electricity export of CSP from MENA to EU is still an efficient option due to the high correlation of CSP transmission via an overlay grid.

However, a construction of an overlay grid - as a first step - would not be the best way due to barriers such as social acceptance, high planning effort over a large area, unknown or missing business cases and its potential difficult operation in a multinational environment. These barriers may be overcome stepwise with lessons learned of an expansion of the existing transmission grid and construction of point-to-point lines (also CSP-HVDC) as steps towards the overlay grid. This may finally lead to an overlay grid using the spatial flexibility to reduce infrastructural impacts and curtailment for an efficient and successful integration of renewable energies.

### 5.1.3 Step 3: Regional integration probability and the role of CSP-HVDC and CSP for the energy system

In this section an empirical probability of the integration of CSP-HVDC, CSP and other dispatchable energies, such as nuclear power plants and CCS technologies is determined by cost sensitivity scenarios. Because of their low carbon emission and possible competition of dispatchability to CSP-HVDC and CSP, nuclear and CCS are considered. Hereby, each region in EUMENA is analysed separately in a modelling framework of isolated regions (Figure 19b) in a “greenfield” approach.

At the end of this section the CSP-HVDC and CSP configuration values out of the sensitivity scenarios are analysed identifying the role of the technology for the energy system in different regions.

The use of an optimization model considering minimal cost as target function leads to a so-called “penny flip” effect which causes an exclusion of technologies. This exclusion can be based on minimal cost differences of technologies. To avoid this effect in the following, different cost relations of technologies are required. Table 16 shows the possible combination of cost assumptions of technologies. These cost relation combinations arise 9 different scenarios. In addition to the described sensitivity framework in Table 16, two transmission line technologies (OHL and UGC) are analysed. Consequently, the complete sensitivity includes  $2 \times 9 = 18$  scenarios.

Table 16: Sensitivity analysis of a single technology in REMix using different technological cost relations

<b>Cost assumption of all technologies</b>	<b>Cost assumption of examined technology</b>
$\max_{\text{all}}$	$\max_{\text{tech}}$
	$\text{mean}_{\text{tech}}$
	$\min_{\text{tech}}$
$\text{mean}_{\text{all}}$	$\max_{\text{tech}}$
	$\text{mean}_{\text{tech}}$
	$\min_{\text{tech}}$
$\min_{\text{all}}$	$\max_{\text{tech}}$
	$\text{mean}_{\text{tech}}$
	$\min_{\text{tech}}$

The integration frequency or probability of a technology of these 18 scenarios is defined as relative empirical probability of technological integration (epti) in Eq.(29).

$$epti_{18} = \frac{|EPTI_{18}|(\text{capacity} > 1GW)}{18} \quad (29)$$

The absolute empirical probability |EPTI| includes the integration of a technology if a minimum of 1 GW power plant capacity is reached. Base cost assumptions ( $\max_{\text{all}}$ ,  $\text{mean}_{\text{all}}$ ,

$\min_{\text{all}}$ ) are set constant for all technologies. Only the examined technology (here: CSP-HVDC, CSP, nuclear plants, CCGT CCS and coal CCS) is calculated with each  $\max_{\text{tech}}$ ,  $\text{mean}_{\text{tech}}$  and  $\min_{\text{tech}}$  cost combination to the base cost assumptions of all other technologies. Thus, the probability of each cost assumption is assumed to be equal.

The aim of this analysis is to quantify the relative empirical probability of the above mentioned technologies in each model region. The modelling framework thus considers only single regions in EUMENA. Showing also empirical probability depending on CO<sub>2</sub> emission, two different CO<sub>2</sub> emission limits with 0 and 16 g CO<sub>2</sub>/kWh<sub>demand</sub> (“0 CO<sub>2</sub> Emission” and “Small CO<sub>2</sub> Emission”) are used. This amounts to an overall sum of 36 (18 x 2) scenarios. CCS technologies are excluded in the first step due to their existing CO<sub>2</sub> emission and incompatible comparability in this framework. In an excursion in section 5.1.3.1 CCS is included showing its value (emission scenario “Small CO<sub>2</sub> Emission with CCS”).

The results in Figure 25 exhibit the integrated capacity of the analysed technologies as dots and capacity bandwidth. The boxplots show the data using quartiles. The technologies are CSP-HVDC (Figure 25a, d), CSP (Figure 25b, e) and nuclear energy (Figure 25c, f) in each model region. The spread of the bandwidth depends on the input cost assumptions and the regional resource and demand profile. It is recognizable that the empirical probability of CSP-HVDC and CSP increase with a lower allowed CO<sub>2</sub> emission limit in some model regions while the empirical probability of nuclear plants does not change (Table 17). A lower CO<sub>2</sub> emission limit benefits therefore the integration of CSP-HVDC and CSP. Based on the results it can be concluded that CSP-HVDC and CSP can substitute carbon emitting technologies, while in this context nuclear power does not.

Table 17: Model region average EPTI considering the CO<sub>2</sub> emission limit reduction from 16 to 0 g CO<sub>2</sub>/kWh<sub>demand</sub>

CSP-HVDC from 37.7% to 43.3% ▲	CSP from 85.0% to 87.2% ▲	Nuclear power plants no change of 32.2% ◀▶
-----------------------------------	------------------------------	---

The average EPTI for all model regions in Table 17 shows that an integration of CSP-HVDC is more supposable than nuclear power plants. CSP has with 85% and above the highest integration probability. CSP in MENA regions, Iberia and Turkey is therefore highly probable to be integrated.

In Germany the EPTI of CSP-HVDC is 50%. An integration of this technology according to cost is therefore just as probable as improbable. The analysis of the EPTI therefore leads to the statement that CSP-HVDC can be integrated but also that it can't. Table 18 helps to clarify in more depth which cost and transmission infrastructure combinations lead to an

integration of CSP-HVDC capacity in Germany and which don't. In the case of "UGC" the EPTI of CSP-HVDC is 33% whereas in the case of "OHL" the EPTI is 67%. The use of underground cable makes CSP-HVDC more expensive in relation to other options and therefore decreases the likelihood of an integration in the cost minimizing approach. The cost combination of  $\max_{\text{all}}$  and  $\text{mean}_{\text{all}}$  show that CSP-HVDC is more frequently integrated than in the cost combination  $\min_{\text{all}}$ . The cost input parameters are therefore more favourable for CSP-HVDC when other energy technologies are in the same high or medium cost scenario.

Table 18: Results of cost and transmission infrastructure combination for the integration of CSP-HVDC capacity in Germany

Cost assumption of all technologies	Cost assumption of examined technology	CSP-HVDC capacity [GW] in Germany "UGC"	CSP-HVDC capacity [GW] in Germany "OHL"
$\max_{\text{all}}$	$\max_{\text{tech}}$	0	13
	$\text{mean}_{\text{tech}}$	59	80
	$\min_{\text{tech}}$	98	111
$\text{mean}_{\text{all}}$	$\max_{\text{tech}}$	0	10
	$\text{mean}_{\text{tech}}$	0	0
	$\min_{\text{tech}}$	74	85
$\min_{\text{all}}$	$\max_{\text{tech}}$	0	0
	$\text{mean}_{\text{tech}}$	0	0
	$\min_{\text{tech}}$	0	5

Capacity of CSP-HVDC is the net capacity of the power block. The colours show in green a high capacity and in yellow a small capacity.

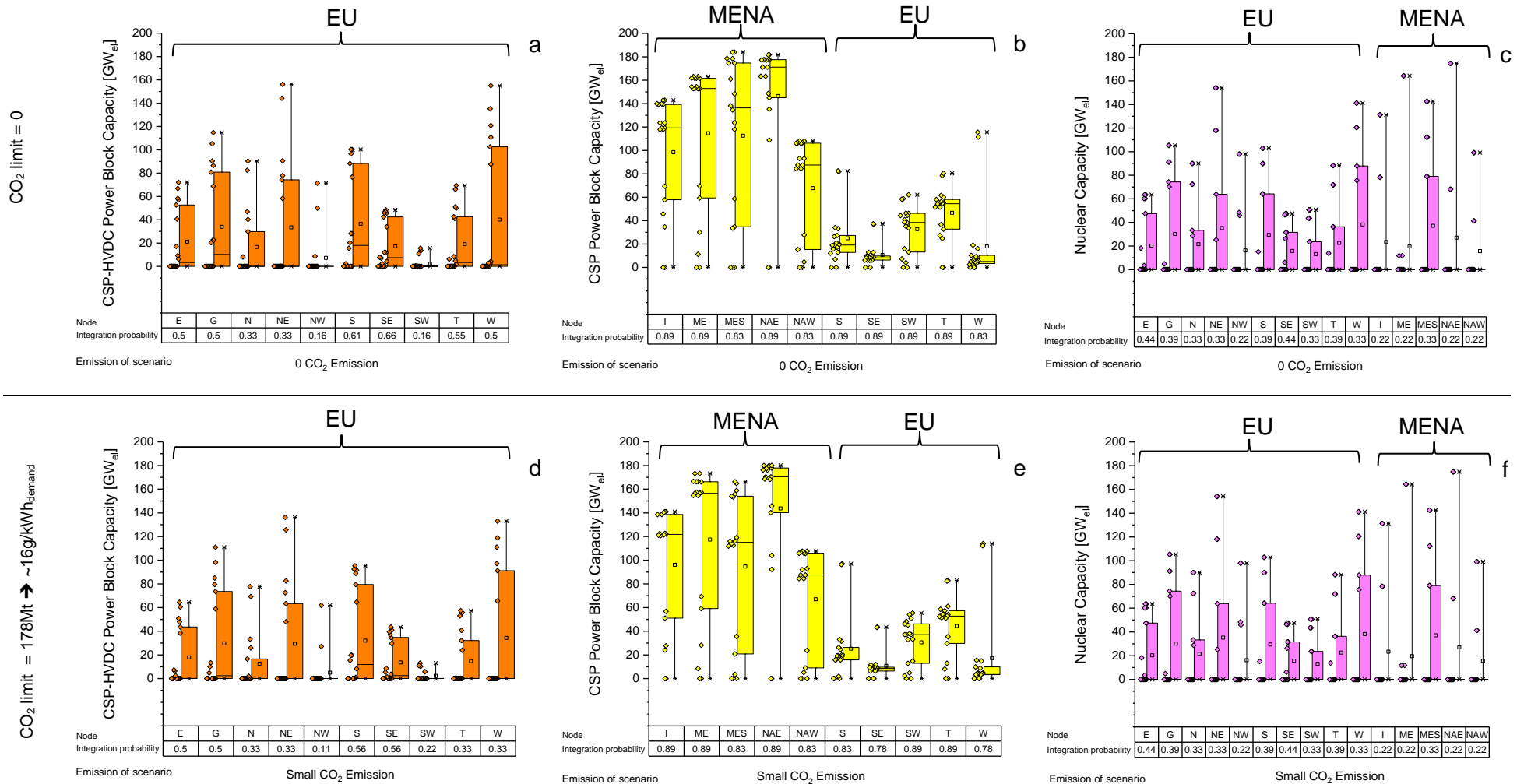


Figure 25: Probability of capacity integration of CSP-HVDC, CSP and nuclear power plants – no CCS allowed

### 5.1.3.1 Excursion: empirical probability of CCS and its value

In this excursion CCGT CCS and Coal CCS are included, showing the empirical probability in Figure 26 of CSP-HVDC (a), CSP (b), nuclear power (c), CCGT CCS (d), Coal CCS (e) and the value of CCS in a radar chart (f). Figure 26 displays the empirical probability of CSP-HVDC, CSP and nuclear plants without and with CCS. The results in Figure 26 reason that the inclusion of CCS decreases the empirical probability of CSP-HVDC and nuclear plants while values of CSP don't change. This leads to the conclusion that CCS may partially replace CSP-HVDC in EU, but it is still probable that CSP-HVDC may be integrated.

Table 19: Comparing average empirical probability of CSP-HVDC, CSP and nuclear power plants in a scenario without CCS with a scenario allowing CCS

CSP-HVDC from 37.7% to 35.6% ▼	CSP no change of 85% ◀▶	nuclear power plants from 32.2% to 30.7% ▼
-----------------------------------	----------------------------	---

First values are the average empirical probability in the scenario without CCS from Table 17.

The average empirical probability of CCGT CCS is 50.7% and of coal CCS is 7.0%. Coal CCS is not very probable to be integrated in a low carbon energy scenario due to better alternatives. A low CO<sub>2</sub> emission limit leads to the use of low specific CO<sub>2</sub> emitting CCS technologies. An analysis of CCS technologies was also performed by (Scholz, et al., 2017). In this paper lower specific CO<sub>2</sub> emitting CCS technologies are preferred with rising CO<sub>2</sub> certificate cost. CCS technologies are thus influenced by an emission limit and CO<sub>2</sub> cost.

Assessing the value of CCS, the average values of the cost sensitivities in EUMENA with and without CCS are illustrated in Figure 26f. The results show that CCS can reduce the electrical storage demand but lead to similar evaluation criteria as a scenario excluding this technology. Yet, it must be noted that the modelling of CCS and other technologies does not include unit commitment constraints e.g. ramping cost, minimal load and part-load behaviour or minimal downtime hours. The result is that the energy system would need more flexibility options than the model suggests. The flexibility of nuclear, coal and gas fired power plants and CCS is overestimated whereby the storage demand is underestimated (Cebulla, et al., 2017). In contrast, the flexibility of CSP is not underestimated because its components are designed to cover the demand flexible (Fichter, 2017). The value of CCS is seen as non-dominant because the saving of storage as shown in Figure 26f would be compensated with the higher storage need when modelling unit commitment constraints. Thus, CCS can be neglected.

⇒ ***This leads to an exclusion of CCS in the last step (Step 5 in section 5.1.5) of the scenario analysis.***

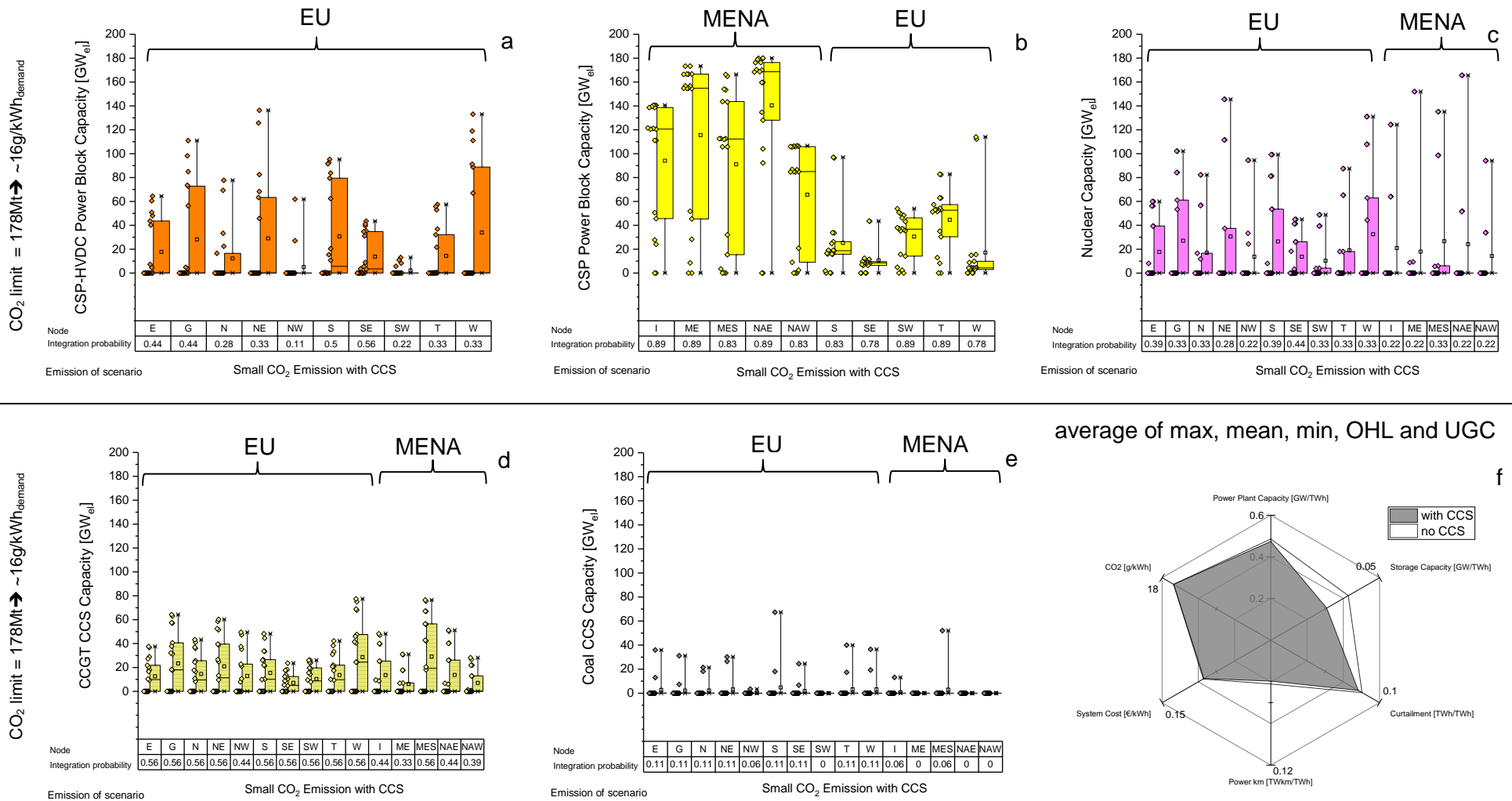


Figure 26: Probability of capacity integration of CSP-HVDC, CSP, nuclear power plants, CCGT CCS, Coal CCS and the value of CCS



### 5.1.3.2 The role of CSP-HVDC and CSP for the energy system

Taking a more detailed look on CSP-HVDC and CSP, this section depicts their optimized configuration of the emission scenario “Small CO<sub>2</sub> Emission”. The configuration criteria solar multiple (Figure 27a, b) and thermal energy storage full load hours (Figure 27c, d), are chosen to clarify the role of the technologies in the energy system and the potential differences of the cost optimal configurations of CSP-HVDC for EU, domestic CSP in MENA and domestic CSP in EU.

#### **Solar Multiple:**

The solar multiple is an indicator of full load hour hours, availability and therefore also dispatchability of the renewable energy share of CSP. The higher the solar multiple the more full load hours a CSP power plant has. The solar multiple is defined as ratio of solar field capacity  $P_{SF,CSP}$  and power block capacity  $P_{PB,CSP}$  according to equation (30). The efficiency of the power block  $\eta_{generator}$  is the product of the thermal and electrical efficiency. A solar multiple of 1 describes a system with a solar field which is large enough to provide nominal capacity for the power block under nominal irradiance (here 800 W/m<sup>2</sup>). A solar multiple of 2 characterises a system with a solar field twice as large as with a solar multiple of 1 (with the same power block capacity). This solar field can provide energy for the power block and for a thermal storage. Thus, one solar field will directly drive the turbine while the other solar field will serve to fill the storage for night time operation (Trieb, et al., 2012).

$$\text{Solar Multiple:} \quad SM = \frac{P_{SF,CSP} [GW_{th}]}{P_{PB,CSP} [GW_{el}] \cdot \eta_{generator}} \quad (30)$$

Figure 27a and b shows that CSP-HVDC has a higher solar multiple than CSP. This result occurs because CSP is in competition with more cost-efficient use of PV in MENA compared to PV in EU. CSP-HVDC has with its high solar multiple a flexible base load characteristic, providing dispatchable energy according to demand.

Another effect is that CSP has a small solar multiple in southern EU regions like in **S**, **SE**, **T** and **W** because it is more efficient to use other technologies than building a larger solar field in such regions with a seasonal lack of DNI irradiance. Also the absolute configuration values of CSP in these EU regions are comparably small. Thus, CSP can be used efficiently in southern EU but only in a comparable small scale. An exception is the EU region **SW** in which the solar multiple can also achieve higher values but also comparable small values.

### Thermal Energy Storage:

The thermal energy storage (TES) for the analysed regions is described in Figure 27c, d with full load hours of the storage. These full load hours can be calculated according to Eq. (31) with a ration of TES capacity,  $P_{TES,CSP}$  and power block capacity  $P_{PB,CSP}$ .

$$TES \text{ full load hours} = \frac{P_{TES,CSP} [GWh_{th}]}{P_{PB,CSP} [GW_{el}]} \cdot \eta_{generator} \quad (31)$$

The results in Figure 27c reveal that the thermal energy storage of CSP-HVDC has about 13 full load hours and is thus considered as medium-term storage. The thermal energy storage of CSP has about the same range of full load hours. However, CSP thermal energy storage full load hours are lower than for CSP-HVDC. The lower full load hour is attended by the lower solar multiple for CSP.

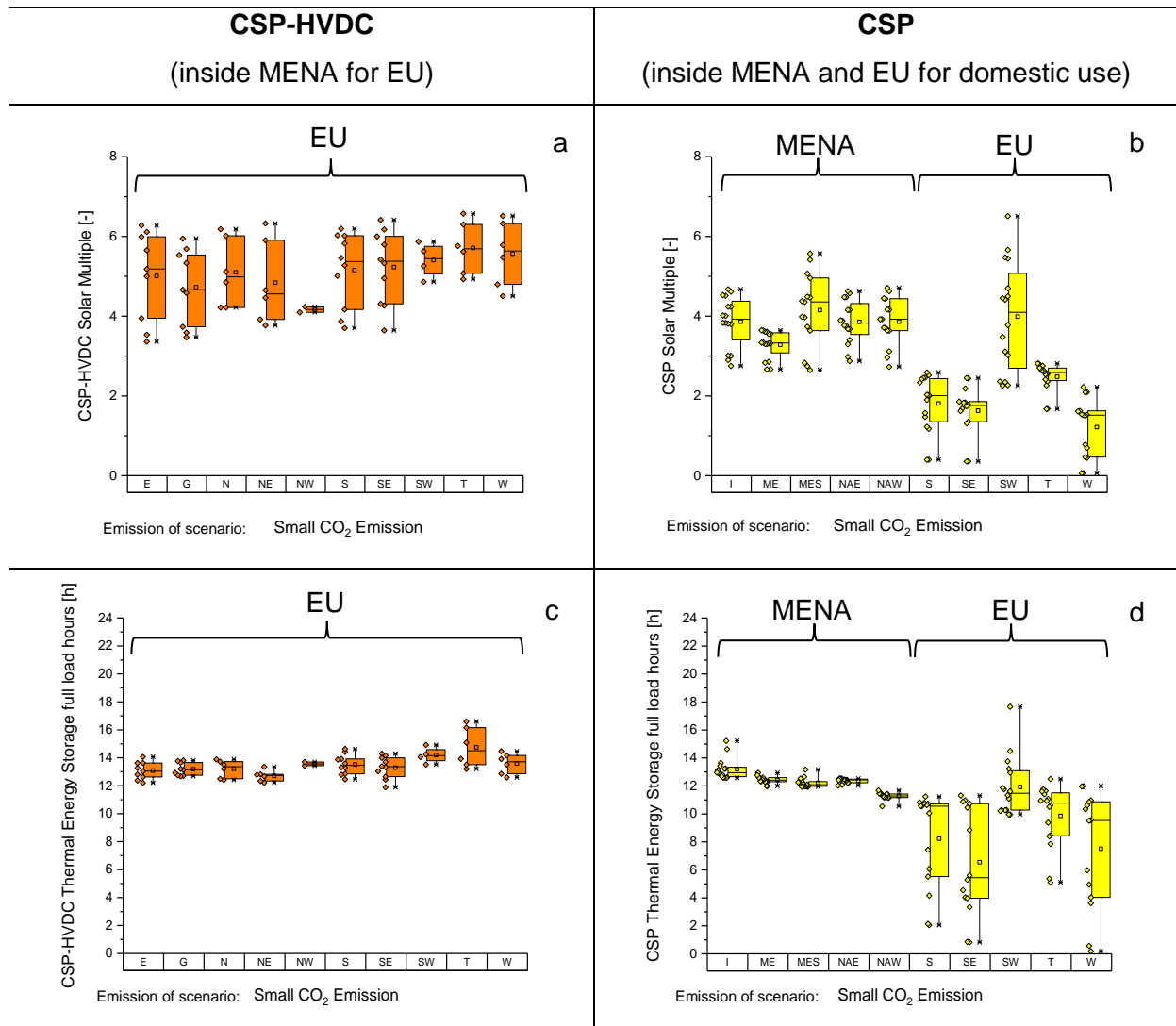


Figure 27: Solar Multiple (a, b) and Thermal Energy Storage full load hours (c, d) of CSP-HVDC (in MENA for EU) and CSP (in MENA and southern EU)

### Demand for land:

The demand for land of the power plant can be calculated by the solar field capacity of CSP-HVDC and CSP. Equation (32) shows how the needed area of the solar field can be calculated. This indicates how much space in desert regions is needed or in other words how much space can be used and cultivated.

$$\text{power plant size [km}^2\text{]} = \frac{P_{SF,CSP} [GW_{th}]}{0.1762} \quad (\text{Stetter, 2012}) \quad (32)$$

Figure 28 reveals the resulting CSP and CSP-HVDC demand for land of the empirical probability analysis in this section. The boxplots in Figure 28 show the data using quartiles. It is remarkable that the median of the demand for land of CSP-HVDC is quite similar compared to the domestic use of CSP inside the MENA region. In other words: “one mirror for MENA, one mirror for EU”. However, the resulting median demand for land of CSP-HVDC is a little lower than CSP inside MENA. The median value of the demand of land for CSP inside MENA for its regional use is in the scale of the area of Switzerland (41.285 km<sup>2</sup>). The accumulation of the values for CSP inside MENA for MENA demonstrates that its median demand for land is more robust than the median value of CSP-HVDC. An accumulation of the demand for land for CSP-HVDC is visible in the under scale of the bar. Based on the large bandwidth of CSP-HVDC, a specific statement of how much area might be used for CSP-HVDC in MENA can't be done with these results.

The area of CSP inside EU for EU is comparable small with a median value of 5000 km<sup>2</sup> which equates twice the German federal state of the Saarland (2570 km<sup>2</sup>).

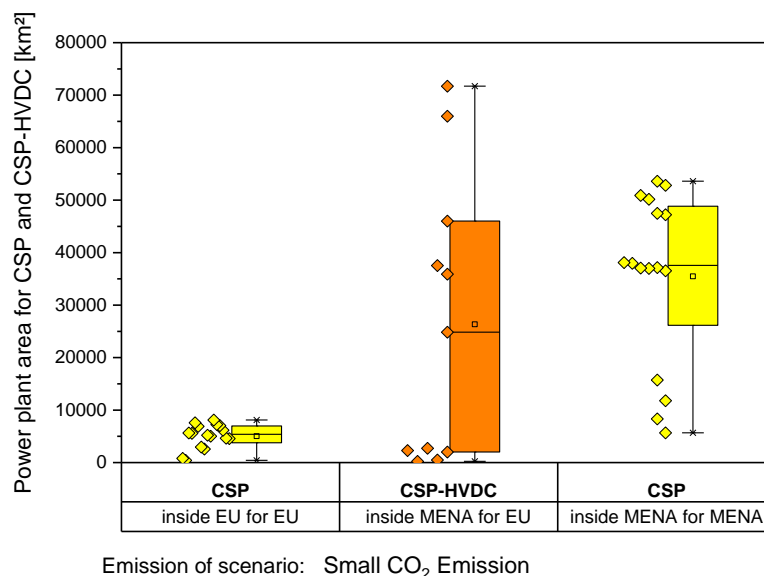


Figure 28: Bandwidth of possible area use [km<sup>2</sup>] of CSP and CSP-HVDC in EU and MENA

Table 20 supplements the configuration criteria of Figure 27 with the power block capacity, net electrical generation and the co-firing. Compared to CSP the average power block

capacity and net electrical generation for CSP-HVDC are smaller. Thus, CSP in MENA has a dominant use while CSP-HVDC is more seen as a supplement for EU. Whereas CSP use a co-firing in small shares, CSP-HVDC provides energy without co-firing usage.

Table 20: CSP-HVDC and CSP configuration in sensitivity scenario of Figure 25 with small CO<sub>2</sub> emissions (16 g CO<sub>2</sub>/kWh<sub>demand</sub>)

Configuration	CSP-HVDC		CSP	
	min - max	average	min - max	average
Solar multiple [-]	3.4 - 6.6	5.1	0.1 – 6.5	3.0
Solar field size [km <sup>2</sup> ]	73.7 – 12899.6	4261.9	76.3 – 13684.5	4236.8
Solar field [GW <sub>th</sub> ]	12.8 - 2272.7	751.0	13.4 - 2411.2	746.5
Thermal energy storage full load hours [h]	11.9 – 16.6	13.4	0.2 – 17.7	10.6
Thermal energy storage [GWh <sub>th</sub> ]	41.8 - 5091.6	1854.6	55.4 - 6044.4	2366.9
Power block capacity [GW]	1.3 - 136.3	50.5	1.9 – 180.0	76.1
Net electrical generation [TWh/y]	7.5 - 842.9	321.7	9.0 - 1256.2	444.3
Co-firing with natural gas [TWh/y]	0	-	0.2 - 20.5	3.6

Average values are calculated considering all regions equally. The relative values (in grey) reflect the configuration of the power plants. The absolute values show their dimension just in a possible bandwidth.

The results are achieved using a simplified technological model. A detailed technological CSP model regarding this configuration is needed. The model doesn't consider scale effects such as higher internal demand with a rising solar multiple so-called parasitic losses.

Detailed regional configuration values of CSP-HVDC and CSP with the frame conditions of 0 and 16 g CO<sub>2</sub>/kWh<sub>demand</sub> also with CCS are shown in the appendix Figure 53 to Figure 56.

### 5.1.3.3 Statement of the section

In this section the empirical probability of CSP-HVDC, CSP, nuclear power and CCS are introduced. It can be concluded that the probability of CSP-HVDC implies a possible integration of this technology according to its cost and HVDC topology assumptions.

However, it should be noted that the cost assumptions of CSP and the pathway of HVDC are assumed as relative conservative and that CSP still renders a cost reduction till 2050 due to its advancing learning curve. Therefore CSP-HVDC has a high potential to be integrated. Nuclear plants and CCS are also possibly integrated yet with a lower probability of nuclear plants than CSP-HVDC or under the very optimistic modelling conditions for CCS.

As a result of the configuration values of CSP-HVDC and CSP it is concluded that the two technologies fulfil different roles in the analysed regions. CSP-HVDC has a high solar multiple and a base load characteristic. CSP in MENA has a lower solar multiple due to efficient combination of CSP and PV in the domestic energy mix. Based on comparable high thermal energy storage full load hours, the medium-term thermal storage of CSP in MENA is frequented like in the CSP-HVDC configuration. Thus, CSP in MENA has also a baseload characteristic but a lower use of the solar field than CSP-HVDC. The CSP power plants in the EU for domestic use have a lower solar multiple and lower thermal energy storage full load hours due to other more efficient technologies and the drastic reduction of DNI in winter. CSP in EU for domestic use shows therefore a commitment to medium load levels.

#### **5.1.4 Step 4: CSP-HVDC - direct comparison of CSP, nuclear energy and CCS**

In this section of the scenario analysis the dispatchable technologies CSP-HVDC, nuclear plants, CCGT CCS and coal CCS are compared and their system impact is quantified applying energy evaluation criteria and system cost deviation and annual full load hours. For this purpose the same power block capacity of these technologies is integrated exogenously. Hereby, each region in EUMENA is analysed separately in a modelling framework of isolated regions (Figure 19b) in a “partial greenfield” approach.

A “partial greenfield approach” means that a capacity optimization of all technologies is allowed and exogenously set capacities are considered in one approach. The exogenous capacity values and their selection criteria are made available in the appendix Table 42. An interconnected overly grid in EUMENA is excluded so that each region is able to balance its own power plant park.

##### **5.1.4.1 Comparison of evaluation criteria**

Three cost sensitivity scenarios are calculated (“all max”, “all mean” and “all min”). The results of these cost sensitivity scenarios are averaged and shown in Figure 29. The results are compared according to selected evaluation criteria, system cost uncertainty and operational behaviour.

In the radar chart Figure 29a the comparison of CSP (incl. CSP-HVDC) and nuclear plants in a zero carbon emission scenario is illustrated. The other charts of Figure 29b-d evidence the comparison of CSP (incl. CSP-HVDC) with nuclear plants, CCGT CCS and coal CCS in a framework with small CO<sub>2</sub> emissions.

Partial greenfield: in each comparison the same capacity amount of the examined technology is set exogenously with optimization possibility of all other technologies

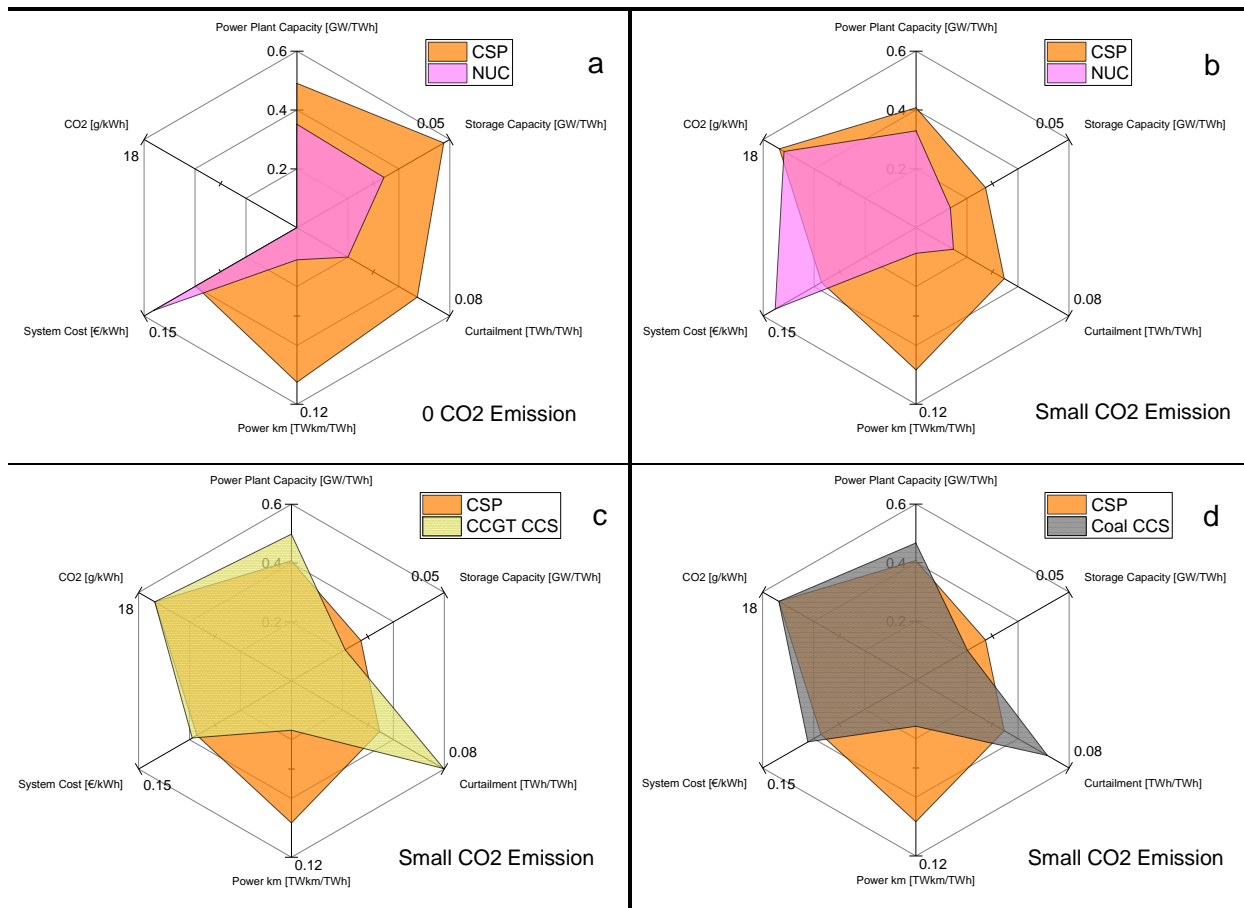


Figure 29: Comparison of CSP, nuclear energy, CCGT CCS and Coal CCS in multi criteria

The results of the zero CO<sub>2</sub> emission scenario in Figure 29a and the low CO<sub>2</sub> emission scenario in Figure 29b points out that the use of nuclear plants lead to lower power plant and electrical storage capacity, curtailment, node internal expansion grid and point-to-point line expansion (power km). Storage and curtailment may be influenced by too optimistic modelling assumptions of nuclear plants with respect to flexibility and are hence seen critical. Nuclear and CCS power plants are not modelled with unit commitment constraints and would therefore cause more storage demand in the system (Cebulla, et al., 2017). System cost in using nuclear power is higher compared to the CSP scenario (Figure 29a and Figure 29b). Other possible higher environmental impacts (waste) or social impacts (acceptance) are not analysed and would make a more comprehensive comparison difficult. From this situation

arises that nuclear power plants may have advantages compared with CSP but probably cause higher system cost.

⇒ ***In the last step of the scenario analysis (Step 5 in section 5.1.5) nuclear plants are excluded due to their average higher system cost.***

The comparison of CCS and CSP in Figure 29 c and d leads to the result, that CCS induces less storage capacity and grid and transmission line expansion (power km) but brings about higher system cost, power plant capacity and curtailment. Both CCS technologies show a similar characteristic in the radar charts. The integration of CCS with the same capacity as CSP and nuclear leads to relative high curtailment. This result occurs because CCS has relative high variable O&M and is used as peak load power plant (Figure 30b) thus energy from other power plants is more cost-efficient than using CCS. The model integrates therefore more capacity of other - almost fluctuating - power plants (visible in Figure 29 c and d) which leads to a high curtailment.

5.1.4.2 Comparison of system cost deviation and annual full load hours

Table 21 defines the framework of analysing system cost deviation using cost sensitivities. The cost sensitivities are based on different cost relations of input parameters. The cost sensitivity scenarios result in different system costs. System cost deviation is defined according to Table 21 as deviation from system cost<sub>all</sub> to system cost<sub>tech</sub>. For example mean cost assumption for all technologies and a min cost assumption for CSP are used. The system cost deviation in this scenario is the difference of these two system costs. System cost deviation is strongly dependant on technological cost bandwidth thereby indicating cost uncertainty of each technology. Figure 30 depicts the system cost deviation

Table 21: Sensitivity analysis of a single technology using different technological cost relations resulting in system cost

<b>Cost assumption of all technologies</b>	<b>Cost assumption of examined technology</b>
$\text{max}_{\text{all}} \rightarrow \text{cost}_{\text{all}}$	$\text{max}_{\text{tech}} \rightarrow \text{cost}_{\text{tech}}$
	$\text{mean}_{\text{tech}} \rightarrow \text{cost}_{\text{tech}}$
	$\text{min}_{\text{tech}} \rightarrow \text{cost}_{\text{tech}}$
$\text{mean}_{\text{all}} \rightarrow \text{cost}_{\text{all}}$	$\text{max}_{\text{tech}} \rightarrow \text{cost}_{\text{tech}}$
	$\text{mean}_{\text{tech}} \rightarrow \text{cost}_{\text{tech}}$
	$\text{min}_{\text{tech}} \rightarrow \text{cost}_{\text{tech}}$
$\text{min}_{\text{all}} \rightarrow \text{cost}_{\text{all}}$	$\text{max}_{\text{tech}} \rightarrow \text{cost}_{\text{tech}}$
	$\text{mean}_{\text{tech}} \rightarrow \text{cost}_{\text{tech}}$
	$\text{min}_{\text{tech}} \rightarrow \text{cost}_{\text{tech}}$

and full load hours of the examined technologies. The results in Figure 30a show that CCGT CCS has the lowest system cost deviation and nuclear has the highest. This result seems reasonable due to an already passed learning curve for CCGT and coal power plants with

quite predictable cost. Furthermore high cost uncertainty for nuclear plants is retraceable because nuclear projects have a high cost deviation (European Commission, 2014). Nuclear plants have thus the highest possible system cost expenditures but also high possible system cost saving. The system cost deviation for CSP is understandable since CSP technology still has to pass a learning curve and leaves us with a noticeable cost uncertainty for the time being.

Comparing the quality of each technology (considering capacity but also annual energy), the annual full load hours in Figure 30b reveal that CSP and nuclear power plant are appropriate for base load configuration with up to 18 times higher annual full load hours than CCS technologies covering only peaks due to their higher O&M cost.

The results show that CSP and nuclear have comparable operational behaviour in the model but CSP has a lower system cost uncertainty than nuclear power plants.

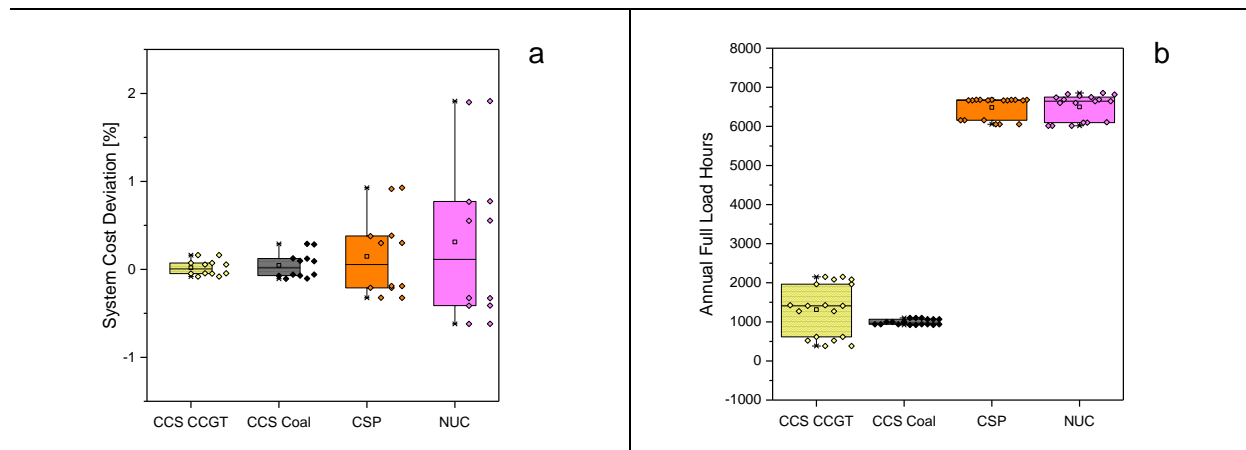


Figure 30: Comparison of some exogenous capacities of CSP, nuclear energy, CCGT CCS and coal CCS in system cost deviation and annual full load hours

#### 5.1.4.3 Statement of the section

The direct comparison of CSP (incl. CSP-HVDC), nuclear and CCS plants shows that CSP is cost competitive and has an operational characteristic that leads to little curtailment and low system cost uncertainty in the energy system. Nuclear and CCS may have some advantages especially in the reduction of grid and transmission capacity (power km). Yet, the drawbacks of transport impact of material - additional to the transport of electrons - like fuel transport of uranium, gas or coal is not included in the comparison. Such transportation of material from the mining to the power plant leads definitely to a negative influence on the energy system. CCS technologies are not competitive to CSP and nuclear plants due to their low average utilisation that predominantly serves another demand segment. Thus, only CSP and nuclear power appear to be competitive within the analysed criteria. Future analyses should include a holistic approach regarding other sustainability indicators beside the used evaluation criteria.



### 5.1.5 Step 5: CSP-HVDC – value of CSP-HVDC with different capacity shares

In this last modelling step the insights of the previous steps are used focussing on the evaluation of CSP-HVDC. A scenario with high CSP-HVDC capacity penetration is analysed. This used capacity of CSP-HVDC is reduced systematically in 25% steps till a 100% reduction. The scenario without CSP-HVDC is the reference. The value of this technology for the energy system is shown with the evaluation criteria considering cost, infrastructure, operational behaviour and emission.

The analysis of these scenarios respects the following modelling framework:

- Cost assumption are “all mean” with an overhead line transmission infrastructure.
- In order to avoid the possibility of penny flips and disproportional expansion of the overlay grid, the capacities of power plants and storages are exogenously set. They are available in the appendix Table 43 to Table 46.
- Knowing that REMix only respects cost does not minimize other evaluation criteria. The modelling of the scenario has the aim to minimize capacities, and curtailment. This can be achieved, if the demand is covered directly (power to demand) using dispatchable renewable energies. Therefore, the potential of renewable dispatchable energies for each region inside EU is modelled at its limit.
- The maximum capacity share of CSP-HVDC in EU is designed to achieve a 50% dispatchable energy share, integrating at first the dispatchable renewable energies of each region inside EU.
- CCS and nuclear plants are excluded due to the previously shown high cost (nuclear) and by reason of too optimistic modelled operational characteristic (no partial load behaviour).
- An overlay grid is used with limited capacity of transmission lines. The transmission line capacities are assumed to be 2 GW for each connection between model regions in 2010. The capacity of overlay grid transmission lines expand in the same manner as the demand of the model regions rises from 2010 to 2050.

Based on these constraints a stepwise approach is used:

1. Expansion of exogenous capacities in a framework of isolated model regions with a CO<sub>2</sub> emission limit (greenfield).  
→ Regional optimized placement of capacities
2. Due to overcapacities of storages in isolated model regions (see section 5.1.2) the resulting storage capacities are extinguished in the next step and all capacities are optimized again in a restricted overlay grid (partial greenfield).  
→ Integration of an overlay grid and new calculation of storage capacities
3. Systematic reduction of CSP-HVDC capacity (power block and solar field). Optimization of all capacities additionally to the exogenous capacities (partial greenfield).  
→ Cost-efficient replacement of CSP-HVDC showing the system influence of this technology

The radar charts in Figure 31 constitute the results of the analysed evaluation criteria for the overall region EUMENA, the sub-regions EU, MENA and on national scale the region of Germany. The ochre charts are the analysed scenarios (base and 50% CSP-HVDC capacity reduction). The grey charts represent the reference scenario without CSP-HVDC.

The results are analysed to show the reader the value and impact of CSP-HVDC with different shares and the consequence of the exclusion of this technology in different regions. The impact of the energy system can be evaluated when summarizing all evaluation criteria. In other words regarding the radar charts show that the smaller the area is the lower is the impact. For a suitable quantification of the impact there is still no answer to the open question how to scale the evaluation criteria in the right relation to each other. In this analysis each evaluation criteria is scaled according to a value near the maximum. This allows assessing the criteria in the same relation to each other. Also a comparison of the analysed regions can be drawn due to the same specific scale (per annual net electricity demand) of the evaluation criteria in each region.

Figure 31a and Figure 31b show the EUMENA region. It is visible that the missing of CSP-HVDC leads to a higher need of power plant and electrical storage capacities and causes more electrical curtailment. However, more power kilometre may be needed due to long distances with CSP-HVDC (keeping in mind an optimistic modelling of the transmission and

distribution grid power km). Regarding the area of the radar charts, it is obvious that scenarios with CSP-HVDC lead to smaller areas.

In Figure 31c-f the focus is on a more regional scale considering EU and MENA separately. It is evident that the MENA region has lower specific values in all categories than in the EU region except specific CO<sub>2</sub> emission. Due to the local possible use of dispatchable CSP, it may be easier for MENA to implement a low carbon energy system compared to the EU region.

Furthermore the regions are compared. CSP-HVDC is used per definition in the thesis only for EU. However, different results for MENA do occur when neglecting this technology. The reason therefore is that all regions are interconnected with a grid which leads to an interdependency among the regions. Another reason is the global CO<sub>2</sub> emission limit which leads to a regional optimization of CO<sub>2</sub> emission. Therefore a different use of power plants commences. The results in Figure 31e show that a use of CSP-HVDC leads to higher CO<sub>2</sub> emission in MENA. This means that CO<sub>2</sub> in EU can be avoided more efficiently using CSP-HVDC. Thus, the region EU contributes to a higher degree of freedom for CO<sub>2</sub> emissions in the MENA region with an integration of CSP-HVDC for the EU. Nevertheless, the specific CO<sub>2</sub> emission is already low and the difference between EU and MENA has not a significant impact.

For a national view towards the results, Figure 31g and Figure 31h display the evaluation criteria for the model region of Germany. This region has the highest specific values compared to EU and MENA and therefore generates a higher impact on its energy system. In the case of the use of CSP-HVDC all evaluation criteria are smaller except the power kilometre. Reducing CSP-HVDC capacity leads to a dominant increase of electrical storage capacities and curtailment. All regional results of the comparison of CSP-HVDC shares are in the appendix Figure 59 to Figure 62.

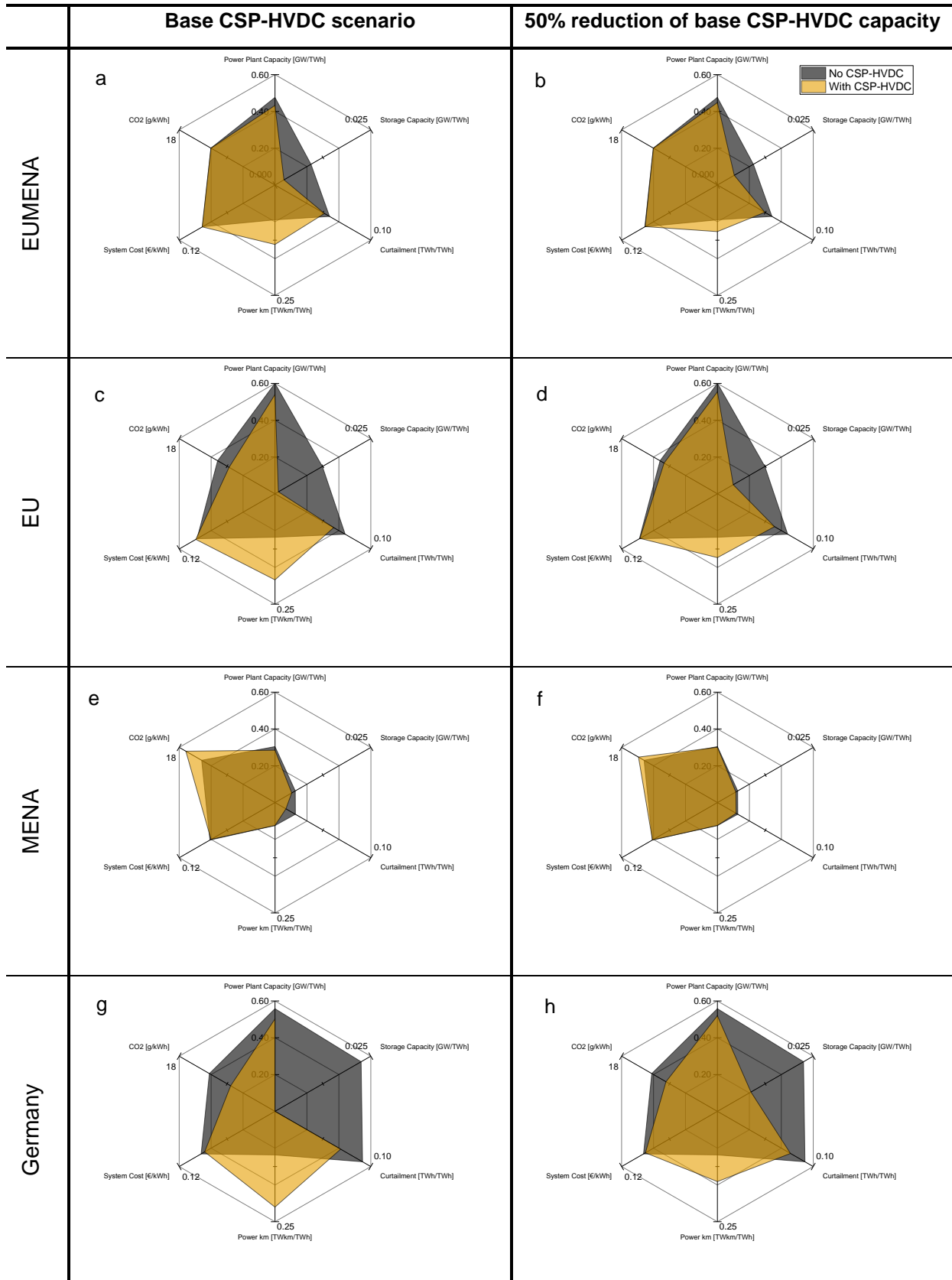


Figure 31: Radar charts showing the value of CSP-HVDC. Base scenario is shown in the left column in ochre, 50% reduction of CSP-HVDC capacity of base scenario in the right column in ochre. Grey radar charts show an energy system without CSP-HVDC as reference. Specific evaluation criteria per annual net electricity demand of each region are applied.

#### 5.1.5.1 Statement of the section

The value of CSP-HVDC can be measured in a radar chart showing that this dispatchable energy can efficiently reduce power plant and storage capacities and curtailment. System cost does not play a major role due to insignificant cost differences in the used medium cost scenario. However, CSP-HVDC might lead to overall more power kilometre depending on its share in the energy system.

### 5.2 Value of CSP-HVDC – discussion of results

Considering the results of the previous scenario analysis, this section takes a more detailed look on the used evaluation criteria. Here the results are discussed on the basis of the modelling assumptions and the used method. Focussing on the value of CSP-HVDC, a critical reflection is undertaken to reveal if this technology can positively contribute to the energy system or if it can be neglected.

#### 5.2.1 Power plant capacity

Power plant capacity can indicate the environmental compatibility of an energy system. This can be measured e.g. in needed area, space and material (Trieb, et al., 2017), (Wetzel, 2015). Regarding the small gain of capacities with CSP-HVDC in Figure 31, review of an exact environmental compatibility requires a deep and detailed examination which goes beyond of the scope of the thesis and should therefore be a research subject of future analyses. A system with CSP-HVDC reduces total power plant capacity in any case.

As for the political assumption, the firm capacity of CSP-HVDC is assumed to be zero, because only domestic firm capacity is considered. The total capacity is a result of neglecting the firm capacity of CSP-HVDC abroad. For each CSP-HVDC capacity a firm capacity is additionally implemented even when CSP-HVDC can provide technically firm capacity but may not be yet accepted as such. Further capacity reduction is therefore possible with an integration of CSP-HVDC.

#### 5.2.2 Electrical storage capacity

The results of the specific electrical storage capacity show how much capacity is needed for a temporal shift of capacity. The used electrical storages are listed in Table 25. A reduction of CSP-HVDC in Figure 31a-d and Figure 31g,h leads to a higher expansion of electrical storage capacity but reduces the needed power kilometre. Thus, a trade-off occurs between electrical storage capacity and grid and transmission line expansion.

In this analysis the electrical storage capacity is considered as evaluation criteria and not the thermal storage capacity of CSP because the thermal storage of CSP can be used solely by CSP and is therefore not accessible by the whole energy system. The electrical storages can be applied by the entire energy system and are therefore a very flexible option. Comparing the influence of CSP and electrical storages needs to separate these technologies.

A possible future option for the thermal storage of CSP could be also a possible use for the whole energy system storing electricity in the thermal storage of CSP as medium term storage.

### 5.2.3 Curtailment

Today curtailment is a result of transmission constraints, balancing issues such as exhaustion of reserves, voltage control but also oversupply (Bird, et al., 2014). The REMix model considers the electrical curtailment of fluctuating energies such as Wind turbines, PV and hydro power plants. The criterion of curtailment in the model is only according to cost. This means that the model can decide e.g. to build an electrical storage, enlarge the node internal grid or curtail energy. Power plants of fluctuating energies with high O&M will be curtailed at first.

Managing high curtailment is a major challenge. If newly build capacities of Wind and PV are more restricted in feeding-in their electricity into the grid compared to the stock, these capacities might be more economical pressure through higher curtailment. This effect may occur if the stock keeps its status quo of former operating Wind and PV capacities. This can cause missing incentives in building new power plants due to a lower or missing profit. Thus, the question arises: Who will build such capacities when these are predominantly curtailed? How much money is needed to compensate curtailed capacity?

*- Cost of curtailment compensation (EinsMan – feed-in management) was around 0.10 €/kWh (Bundesnetzagentur, 2015) in the first quarter of the year 2015 in Germany. If this cost is realised in a future energy system, high fluctuating energy shares would lead to an increase of the energy system cost. For example a curtailed energy amount of 10% of the net electricity demand in Germany would lead to an increase of system cost of around 7 bn €/y with such a compensation payment. –*

Figure 31 on page 84 shows the curtailment according to the share of CSP-HVDC. It is obvious that lower curtailment is achieved using more dispatchable energy. Thus, an equal distribution of electrical curtailment is accomplished. In other words high full load hours for each power plant or market participant can be achieved if more dispatchable energies are used. Also less intervention in power plant and transmission operation is the result of lower curtailment. Thus, CSP-HVDC can help to imply a low carbon energy system with a less complicated operation of the energy system.

## 5.2.4 Power kilometre and utilisation of the overlay grid

### 5.2.4.1 Power kilometre

Grid and transmission line expansion is a major indicator dealing with high shares of renewable energies. The indicator quantifies the spatial flexibility of the energy system. The power kilometres are divided in three categories: transmission capacity over distance of overlay grid (HVDC 600kV and AC 380kV), nodal grid (transmission and distribution grid) and point-to-point lines (CSP-HVDC and hydro reservoir import). In Figure 32 and Figure 34 the total power km are compared, considering scenarios with different capacity shares of CSP-HVDC. Under this influence, the aim of Figure 32 is to compare the regional difference of resulting power kilometre. Figure 34 compares the power kilometre categories. The maps of Figure 32 show the nodal and point-to-point power kilometre inside the regions. The power kilometre of the point-to-point CSP-HVDC and hydro reservoir import power plants are added to the destination node in which the point-to-point infrastructure ends. The power kilometres of the overlay grid are illustrated with the capacity of each overlay grid transmission line. The overlay grid has fixed transmission line capacities. The capacity of overlay grid transmission lines are assumed with about 2GW in the year 2010 and expand until 2050 in the same manner as the demand of the model regions rises from 2010 to 2050. Therefore MENA countries have higher overlay grid capacities than regions in EU (appendix Table 46).

The results in Figure 32 show the used overlay grid and the absolute regional power kilometre [TWkm] with different CSP-HVDC capacity shares. Figure 32a presents the power kilometre in the CSP-HVDC base scenario with maximum set CSP-HVDC capacity. Figure 32b illustrates the power kilometre of the scenario with a 50% reduction of CSP-HVDC capacity of the base scenario. Figure 32c shows the power kilometre with an exclusion of CSP-HVDC. Figure 32 clarifies the regional resulting power kilometre. The absolute power kilometre is a result of net electricity demand and expansion of regional grid and point-to-point transmission lines. This means that only the comparison of Figure 32a-c reveals the influence of CSP-HVDC and the resulting regional power kilometre. Due to the cost-efficient use of local CSP in MENA and southern EU, the regional power kilometre in MENA and southern EU are low compared to the regions **NW**, **W**, **G** and **NE**. In the model region **N** the regional power kilometre are lower than in the surrounding regions. This effect is achieved using a high share of dispatchable biomass and hydro reservoir power plants in **N** (see appendix Table 44 and Table 45). Comparing the absolute with the specific power kilometre (according to electricity demand in the appendix Figure 59 to Figure 62) the specific values are also high for the regions **NW**, **W**, **G**, **NE** and **E** high values. These regions may well have a relative intense transmission infrastructure also outside their territory when integrating CSP-HVDC.

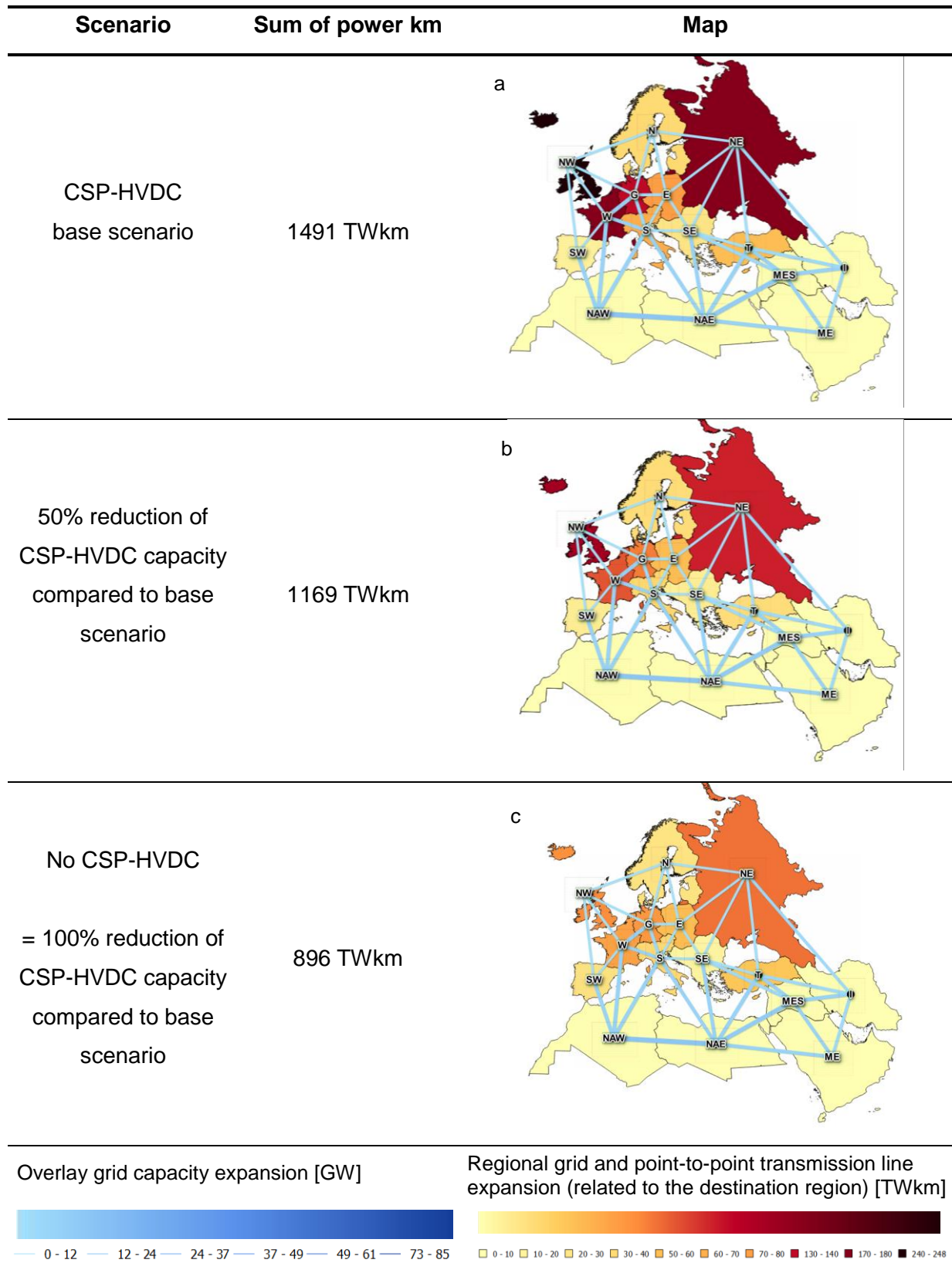


Figure 32: Regional grid and transmission line expansion measured in power km in scenarios with different CSP-HVDC capacity shares related to the base scenario



Figure 33 exhibits the power km over EUMENA according to grid infrastructure categories (overlay grid, P2P and nodal grid). The power kilometres of the overlay grid are fixed. A reduction of CSP-HVDC leads to lower total power km. However, such a reduction of dispatchable energy leads to an increase of nodal grid expansion of transmission grid (red double arrow in Figure 33 and visible in Figure 34) due to higher fluctuating energy shares of Wind and PV. The distribution grid is not expanded and its stock is not listed due to unknown data. Missing CSP-HVDC also leads to a higher use of hydro reservoir import capacity over point-to-point lines (dark blue bulk) from model region **N** to **NW**, **G** and **E**. Such an increase indicates a need of dispatchable energy for an utilisation in the grid.

Lower CSP-HVDC shares can also reduce total power kilometre because nodal grid power kilometre increase. This potential trade-off can be achieved in the analysed case with an adequate share of CSP-HVDC. Such a share can therefore lead to a reduction of total power kilometre. This characteristic is visible in Figure 35 with the falling gradient of CSP-HVDC (P2P lines) and the rising gradient of the transmission grid (nodal grid).

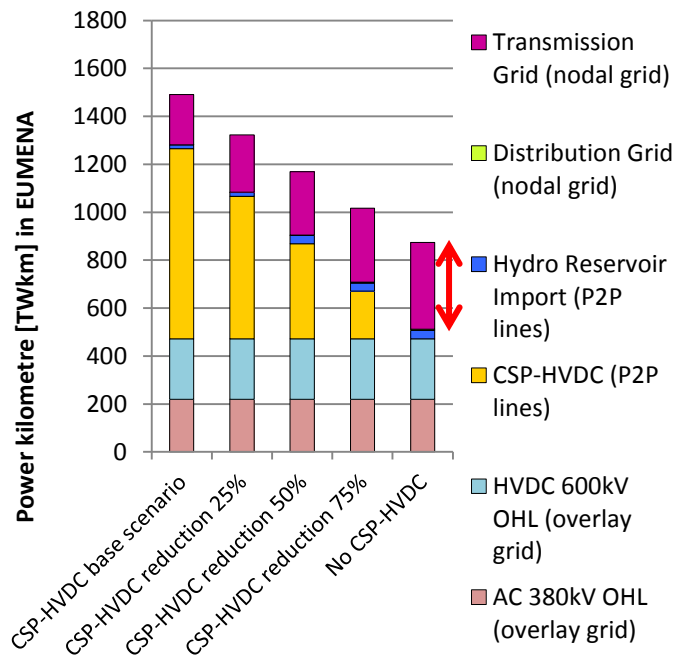


Figure 33: Different shares of CSP-HVDC capacity and resulting expansion of power kilometre according to transmission infrastructure categories

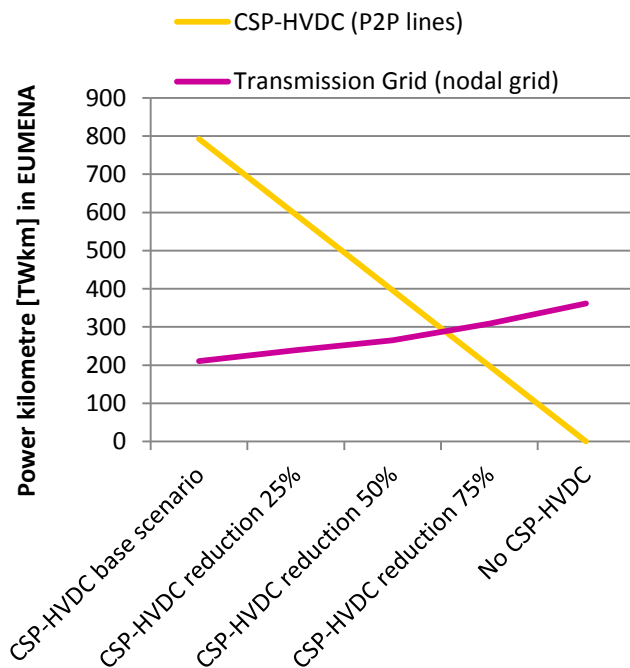


Figure 34: Trade-off of power kilometre between CSP-HVDC (P2P lines) and Transmission grid (nodal grid) in EUMENA

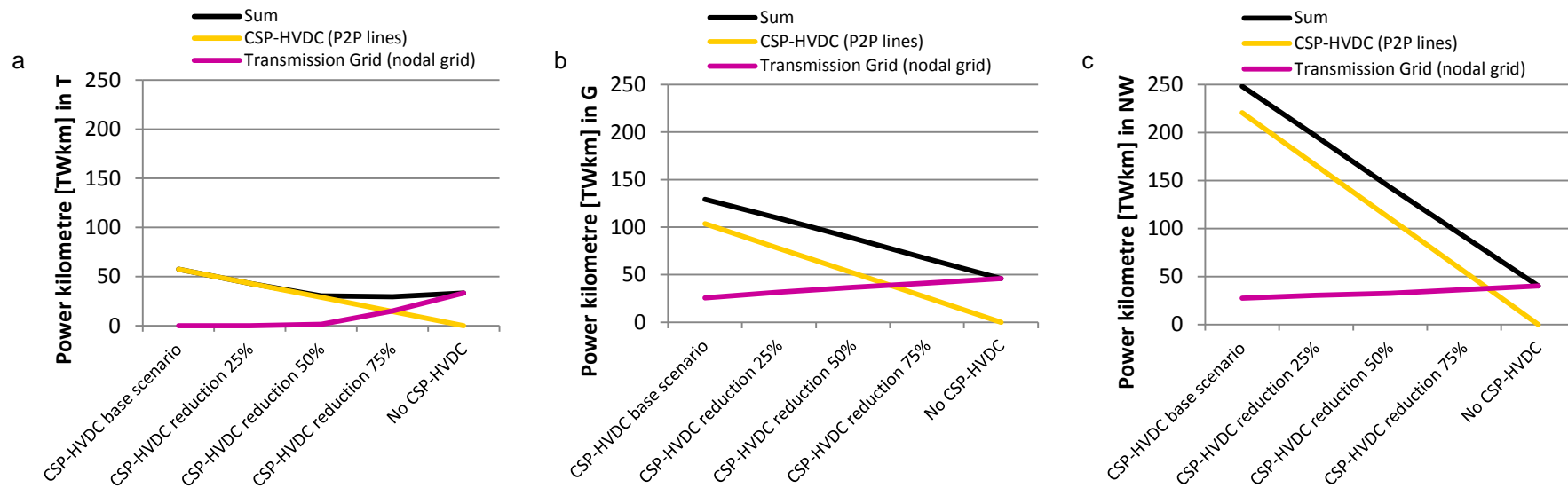


Figure 35: Trade-off of power kilometre between CSP-HVDC (P2P lines) and Transmission grid (nodal grid). In (a) of model region **T**, in (b) of model region **G** and in (c) of model region **NW**

If the rising gradient of the transmission grid is higher than the falling gradient of CSP-HVDC a reduction potential of total power kilometre occurs. This reduction is also visible with the sum of both shown power kilometre categories. Figure 35a reveals that gradient of transmission grid is higher than the gradient of CSP-HVDC in model region **T**. Thus, including CSP-HVDC can reduce total power kilometre. The northern the region the higher is the gradient of CSP-HVDC due to higher distance between CSP and offtaker. This is visible in Figure 35b with model region **G** and in Figure 35c with model region **NW**. Thus, the reduction potential of total power kilometre decreases in the northern model regions. However, the grid model is conservatively calibrated and bears a potential higher gradient of the nodal grid than assumed! Thus, more northern regions may profit from a reduction of total power kilometre. A reduction of nodal grid power kilometre can be achieved in almost every model regions and reduces therefore the effort in building new transmission lines spread inside a spatial area. The power kilometre of CSP-HVDC outside the territory of an offtaker model region should be designed as a cooperative project (see chapter 6). All regional results of power kilometre are available in the appendix in Figure 58.

#### 5.2.4.2 Utilisation of the overlay grid

In this section the influence of CSP-HVDC on the operation of the overlay is analysed. Therefore the focus of the analysis is the comparison of average utilisation and the number of capacity peaks of transmission lines.

The results in Table 22 show that higher shares of CSP-HVDC can lead to a reduction of the average utilisation and a reduction of capacity peaks of the overlay grid. Thus, an integration of CSP-HVDC yields a protective effect for the overlay grid against high stress.

Table 22: Comparison of the overlay grid utilisation

Grid utilisation	CSP-HVDC base scenario	-25% CSP-HVDC	-50% CSP-HVDC	-75% CSP-HVDC	No CSP-HVDC
Reduction of average utilisation	11%	2%	-7%	-3%	Reference
Reduction of capacity peaks* in link flow direction	29%	18%	11%	5%	Reference
against link flow direction	14%	10%	7%	4%	Reference

\*Peak is defined as 95% of max. link capacity

In the previous analysis it is outlined that a reduction of CSP-HVDC capacity leads to a higher capacity expansion of hydro reservoir and CSP in MENA. Thus, the question arises: is CSP in MENA is used for export to EU using the overlay grid? In section 5.1.2 it is delineated that electricity of CSP is probably transferred within the overlay grid, however it is not yet shown what happens if CSP-HVDC is excluded.

Figure 36 shows the effect of imports/exports via the overlay grid including and excluding CSP-HVDC. This comparison shows the regional difference in import/export of neglecting (Figure 36a) and integrating CSP-HVDC (Figure 36b). In the red ovals the results constitute a higher export from **NAE** and **NAW** in the case of the scenario "No CSP-HVDC" (Figure 36a). This indicates that CSP may be advantageous in Europe and transmitted through the grid. To verify this hypothesis, a correlation analysis of hourly technological generation in model region NAW and time series of export over selected transmission lines is done. The results of the correlation analysis are shown in Table 23.

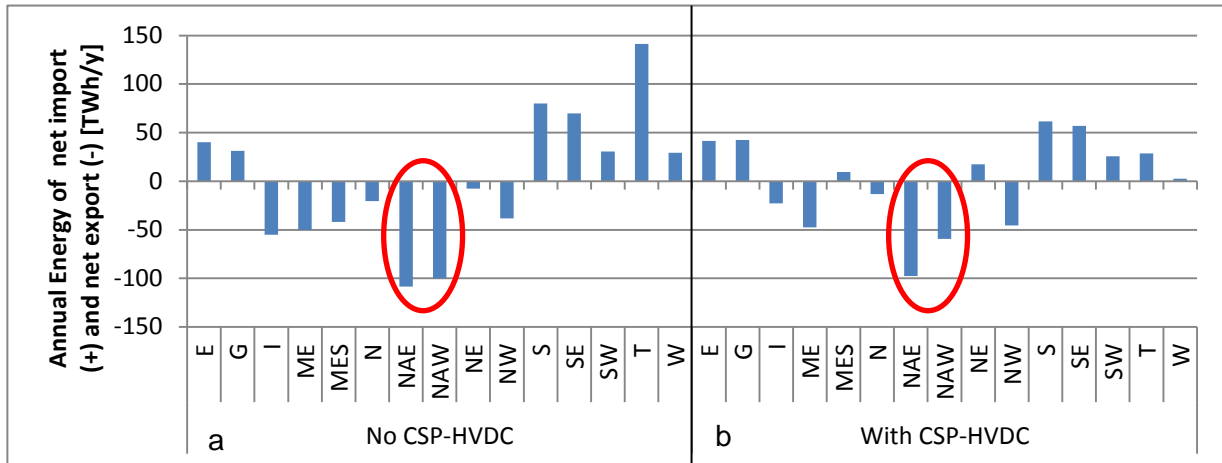


Figure 36: Annual Energy of import (positive) and export (negative) in the scenarios “No CSP-HVDC” (a) and “With CSP-HVDC” (b). Energy is transmitted over the overlay grid.

Table 23: Correlation based on hourly time series of generation out of CSP, PV, Wind Onshore and Wind Offshore in NAW and transmitted electricity from selected regions to surrounding regions – scenario “No CSP-HVDC”

Electricity generation in	Transmission line / export from - to	Transmission		Wind	Wind	PV and	Sum all
		CSP	PV	Onshore	Offshore	Wind	
NAW	NAW-W	58%	19%	-2%	-26%	21%	60%
NAW	NAW-SW	30%	-2%	7%	-8%	4%	29%
NAW	NAW-S	52%	7%	1%	-18%	9%	50%
NAW	NAW-NAE	-3%	-16%	16%	14%	-5%	-5%
NAW	SW-W	38%	21%	-7%	-30%	18%	41%
NAW	W-G	22%	17%	-20%	-18%	1%	20%
NAW	W-NW	27%	14%	-7%	-14%	10%	29%
NAW	S-G	43%	23%	-18%	-29%	11%	43%

Table 23 reveals that it is highly probable that CSP is exported in the scenario “No CSP-HVDC” (Figure 36a). Compared to PV and Wind, CSP has a higher correlation with the export time series of the analysed transmission lines. Thus, this technology is preferred as an exporting/importing energy resource.

### 5.2.5 System cost and annual cost

As illustrated in Figure 31 on page 84, system cost does not differ strongly in the scenarios with and without CSP-HVDC. Thus, system cost may not play the major role deciding if CSP-HVDC is advantageous for the energy system or not. Comparing the annual cost in MENA,

EU and Germany in Figure 31 on page 84, it is remarkable that the MENA region has about 18% lower annual cost than EU and about 8% lower annual cost than Germany.

Having in mind that different cost assumptions or learning curve development still may influence system cost significantly, an adequate energy mix can save billions due to high future system cost uncertainty (see Figure 17f on page 47).

### 5.2.6 CO<sub>2</sub> emission

The scenarios shown in Figure 31 on page 84 have an equal CO<sub>2</sub> emission limit in EUMENA. A CO<sub>2</sub> emission limit for the entire examination area EUMENA leads to a regional optimization of the use of carbon emitting energy. Thus, the sum of emissions in entire EUMENA is constant but varies depending on the region. As mentioned in section 5.1.5, CSP-HVDC can support the use of carbon emitting technologies in MENA countries if EU countries integrate this technology. This is an advantageous possibility for MENA having a higher degree of freedom to emit CO<sub>2</sub>.

## 5.3 Used techno-economic data

The objective of the analysis is to model CSP-HVDC and CSP relative conservatively compared to other technologies. This facilitates a conservative examination of CSP-HVDC and CSP to analyse their value strictly avoiding an overestimation of this technology. Therefore the applied techno-economic data for other technologies are rather optimistic.

The bandwidth of cost assumptions (€<sub>2015</sub>) and technological characteristics in Table 24 to Table 30 are assumed from today's point of view and can differ from reality especially when projecting an energy system in the year 2050.

Table 24 to Table 30 include an exchange rate with 1\$ at the parity of 1.35 €. Some values are based on a time value of money the year 2010. Therefore an inflation rate of 10% is considered from 2010 to 2015 to calculate the time value of money of the year 2015. The mean values are not listed in the tables but are calculated according to the average of max and min values.

Table 24: Cost and technology parameters for power plants in the year 2050 based on expert assumptions

Technology	Cost sensitivity	Specific investment [k€/MWe]	O&M Fix [%/y] of investment	O&M Variable [€/MWh]	Fuel cost [€/MWh]	Amortisation Time [y]	Interest Rate	Efficiency [-] net	Availability	Capacity Credit [-]																																																																																																																																																														
Photovoltaic	max	1150	0.04	0.00		20	9%	1	98%	0																																																																																																																																																														
	min	597	1.10	0.00		40	3%				Wind Onshore	max	1272	2.10	4.33		18	9%	1	95%	0	min	769	1.61	2.44		24	3%	Wind Offshore	max	2275	3.64	13.87		16	9%	1	95%	0	min	1052	3.49	9.55		22	3%	Run-Of-River	max	5541	5.50	4.84		40	9%	1	95%	0	min	5541	2.75	2.44		60	3%	Hydro Reservoir	max	2113	5.00	1.00		40	9%	1	98%	0	min	1017	5.00	1.00		30	3%	Solid Biomass	max	3833	1.98	3.20	40.0	20	9%	0.35	90%	0.9	min	1647	5.60	2.90	25.0	30	3%	Geothermal	max	6797	3.00	0.10		20	9%	1	90%	0.9	min	3826	3.00	0.10		30	3%	CSP power block	max	1098	2.50	2.22		35	9%	0.37	95%	modelled with 0, however 0.9 is possible accepting firm capacity abroad	min	857	2.50	2.22		45	3%	CSP solar field	max	356 k€/MW <sub>thermal</sub>	2.50			20	9%		95%	-	min	166 k€/MW <sub>thermal</sub>	2.50			30	3%	CSP thermal storage	max	18 k€/MWh <sub>thermal</sub>	2.50			20	9%	0.95 and 0.05%/h self-discharge rate	95%	-	min	11 k€/MWh <sub>thermal</sub>	2.50
Wind Onshore	max	1272	2.10	4.33		18	9%	1	95%	0																																																																																																																																																														
	min	769	1.61	2.44		24	3%				Wind Offshore	max	2275	3.64	13.87		16	9%	1	95%	0	min	1052	3.49	9.55		22	3%	Run-Of-River	max	5541	5.50	4.84		40	9%	1	95%	0	min	5541	2.75	2.44		60	3%	Hydro Reservoir	max	2113	5.00	1.00		40	9%	1	98%	0	min	1017	5.00	1.00		30	3%	Solid Biomass	max	3833	1.98	3.20	40.0	20	9%	0.35	90%	0.9	min	1647	5.60	2.90	25.0	30	3%	Geothermal	max	6797	3.00	0.10		20	9%	1	90%	0.9	min	3826	3.00	0.10		30	3%	CSP power block	max	1098	2.50	2.22		35	9%	0.37	95%	modelled with 0, however 0.9 is possible accepting firm capacity abroad	min	857	2.50	2.22		45	3%	CSP solar field	max	356 k€/MW <sub>thermal</sub>	2.50			20	9%		95%	-	min	166 k€/MW <sub>thermal</sub>	2.50			30	3%	CSP thermal storage	max	18 k€/MWh <sub>thermal</sub>	2.50			20	9%	0.95 and 0.05%/h self-discharge rate	95%	-	min	11 k€/MWh <sub>thermal</sub>	2.50			30	3%														
Wind Offshore	max	2275	3.64	13.87		16	9%	1	95%	0																																																																																																																																																														
	min	1052	3.49	9.55		22	3%				Run-Of-River	max	5541	5.50	4.84		40	9%	1	95%	0	min	5541	2.75	2.44		60	3%	Hydro Reservoir	max	2113	5.00	1.00		40	9%	1	98%	0	min	1017	5.00	1.00		30	3%	Solid Biomass	max	3833	1.98	3.20	40.0	20	9%	0.35	90%	0.9	min	1647	5.60	2.90	25.0	30	3%	Geothermal	max	6797	3.00	0.10		20	9%	1	90%	0.9	min	3826	3.00	0.10		30	3%	CSP power block	max	1098	2.50	2.22		35	9%	0.37	95%	modelled with 0, however 0.9 is possible accepting firm capacity abroad	min	857	2.50	2.22		45	3%	CSP solar field	max	356 k€/MW <sub>thermal</sub>	2.50			20	9%		95%	-	min	166 k€/MW <sub>thermal</sub>	2.50			30	3%	CSP thermal storage	max	18 k€/MWh <sub>thermal</sub>	2.50			20	9%	0.95 and 0.05%/h self-discharge rate	95%	-	min	11 k€/MWh <sub>thermal</sub>	2.50			30	3%																																
Run-Of-River	max	5541	5.50	4.84		40	9%	1	95%	0																																																																																																																																																														
	min	5541	2.75	2.44		60	3%				Hydro Reservoir	max	2113	5.00	1.00		40	9%	1	98%	0	min	1017	5.00	1.00		30	3%	Solid Biomass	max	3833	1.98	3.20	40.0	20	9%	0.35	90%	0.9	min	1647	5.60	2.90	25.0	30	3%	Geothermal	max	6797	3.00	0.10		20	9%	1	90%	0.9	min	3826	3.00	0.10		30	3%	CSP power block	max	1098	2.50	2.22		35	9%	0.37	95%	modelled with 0, however 0.9 is possible accepting firm capacity abroad	min	857	2.50	2.22		45	3%	CSP solar field	max	356 k€/MW <sub>thermal</sub>	2.50			20	9%		95%	-	min	166 k€/MW <sub>thermal</sub>	2.50			30	3%	CSP thermal storage	max	18 k€/MWh <sub>thermal</sub>	2.50			20	9%	0.95 and 0.05%/h self-discharge rate	95%	-	min	11 k€/MWh <sub>thermal</sub>	2.50			30	3%																																																		
Hydro Reservoir	max	2113	5.00	1.00		40	9%	1	98%	0																																																																																																																																																														
	min	1017	5.00	1.00		30	3%				Solid Biomass	max	3833	1.98	3.20	40.0	20	9%	0.35	90%	0.9	min	1647	5.60	2.90	25.0	30	3%	Geothermal	max	6797	3.00	0.10		20	9%	1	90%	0.9	min	3826	3.00	0.10		30	3%	CSP power block	max	1098	2.50	2.22		35	9%	0.37	95%	modelled with 0, however 0.9 is possible accepting firm capacity abroad	min	857	2.50	2.22		45	3%	CSP solar field	max	356 k€/MW <sub>thermal</sub>	2.50			20	9%		95%	-	min	166 k€/MW <sub>thermal</sub>	2.50			30	3%	CSP thermal storage	max	18 k€/MWh <sub>thermal</sub>	2.50			20	9%	0.95 and 0.05%/h self-discharge rate	95%	-	min	11 k€/MWh <sub>thermal</sub>	2.50			30	3%																																																																				
Solid Biomass	max	3833	1.98	3.20	40.0	20	9%	0.35	90%	0.9																																																																																																																																																														
	min	1647	5.60	2.90	25.0	30	3%				Geothermal	max	6797	3.00	0.10		20	9%	1	90%	0.9	min	3826	3.00	0.10		30	3%	CSP power block	max	1098	2.50	2.22		35	9%	0.37	95%	modelled with 0, however 0.9 is possible accepting firm capacity abroad	min	857	2.50	2.22		45	3%	CSP solar field	max	356 k€/MW <sub>thermal</sub>	2.50			20	9%		95%	-	min	166 k€/MW <sub>thermal</sub>	2.50			30	3%	CSP thermal storage	max	18 k€/MWh <sub>thermal</sub>	2.50			20	9%	0.95 and 0.05%/h self-discharge rate	95%	-	min	11 k€/MWh <sub>thermal</sub>	2.50			30	3%																																																																																						
Geothermal	max	6797	3.00	0.10		20	9%	1	90%	0.9																																																																																																																																																														
	min	3826	3.00	0.10		30	3%				CSP power block	max	1098	2.50	2.22		35	9%	0.37	95%	modelled with 0, however 0.9 is possible accepting firm capacity abroad	min	857	2.50	2.22		45	3%	CSP solar field	max	356 k€/MW <sub>thermal</sub>	2.50			20	9%		95%	-	min	166 k€/MW <sub>thermal</sub>	2.50			30	3%	CSP thermal storage	max	18 k€/MWh <sub>thermal</sub>	2.50			20	9%	0.95 and 0.05%/h self-discharge rate	95%	-	min	11 k€/MWh <sub>thermal</sub>	2.50			30	3%																																																																																																								
CSP power block	max	1098	2.50	2.22		35	9%	0.37	95%	modelled with 0, however 0.9 is possible accepting firm capacity abroad																																																																																																																																																														
	min	857	2.50	2.22		45	3%				CSP solar field	max	356 k€/MW <sub>thermal</sub>	2.50			20	9%		95%	-	min	166 k€/MW <sub>thermal</sub>	2.50			30	3%	CSP thermal storage	max	18 k€/MWh <sub>thermal</sub>	2.50			20	9%	0.95 and 0.05%/h self-discharge rate	95%	-	min	11 k€/MWh <sub>thermal</sub>	2.50			30	3%																																																																																																																										
CSP solar field	max	356 k€/MW <sub>thermal</sub>	2.50			20	9%		95%	-																																																																																																																																																														
	min	166 k€/MW <sub>thermal</sub>	2.50			30	3%				CSP thermal storage	max	18 k€/MWh <sub>thermal</sub>	2.50			20	9%	0.95 and 0.05%/h self-discharge rate	95%	-	min	11 k€/MWh <sub>thermal</sub>	2.50			30	3%																																																																																																																																												
CSP thermal storage	max	18 k€/MWh <sub>thermal</sub>	2.50			20	9%	0.95 and 0.05%/h self-discharge rate	95%	-																																																																																																																																																														
	min	11 k€/MWh <sub>thermal</sub>	2.50			30	3%																																																																																																																																																																	

Sources: (Mai et al., 2012), (IEA, 2010), (Agency, 2010), (Department of Energy, 2011), (IEA, 2009), (OPENEI NREL), (Environmental Protection Agency, 2010), (IRENA, 2012), (Nitsch, et al., 2012), own assumptions

Table 25: Cost and technology parameters for storages in the year 2050

Technology	Cost sensitivity	Specific investment [k€/MWh]	O&M Fix [%/y] of investment	O&M Variable [€/MWh]	Amortisation Time [y]	Interest Rate	Efficiency [-] net	Availability	Capacity Credit [-]
Pump Storage storage	max	40 k€/MWh	2.80	-	30	9%	0%/h self-discharge rate		-
	min	5 k€/MWh	1.86	-	40	3%			
Pump Storage charge	max	400	2.80	3.80	20	9%	0.89	95%	-
	min	180	1.86	3.80	30	3%			
Pump Storage discharge	max	400	2.80	-	20	9%	0.90		0
	min	170	1.86	-	30	3%			
Power-to-Gas-to-Power (P2G2P) Storage	max	0.20 k€/MWh	3.00	-	25	9%	0%/h self-discharge rate		-
	min	0.20 k€/MWh	2.42	-	35	3%			
Power-to-Gas-to-Power (P2G2P) charge	max	1206 = 606 (alkali electrolysis) +600 (methanation)	3.00	2.30	15	9%	0.70* = 0.87 (electrolysis) x 0.85 (methanation) x 0.95 (compression)	95%	-
	min	922 = 322 (PEMFC) +600 (methanation)	2.42	1.64	20	3%			
Power-to-Gas-to-Power (P2G2P) discharge (gas turbine)	max	713	3.00	-	25	9%	0.465*		0.95
	min	417	2.42	-	40	3%			
Compressed Air Storage storage	max	60 k€/MWh	1.30	-	25	9%	0.125%/h self-discharge rate		-
	min	38 k€/MWh	1.30	-	35	3%			
Compressed Air Storage charge	max	310	1.30	2.70	20	9%	0.88	95%	-
	min	200	1.30	0.10	30	3%			
Compressed Air Storage discharge	max	400	1.30	-	25	9%	0.70		0
	min	260	1.30	-	35	3%			
Lithium Ion storage	max	220 k€/MWh	2.00	-	15	9%	0.001%/h self-discharge rate		-
	min	150 k€/MWh	2.00	-	25	3%			
Lithium Ion charge	max	25	2.00	0.22	15	9%	0.97	95%	-
	min	12.5	2.00	0.22	25	3%			
Lithium Ion discharge	max	25	2.00	-	15	9%	0.97		0
	min	12.5	2.00	-	25	3%			

Sources: (Mai et al., 2012), (Pregger, 2015), (Albrecht, et al., 2013), (Fürstenwerth, et al., 2014), own assumptions.

\*The overall efficiency of P2G2P is 0.70 (charge) x 0.465 (discharge) = 0.3255

Table 26: Cost and technology parameters for carbon emitting and nuclear technologies in the year 2050

Technology	Cost sensitivity	Specific investment [k€/MWe]	O&M Fix [%/y]	O&M Variable [€/MWh]	Fuel cost [€/MWh <sub>chem</sub> ]	Amortisation Time [y]	Interest Rate	Efficiency [-] net	CO <sub>2</sub> sequestration [-]	Availability	Capacity Credit [-]
Coal CCS Steam Turbine	max	2460	4	9.2	30	25	9%	0.299	0.85	0.896	0.9
	min	1807	4	9.2	18.9	40	3%				
Coal Steam Turbine	max	1418	4	0.1	30	25	9%	0.509	0	0.896	0.9
	min	1108	4	0.1	18.9	40	3%				
Combined CCS Cycle Gas Turbine	max	1203	4	3.5	65.2	25	9%	0.428	0.86	0.96	0.9
	min	867	4	3.5	40.1	40	3%				
Combined Cycle Gas Turbine	max	691	4	0.3	65.2	25	9%	0.621	0	0.96	0.9
	min	491	4	0.3	40.1	40	3%				
Gas Turbine	max	713	4	0.3	65.2	25	9%	0.465	0	0.95	0.9
	min	417	4	0.3	40.1	40	3%				
Lignite Steam Turbine	max	1750	4	0.1	11.1	25	9%	0.491	0	0.902	0.9
	min	1250	4	0.1	9.1	40	3%				
Nuclear Steam Turbine	max	13030	4	0.1	5.5	25	9%	0.309	-	0.90	0.9
	min	4684	4	0.1	5	40	3%				

Sources: (Nitsch, et al., 2012), (Nitsch, et al., 2013), (Rubin, et al., 2007), (European Commission, 2014), own assumptions, CCS O&M Variable are based on cost for CO<sub>2</sub> transport (3€/t) and CO<sub>2</sub> storage (4.45 €/t) (Goerne, 2009)



Table 27: Specific CO<sub>2</sub> emission

Fuel	tCO <sub>2</sub> /MWh <sub>chem</sub>
Coal	0.3348
Lignite	0.3996
Natural Gas	0.2016
Nuclear	0
Biomass	0

Source: (Nitsch, et al., 2012)

Table 28: CO<sub>2</sub> certificate cost representing environmental impact

Cost sensitivity	€/tCO <sub>2</sub>
max	82.5
mean	62.7
min	49.5

Source: (Nitsch, et al., 2012)

Table 29: Techno-economic parameters of AC and DC infrastructure in the scenario analysis

	AC	DC	DC converter	Losses
OHL	500.000 €/km	786.000 €/km	148.730.000 € per station	20.7 (AC), 4.5 (DC) %/1000km
UGC	944.000 €/km	2.271.350 €/km	148.730.000 € per station	5.7 (AC), 3.5 (DC) %/1000km
Sea cable	1.132.000 €/km	2.672.000 €/km	148.730.000 € per station	2.7 %/1000km
Specific Capacity	1005 MW	1500 MW	1500 MW	
Specific Voltage	380 kV	600 kV		

Losses of converter station are assumed with 0.7%. Sources: (Brakelmann, 2004), (Trieb, et al., 2012), (Hess, 2013). Here no AC converter station is considered, because of the integration of all grid relevant cost with the node-internal grid model in chapter 5.

Table 30: Learning curve approach of CSP solar field, thermal storage and power block based on installed capacity and progress ratio

Cost sensitivity	Unit	Current state	MAX	MEAN	MIN	Unit	Progress Ratio MAX	Progress Ratio MIN
year		2015	2050	2050	2050			
Installed capacity	MW	4,700	120,000	835,000	1,550,000			
Solar Field	[k€/MW <sub>th</sub> ]	647	355	260	166	[-]	0.88	0.85
Thermal Storage	[k€/MWh <sub>th</sub> ]	50	19	15	11	[-]	0.80	0.83
Power Block	[k€/MW <sub>el</sub> ]	1206	1098	978	857	[-]	0.98	0.96

Sources: based on (Neij, 2008) and (Trieb, et al., 2012), (CSP-Today, 2016), (Viehbahn, et al., 2008), (Greenpeace, 2009)

## 6 Perspective of a CSP transfer option

This chapter provides a perspective how a CSP-HVDC power plant could be implemented. The next possible steps are concretised and it is shown which breakthroughs are still to be achieved.

The perspective on a possible business case examines the example “MEFID Solar Link” as a representative bundled infrastructure for economic regions in Europe.

### 6.1 Potential business case MEFID Solar Link

Due to the mentioned system advantages of CSP-HVDC a real business case is possible if the CSP-HVDC power plant is a closed and manageable system. Until the first power can flow, a feasibility or pilot study is necessary to identify more details for an implementation.

#### 6.1.1 Need of a feasibility study

The EU research project BETTER made clear that an international electricity infrastructure can be supported by the EU (e.g. project of common interest). Multilateral initiatives (producer, transmitter and offtaker) are the basis for a start. Countries and continents worldwide already use a concept of connecting power plants (often water power plants) with bigger cities via HVDC (ABB, 2017). Unfortunately, until today no CSP-HVDC initiative in EUMENA took place.

The next specific step towards an implementation of a CSP-HVDC power plant should be a feasibility study analysing *geographical, technical and financial impact, as well as political and framework assessment* (BETTER, 2015). For this purpose the proposal is the picture of the Four Motors for Europe and Morocco called “MEFID Solar Link” (**M**orocco, **E**spaña, **F**rance, **I**talia, **D**eutschland) as drafted in Figure 37. Each region of the Four Motors has a separate CSP-HVDC power plant but a common bundled HVDC corridor. Geographical routes of each CSP-HVDC plant are illustrated in Figure 38. The advantages of these exemplary economic and progressive European regions are their demand and the experience with CSP in Morocco. A bundling of the point-to-point links and also a common use of the water infrastructure in Morocco are good reasons to start a common project. Morocco and the Four Motors can create with the use of sustainable water new living area in desert regions, agriculture and job possibilities. Renewable dispatchable energy can lead to a WIN-WIN for all participants involved (Hess, et al., 2014).

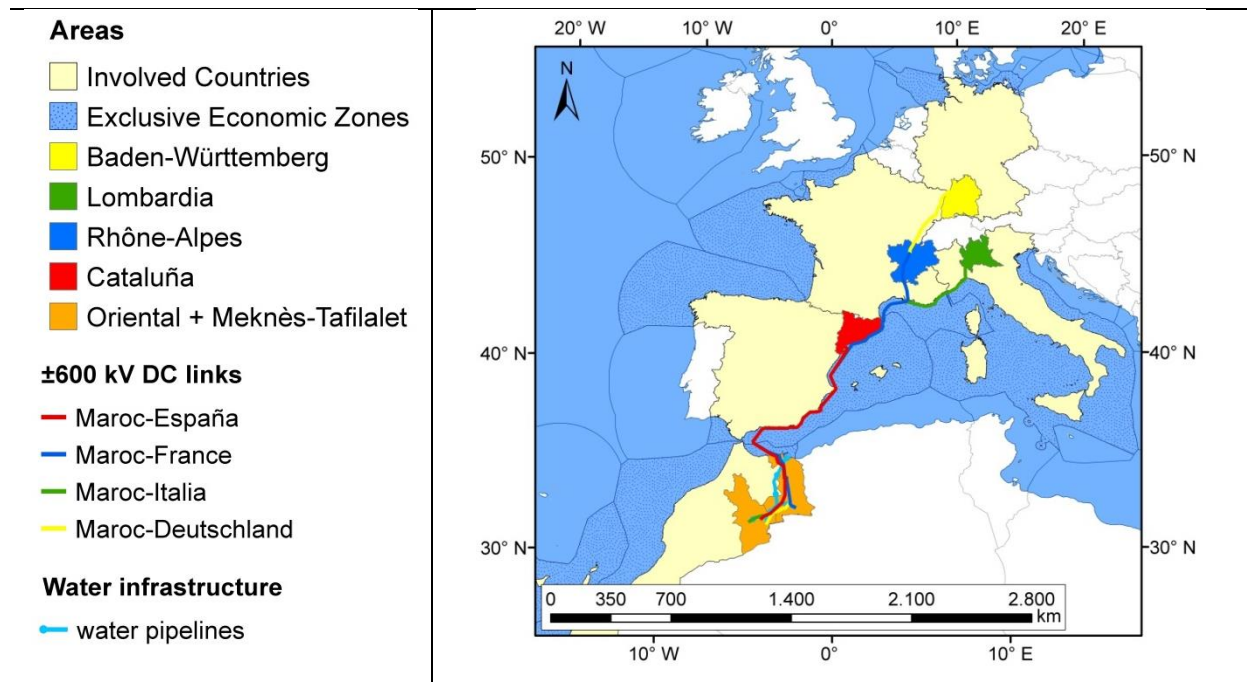


Figure 37: MEFID Solar Link – schematic bundling of common infrastructure

Other CSP-HVDC power plants can follow a successful implementation of such a pilot project. Regarding the rising energy demand of mega cities, communities worldwide might be a suitable off-taker of renewable dispatchable energy from distance to cover their energy needs. Now it can be EUMENA showing the world that it is still possible to cooperate and to build up trust in a multi-national and multi-cultural environment. The entrepreneurial risk of a CSP-HVDC power plant with its high investment (~15 bn € for 1.5GW<sub>net</sub>) should not be underestimated. Thus, it would be an option to disperse the risk among many by simultaneously guaranteeing their energy provision. The call becomes loud for governmental initiatives like it used to be in the start phase of nuclear power plant implementation with direct subsidies. However, with the right framework made from legislative institutions (guarantees, power purchase agreement, etc. – no direct financial subsidies) it is conceivable that a mixture of investors from all parts of society can manage such a project in a participatory enterprise like in many present local initiatives for renewable energy.

Table 31 lists an approximation of the dimension and cost of CSP-HVDC for the example of the Four Motors for Europe. The analysis is based on the learning curve of CSP cost in the year 2025 and HVDC cost assumptions according to (Hess, 2013). To save expenses, a combination of CSP and PV inside a power plant is useful to cover the electrical demand of mirror tracking and pumps with about 13.5% PV of total capacity instead of using CSP solely. The water demand of the four CSP power plant parks is about 17Mm<sup>3</sup>/y for mirror cleaning, supplying workers and using a dry cooling. An additional demand of 20 Mm<sup>3</sup>/y is assumed for agricultural use around the power plants. The cost and dimension of water desalination is

according to (Moser, 2015) with an investment of 1800 €/m<sup>3</sup>/d and 148 GWh/y electrical demand. Cost of the collective water pipeline is assumed with 1300 €/m (1000€ per diameter and meter). The total investment cost of CSP-HVDC including the water infrastructure are between 9600 and 11330 €/kW<sub>net</sub>. LCOE are about 12-13 €/Cent/kWh using the calculation approach according to (Hess, 2013).

Table 31: Approximation of CSP-HVDC configuration and cost for a parabolic trough with HVDC underground cables for the Four Motors for Europe

Region	Catalunya	Rhône-Alpes	Lombardia	Baden-Württemberg
Annual net electrical demand in 2015	48 TWh/y (Instituto Catalán de Energía, 2016)	61 TWh/y (RTE, 2016)	65 TWh/y (TERNA, 2016)	75 TWh/y (Statistisches Landesamt, 2017)
CSP-HVDC net capacity and annual power	1.50 GW → 10.6 TWh/y	1.50 GW → 10.6 TWh/y	1.50 GW → 10.6 TWh/y	1.50 GW → 10.6 TWh/y
CSP and PV power plant gross capacity in Morocco and investment	1.93 GW CSP 0.26 GW PV 10.85 bn €	1.97 GW CSP 0.26 GW PV 11.08 bn €	1.98 GW CSP 0.26 GW PV 11.16 bn €	2.00 GW CSP 0.27 GW PV 11.28 bn €
Point-to-point line length and investment	1440 km 3.3bn €	2150 km 4.7bn €	2440 km 5.3bn €	2670 km 5.7bn €
Collective water infrastructure and investment	37Mm <sup>3</sup> /y (105m <sup>3</sup> /day); 600 km pipelines in Morocco ~1.0bn € (water price of ~1.80 €/m <sup>3</sup> incl. capital and O&M cost)			
Total investment	14.4 bn € 9600 €/kW <sub>net</sub>	16.1 bn € 10730 €/kW <sub>net</sub>	16.7 bn € 11130 €/kW <sub>net</sub>	17.0 bn € 11330 €/kW <sub>net</sub>
LCOE	12 €/Cent/kWh	12 €/Cent/kWh	13 €/Cent/kWh	13 €/Cent/kWh

Total investment can still drop with a decreasing learning curve of CSP if this technology is further implemented. LCOE strongly depend on interest and discount rate and amortization time. Interest can be reduced by guarantees.

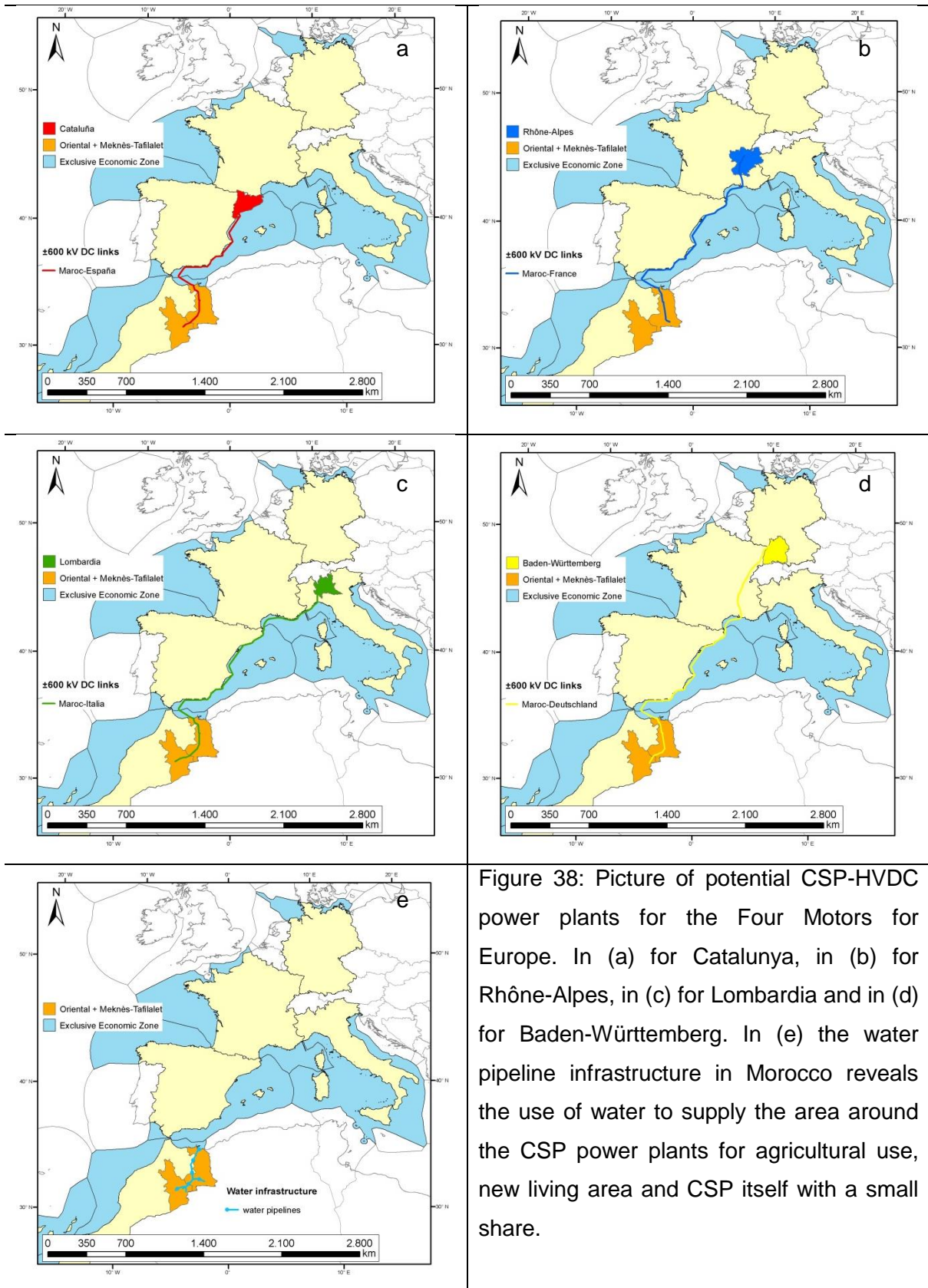


Figure 38: Picture of potential CSP-HVDC power plants for the Four Motors for Europe. In (a) for Catalunya, in (b) for Rhône-Alpes, in (c) for Lombardia and in (d) for Baden-Württemberg. In (e) the water pipeline infrastructure in Morocco reveals the use of water to supply the area around the CSP power plants for agricultural use, new living area and CSP itself with a small share.

## 7 Summary and outlook

This chapter summarizes the major findings for the value of CSP-HVDC, the scientific contribution of the thesis and gives an outlook of further research demand.

Table 32 highlights the qualitative comparison of the used evaluation criteria. It shows higher (-), lower (+) or equal (0) values for two energy systems neglecting CSP-HVDC and integrating CSP-HVDC. This qualitative comparison targets to evidence system advantages and disadvantages. Table 32 reveals with the background colours a final evaluation of the indicators for the two energy systems. The evaluation of the indicators can depend on an integration of CSP-HVDC per se or on the share of CSP-HVDC and model region. The latter concerns system cost uncertainty and total power kilometre.

Table 32: Comparison of evaluation criteria of two energy systems in EUMENA without and with CSP-HVDC

Evaluation criteria	Indicators (higher - / lower + / equal 0)	No CSP-HVDC	With CSP-HVDC
Cost	System cost	0	0
	System cost uncertainty	-	- / + <sup>a</sup>
Infrastructure	Power plant capacity	-	+
	Electrical storage capacity	-	+
	Total power km <sup>*</sup>	- / +	- / + <sup>a</sup>
	Nodal grid power km	-	+
	CSP P2P power km	+	-
Operational behaviour	Grid stress	-	+
	Curtailment	-	+
Emission	CO <sub>2</sub> emission	0	0 / + <sup>b</sup>

Legend of indicator evaluation

	negative		balanced		positive		neutral
--	----------	--	----------	--	----------	--	---------

\* Total power kilometre is defined as capacity of a power line over distance. This includes the overlay grid, P2P and nodal grid.

<sup>a</sup> Evaluation is positive because the indicator can show a lower impact with CSP-HVDC having more options for action. The indicator strongly depends on the share of CSP-HVDC and the model region.

<sup>b</sup> Evaluation is neutral because the influence of the lower indicator is insignificant on the entire energy system. A lower indicator can be achieved depending on the model region and allows a higher degree of freedom and options for action in a model region.

## 7.1 Résumé of evaluation criteria

This section resumes the comparison of two energy systems (without and with CSP-HVDC) in the EUMENA region considering the evaluation criteria of Table 32.

### Cost:

- System cost:

A minimization of system cost is a major objective for an energy system. As shown in Figure 31 on page 84 results of system cost differences between two scenarios can be small. Thus, comparing a system without and with CSP-HVDC, system cost differs not much. Due to high cost uncertainty for a future energy system in the year 2050 (up to  $\pm 50\%$  of medium system cost) a statement of future system cost is not robust. Therefore the indicator is evaluated as neutral to avoid a wrong evaluation.

- System cost uncertainty:

System cost bandwidths represent system cost uncertainty. Such bandwidths are analysed for Germany with different shares of renewable and dispatchable energy shares in Figure 17f on page 47. A well-balanced mix of dispatchable and fluctuating energies to about equal shares can reduce system cost uncertainty up to 7% of maximum system cost bandwidth. Such a mix includes CSP-HVDC as supplementing technology to achieve an adequate dispatchable share. However, a high share of CSP-HVDC can also increase system cost uncertainty. Without CSP-HVDC a minimum system cost uncertainty can't be reached for Germany in a complete renewable energy system. Other dispatchable renewable energies are limited in their resource potential and can't contribute sufficiently to a suitable renewable dispatchable energy share. Thus, CSP-HVDC reduces system cost uncertainty. The indicator system cost uncertainty is therefore considered to be positive for a system that includes an adequate share of CSP-HVDC and negative if this technology option is missing.

### Infrastructure:

- Power plant capacity and electrical storage capacity:

The capacities of energy supply and flexibility options such as electrical storage represent an environmental indicator for the energy system. Higher capacities can have a higher environmental impact. Hence, the assumption of high capacities to low cost needs to be scrutinised. Comparing the scenarios with and without CSP-HVDC, the capacity with CSP-HVDC is lower. Avoiding high supply peaks of fluctuating energies, CSP-HVDC can complement such technologies and avoids a high capacity expansion. Also its firm capacity can reduce back-up capacity in EU, if firm capacity abroad is politically accepted as such.

- **Total power kilometre:**

As shown in Figure 23 on page 61 a transmission of electricity over distance is a cost-efficient flexibility option. The use of an overlay grid, point-to-point transmission lines and the expansion of nodal grid reduces cost, curtailment, power plant and storage capacity expansion. However, high amounts of power kilometre are hard to implement due to low social acceptance (Steinbach, 2013). The consequences of a reduced power kilometre expansion are higher values of evaluation criteria such as power plant and storage capacities and curtailment. Using high shares of CSP-HVDC increases total power kilometre. An adequate share of CSP-HVDC leads to lower total power kilometre for some model regions (see Figure 35 on page 90). This increases the impact with respect to other evaluation criteria but it still leads to lower evaluation criteria than a scenario without CSP-HVDC. The indicator total power kilometre is therefore considered to be positive due to a higher degree of freedom and more options for action including CSP-HVDC. Without this technology the indicator is evaluated as balanced due to a potential higher but also lower impact for the entire EUMENA region.
- **Nodal grid and CSP-HVDC P2P:**

The nodal grid, defined as the combination of transmission and distribution grid inside a region, is expanded in the case of a higher share of fluctuating energy. In other words: the lower the dispatchable share the higher the nodal grid expansion. A scenario that includes CSP-HVDC reduces power kilometre of the nodal grid (see Figure 34 on page 89). However, as mentioned before, higher shares of CSP-HVDC can increase total power kilometre due to more needed CSP-HVDC P2P power kilometre. Thus, a trade-off arises between nodal grid power kilometre and CSP-HVDC P2P power kilometre. An adequate CSP-HVDC share is therefore essential to reduce total power kilometre.

**Operational behaviour:**

- **Grid stress:**

The operational behaviour of the grid is influenced by the capacity limit of transmission lines. The more often the capacity limit is reached the higher the stress for the grid and the more often is the potential intervention by the transmission system operator. Reaching capacity limits of the transmission lines is analysed by numbers of peaks in the grid. Including CSP-HVDC reduces such peaks up to 29% and therefore the grid stress (see Table 22 on page 91). Reducing peaks leads to fewer possible bottlenecks in the grid. Consequently, CSP-HVDC allows a better application possibility of the grid.



- **Curtailment:**

Managing a high share of curtailment is a major challenge for the operation of the energy system. A higher curtailment means a higher intervention to curtail energy of specific power plant parks. Some small power plants such as decentralised PV are difficult to curtail due to missing switches. An open question is also how such interventions can be executed with the acceptance of the power plant operator. CSP-HVDC can reduce the amount of electrical curtailment of up to 25% compared to the scenario without this technology (depending on CSP-HVDC share and region – see Figure 59 on page 167). Thus, CSP-HVDC allows an easier system operation.

**Emission:**

- **CO<sub>2</sub> emission**

CO<sub>2</sub> emission is equal in both scenarios for EUMENA. However, the regional CO<sub>2</sub> emission differs. In the scenario with CSP-HVDC, the MENA regions have a higher degree of freedom to emit CO<sub>2</sub> while they would still stay inside the EUMENA carbon emission limit. This means a small advantage of using CO<sub>2</sub> emitting technologies. The EU region can therefore support the MENA region by integrating CSP-HVDC. However, the difference of regional CO<sub>2</sub> emission is small and has a low impact. Thus, the indicator is considered to be neutral.

**Conclusion: the value of CSP-HVDC**

The summary of Table 32 shows, that the advantages of an inclusion of CSP-HVDC outweigh the disadvantages regarding the applied evaluation criteria. This leads to the conclusion that CSP-HVDC is useful and promising for the energy system in EUMENA, and in its sub-regions EU, MENA and Germany. Having in mind that CSP-HVDC is conservatively modelled, the outlined advantages are underestimated rather than overrated. Finally, it depends on the share of CSP-HVDC capacity that quantifies the resulting advantages and disadvantages for the energy system.

## 7.2 Additional research results

### **Influence of cost assumption on evaluation criteria applying the REMix model**

As shown in section 5.1.1, cost assumptions can influence all other evaluation criteria. The essential point is the cost proportion of technologies to each other which determines the chosen technologies. When minimizing cost with the REMix model, only the minimal cost is chosen. This self-evident statement reveals that also small cost differences of technologies can lead to a complete exclusion of a single technology for the energy system (penny flip effect) which seems unrealistic. Cost sensitivities are a solution for this effect using cost minimisation.

In section 5.1.2, the influence of an unlimited overlay grid compared to its exclusion is demonstrated. Excluding the overlay grid leads to about 7% higher system cost but a massive change in grid expansion (e.g. 176% more power kilometre). Thus, a small system cost change can lead to a recognizable change of all other evaluation criteria. In other words: system cost of different energy systems can be very similar. Other evaluation criteria beside cost may therefore determine a sustainable energy system which may not be extremely cost-optimal.

### **Overlay grid vs. point-to-point CSP-HVDC**

Overlay grid and CSP-HVDC P2P can both reduce power plant and electrical storage capacity and curtailment of the energy system to about same energy system cost (Figure 23 on page 61 and Figure 31 on page 84). The major difference is the increasing stress of the overlay grid when CSP-HVDC is not integrated (Table 22 on page 91).

One of the results of the REMix model is an overlay grid with a huge transmission capacity expansion (Figure 23 on page 61). Such a massive overlay grid capacity is due to its assumed minimal cost characteristic and does not integrate CSP-HVDC in that framework (Figure 22 on page 61). However, CSP is used for a transmission via the overlay grid from MENA to EU (Table 15 on page 65). This result of the model means that CSP in MENA is beneficial for the use in EU. However, the building of such a huge overlay grid is unrealistic especially as a first step.

The major barrier of building an overlay grid is its unclear financing and operation over a large spatial area. As a first step it might be easier to implement CSP-HVDC and additionally to expand specific transmission lines of the overlay grid. Another barrier of the overlay grid is that single regions can be stressed by a large number of power kilometres and do not profit much from such a grid (e.g. model region SW in section 5.1.2). For CSP-HVDC also high power kilometre can occur for some regions. In this case CSP-HVDC can be bundled and may lead to a lower impact than a spatial extend of an overlay grid. CSP-HVDC offers also a specific financial and procedure participation of affected persons due to its project specific

characteristic (Hess, 2013). Each CSP-HVDC can be handled as a single project with precise business case possibility (Hess, 2013). This may also be the case for certain grid expansion corridors in a specific overlay grid. The application of an overlay grid together with CSP-HVDC is essential to use the spatial flexibility of a proportionate overlay grid and a suitable share of renewable dispatchable energy of CSP-HVDC. Their synergetic combination can reduce infrastructural requirements and allow an easier system operation.

### **Probability of an integration of CSP-HVDC and configuration of CSP-HVDC and CSP**

Regarding the cost sensitivity analysis in section 5.1.3, a high empirical probability for CSP-HVDC is reached with up to 66% for some EU regions. Model regions like **E, G, S, SE, T** and **W** feature a relative high probability to integrate this technology while others like **N, NW, NE** and **SW** have a smaller preference.

The configuration of CSP-HVDC in Figure 27 on page 74 shows a high solar multiple of 4-6 and thermal storage full load hours of ~13h. CSP-HVDC is thus configured as a flexible base load power plant in the energy system. The CSP power plants inside the EU for domestic use have a lower solar multiple and lower thermal energy storage full load hours due to other more efficient technologies and the drastic reduction of DNI in winter. CSP in EU for domestic use shows therefore a commitment to medium load levels.

The potential demand for land of CSP-HVDC for EU (in MENA) and CSP for MENA (in MENA) can be in the same extent with around 40.000km<sup>2</sup> each (Figure 28 on page 75). Thus, EU and MENA can implement such technologies hand in hand (one mirror for MENA, one mirror for the EU) and use such desert areas meaningfully. Such desert areas can be transformed to useful arable land. The absolute demand of land for CSP-HVDC for EU is potentially lower than the demand of land for CSP for the use inside MENA.

### **Comparison of CSP with nuclear energy and CCS**

Low carbon dispatchable technologies such as nuclear power plants, coal and CCGT CCS and CSP are compared in section 5.1.3 and 5.1.4. The results show that nuclear power plants have higher cost and therefore a lower probability of an integration (Figure 26a, c on page 72) than CSP-HVDC in the majority of model regions. Compared to CSP, nuclear power plants reveals advantages of other analysed evaluation criteria such as fewer power kilometres (Figure 29 on page 78). CCS technologies do not show a high influence on the energy system (Figure 26f on page 72). Their operational characteristic is not comparable to CSP or nuclear power plants (Figure 30 on page 80). As a model result, low annual full load hours of CCS (~1000h/y) define this technology as peak load power plant. Nuclear and CSP are endogenously designed as base load power plants (~6500h/y). Due to the used and

limited evaluation criteria a holistic comparison of nuclear power plants and CSP can't be done and should therefore be in the focus of further research activities.

### 7.3 Scientific contribution

This section shows as highlights the contribution of the thesis to the scientific body of knowledge with two major novelties. The core of the thesis is to find a suitable framework to assess the value of CSP-HVDC and to show the value of this technology. For such a framework a new node-internal grid model is developed. The analysis of the value of CSP-HVDC includes uncertainty, empirical probability and a multi-criteria view of the energy system.

#### **New methodology of modelling the transmission and distribution grid**

- Introduction of a node-internal grid model which represents the grid and reduces its complexity.
- The model considers major grid expansion drivers and grid integration cost of fluctuating renewable energies
- Calibration of the model using a high spatio-temporal resolution and validation

#### **New analysis of the value of CSP-HVDC using an energy system model**

- Consideration of uncertainty by cost sensitivity analysis
- Introduction of a capacity integration probability as a frequency function (EPTI)
- Multi-criteria analysis applying evaluation criteria

### 7.4 Further research demand

Two important improvements of energy system modelling are the use of adequate high resolution data and diverse methods modelling near reality. Thus, a broad and deep analysis should be the goal of future energy system analysis research. Concretising the idea of CSP-HVDC, a feasibility study is essential to identify more details for an implementation.

#### **7.4.1 Data**

Assuming that the energy system is quite sensitive to short disruptions and possibly affected by load imbalance in short time phases, a higher temporal resolution than hourly would be a major improvement in modelling. However, computational constraints are today's major barriers. Thus, higher computer performance is needed or the complexity of such analyses must be reduced by a representation of system relevant effects (or both). Especially high fluctuating renewable energy shares with high production peaks may influence energy system analysis. Analysing e.g. short-term storages needs a tighter than hourly temporal resolution (Haas, et al., 2017). Isolated technological systems like PV and battery are already analysed in temporal sensitivity (Beck, et al., 2016). Moreover, a quantification of the temporal effect on an entire energy system may be the focus of further research activities.

#### **7.4.2 Multi-criteria consideration, optimization, simulation and evaluation**

An energy system is often characterised by pluralism. Considering only the cost or cost dependent objective functions reduces the energy system to cost driven impacts alone. Future analyses should use a multi-objective consideration including diverse sustainability criteria such as economy, ecology, social and institutional factors (Kopfmüller, et al., 2001). Interdependencies of multi-criteria may show a better understanding of their impact to each other and to the system. Primarily a sustainable energy provision combined with the secure supply of water and food should be included in a multi-criteria analysis thereby considering an increasing world population in a time with increasing conflicts. The “water, energy, and food security nexus” considers such sustainability criteria (EU, 2017).

Optimizing with several objective functions some unrecognized frame conditions may still exist. This can lead to one-sided results such as the consideration of only the cost objective function. A suitable weighting of the objective functions among each other is therefore essential to quantify their impact. The method of multi-objective optimization can still be constituted by a linear model but also a genetic or evolutionary optimization such as particle swarm optimization can be taken into consideration (Coello, et al., 2004). Other research activities to date in multi-criteria optimization e.g. (Rabbani, et al., 2018) using such optimization methods, focus on self-contained technological models but not on a complete energy system.

Beside an optimization also a simulation can be performed showing if a power plant park, its grid and storage can be comprehensibly financed, manageably constructed and meaningfully operated. Thereby, different results of an optimization might be used and compared with such a simulation leading to a multi-criteria evaluation of an energy system.

#### **7.4.3 System configuration of CSP and conceptual technological alternatives**

The conservative techno-economic assumptions of CSP in the thesis lead to the research question of optimizing this technology in its profitable function for the energy system. Such an optimization can be a combination of CSP and PV. The use of the thermal storage as a medium term storage by the entire energy system can be also a promising possibility for CSP because electricity can be stored in the thermal storage of CSP to avoid otherwise higher electrical storage capacity and curtailment of the energy system. The high solar multiple of CSP-HVDC (4-6) leads to potential constructional questions especially regarding parasitics in a large solar field size. Transforming desert areas in arable land raises the question which of the CSP technologies (tower, trough or Fresnel) is favourable to be used for this purpose and at the same time efficient for an export via HVDC.

Conceptual technological alternatives to CSP-HVDC have a low technology readiness level such as Wind or PV combined with a thermal/electrical storage, heat pump and co-firing option, or nuclear fusion and are therefore intangible. Technological breakthroughs are

uncertain from today's point of view. Such technological concepts are important for further research activities but should be definitely no obstacles to concretise technically functioning CSP-HVDC reaching climate protection targets as soon as possible.

#### 7.4.4 Feasibility study

Further research in the field of applied energy infrastructures should be in the focus to accelerate the energy transition towards low carbon emissions. A major barrier but also a people-uniting chance could be the point-to-point connection of CSP-HVDC in a multinational environment. The most important spark is the human willingness for a specific project implementation. To implement such a system beneficial technology, it needs at first a CSP-HVDC feasibility study and the will to finance such a study. Secondly, it requires the intention from offtakers in the EU to purchase such electricity. Power purchase agreement and guarantees are essential for financial issues (Hess, 2013). Thirdly, it needs the agreement of a region in MENA to provide suitable land for the CSP-HVDC power plant. Than a convenient HVDC point-to-point transmission pathway must be found including participatory issues. Neglecting other essential details in between which might emerge only in a feasibility study, investors must be found, approvals must be granted and the construction can begin. Open questions remain for a specific implementation of this technology if no interdisciplinary feasibility study e.g. in *geographical, technical and financial impact, political and framework assessment* is realised (BETTER, 2015). Thus, such a study is essential for a further step benefiting from the multifaceted system advantages of CSP-HVDC.

#### 7.5 Final conclusion

Today the option of CSP-HVDC is not on the agenda for the energy transition in the EU or in national action plans. However, CSP-HVDC offers great chances of an energy transition towards low CO<sub>2</sub> emission. CSP-HVDC provides dispatchable renewable energy according to demand. This feature is rarely available in the EU. Therefore, the EU and MENA can profit mutually (WIN-WIN) from a business case opportunity of a transfer of such dispatchable energy. In EU the energy system benefits from lower system cost uncertainty, less capacities of power plants and electrical storages, lower nodal grid expansion, lower grid stress with fewer bottlenecks and lower curtailment. The technological option of CSP-HVDC reduces the amount of open questions and unknown barriers and therefore provides more reliable implementing possibilities for a successful energy transition ahead of us. Especially the operation of an energy system with a small share of dispatchable energy is rather unclear. The inclusion of a technology such as CSP-HVDC implies also a higher technological degree of freedom, more options for action and greater diversity.

Finally, it is a decision of the society in EUMENA if CSP-HVDC should be implemented within an international cooperation that can build common ways connecting people.

## 8 Data Sets

GADM (2012): Database of Global Administrative Areas <https://www.gadm.org/>

Marine Regions (2013): Claus S. et al. <http://www.marineregions.org>

Load time series (hourly):

- ENTSO-e in 2006 <https://transparency.entsoe.eu/>
- Arab Union of Electricity (AUE) in 2010
- Synthetic load profile from (Gruber, 2012)

## 9 References

**ABB. 2017.** HVDC. [Online] 2017. [Zitat vom: 06. 22 2017.]

<http://new.abb.com/systems/hvdc>.

**Abdalla, O. H., Al-Hadi, H. und Al-Riyami, H. 2009.** Development of a Digital Model for Oman Electrical Transmission Main Grid. *IEEE*. 01. 06 2009.

**Afridi, M. und Baryalay, H. 2012.** United Arab Emirates - Energy Regulation and Markets Review. [Online] 10. 10 2012. [Zitat vom: 16. 02 2017.] <http://www.afridi-angell.com/items/limg/Energy-Regulation-and-Markets-Review-2012-MKA-HB1.pdf>.

**Agency, Environmental Protection. 2010.** *Data from Integrated Power Model (IPM), ICF International*. 2010.

**Albrecht, U. und et al. 2013.** *Analyse der Kosten erneuerbarer Gase*. s.l. : BWE, 2013.

**Alsayegh, O. A. 2008.** Restructuring Kuwait Electric Power System: Mandatory or Optional? *International Journal of Social, Behavioral, Educational, Economic, Business and Industrial Engineering*. 2008, Bd. 2, 9.

**Al-Shibani, K. 2013.** Yemen - Second National Communication. [Online] 05 2013. [Zitat vom: 16. 02 2017.] <http://unfccc.int/resource/docs/natc/yemnc2.pdf>.

**Bach, Paul-Frederik. 2014.** Denmark - Dependent on Foreign Balancing Services. [Online] 04. 07 2014. [Zitat vom: 16. 02 2017.] [http://www.pfbach.dk/firma\\_pfb/news\\_2014\\_5\\_e.htm](http://www.pfbach.dk/firma_pfb/news_2014_5_e.htm).

**Bahrain Electricity and Water Authority. 2015.** Bahrain - Electricity. [Online] 2015. [Zitat vom: 16. 02 2017.] <http://www.mew.gov.bh/default.asp?action=category&id=64>.

**Bank, World. 2011.** Armenia - ENERGY SECTOR NOTE. [Online] 10 2011. [Zitat vom: 16. 02 2017.] <http://r2e2.am/wp-content/uploads/2012/07/Charged-DecisionsDifficult-Choices-in-Armenias-Energy-Sector.pdf>.

**Beck, T., et al. 2016.** Assessing the influence of the temporal resolution of electrical load and PV generation profiles on self-consumption and sizing of PV-battery systems. *Applied Energy*. 2016, Bd. 173, S. 331-342.

- BETTER. 2015.** *Bringing Europe and Third countries closer together through renewable Energies*. EU. 2015.  
[http://www.dlr.de/dlr/Portaldata/1/Resources/documents/2015/DLR\\_Stuttgart\\_BETTER-Studie\\_English.pdf](http://www.dlr.de/dlr/Portaldata/1/Resources/documents/2015/DLR_Stuttgart_BETTER-Studie_English.pdf).
- Bird, Lori, Cochran, Jaquelin und Wang, Xi. 2014.** *Wind and Solar Energy Curtailment: Experiences and Practices in the United States*. Denver : NREL, 2014.
- Board, Energy Community Regulatory. 2008.** Albania - National Report. [Online] 01. 09 2008. [Zitat vom: 15. 02 2017.] [https://www.energy-community.org/portal/page/portal/ENC\\_HOME/DOCS/244177/0633975AA5A97B9CE053C92FA8C06338.PDF](https://www.energy-community.org/portal/page/portal/ENC_HOME/DOCS/244177/0633975AA5A97B9CE053C92FA8C06338.PDF).
- Boie, Inga, et al. 2016.** Opportunities and challenges of high renewable energy deployment and electricity exchange for North Africa and Europe – Scenarios for power sector and transmission infrastructure in 2030 and 2050. *Renewable Energy*. 2016, Bd. 87, S. 130–144.
- Brakelmann, Heinrich. 2004.** *Netzverstärkungs-Trassen zur Übertragung von Windenergie: Freileitung oder Kabel ?* Rheinberg : s.n., 2004.
- Brand, Bernhard. 2015.** *The integration of renewable energy into North African electricity systems*. Hamburg : s.n., 2015. ISBN 978-3-8300-8311-5.
- Büchner, J. und et al. 2014.** *Verteilernetzstudie*. s.l. : BMWi, 2014.
- Bundesnetzagentur. 2015.** *Bedarfsermittlung 2024 - NEP- Netzentwicklungsplan*. 2015.
- . 2015. *Quartalsbericht zu Netz- und Systemsicherheitsmaßnahmen 1.+2. Quartal 2015*. s.l. : BNetzA, 2015. Tabelle 7.
- Cebulla, F. 2017.** *Storage demand in highly renewable energy scenarios for Europe*. s.l. : University of Stuttgart, 2017.
- Cebulla, F. und Fichter, T. 2017.** Merit order or unit-commitment: How does thermal power plant modeling affect storage demand in energy system models? *Renewable Energy*. 2017, Bd. 105, S. 117-132.
- CIGRE. 2014.** Algeria - The Electric Power System. [Online] 2014. [Zitat vom: 15. 02 2017.] <http://www.cigre.org/var/cigre/storage/original/application/1ec62202f27aaa674c271ace096089f3.pdf>.
- . 2014. Estonia - The Electric Power System. [Online] 2014. [Zitat vom: 15. 02 2017.] <http://www.cigre.org/var/cigre/storage/original/application/feae6a009214588134996158e93de379.pdf>.
- . 2011. Finland - The Electric Power System. [Online] 2011. [Zitat vom: 15. 02 2017.] <http://www.cigre.org/var/cigre/storage/original/application/67cf88dc73b65038be83214053dae45d.pdf>.



- . **2014.** Great Britain - The Electric Power System. [Online] 2014. [Zitat vom: 15. 02 2017.] <http://www.cigre.org/var/cigre/storage/original/application/f61d0ebd5531fcbcd39ef222fc7e8948.pdf>.
- . **2015.** Greece - The Electric Power System. [Online] 20. 10 2015. [Zitat vom: 16. 02 2017.] <http://www.cigre.org/var/cigre/storage/original/application/c5729776471a98524c7b244696a2cc95.pdf>.
- . **2016.** Iceland - The Electric Power System. [Online] 03. 08 2016. [Zitat vom: 16. 02 2017.] <http://www.cigre.org/var/cigre/storage/original/application/0e6b49d276197c815b453f89a96d6f1d.pdf>.
- . **2015.** Iran - The Electric Power System. [Online] 10. 05 2015. [Zitat vom: 16. 02 2017.] <http://www.cigre.org/var/cigre/storage/original/application/48aad4ca93bc0f8a5919ac5122a6ce1b.pdf>.
- . **2015.** Ireland - The Electric Power System. [Online] 2015. [Zitat vom: 15. 02 2017.] <http://www.cigre.org/var/cigre/storage/original/application/d265c3b09604c7fe99501f2036459645.pdf>.
- . **2016.** Israel - The Electric Power System. [Online] 2016. [Zitat vom: 15. 02 2017.] <http://www.cigre.org/var/cigre/storage/original/application/bbc083b09021694c44096901db84efc6.pdf>.
- . **2014.** Macedonia - The Electric Power System. [Online] 2014. [Zitat vom: 15. 02 2017.] <http://www.cigre.org/var/cigre/storage/original/application/a0c5760448b5d0f9370840b4f34848e8.pdf>.
- . **2013.** Norway - The Electric Power System. [Online] 2013. [Zitat vom: 15. 02 2017.] <http://www.cigre.org/var/cigre/storage/original/application/6f712b7cf070d717dc1a19fa5d26cdf9.pdf>.
- . **2014.** Schweden - The Electric Power System. [Online] 2014. [Zitat vom: 15. 02 2017.] <http://www.cigre.org/var/cigre/storage/original/application/e589ee228cf72f7e222c7d45033ec0d3.pdf>.
- . **2014.** Turkey - The Electric Power System. [Online] 2014. [Zitat vom: 15. 02 2017.] <http://www.cigre.org/var/cigre/storage/original/application/affeb24295861859ceec4db5e0a28d04.pdf>.
- Coello, C.A.C., Pulido, G.T. und Lechuga, M.S. 2004.** Handling multiple objectives with particle swarm optimization. *IEEE Transactions on Evolutionary Computation*. 2004, Bd. 8, S. 256 - 279.
- Cole, Stijn, et al. 2011.** *A European Supergrid: Present state and future challenges*. Stockholm : s.n., 2011. 17th Power Systems Computation Conference.

- Comission, European.** Lithuania - Country Report. [Online] [Zitat vom: 15. 02 2017.] [https://ec.europa.eu/energy/sites/ener/files/documents/2014\\_countryreports\\_lithuania.pdf](https://ec.europa.eu/energy/sites/ener/files/documents/2014_countryreports_lithuania.pdf).
- Commission, European. 2014.** Greece - Country Report. [Online] 23. 10 2014. [Zitat vom: 16. 02 2017.] [https://ec.europa.eu/energy/sites/ener/files/documents/2014\\_countryreports\\_greece.pdf](https://ec.europa.eu/energy/sites/ener/files/documents/2014_countryreports_greece.pdf).
- Company, Egyptian Electricity Holding. 2014.** Annual Report. [Online] 2014. [Zitat vom: 15. 02 2017.] [http://www.moee.gov.eg/english\\_new/EEHC\\_Rep/2014-2015en.pdf](http://www.moee.gov.eg/english_new/EEHC_Rep/2014-2015en.pdf).
- Company, Saudi Electricity. 2015.** Saudi Arabia - BACKGROUND ON CORE BUSINESS. [Online] 2015. [Zitat vom: 15. 02 2017.] <https://www.se.com.sa/en-us/invshareholder/Pages/BackgroundOnBusinessSegment.aspx>.
- Cossent, Rafael, et al. 2011.** Distribution network costs under different penetration levels of distributed generation. *EUROPEAN TRANSACTIONS ON ELECTRICAL POWER*. 2011, Bd. 21, S. 1869–1888.
- CSP-Today. 2016.** CSP-Today. [Online] 15. 02 2016. <http://www.csptoday.com/>.
- Denholm, P., et al. 2012.** *The Potential Role of Concentrating Solar Power in Enabling High Renewables Scenarios in the United States*. s.l. : NREL, 2012. <http://www.nrel.gov/docs/fy13osti/56294.pdf>.
- Department of Energy. 2011.** *Estimate Value 2030*. 2011. Deutsche Gesellschaft für Sonnenenergie e.V. EEG-Anlagenregister. [Online] [Zitat vom: 14. 02 2017.] <http://www.energymap.info/download.html>.
- DLR. 2005.** *Med-CSP*. 2005.
- .** 2006. *TRANS-CSP*. 2006.
- DOE. 2004.** Azerbaijan - An Energy Overview of the Republic of Azerbaijan. [Online] 21. 06 2004. [Zitat vom: 16. 02 2017.] <https://www.osti.gov/scitech/servlets/purl/821116>.
- Electric Power System of Libya and its Future.* **NASR, Maher. 2010.** FEI TU of Košice, Slovak Republic : s.n., 2010. 10th Scientific Conference of Young Researchers.
- Enemalta.** Electricity Distribution. [Online] [Zitat vom: 15. 05 2017.] <http://www.enemalta.com.mt/index.aspx?cat=2&art=6>.
- Energetici, Gestore dei Servizi. 2013.** Tunisia - Energy Country Report. [Online] 05 2013. [Zitat vom: 15. 02 2017.] [http://www.qualenergia.it/sites/default/files/articolo-doc/%252fCOUNTRY\\_REP\\_TUNISIA.PDF](http://www.qualenergia.it/sites/default/files/articolo-doc/%252fCOUNTRY_REP_TUNISIA.PDF).
- EnergiNetDK. 2014.** Denmark - Electricity facilities. [Online] 01. 01 2014. [Zitat vom: 15. 02 2017.] <http://www.energinet.dk/EN/ANLAEG-OG-PROJEKTER/Generelt-om-elanlaeg/Sider/default.aspx>.
- Energy, PISG Energy Office. 2004.** Kosovo - ELECTRIC POWER SYSTEM DEVELOPMENT STRATEGY White Paper. [Online] 14. 06 2004. [Zitat vom: 16. 02 2017.] <http://www.esiweb.org/pdf/bridges/kosovo/10/4.pdf>.

**Energypedia. 2012.** Tunisia - Energy Situation . [Online] 2012. [Zitat vom: 15. 02 2017.]  
[https://energypedia.info/wiki/Tunisia\\_Energy\\_Situation](https://energypedia.info/wiki/Tunisia_Energy_Situation).

**ENTSO-e. 2013.** ENTSO-e peak load. [Online] 2013. [Zitat vom: 15. 06 2015.] peak load.  
[https://www.entsoe.eu/fileadmin/user\\_upload/\\_library/publications/entsoe/outlookreports/131128\\_Winter\\_Outlook.pdf](https://www.entsoe.eu/fileadmin/user_upload/_library/publications/entsoe/outlookreports/131128_Winter_Outlook.pdf).

— **2013.** INFORMATION UPON THE LENGTHS OF CIRCUITS. [Online] 2013. [Zitat vom: 15. 02 2017.]  
<https://www.entsoe.eu/db-query/miscellaneous/lengths-of-circuits>.

— **2016.** Lengths of circuits. [Online] 2016. [Zitat vom: 03. 06 2015.]  
<https://www.entsoe.eu/db-query/miscellaneous/lengths-of-circuits>.

ENTSO-E load data. [Online] load data from 2006 for Germany.  
<https://www.entsoe.eu/data/data-portal/consumption/Pages/default.aspx>.

**ENTSO-e. 2010.** NTC Matrix. [Online] 2010. [Zitat vom: 14. 02 2017.] Winter 2010/11.  
<https://www.entsoe.eu/publications/market-reports/ntc-values/ntc-matrix/Pages/default.aspx>.

— **2012.** YS&AR report. [Online] 2012. [Zitat vom: 15. 02 2017.]  
[https://ec.europa.eu/energy/sites/ener/files/documents/2014\\_countryreports\\_latvia.pdf](https://ec.europa.eu/energy/sites/ener/files/documents/2014_countryreports_latvia.pdf).

**Environmental Protection Agency. 2010.** Data from Integrated Power Model (IPM), ICF International. 2010.

**EU. 2017.** The Water, Energy & Food Security NEXUS. [Online] 2017. [Zitat vom: 22. 09 2017.]  
<https://www.water-energy-food.org>.

**European Commission. 2014.** Press releases database. *Hinkley Point*. [Online] 08. 10 2014. [Zitat vom: 20. 03 2015.]  
[http://europa.eu/rapid/press-release\\_IP-14-1093\\_de.htm](http://europa.eu/rapid/press-release_IP-14-1093_de.htm).

**Federal Grid Company. 2015.** Russia - Annual Report. [Online] 2015. [Zitat vom: 16. 02 2017.]  
[http://www.fsk-ees.ru/upload/docs/2015\\_AR\\_FGC\\_UES\\_app.pdf](http://www.fsk-ees.ru/upload/docs/2015_AR_FGC_UES_app.pdf).

**FIAS. 2017.** [Online] 2017. [Zitat vom: 03. 05 2016.]  
<https://github.com/FRESNA/powerplantmatching>.

**Fichter, T., et al. 2014.** Optimized Integration of Renewable Energies into Existing Power Plant Portfolios. *Energy Procedia*. 2014, Bd. 49, S. 1858-1868.

**Fichter, Tobias. 2017.** *Long-term Capacity Expansion Planning with Variable Renewable Energies - Enhancement of the REMix Energy System Modelling Framework*. Stuttgart : Universität Stuttgart, 2017.

**Funds, Climate Investment. 2014.** INDEPENDENT REVIEW OF THE MOROCCO-CLEAN AND EFFICIENT ENERGY PROJECT. [Online] 2014. [Zitat vom: 15. 02 2017.]  
[https://www.cif.climateinvestmentfunds.org/sites/default/files/2014\\_Independent%20Review%20CTF\\_MOCCO\\_V6\\_rev.pdf](https://www.cif.climateinvestmentfunds.org/sites/default/files/2014_Independent%20Review%20CTF_MOCCO_V6_rev.pdf).

**Fürstenwerth, D. und et al. 2014.** *Stromspeicher in der Energiewende*. s.l. : Agora, 2014.

**Gauché, Paul. 2016.** *Spatial-temporal model to evaluate the system potential of concentrating solar power in South Africa*. 2016.

- Georgian State Electrosystem. 2014.** Georgia - Annual Report. [Online] 2014. [Zitat vom: 16. 02 2017.] [http://www.gse.com.ge/new/wp-content/uploads/2015/07/SSA-ANNUAL\\_FORWEB\\_012.pdf](http://www.gse.com.ge/new/wp-content/uploads/2015/07/SSA-ANNUAL_FORWEB_012.pdf).
- Gils, H.C. 2014.** Assessment of the theoretical demand response potential in Europe. doi:10.1016/j.energy.2014.02.019. *Energy*. 2014, Bd. 67, S. 1-18.
- **2016.** Economic Potential for Future Demand Response in Germany – Modelling Approach and Case Study. doi:10.1016/j.apenergy.2015.10.083. *Applied Energy*. 2016, Bd. 162, S. 401–415. doi:10.1016/j.apenergy.2015.10.083.
- Gils, H.C., et al. 2017.** Integrated modelling of variable renewable energy-based power supply in Europe. *Energy*. 2017, Bd. 123, S. 173–188.
- Gils, Hans Christian. 2016.** Economic potential for future demand response in Germany – Modeling approach and case study. *Applied Energy*. 2016, Bd. 162, S. 401-415.
- Goerne, Gabriela von. 2009.** *CO<sub>2</sub>-Abscheidung und -Lagerung(CCS) in Deutschland*. s.l. : Germanwatch Nord-Süd Initiative e.V., 2009. ISBN-10: 3939846465.
- Greenpeace. 2009.** scenario optimistic. 2009.
- Gruber, L. 2012.** *Synthese globaler, elektrischer Lastganglinien*. Berlin : s.n., 2012.
- Haas, J., et al. 2017.** Challenges and trends of energy storage expansion planning for flexibility provision in low-carbon power systems – a review. *Renewable and Sustainable Energy Reviews*. 2017, Bd. 80, S. 603–619.
- Haller, Markus, Ludig, Sylvie und Bauer, Nico. 2012.** Decarbonization scenarios for the EU and MENA power system: Considering spatial distribution and short term dynamics of renewable generation. *Energy Policy*. 2012, Bd. 47, S. 282-290.
- Hess, Denis. 2013.** *FERNÜBERTRAGUNG REGELBARER SOLARENERGIE VON NORDAFRIKA NACH MITTELEUROPA*. Stuttgart : University Library of the University of Stuttgart, 2013. urn:nbn:de:bsz:93-opus-86283.
- Hess, Denis und Pfenning, Uwe. 2014.** MIN-MIN + WIN-WIN Risiken und Chancen lokaler Energieautonomie. *VDE-Kongress 2014 - Smart Cities – Intelligente Lösungen für das Leben in der Zukunft*. Frankfurt am Main : VDE, 2014. S. 1-6. ISBN 978-3-8007-3641-6.
- Hitchcock, Frank L. 1941.** The Distribution of a Product from Several Sources to Numerous Localities. *Studies in Applied Mathematics*. 1941, Bd. 20, S. 224–230.
- IEA. 2009.** *Data from Market Allocation (MARKAL) model, International Energy Agency and Brookhaven National Laboratory*. 2009.
- **2017.** Internatioanl Energy Agency Statistics. [Online] 2017. [Zitat vom: 14. 02 2015.] <http://www.iea.org/statistics/>.
- **2010.** *PV Roadmap*. 2010.
- **2005.** *Russian Electricity Reform*. Paris : s.n., 2005. 56.6% of of total Russia (electricity production in 2000).

**IIASA. 2013.** Shared Socioeconomic Pathways Database. [Online] 1.1, 03 2013. [Zitat vom: 03. 08 2015.] SSP1-26-SPA1-V12.

**INMR. 2014.** Qatar Power Grid Faces Combined Challenges of Pollution and Rapid Expansion. [Online] 08. 09 2014. [Zitat vom: 16. 02 2017.] <http://www.inmr.com/qatar-power-grid-faces-combined-challenges-pollution-rapid-expansion-2/3/>.

**Institute, Global Energy Network. 2016.** Armenia - National Energy Grid. [Online] 30. 06 2016. [Zitat vom: 15. 02 2017.] [http://geni.org/globalenergy/library/national\\_energy\\_grid/armenia/index.shtml](http://geni.org/globalenergy/library/national_energy_grid/armenia/index.shtml).

**Instituto Catalán de Energía. 2016.** [Online] 2016. [Zitat vom: 17. 09 2017.] [http://icaen.gencat.cat/es/energia/estadistiques/resultats/annuals/balanc\\_energia/](http://icaen.gencat.cat/es/energia/estadistiques/resultats/annuals/balanc_energia/).

**International Energy Agency. 2005.** Russia - RUSSIAN ELECTRICITY REFORM. [Online] 2005. [Zitat vom: 16. 02 2017.] <https://www.iea.org/publications/freepublications/publication/russianelec.pdf>.

**IPCC. 2014.** *Mitigation of Climate Change*. 2014. p. 714, figure 9.23 and p.713.

—, **2014.** *Mitigation of Climate Change*. 2014. p. 640, figure 8.12.

**Iraq - MINISTRY OF ELECTRICITY. 2010.** Iraq - IRAQ ELECTRICITY MASTERPLAN. [Online] 2010. [Zitat vom: 16. 02 2017.] <http://iraqieconomists.net/ar/wp-content/uploads/sites/2/2015/09/Iraq-Electricity-Master-Plan-2010-Volume-1-Executive-Summary.pdf>.

**IRENA. 2012.** IRENA Hydro Power. [Online] 2012. values are estimated but are based reference assumption on p. 22. [http://www.irena.org/documentdownloads/publications/re\\_technologies\\_cost\\_analysis-hydropower.pdf](http://www.irena.org/documentdownloads/publications/re_technologies_cost_analysis-hydropower.pdf).

—, **2017.** *Planning for the Renewable Future: Long-term modelling and tools to expand variable renewable power in emerging economies*. Abu Dhabi : International Renewable Energy Agency, 2017.

**JSC Georgian State Electrosystem. 2014.** Georgia - About us. [Online] 2014. [Zitat vom: 16. 02 2017.] [http://www.gse.com.ge/new/?page\\_id=179&lang=en](http://www.gse.com.ge/new/?page_id=179&lang=en).

**Jung, R., et al. 2002.** *Abschätzung des technischen Potenzials der geothermischen Stromerzeugung und der geothermischen Kraft-Wärmekopplung (KWK) in Deutschland*. 2002. [https://www.foederal-erneuerbar.de/landesinfo/bundesland/BW/kategorie/erdwaerme/auswahl/815-technisches\\_potenzia](https://www.foederal-erneuerbar.de/landesinfo/bundesland/BW/kategorie/erdwaerme/auswahl/815-technisches_potenzia).

**KISR. 2014.** Kuwait - Energy Efficiency in Kuwait: Past, Current & Future. [Online] 20. 06 2014. [Zitat vom: 04. 06 2016.] <http://css.escwa.org.lb/SDPD/3457/PPT1-1.pdf>.

- Klobasa, M. und Mast, D. 2014.** *ImpRES Project, Monitoringbericht BNetzA 2013*. s.l. : Bundesnetzagentur 2013b, 2014. [http://www.impres-projekt.de/impres-wAssets/docs/2014\\_08\\_03\\_Netzausbaukosten-ImpRES\\_final.pdf](http://www.impres-projekt.de/impres-wAssets/docs/2014_08_03_Netzausbaukosten-ImpRES_final.pdf).
- Knies, Gerhard und Bennouna, Abdelaziz. 1997.** *Nordafrikanisch - Europäischer Solarenergie Verbund. Workshop des Hamburger Klimaschutz-Fonds HKF am 9.4. 1997 an der TU Hamburg Harburg* . 1997.
- Kontos, Adamos. 2015.** Cyprus - Net metering Policy and Electricity Market in Cyprus. [Online] 06. 03 2015. [Zitat vom: 16. 02 2017.] [http://www.raee.org/fileadmin/user\\_upload/mediatheque/raee/Documents/Publications/Recueil\\_interventions/2015/PVNET\\_MARS2015/2\\_CYPRUS\\_DSO\\_06\\_March\\_2015.pdf](http://www.raee.org/fileadmin/user_upload/mediatheque/raee/Documents/Publications/Recueil_interventions/2015/PVNET_MARS2015/2_CYPRUS_DSO_06_March_2015.pdf).
- Kopfmüller, J., et al. 2001.** *Nachhaltige Entwicklung integrativ betrachtet. Konstitutive Elemente, Regeln, Indikatoren*. Berlin : edition sigma, 2001. ISBN 3-89404-571-X.
- 2016.** *Kraftwerksliste Bundesnetzagentur Stand 10.05.2016*. s.l. : BNetzA, 2016.
- Kühnel, S. 2013.** *Investigation of the variability of solar and wind electricity generation potentials in Europe and North Africa*. Oldenburg : Karl von Ossietzky University, 2013.
- Laâbi, Taoufik. 2014.** Wind Power Support in Morocco. [Online] 09. 10 2014. [Zitat vom: 15. 02 2017.] <http://wind.vdma.org/documents/106078/2159140/2014-10-09-WEED-2014-Laabi-ONEE-Marocco/a40e9cbb-d200-4836-9aa6-e79452e13c66>.
- Liban, Électricité Du. 2014.** Lebanon - EDL Power Structure. [Online] 01. 05 2014. [Zitat vom: 15. 02 2017.] <http://www.edl.gov.lb/aboutedl.htm>.
- Limberger, J., et al. 2014.** Assessing the prospective resource base for enhanced geothermal systems in Europe. *Geoth. Energ. Sci.* 2014, Bd. 2, S. 55-71.
- Litgrid. 2016.** Lithuania - Power system. [Online] 01. 07 2016. [Zitat vom: 15. 02 2017.] <http://www.litgrid.eu/index.php/power-system/power-system-information/grid-scheme-and-data/545>.
- Liudmyla, Vlasenko. 2013.** Ukraine - Ministry of Energy and Coal Industry. [Online] 2013. [Zitat vom: 15. 02 2017.] <https://eneken.ieej.or.jp/data/5026.pdf>.
- Mai et al. 2012.** *COST AND PERFORMANCE DATA FOR POWER GENERATION TECHNOLOGIES*. 2012.
- Marcos, Gimeno-Gutiérrez und Roberto, Lacal-Aránzategui. 2013.** *Assessment of the European potential for pumped hydropower energy storage: A GIS-based assessment of pumped hydropower storage potential*. 2013.
- May, Nadine. 2005.** *Ökobilanz eines Solarstromtransfers von Nordafrika nach Europa*. 2005.
- Medjroubi, W., Matke, C. und D., Kleinhans. 2015.** *SciGRID - An Open Source Reference Model for the European Transmission Network (v0.2)*. November 2015.
- Metzdorf, Johannes. 2016.** *Development and implementation of a spatial clustering approach using a transmission grid energy system model*. Stuttgart : s.n., 2016.

- Moldova, Ministry of Economy of the Republic of. 2013.** Moldova - Security of Supply Statements. [Online] 2013. [Zitat vom: 15. 02 2017.] [https://www.energy-community.org/portal/page/portal/ENC\\_HOME/DOCS/2440189/0633975AD4447B9CE053C92FA8C06338.PDF](https://www.energy-community.org/portal/page/portal/ENC_HOME/DOCS/2440189/0633975AD4447B9CE053C92FA8C06338.PDF).
- Monfared, M.A.S. und Alipour, Z. 2013.** Structural Properties and vulnerability of Iranian 400kv Power Transmission Grid: a Complex Systems Approach. *Industrial Engineering & Management*. 2013, Bd. 2, 3.
- Moser, Albert. 2014.** *Unterstützung der Energiewende in Deutschland durch einen Pumpspeicherausbau*. 2014.  
[http://www.wasserkraft.info/application/media/documents/Abschlussbericht\\_RWTH\\_PSW\\_Voith\\_final.pdf](http://www.wasserkraft.info/application/media/documents/Abschlussbericht_RWTH_PSW_Voith_final.pdf).
- Moser, Massimo. 2015.** *Combined electricity and water production based on solar energy*. s.l. : Universität Stuttgart, 2015. <http://dx.doi.org/10.18419/opus-2365>.
- Neij, L. 2008.** Cost development of future technologies for power generation—A study based on experience curves and complementary bottom-up assessments. *Energy Policy* 36. 2008, S. 2200– 2211.
- NEPCO. 2013.** Jordan - Annual Report. [Online] 2013. [Zitat vom: 15. 02 2017.] [http://www.nepco.com.jo/store/docs/web/2013\\_en.pdf](http://www.nepco.com.jo/store/docs/web/2013_en.pdf).
- Nitsch, J. und et al. 2012.** *Long-term scenarios and strategies for the deployment of renewable energies in Germany in view of European and global developments*. 2012.
- Nitsch, Joachim und Pregger, Thomas. 2013.** Kostenbilanz des Ausbaus erneuerbarer Energien in der Stromerzeugung bei unterschiedlichen Preisbildungen am Strommarkt. *Vierteljahrshefte zur Wirtschaftsförderung*. 2013, Bd. 82, S. 45-59.
- OFFICE, ENERGY REGULATORY. 2005.** Kosovo - Kosovo within the framework of Energy Community of SEE. [Online] 22. 12 2005. [Zitat vom: 16. 02 2017.] [http://www.ero-ks.org/ERO%20Presentation/Kosovo\\_energy\\_sector\\_profile\\_18\\_12\\_05\\_eng.pdf](http://www.ero-ks.org/ERO%20Presentation/Kosovo_energy_sector_profile_18_12_05_eng.pdf).
- OPENEI NREL.** *The data below was downloaded from the Transparent Cost Database at <http://en.openei.org/apps/TCDB/>.*
- Pfenninger, S., Hawkes, A. und Keirstead, J. 2015.** Energy system modeling for twenty-first century energy challenges. *Renewable and Sustainable Energy Reviews*. 2015, Bd. 33, S. 74-86.
- Pfenninger, Stefan, et al. 2014.** Potential for concentrating solar power to provide baseload and dispatchable power. *Nature Climate Change*. 2014, Bd. 4, S. 689–692.
- Pleißmann, Guido, et al. 2014.** Global Energy Storage Demand for a 100% Renewable Electricity Supply. *Energy Procedia*. 2014, Bd. 46, S. 22-31.
- Pregger. 2015.** *Vergleichende Bewertung der Integration einer zentralen versus einer dezentralen Wasserstoffherzeugung in die zukünftige Stromversorgung Deutschlands* . 2015.

- Rabbani, Masoud, Mohammadi, Setare und Mobini, Mahdi. 2018.** Optimum design of a CCHP system based on Economical, energy and environmental considerations using GA and PSO. *International Journal of Industrial Engineering Computations*. 2018, Bd. 9, S. 99–122.
- Rehtanz, C. und et al. 2012.** *Dena Verteilnetzstudie Szenario Bundesländer*. s.l. : Deutsche Energieagentur (dena), 2012.
- Rogelj, Joeri, et al. 2015.** Energy system transformations for limiting end-of-century warming to below 1.5 °C. *Nature Climate Change*. 2015, Bd. 5, S. 519–527.
- RTE. 2016.** *Bilan électrique et perspectives*. 2016. [http://www.rte-france.com/sites/default/files/2016\\_12\\_04\\_bilan\\_electrique\\_auvergne\\_rhones-alpes\\_1.pdf](http://www.rte-france.com/sites/default/files/2016_12_04_bilan_electrique_auvergne_rhones-alpes_1.pdf).
- Rubin, Edward S., Chen, Chao und Rao, Anand B. 2007.** Cost and performance of fossil fuel power plants with CO<sub>2</sub> capture and storage. *Energy Policy*. 2007, Bd. 35, S. 4444–4454.
- Russian Federal State, Statistics Service. 2010.** *All-Russian Population Census*. 2010.
- SACM, Servicios Avanzados de Comunicación y Marketing SL. 2017.** CSP World Map. [Online] 2017. [Zitat vom: 02. 06 2017.] <http://cspworld.org/cspworldmap>.
- Schaber, K., et al. 2012.** Parametric study of variable renewable energy integration in Europe: Advantages and costs of transmission grid extensions. *Energy Policy*. 2012, Bd. 42, S. 498–508.
- Scholz, Y. 2012.** *RENEWABLE ENERGY BASED ELECTRICITY SUPPLY AT LOW COSTS: DEVELOPMENT OF THE REMIX MODEL AND APPLICATION FOR EUROPE*. Stuttgart : University Library of the University of Stuttgart, 2012. urn:nbn:de:bsz:93-opus-76350.
- Scholz, Yvonne, Gils, Hans Christian und Pietzcker, Robert C. 2017.** Application of a high-detail energy system model to derive power sector characteristics at high wind and solar shares. *Energy Economics*. 2017, Bd. 64, S. 568-582.
- 2015.** *Statistisches Bundesamt, Zensus 2011*. Wiesbaden : Statistisches Bundesamt, 2015.
- Statistisches Landesamt. 2017.** *Energiebericht kompakt 2017*. s.l. : Statistisches Landesamt Baden-Württemberg, 2017.
- Steinbach, Armin. 2013.** Barriers and solutions for expansion of electricity grids - the German experience. *Energy Policy*. 2013, Bd. 63, S. 224-229.
- Stetter, D. 2012.** *ENHANCEMENT OF THE REMIX ENERGY SYSTEM MODEL: GLOBAL RENEWABLE ENERGY POTENTIALS, OPTIMIZED POWER PLANT SITING AND SCENARIO VALIDATION*. Stuttgart : University Library of the University of Stuttgart, 2012. urn:nbn:de:bsz:93-opus-94531.
- Syria, Atomic Energy Commission of. 2011.** SELF-EVALUATION OF THE DEVELOPMENT OF THE NATIONAL NUCLEAR INFRASTRUCTURE OF SYRIA. [Online] 02 2011. [Zitat vom: 15. 02 2017.]



[https://www.iaea.org/NuclearPower/Downloads/Infrastructure/meetings/2011-02-TM-WS-Vienna/Day-2/Jouhara\\_SYRIA.pdf](https://www.iaea.org/NuclearPower/Downloads/Infrastructure/meetings/2011-02-TM-WS-Vienna/Day-2/Jouhara_SYRIA.pdf).

**TERNA. 2016.** Bilanci Regionali. [Online] 2016. [Zitat vom: 09. 17 2017.]

<https://www.terna.it/it->

[it/sistemaelettrico/statisticheeprevisioin/bilancienergiaelettrica/bilanciregionali.aspx](https://www.terna.it/it-sistemaelettrico/statisticheeprevisioin/bilancienergiaelettrica/bilanciregionali.aspx).

**2016.** *The Report: Qatar 2015*. s.l. : Oxford Business Group, 2016. S. 137.

**tīkls, Augstsprieguma. 2014.** Latvia - Transmission network characteristic Annual Report.

[Online] 2014. [Zitat vom: 15. 02 2017.]

[http://www.ast.lv/files/ast\\_files/gadaparskzinoj/0614\\_001.pdf](http://www.ast.lv/files/ast_files/gadaparskzinoj/0614_001.pdf).

**timesofmalta, Malta -. 2015.** National electricity peak load record registered. [Online] 23. 07 2015. [Zitat vom: 15. 02 2017.]

<http://www.timesofmalta.com/articles/view/20150723/local/national-electricity-peak-load-record-registered.577769>.

**Tomaschek, J., et al. 2013.** Integrated Analysis of dispatchable Concentrated Solar Power. *Energy Procedia*. 2013, Bd. 69, S. 1711-1721.

**Trieb, Franz und Hess, Denis. 2017.** Wege zur regenerativen Stromversorgung.

*Energiewirtschaftliche Tagesfragen*. 2017, Bd. 3.

**Trieb, Franz und Klann, Uwe. 2006.** *Modeling the Future Electricity Demand of Europe, Middle East and North Africa*. Stuttgart : s.n., 2006. Internal Report.

**Trieb, Franz, et al. 2012.** Solar electricity imports from the Middle East and North Africa to Europe. *Energy Policy*. 2012, Bd. 42.

**Tum, Markus, et al. 2013.** Sustainable Bioenergy Potentials for Europe and the Globe. *Geoinformatics & Geostatistics: An Overview*. 2013, S. 1-10.

**UNDP, Moe. 2004.** Lebanon - VULNERABILITY AND ADAPTATION OF THE ELECTRICITY SECTOR. [Online] 2004. [Zitat vom: 15. 02 2017.]

<http://test.moe.gov.lb/ClimateChange/pdf/SNC/b-Electricity%20sector.pdf>.

**UNESCWA. 2011.** Statistical Abstract of the Arab Region. [Online] 2011. [Zitat vom: 16. 02 2017.] <http://taqaway.net/statistics-indicators/electricity-peak-load-united-arab-emirates-2011>.

—. **2000.** Yemen - Statistical Abstract of the Arab Region. [Online] 2000. [Zitat vom: 16. 02 2017.] <http://taqaway.net/statistics-indicators/electricity-peak-load-yemen-2000-0>.

**United Nations. 2010.** *World Population Prospects*. 2010.

—. **2015.** *World Population Prospects: The 2015 Revision*. Department of Economic and Social Affairs, Population Division. 2015. Medium fertility variant, 2015 - 2100.

**United States Agency for International Development. 2013.** Azerbaijan - REGIONAL ELECTRICITY MARKET OVERSIGHT. [Online] 31. 07 2013. [Zitat vom: 16. 02 2017.]

[http://pdf.usaid.gov/pdf\\_docs/PA00JCTR.pdf](http://pdf.usaid.gov/pdf_docs/PA00JCTR.pdf).

**Viehbahn, P. und et al. 2008.** *EU-NEEDS scenario pesimistic.* 2008.

**Wetzel, Manuel. 2015.** *Materialbedarf von Stromerzeugungssystemen: Szenarienpfadanalyse für Deutschland.* 2015.

**Yakushau, Anatoli. 2010.** IAEA Interregional workshop on Long Range NE Program

Planning. [Online] 15. 06 2010. [Zitat vom: 16. 02 2017.]

[https://www.iaea.org/INPRO/activities/WS\\_on\\_Long-range\\_planning/Belarus\\_Yakushau\\_June\\_13\\_2010\\_FD\\_AK\\_2.pdf](https://www.iaea.org/INPRO/activities/WS_on_Long-range_planning/Belarus_Yakushau_June_13_2010_FD_AK_2.pdf).

## 10 Appendix

### 10.1 Chapter 2 - The concept of a CSP transfer to Europe

#### 10.1.1 CSP sites, HVDC point-to-point transmission lines and offtakers

##### 10.1.1.1 Pathway lengths

In Table 33 the used pathway lengths are shown assuming two different pathway configurations (onshore and offshore laying). The used pathways are a manual selection out of all 1230 combinations using short but also diversified resources of possible CSP hotspots and offtakers.

Table 33: Selection of 124 pathway lengths from a potential CSP hot spot in MENA plant to potential offtaker in EU – grey rows show potential CSP hotspots and pathways for offtakers in Germany

From potential CSP hotspot	To potential offtaker	Offtaker in model region	Dominant onshore pathway		Dominant offshore pathway	
			Total length [km]	Sea cable section [km]	Total length [km]	Sea cable section [km]
Algeria1	Amsterdam	W	2405	202	2801	1663
Tunisia1	Amsterdam	W	2483	344	2935	1959
Jordan1	Ankara	T	1423	0	893	263
Syria1	Athens	SE	2007	212	1619	1366
Iran1	Baku	NE	711	0	1246	302
Iraq1	Baku	NE	1257	0	675	360
Algeria2	Barcelona	SW	1701	185	1214	834
Morocco2	Barcelona	SW	1304	134	1944	1466
Libya1	Belgrade	SE	2240	564	1873	1315
Tunisia1	Belgrade	SE	1967	564	1964	1274
Morocco2	Berlin	G	3079	134	3031	1615
Syria1	Brandenburg	G	3679	100	3722	2622
Algeria2	Bremen	G	2498	401	2484	1042
Algeria2	Brussels	W	2743	185	2307	1128
Morocco2	Brussels	W	2346	134	2376	1079
Libya1	Bucharest	E	2704	538	2725	1984
SaudiArabia1	Bucharest	E	2540	100	2454	1464
Algeria2	Budapest	SE	2442	410	2678	1829
Libya2	Budapest	SE	2870	788	2603	1596
Algeria1	Cardiff	NW	2587	426	3237	2850
Morocco1	Cardiff	NW	2808	369	2618	1828
Iraq1	Chisinau	NE	3513	37	2563	1238

Jordan1	Cluj-Napoca	SE	2745	100	2247	1232
Libya1	Cluj-Napoca	SE	2592	564	2611	1647
Algeria2	Cologne	G	2863	185	2431	1177
Morocco2	Cologne	G	2465	134	2250	1042
Algeria2	Copenhagen	N	2717	434	2768	1283
Libya1	Copenhagen	N	2981	358	2666	1107
Iran2	Donetsk	NE	2662	25	2128	1228
Syria1	Donetsk	NE	2903	25	3035	1457
Algeria2	Dresden	G	2382	401	2338	1100
Algeria2	Dublin	NW	3033	666	3292	2891
Morocco1	Dublin	NW	2822	616	3399	2545
Algeria2	Erfurt	G	2230	401	2219	1042
Algeria2	Frankfurt	G	2120	401	2653	1615
Morocco2	Frankfurt	G	2494	134	2113	1042
Morocco2	Freiburg City	G	2269	134	2465	1615
Algeria1	Gothenburg	N	3408	347	3106	1644
Libya1	Gothenburg	N	3293	458	4032	2939
Morocco2	Hamburg	G	2953	134	4467	3306
Algeria2	Hanover	G	2373	401	2934	1615
Morocco2	Hanover	G	2915	134	2363	1042
Algeria2	Helsinki	N	3850	468	4652	2134
Iran1	Helsinki	N	4303	82	3968	2260
Egypt1	Istanbul	T	1949	504	2409	1936
SaudiArabi a1	Istanbul	T	1988	32	2662	2138
Egypt1	Kaliningrad	NE	3958	572	4696	2698
Algeria2	Karlsruhe City	G	2007	401	2015	1042
Libya1	Kiel	G	2807	325	2630	1217
Libya1	Kirkop	S	729	339	726	382
Algeria1	Koblenz	G	2400	185	2378	1132
Jordan1	Kosice	E	3072	100	2926	1669
Egypt1	Kyiv	NE	3234	572	2954	2246
Syria1	Kyiv	NE	3744	25	3643	2677
Algeria1	Lisbon	SW	1324	25	1453	997
Libya1	Ljubljana	S	2162	334	2142	1710
Algeria1	London	NW	2314	290	3553	2886
Morocco2	London	NW	2450	118	2684	1644
Algeria2	Luxembourg	W	2713	185	2176	1079
Syria1	Lviv	NE	2832	100	2491	1315
Tunisia1	Lviv	NE	3047	334	2918	1810
Morocco2	Lyon	W	1864	134	2075	1572
Tunisia1	Lyon	W	1884	370	1783	1128
Algeria1	Madrid	SW	1038	185	1268	617
Morocco1	Madrid	SW	1184	103	1024	244
Libya1	Magdeburg	G	2613	325	2461	1217
Algeria1	Manchester	NW	2789	295	3506	2916
Morocco1	Manchester	NW	2855	369	2887	1894

Algeria2	Marseille	W	1769	466	1632	1232
Morocco2	Marseille	W	1781	341	1834	1354
Morocco2	Milan	S	2342	134	1556	1195
Tunisia1	Milan	S	1591	325	2178	1615
Egypt2	Minsk	NE	3436	162	3186	1173
Iraq1	Minsk	NE	4176	0	3637	2462
Egypt2	Moscow	NE	4023	0	2868	1175
Syria1	Moscow	NE	3631	0	3225	1505
Tunisia1	Munich	G	1950	325	1966	1042
Libya2	Naples	S	2073	748	1310	1077
Tunisia1	Naples	S	1303	565	1856	1510
Egypt2	Nicosia	T	698	375	698	461
Libya1	Nuremberg	G	2321	325	2606	1615
Libya1	Oslo	N	3489	497	3116	1803
Tunisia1	Oslo	N	3222	497	3281	1825
Algeria2	Paris	W	2404	185	2040	1067
Morocco2	Paris	W	2007	134	2770	1699
Libya2	Podgorica	SE	2388	767	2198	1814
Morocco2	Porto	SW	1238	24	1291	809
Algeria2	Prague	E	2220	410	3034	2176
Libya2	Prague	E	3783	334	2215	1100
Jordan1	Pristina	SE	2811	100	2394	1794
Morocco1	Reykjavik	NW	5560	1850	5452	4887
SaudiArabia1	Riga	N	5438	0	4303	2462
Algeria2	Rome	S	1457	526	1320	1089
Tunisia1	Rome	S	1453	449	1384	935
Morocco2	Saarbrücken	G	2329	134	2262	1177
Jordan1	Sarajevo	SE	3072	100	1752	1274
Libya1	Sarajevo	SE	1985	572	2833	2301
Libya1	Schwerin	G	2786	325	2620	1217
Egypt2	Skopje	SE	2739	162	2293	1859
Tunisia1	Sofia	SE	2088	499	1932	1273
Algeria1	Southampton	NW	2266	317	3212	2663
Morocco2	Southampton	NW	2286	207	2380	1456
Iran1	St Petersburg	NE	3714	0	3702	1184
Iraq1	St Petersburg	NE	4099	0	3649	1043
Algeria2	Tallinn	N	3763	410	3918	2169
Iran1	Tbilisi	NE	1016	0	1320	0
Libya2	Thessaloniki	SE	2614	794	2385	1782
Libya2	Tirana	SE	2374	742	2083	1718
Algeria1	Toulouse	W	1437	185	1947	1423
Morocco1	Toulouse	W	1806	103	1419	767
Libya1	Vaduz	S	2023	325	1881	1217
Algeria2	Vienna	S	2238	410	2938	2220
Libya2	Vienna	S	2923	750	2282	1354
Libya1	Vilnius	N	3712	334	3111	1274
Iran2	Volgograd	NE	2273	0	2302	901

Iraq1	Volgograd	NE	2191	0	2190	1160
Algeria2	Warsaw	E	2927	410	2693	1274
Libya1	Warsaw	E	3190	334	2918	1324
Libya1	Wroclaw	E	2854	334	2601	1689
Tunisia1	Wroclaw	E	2587	334	2692	1648
Iraq1	Yerevan	NE	1213	0	968	0
Algeria2	Zagreb	SE	2061	410	2077	1341
Algeria1	Zurich	S	2223	185	2373	1615
Morocco2	Zurich	S	2247	134	2378	1570

Table 34: Link lengths of point-to-point hydro reservoir (not optimized)

<b>From potential exporting model region</b>	<b>To potential offtaker model region</b>	<b>Total length [km]</b>	<b>Sea cable section [km]</b>
N	G	1570	160
N	E	1704	350
N	NW	2502	850

## 10.2 Chapter 3 - Energy System Model

### 10.2.1 Energy supply and demand

#### 10.2.1.1 Supply technologies and their resource potentials

Table 35 shows the model limitations by resource potential of the listed technologies. Other used technologies or technological components (e.g. storage size) have unlimited potentials.

Table 35: Limited resource potentials of used technologies

Technology/ Model region	Pump storage discharge [MW <sub>e</sub> ]	Hydro run-of-river [MW <sub>e</sub> ]	Hydro-reservoir regional, turbine [MW <sub>e</sub> ]	Hydro-reservoir import from N, turbine [MW <sub>e</sub> ]*	Geothermal energy [TWh <sub>e</sub> ]	Solid biomass [TWh <sub>chem</sub> ]	CSP regional, solar field [GW <sub>th</sub> ]
G	15875	4377	430	6153	26	216	0
N	4781	39326	25813	-	1	832	0
E	3500	4504	963	3748	17	338	0
S	20014	31924	16500	-	18	317	105
W	7743	13943	11660	-	12	329	19
NW	3853	3507	328	7308	24	57	0
NE	2612	32448	0	-	1	2580	0
SE	4149	21721	8330	-	8	520	42
NAE	0	3033	0	-	13	12	242239
NAW	932	1724	0	-	9	80	234089
SW	19588	8560	12999	-	22	314	1566
T	571	14611	679	-	75	212	373
MES	0	3313	0	-	0	12	58426
I	0	1044	0	-	6	38	37867
ME	0	0	0	-	68	3	224692

\*The import potential of hydro reservoir from model region N to G, E and NW is calculated with 40% of the available potential in N and distributed due to the electricity of the destination model regions. Thus, 60% of the original potential remains in model region N.

Potential of pump storage discharge is taken from (Marcos, et al., 2013) "T2 realisable (5km)" with energy to power ratio of 7 and a reduced potential of 75.5%. This reduced potential is achieved comparing the cost-efficient pump storage discharge potential in Germany of 15GW (Moser, 2014) to the study values with 20GW (Marcos, et al., 2013).

Potential of hydro run-of-river and CSP is taken from (Scholz, 2012) for Europe and from (Stetter, 2012) for MENA. Potential of hydro-reservoir is taken from (FIAS, 2017) using a power plant matching in Europe and for Turkey from (Scholz, 2012). Potential of geothermal energy is taken from (DLR, 2005), (DLR, 2006) and for Germany from (Jung, et al., 2002). Net primary production (NPP) potential of solid biomass is taken from model values of (Tum, et al., 2013). The assumed usable energy potential consists of 25% of total tree NPP and of 20% of total straw NPP of the year 2010.

#### 10.2.1.2 Demand model

As described in (Trieb, et al., 2006) the electricity demand model depends on population and GDP. Table 36 lists the assumed GDP growth rate. This is based on a scenario which closes the GDP gap between each country and here the USA (with a comparable high GDP per capita) of 50% in the year 2050. Higher GDP growth rates of 7% are avoided. The population data is used from (United Nations, 2010). Starting in the year 2010 with electricity final consumption values from IEA country statistics, the resulting electricity demand and electrical demand in heat and mobility sector is also shown in Table 36 for the year 2050.

Table 36: GDP growth rate assumption and resulting annual electrical national demand following (Trieb, et al., 2006)

Country	Average growth rate for GDP per capita in %/y (2010 - 2050)	Electricity demand 2010 [TWh]	Electricity demand 2050 [TWh]	Electrical heat demand 2050 [TWh]	Electrical mobility demand 2050 [TWh]	Load time serie
Albania	4.10	5.67	13.67	0.10	0.33	ENTSO-e
Algeria	3.50	33.47	292.32	61.78	12.84	AUE
Armenia	4.95	4.67	13.54	0.95	0.09	Synthetic
Austria	1.40	62.32	51.20	14.41	4.18	ENTSO-e
Azerbaijan	3.05	12.24	57.23	14.80	1.28	Synthetic
Bahrain	1.46	22.20	13.68	0.00	1.16	AUE
Belarus	3.05	29.38	42.21	6.79	1.29	ENTSO-e (Poland)
Belgium	1.48	83.31	71.79	47.36	5.94	ENTSO-e
Bosnia Herzegovina	4.25	10.35	15.46	0.13	0.37	ENTSO-e
Bulgaria	3.15	27.19	26.72	0.21	0.62	ENTSO-e
Croatia	2.65	15.86	20.55	1.63	0.70	ENTSO-e
Cyprus	1.70	4.87	7.89	0.02	0.63	ENTSO-e



Czech Republic	2.02	57.20	61.38	14.42	2.56	ENTSO-e
Denmark	1.40	32.11	60.88	7.02	2.90	ENTSO-e
Djibouti	5.93	0.29	5.02	0.31	0.09	AUE (Yemen)
Egypt	3.86	125.16	1048.72	19.22	25.83	AUE
Estonia	2.45	6.91	6.01	0.33	0.28	ENTSO-e
Finland	1.50	83.40	88.89	2.28	2.47	ENTSO-e
France	1.61	443.86	468.15	88.94	26.89	ENTSO-e
Georgia	5.20	7.29	17.31	0.67	0.24	Synthetic
Germany	1.65	532.42	510.40	173.47	21.83	ENTSO-e
Greece	1.92	53.12	61.19	2.63	2.89	ENTSO-e
Hungary	2.45	34.21	48.71	14.53	1.39	ENTSO-e
Iceland	1.58	15.71	9.91	0.02	0.22	Synthetic
Iran	2.93	186.06	484.45	361.75	28.19	AUE (Syria)
Iraq	2.73	36.76	389.93	83.64	35.92	AUE (Syria)
Ireland	1.35	25.29	39.36	17.58	3.14	ENTSO-e
Israel	1.95	48.72	73.66	0.80	6.12	AUE (Syria)
Italy	1.65	299.31	387.24	96.46	16.73	ENTSO-e
Jordan	3.75	12.84	63.13	2.90	2.96	AUE
Kosovo	4.50	4.10	24.92	0.23	0.46	ENTSO-e (Serbia)
Kuwait	0.72	37.22	46.93	0.00	8.29	AUE
Latvia	2.82	6.22	8.38	0.94	0.32	ENTSO-e
Lebanon	3.00	15.09	29.29	0.15	1.52	AUE (Syria)
Libya	1.90	25.43	78.15	0.09	5.66	AUE
Lichtenstein	0.48	0.61	0.29	0.11	0.02	ENTSO-e
Lithuania	2.55	8.33	12.61	0.92	0.43	ENTSO-e
Luxembourg	0.60	6.59	11.46	5.75	2.79	ENTSO-e
Macedonia	3.69	6.78	9.92	0.08	0.21	ENTSO-e
Malta	2.07	1.80	2.25	0.00	0.09	ENTSO-e
Moldova	6.15	5.56	15.85	2.05	0.32	ENTSO-e (Poland)
Montenegro	3.33	3.21	2.95	0.00	0.10	ENTSO-e (Serbia)
Morocco	4.95	23.71	218.13	7.69	4.29	AUE
Netherlands	1.30	106.87	121.84	62.95	6.53	ENTSO-e
Norway	0.96	113.45	152.98	0.00	4.48	ENTSO-e
Oman	1.20	16.13	46.99	0.00	5.89	AUE
Palestine	3.48	3.28	39.11	3.24	3.32	AUE (Syria)

Poland	2.50	119.06	196.58	50.75	6.01	ENTSO-e
Portugal	2.05	49.89	64.24	0.59	2.40	ENTSO-e
Qatar	0.27	24.62	34.29	0.00	5.97	AUE
Romania	2.95	41.47	83.95	8.85	1.33	ENTSO-e
		411.27				
Russia until Ural	2.55	(IEA, 2005)	513.70	50.52	17.85	ENTSO-e (Poland)
Saudi-Arabia	1.30	202.82	387.16	0.00	49.57	AUE
Serbia	3.60	27.57	38.53	1.53	1.06	ENTSO-e
Slovakia	2.22	24.14	29.94	1.95	0.88	ENTSO-e
Slovenia	2.00	11.97	11.61	1.75	0.81	ENTSO-e
Spain	1.76	245.39	250.61	8.77	15.54	ENTSO-e
Sweden	1.40	131.21	210.97	1.45	6.02	ENTSO-e
Switzerland	1.13	59.77	68.95	28.21	4.91	ENTSO-e
Syria	5.29	33.65	200.65	8.07	6.07	AUE
Tunisia	3.90	13.55	71.07	4.72	1.65	AUE
Turkey	2.95	170.01	501.43	89.91	13.19	ENTSO-e (Greece)
Ukraine	4.50	134.03	175.08	40.20	2.70	ENTSO-e (Poland)
United Arab Emirates	1.03	84.42	118.75	0.00	11.14	AUE
United Kingdom	1.61	328.96	502.46	183.57	28.87	ENTSO-e
Yemen	4.50	5.04	215.97	17.53	5.06	AUE

Especially in MENA countries the electrical demand rises until 2050. However, e.g. in the demand scenario of Iran the electrical heat demand is dominant, which indicates that a major transition need – achieving climate targets – is also the restructuring of the heat sector by renewable energies.

## 10.2.2 Basic modelling assumptions

### 10.2.2.1 Annual characteristic of load and renewable resources

For a regional comparison of renewable resources and demand Table 37 shows peak load and average full load hours of model regions.

Table 37: Peak load and average resource full load hours of model regions

Model region	Peak Load [GW]	Average resource full load hours [h/y]					
		PV	Wind Onshore	Wind Offshore	Hydro Run Of River	CSP solar field national	CSP solar field import
G	112	836	2107	4125	5015	-	1934
N	99	867	2023	3810	4137	-	1980
E	69	1016	1731	3207	2396	-	2011
S	112	1139	1353	1917	3033	1914	1943
W	155	1027	2110	3626	2543	1881	1926
NW	134	789	3721	4309	3606	-	1916
NE	170	1011	2251	3260	3220	-	1939
SE	54	1118	1290	2265	2432	1938	1997
NAE	182	1747	1257	1939	4219	2135	-
NAW	112	1701	2179	3096	1925	2026	-
SW	57	1309	1555	2418	1551	2034	1897
T	113	1494	1312	1767	3266	1847	1966
MES	165	1620	1661	1400	4096	1881	-
I	152	1671	1591	1725	4957	1972	-
ME	170	1749	1577	1765	-	2105	-

The average resource full load hours are a result of an aggregation of the spatial availability of the resource. Full load hours of CSP solar field import represent an average of selected sites in EUMENA which leads to a more conservative approach than for CSP solar field nat.

### 10.2.2.2 Isoleth diagrams of electrical load and technological time series

In this section isopleth diagrams show regional technological availability. Comparing e.g. load curves in MENA and EU, the peak demand in MENA is higher in summer than in winter probably due to cooling efforts. Another visible effect is that in MENA the solar resource are more constantly available during the year while in the EU the availability decrease in winter. Some regions do not have hydro reservoir due to missing data or missing potentials.

### 10.2.2.3 Hourly time series profiles for EU of the year 2006 based on (Scholz, 2012) and for MENA of the year 2002 based on (Stetter, 2012)

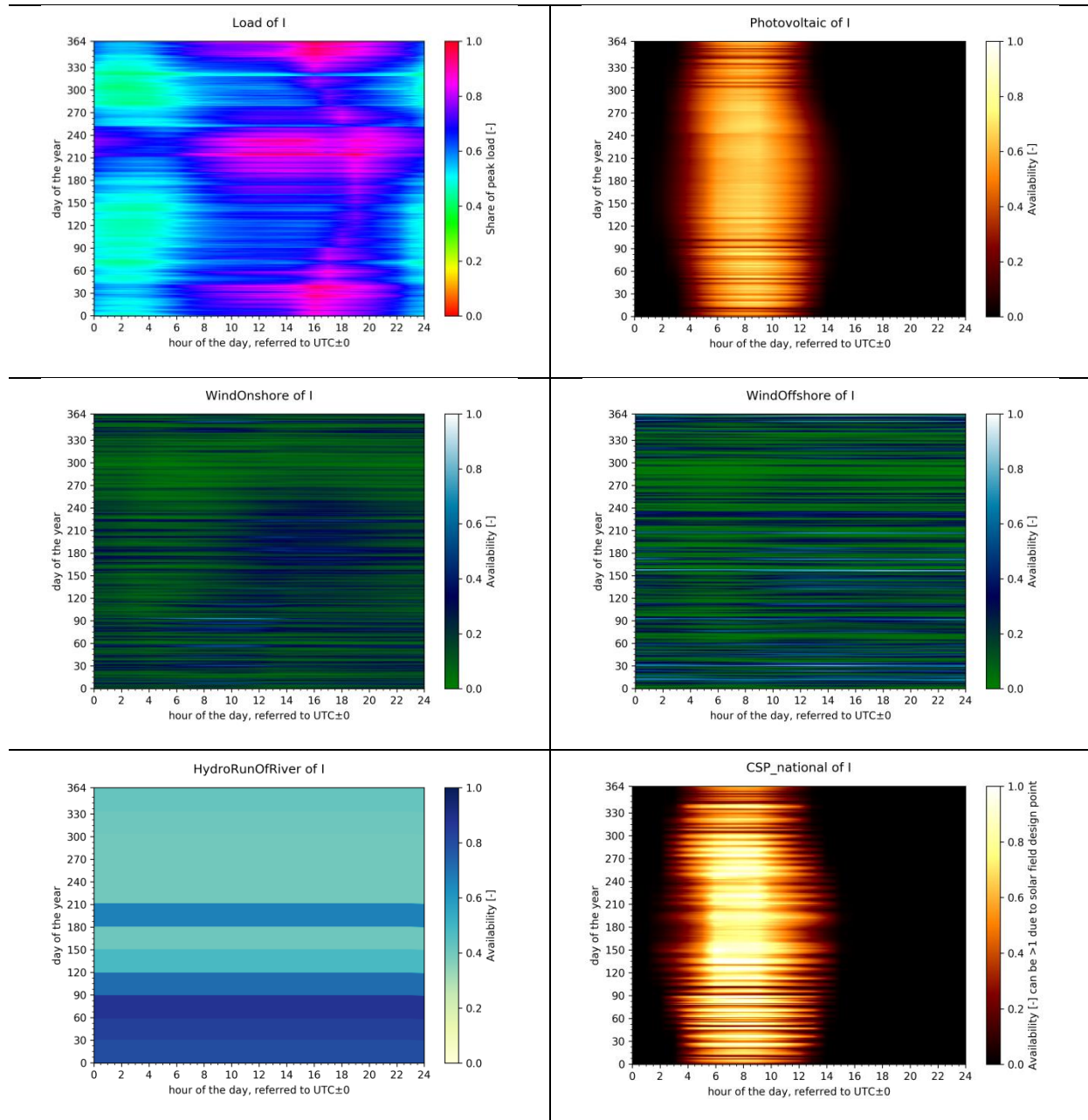


Figure 39: Load and technological time series of model region I

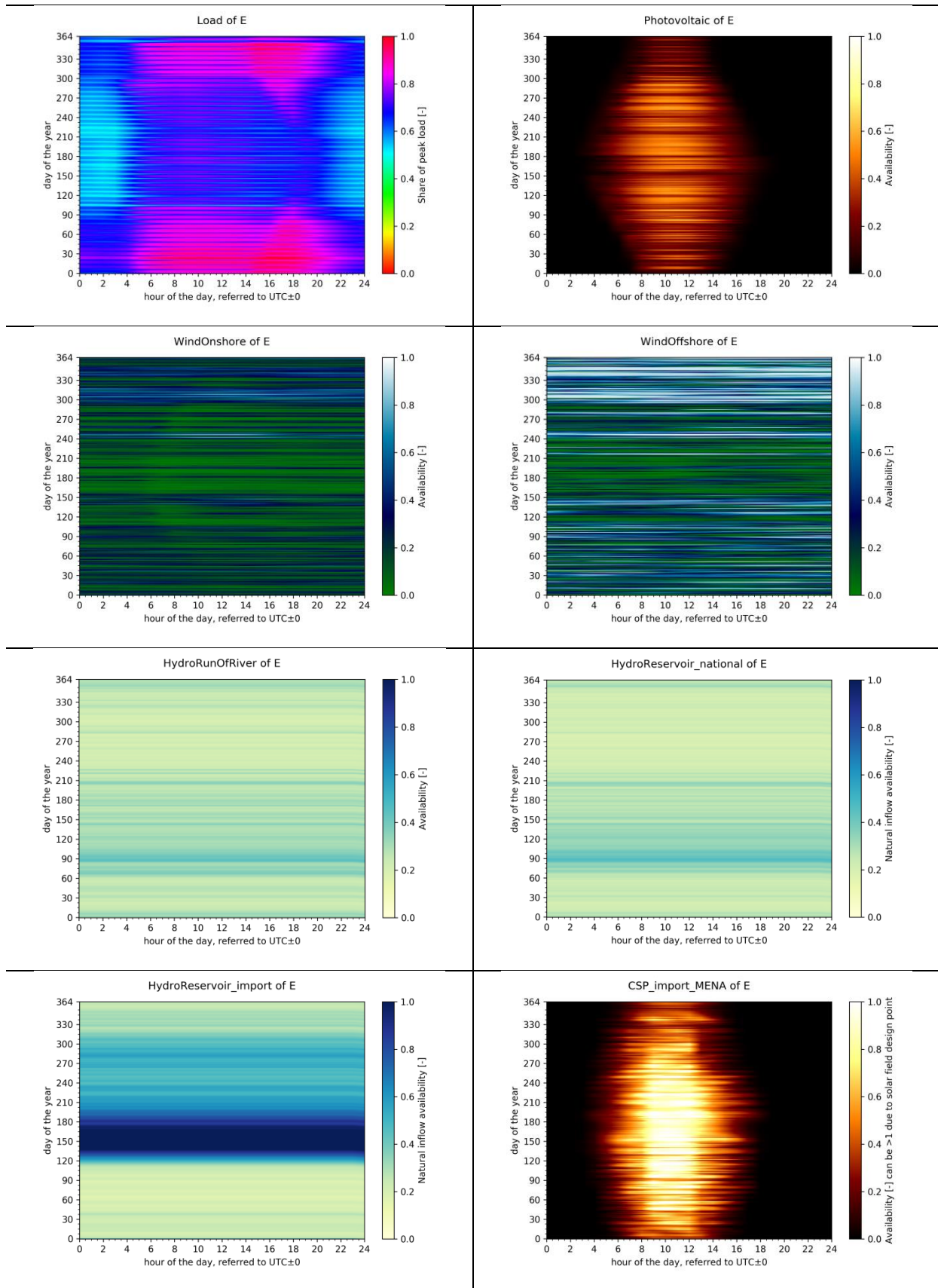


Figure 40: Load and technological time series of model region E

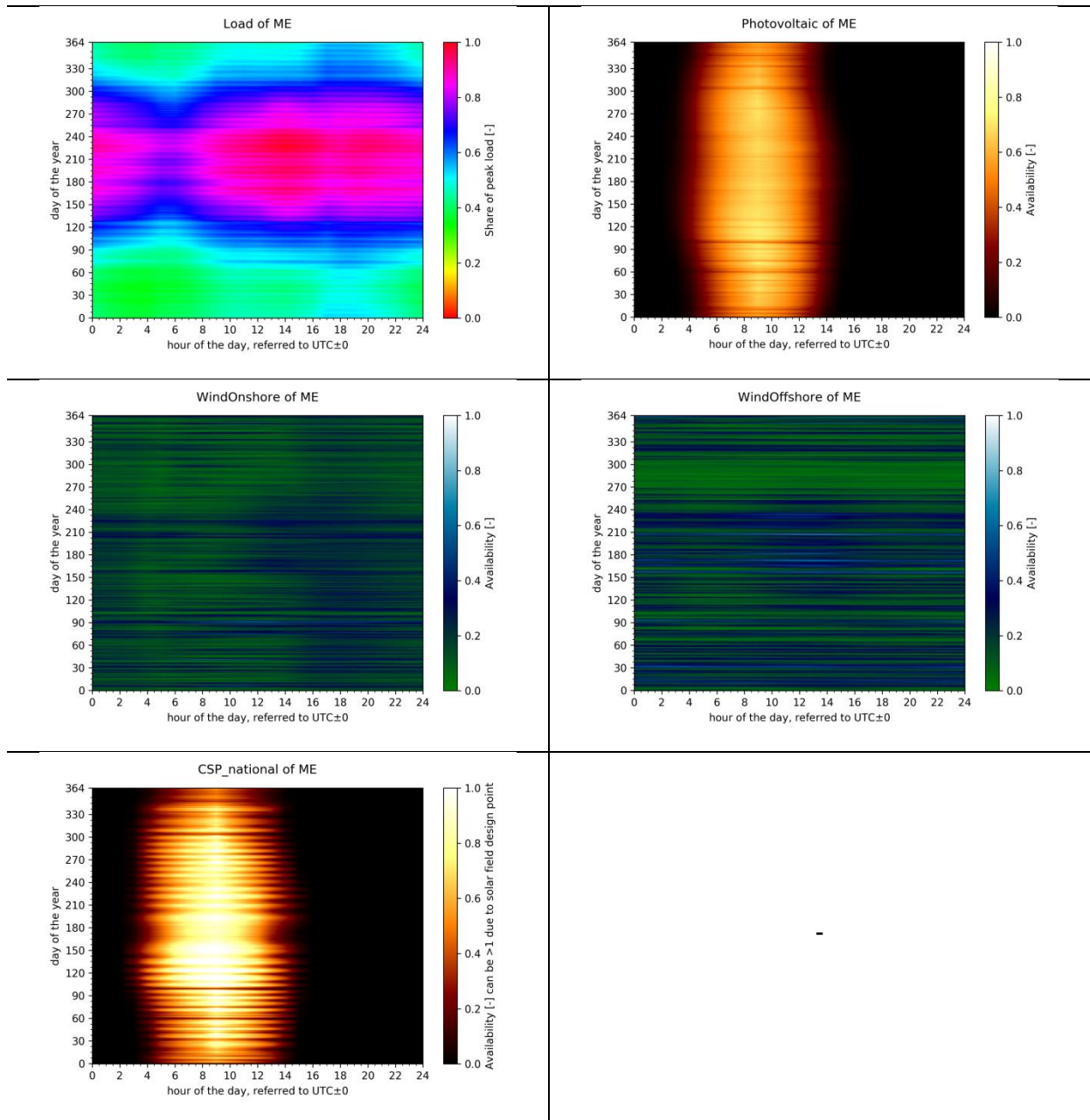


Figure 41: Load and technological time series of model region ME

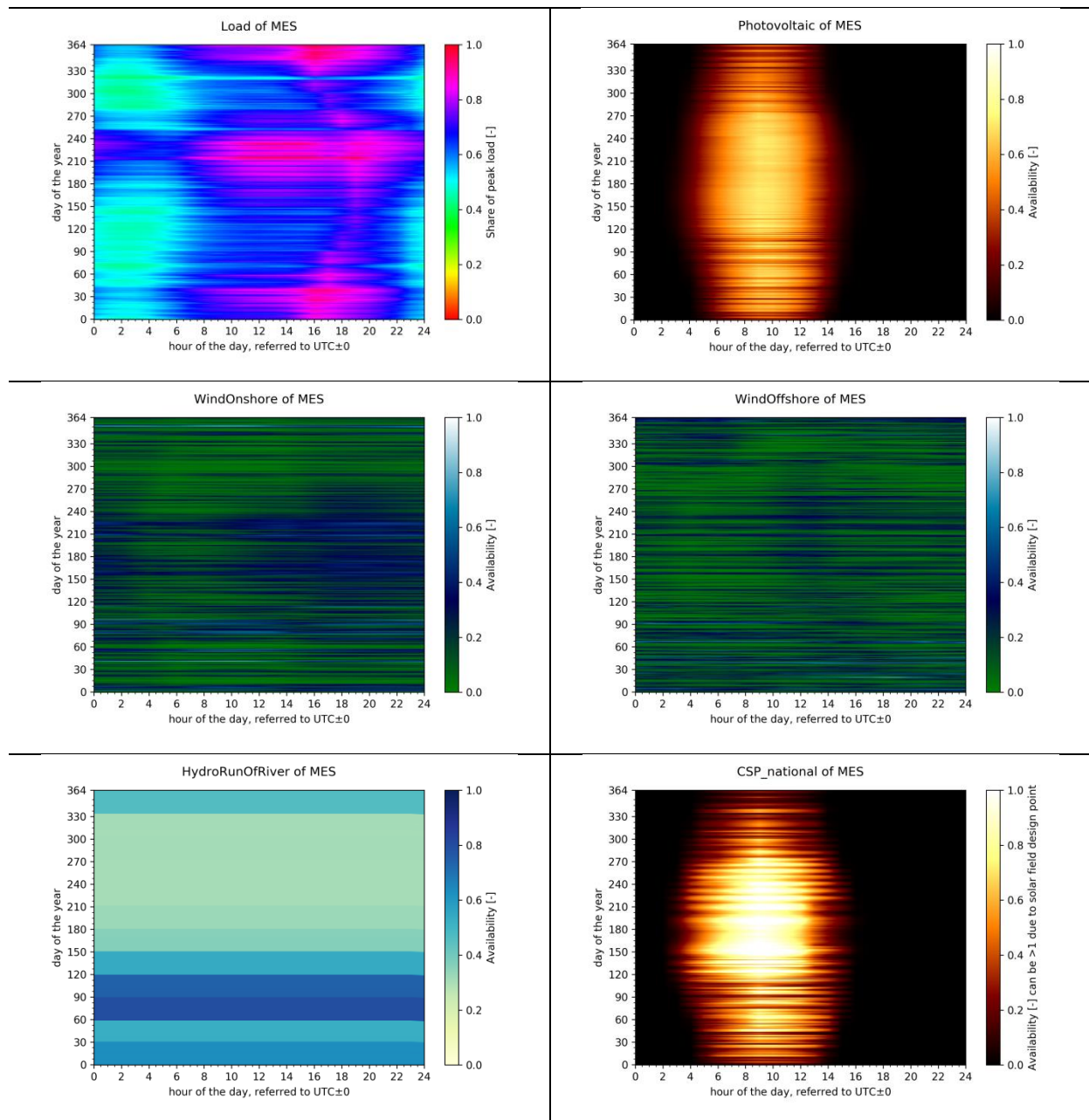


Figure 42: Load and technological time series of model region MES

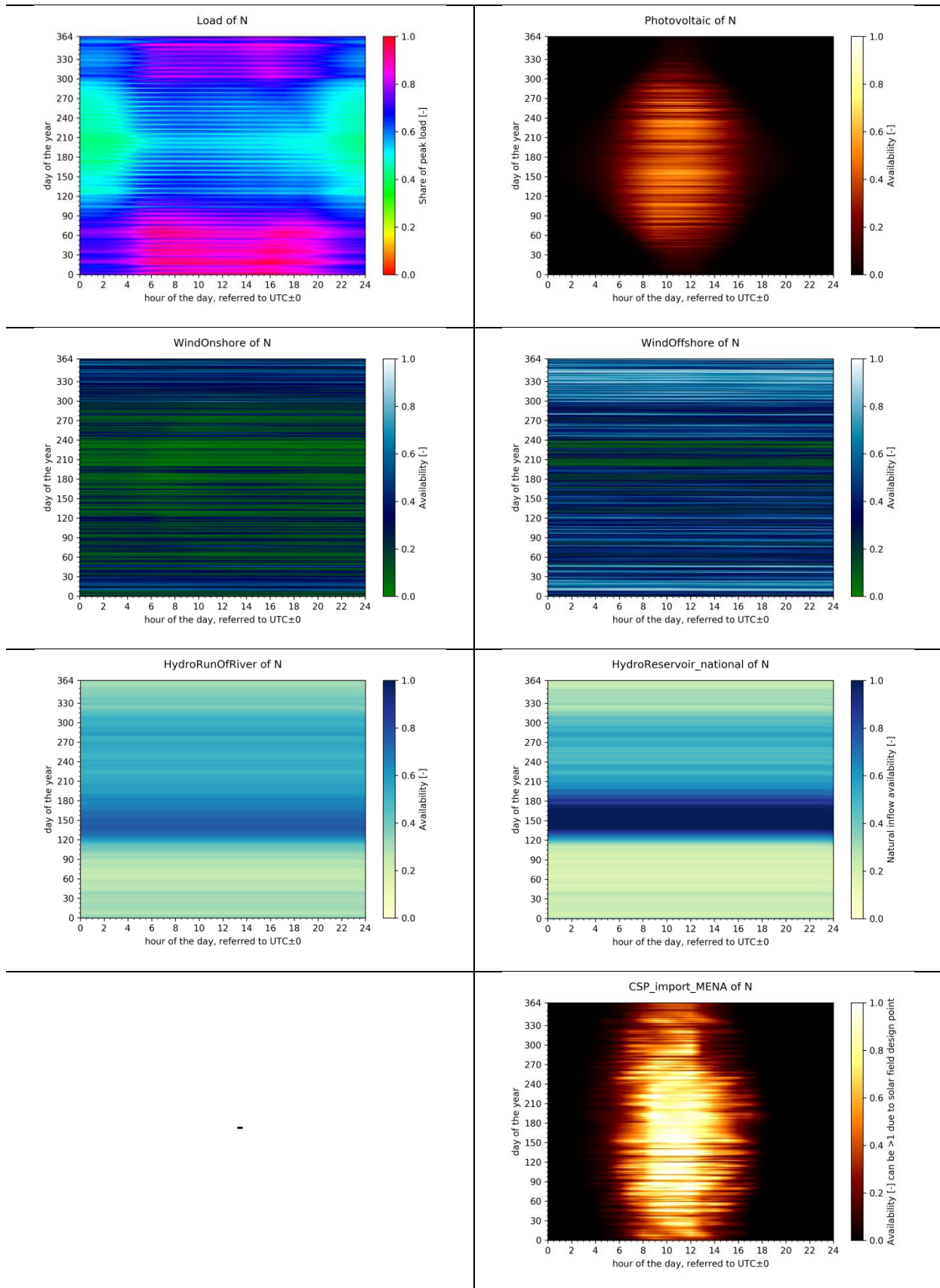


Figure 43: Load and technological time series of model region N



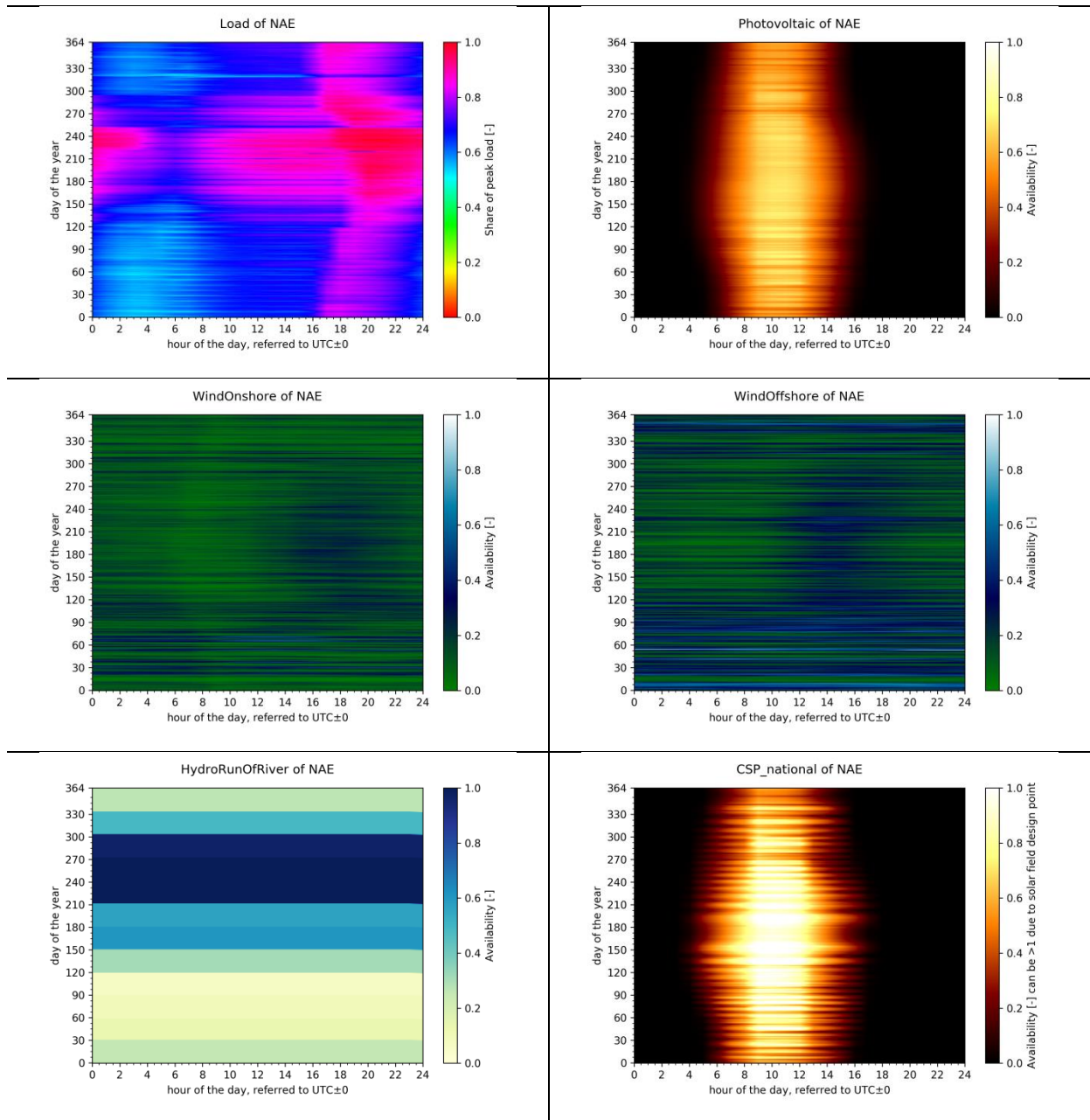


Figure 44: Load and technological time series of model region NAE

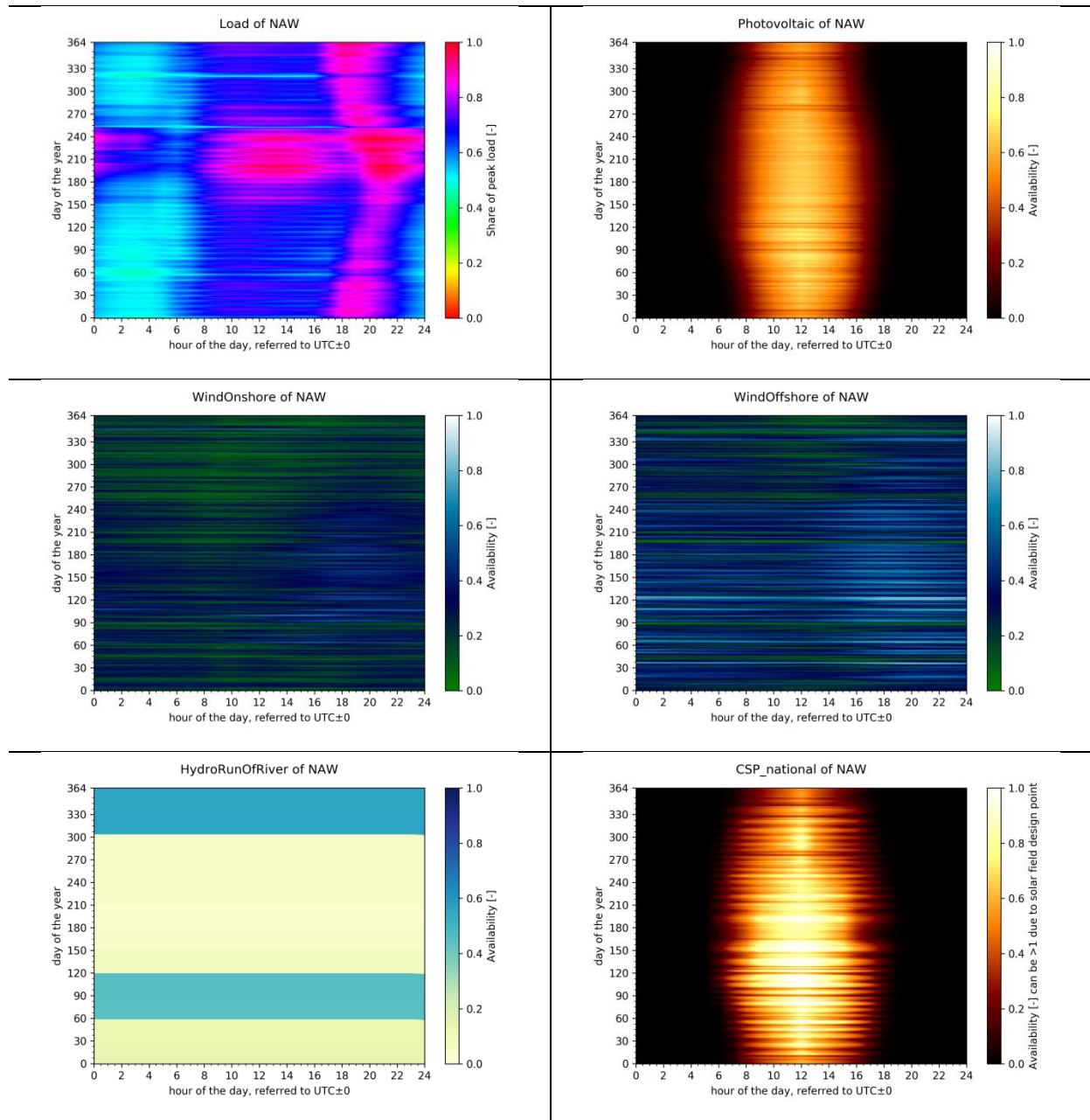


Figure 45: Load and technological time series of model region NAW

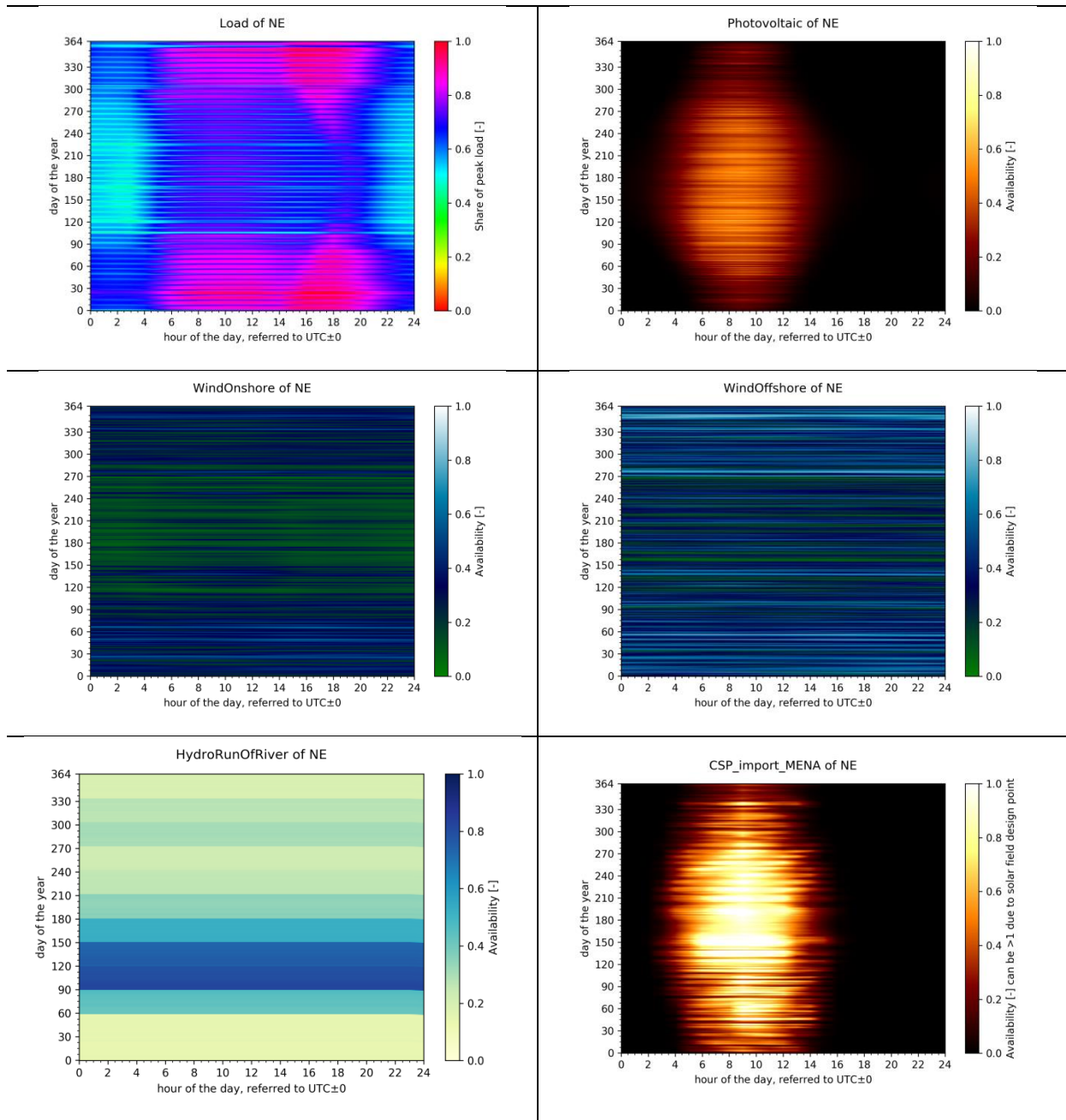


Figure 46: Load and technological time series of model region NE

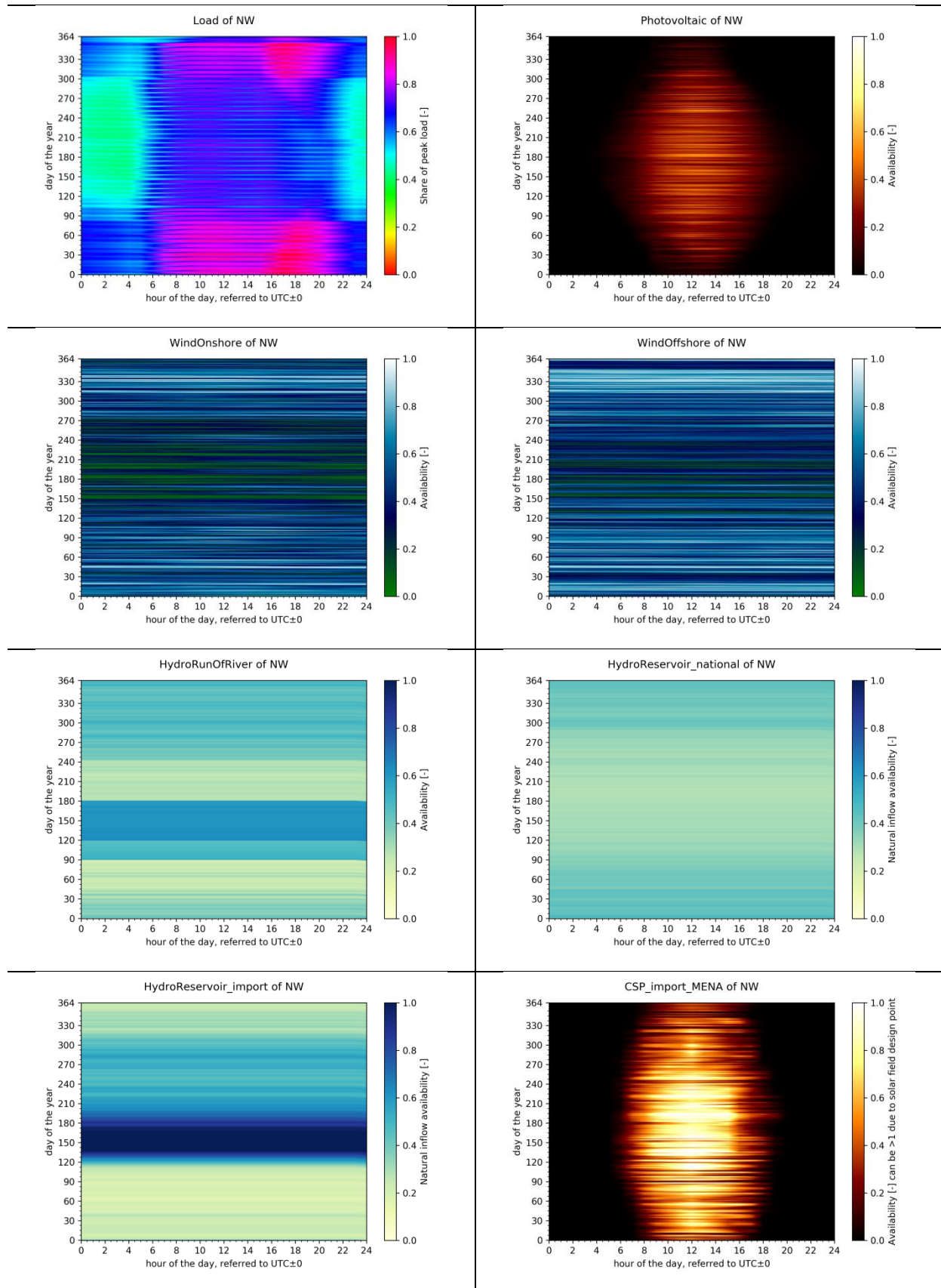


Figure 47: Load and technological time series of model region NW

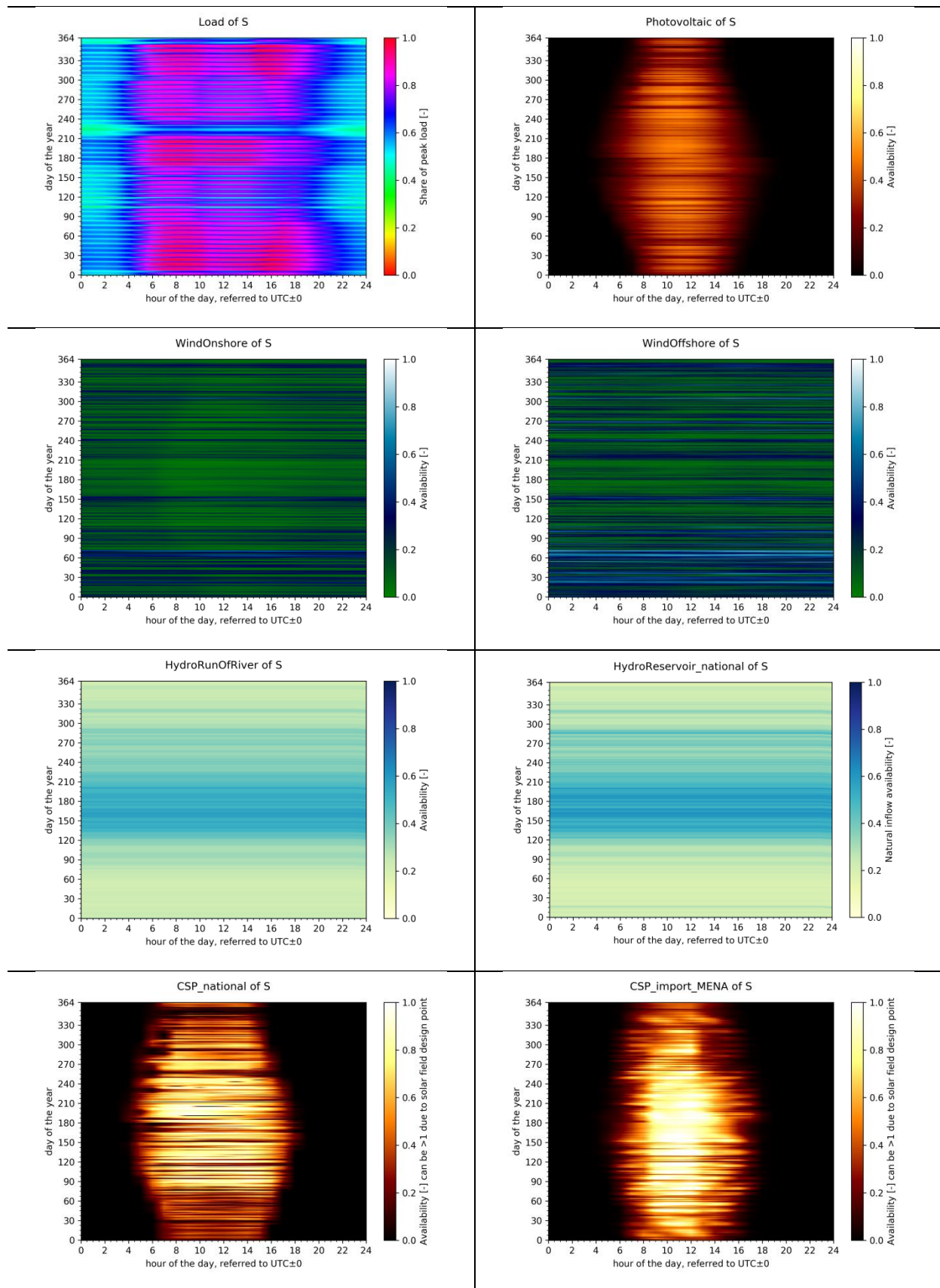


Figure 48: Load and technological time series of model region S

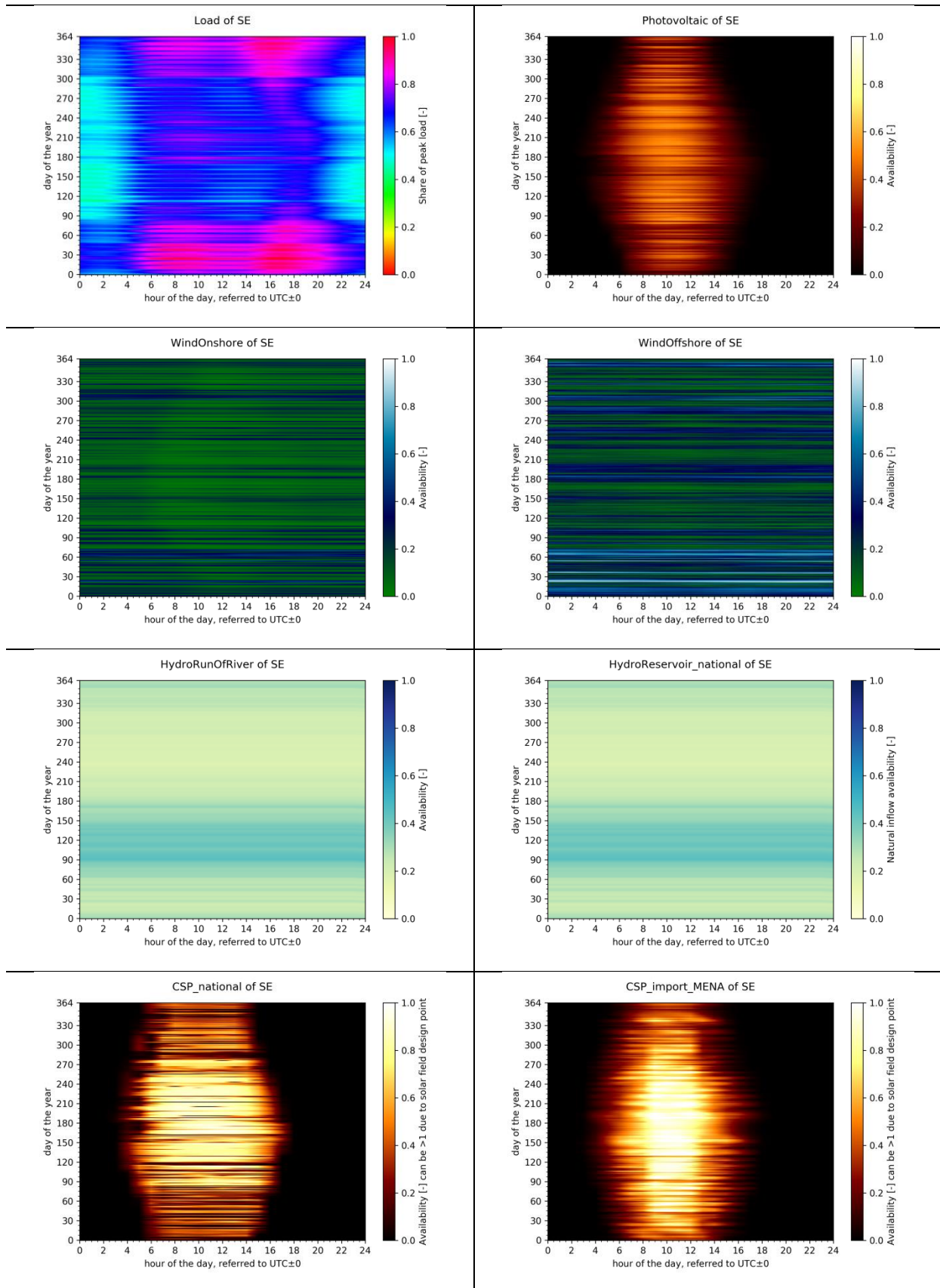


Figure 49: Load and technological time series of model region SE

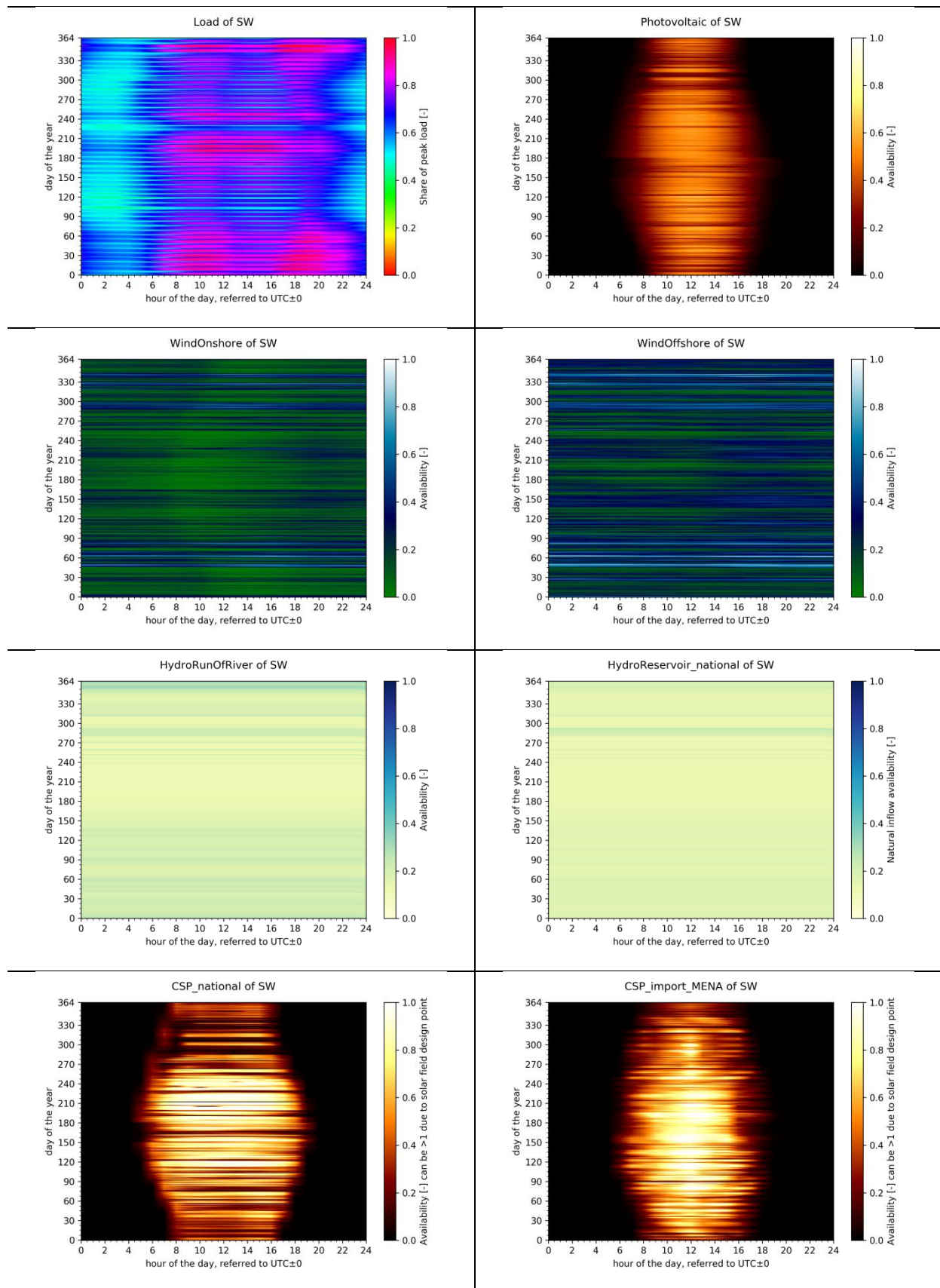


Figure 50: Load and technological time series of model region SW

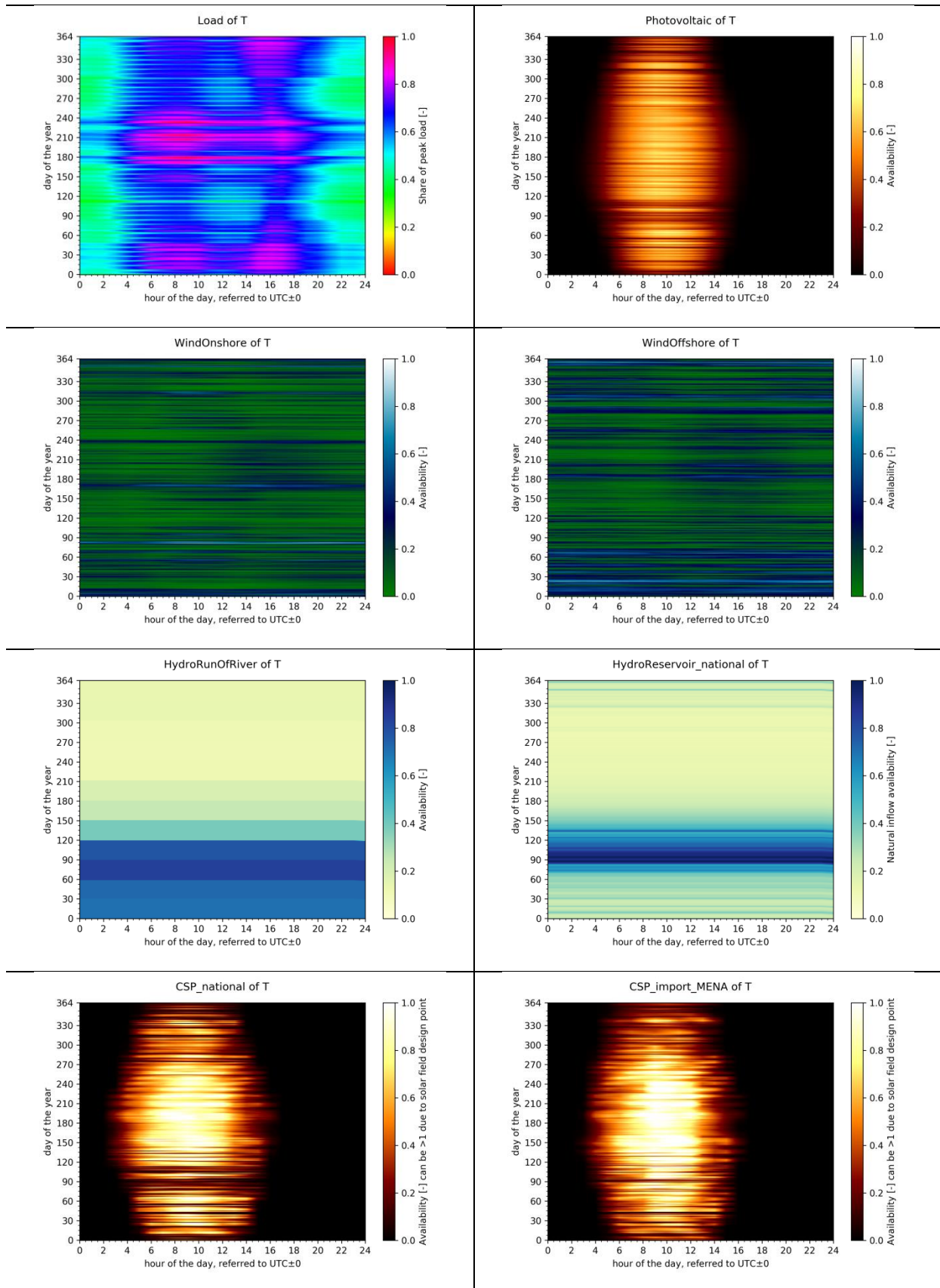


Figure 51: Load and technological time series of model region T



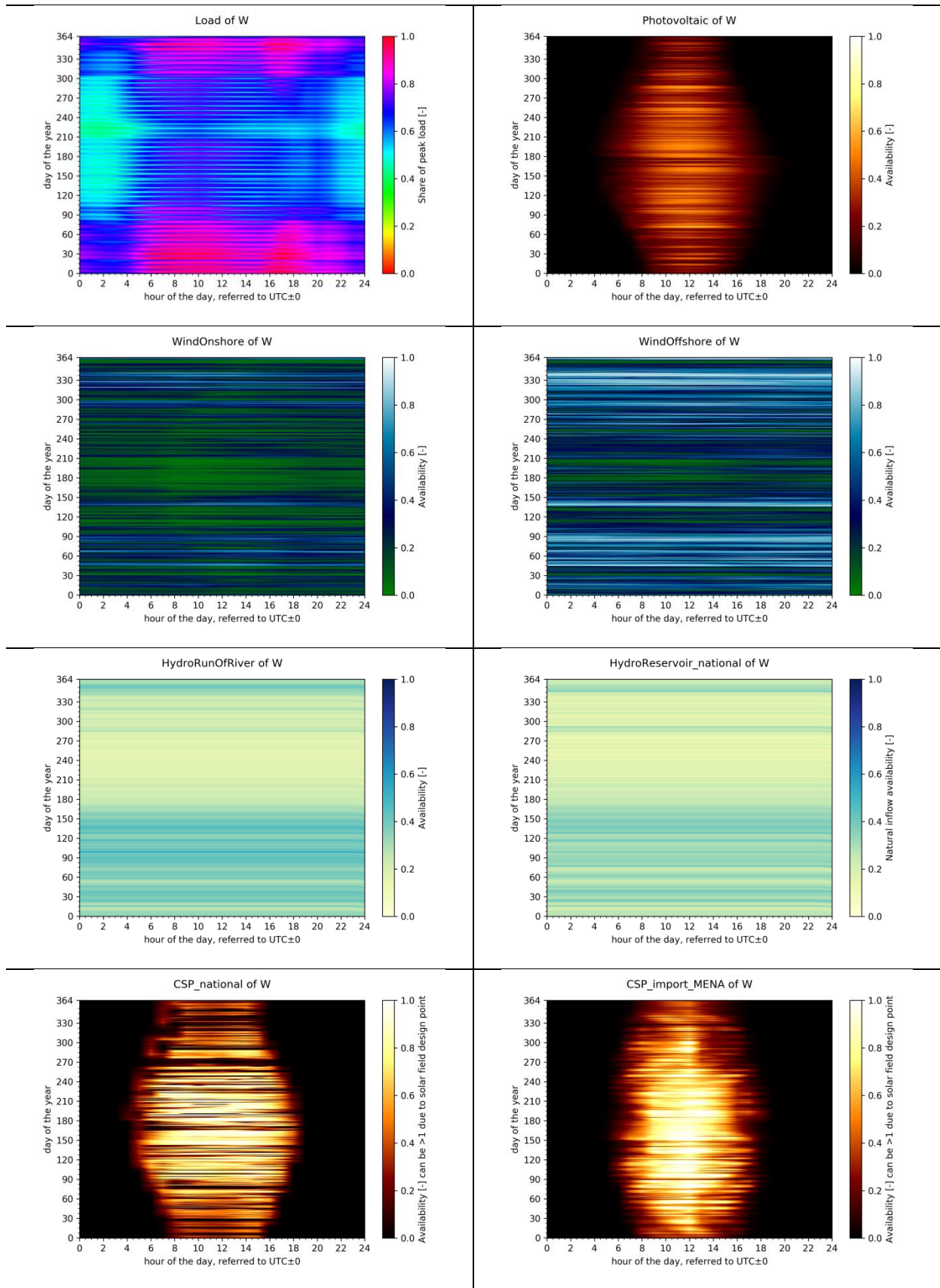


Figure 52: Load and technological time series of model region W

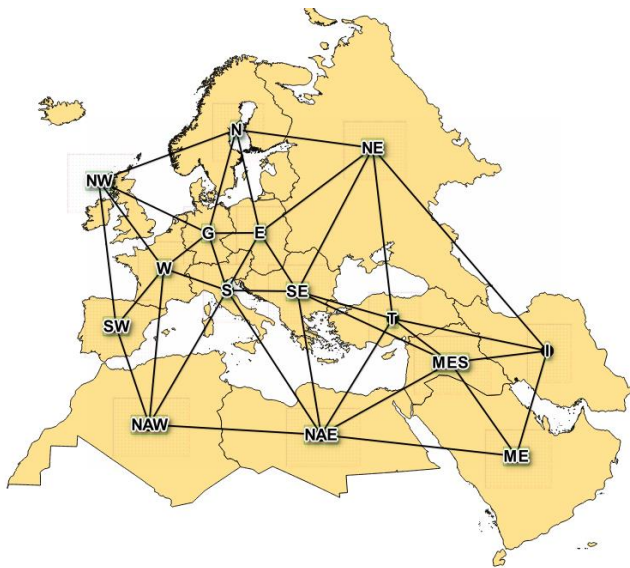
## 10.2.3 Grid method and validation

### 10.2.3.1 Overlay grid modelling

In Table 38 the link lengths of the overlay grid are shown. Using air-line distance this value is multiplied with a length correction factor of 1.2 for a more realistic length assumption.

Table 38: Assumed overlay grid link length

Link	Link length land [km]	Link length sea [km]	Map
G_N	1410	160	
G_E	535	0	
G_S	772	0	
G_W	703	0	
G_NW	1414	700	
N_NE	1458	0	
N_E	1354	350	
N_NW	1652	850	
NE_E	1772	0	
NE_SE	2134	630	
NE_T	2141	630	
NE_I	2891	1090	
NW_W	1379	660	
NW_SW	1929	1220	
W_S	795	0	
W_NAW	2060	530	
W_SW	950	0	
SW_NAW	1356	200	
S_E	865	0	
S_SE	838	220	
S_NAE	2145	930	
S_NAW	2018	785	
SE_T	1160	0	
SE_MES	1972	300	
SE_NAE	1849	440	
NAE_NAW	2178	0	
NAE_T	1790	750	
NAE_MES	1933	0	
NAE_ME	2477	250	
MES_I	1228	0	
MES_ME	1315	0	
MES_T	836	0	
I_T	1869	0	
I_ME	1359	230	
E_SE	849	0	



### 10.2.3.2 Transmission and distribution grid modelling

Table 39 shows the resulting capacity of the “greenfield” optimization as result of pre-assumption of the node-internal grid model and input of the node-internal grid model calibration. This capacity is distributed in the 491 node model according to Figure 14.

Table 39: Capacity [GW] in Germany using the node-internal grid model (916 €/kW<sub>AC trans</sub> OHL and 1758 €/kW<sub>AC trans</sub> UGC).

Scenario	Max UGC	Min OHL	Max UGC	Min OHL	Max UGC	Min OHL	Max UGC	Min OHL	Max UGC	Min OHL
	10_90	10_90	30_70	30_70	50_50	50_50	70_30	70_30	90_10	90_10
Solid Biomass	26.4	0.0	21.1	0.0	22.4	0.0	27.3	0.0	19.3	0.0
Geothermal	3.7	3.8	4.1	3.6	4.0	4.6	4.0	4.3	4.1	4.7
Photovoltaic	0.0	0.0	0.0	4.7	41.6	73.4	95.5	144.5	147.0	182.8
Hydro Run Of River	0.0	0.0	0.0	0.0	0.0	0.0	0.0	0.0	0.0	0.0
Wind Offshore	0.0	14.8	36.7	37.1	53.7	44.9	77.9	64.6	109.0	97.5
Wind Onshore	43.1	35.9	45.5	56.6	73.0	85.4	86.3	109.5	117.9	119.7
CSP Power Block	91.7	98.8	70.7	78.5	47.7	56.5	23.7	33.9	0.0	10.0
CSP Solar Field [GWth]	1076.2	1402.5	749.4	995.8	474.2	685.6	225.5	382.5	0.0	98.5
CSP Thermal Storage [GWh]	3190.8	3560.5	2381.5	2747.1	1622.8	1974.5	813.6	119.8	0.0	351.3
P2G2P Discharge	88.6	113.5	93.2	113.8	92.1	112.8	87.5	113.0	95.0	112.7
P2G2P Charge	12.4	9.2	9.8	8.5	14.9	11.3	15.7	15.8	27.7	22.9
P2G2P Storage [GWh]	10.9	16.3	8.7	13.3	9.2	15.1	9.8	15.6	12.3	13.3
Compressed Air Discharge	0.0	0.0	0.0	0.0	0.0	0.0	0.0	2.1	0.0	12.2
Compressed Air Charge	0.0	0.0	0.0	0.0	0.0	0.0	0.0	1.3	0.0	8.8
Compressed Air Storage [GWh]	0.0	0.0	0.0	0.0	0.0	0.0	0.0	0.0	0.0	0.2
Pump Storage Discharge	0.0	11.2	2.9	2.9	6.2	15.9	10.8	15.9	15.9	15.9
Pump Storage Charge	0.0	15.7	1.9	14.6	4.1	19.4	9.3	22.4	18.9	22.8
Pump Storage Storage [GWh]	0.0	0.7	0.0	1.3	0.1	1.6	0.3	2.2	0.5	3.4
Lithium Ion Discharge	0.0	0.0	0.0	0.0	0.0	0.0	1.3	5.9	5.6	8.3
Lithium Ion Charge	0.0	0.0	0.0	0.0	0.0	0.0	0.7	3.5	3.7	4.9
Lithium Ion Storage [GWh]	0.0	0.0	0.0	0.0	0.0	0.0	0.0	0.0	0.0	0.0

Table 40 shows the resulting capacity of the “greenfield” optimization as result of the calibrated node-internal grid model. The sum of these capacities are shown in Figure 17g.

Table 40: Capacity [GW] in Germany using the node-internal grid model (585 €/kW<sub>AC trans</sub> OHL and 900 €/kW<sub>AC trans</sub> UGC).

Scenario	Max UGC	Min OHL	Max UGC	Min OHL	Max UGC	Min OHL	Max UGC	Min OHL	Max UGC	Min OHL
fluctuating_dispatchable share	10_90	10_90	30_70	30_70	50_50	50_50	70_30	70_30	90_10	90_10
Solid Biomass	25.9	0.0	20.8	0.0	22.5	0.0	25.5	0.0	18.6	0.0
Geothermal	3.7	3.7	4.1	3.5	4.0	4.5	4.0	4.8	4.2	4.7
Photovoltaic	0.0	0.0	1.8	6.7	41.4	78.6	92.0	140.7	137.2	183.0
Hydro Run Of River	0.0	0.0	0.0	0.0	0.0	0.0	0.0	0.0	0.0	0.0
Wind Offshore	7.7	21.4	39.6	42.7	53.6	47.1	77.8	62.3	111.2	96.7
Wind Onshore	28.2	21.1	40.1	45.6	73.3	80.6	86.0	109.2	106.7	117.5
CSP Power Block	92.0	99.0	70.5	77.7	47.7	56.4	22.6	34.1	0.0	9.5
CSP Solar Field [GWth]	1075.0	1404.0	751.0	1014.0	474.0	688.0	213.0	381.2	0.0	93.4
CSP Thermal Storage [GWh]	3160.0	3557.0	2379.0	2732.0	1624.0	1974.0	774.0	1197.0	0.0	336.0
P2G2P Discharge	89.1	113.6	93.6	113.9	92.0	113.0	89.0	112.6	95.5	112.7
P2G2P Charge	13.2	9.6	10.8	8.7	14.9	11.6	19.2	16.1	32.8	24.8
P2G2P Storage [GWh]	11.5	17.0	8.8	13.5	9.2	15.6	10.7	15.4	13.9	13.8
Compressed Air Discharge	0.0	0.0	0.0	0.0	0.0	0.0	0.0	1.6	0.0	12.1
Compressed Air Charge	0.0	0.0	0.0	0.0	0.0	0.0	0.0	1.0	0.0	8.3
Compressed Air Storage [GWh]	0.0	0.0	0.0	0.0	0.0	0.0	0.0	0.0	0.0	0.2
Pump Storage Discharge	0.0	10.7	3.3	15.9	6.1	15.9	11.9	15.9	15.9	15.9
Pump Storage Charge	0.0	15.4	2.2	14.1	4.1	20.2	9.9	23.0	18.9	24.3
Pump Storage Storage [GWh]	0.0	0.6	0.1	1.2	0.1	1.4	0.3	2.3	0.6	3.4
Lithium Ion Discharge	0.0	0.0	0.0	0.0	0.0	0.0	0.0	6.2	1.6	7.1
Lithium Ion Charge	0.0	0.0	0.0	0.0	0.0	0.0	0.0	3.4	1.7	4.3
Lithium Ion Storage [GWh]	0.0	0.0	0.0	0.0	0.0	0.0	0.0	0.0	0.0	0.0

Table 41 shows the used grid data based on historical data of each country in EUMENA for the calculation of grid expansion cost depending on fluctuating energies.

Table 41: Country specific grid values, peak load and cost of fluctuating feed-in power

country	220 kV [km]	≥380 kV [km]	Today's grid cost [bn. € <sub>2015</sub> ]	Power kilomet res [TWkm]	Peak Load [GW]	Assumed grid capacity [GW]	$C_{cb,grid\ trans}$ OHL per fluc feed-in [€ <sub>2015</sub> /kW]	$C_{cb,grid\ trans}$ UGC per fluc feed-in [€ <sub>2015</sub> /kW]
<b>Central ENTSO-e</b>								
Austria	3667 (ENTSO-e, 2013)	2838 (ENTSO-e, 2013)	2.89	4.99	11.44 (ENTSO-e, 2013)	2.39	772	1188
Belgium	432 (ENTSO-e, 2013)	1326 (ENTSO-e, 2013)	0.84	1.58	13.35 (ENTSO-e, 2013)	2.78	192	295
Bosnia-Herzegovina	1525 (ENTSO-e, 2013)	865 (ENTSO-e, 2013)	1.04	1.76	2.07 (ENTSO-e, 2013)	0.43	1540	2370
Bulgaria	2837 (ENTSO-e, 2013)	2419 (ENTSO-e, 2013)	2.34	4.08	6.74 (ENTSO-e, 2013)	1.41	1065	1639
Croatia	1210 (ENTSO-e, 2013)	1248 (ENTSO-e, 2013)	1.11	1.96	2.81 (ENTSO-e, 2013)	0.59	1206	1857
Czech Republic	1909 (ENTSO-e, 2013)	3510 (ENTSO-e, 2013)	2.52	4.64	10.09 (ENTSO-e, 2013)	2.10	764	1177
France	26640 (ENTSO-e, 2013)	21752 (ENTSO-e, 2013)	21.53	37.37	92.90 (ENTSO-e, 2013)	19.35 17.30	710	1093
Germany	14053 (ENTSO-e, 2013)	20455 (ENTSO-e, 2013)	15.85	28.74	83.10 (ENTSO-e, 2013)	(ENTSO-e, 2010)	585	900
Hungary	1394 (ENTSO-e, 2013)	2978 (ENTSO-e, 2013)	2.05	3.8	5.86 (ENTSO-e, 2013)	1.22	1069	1645
Italy	11149 (ENTSO-e, 2013)	10746 (ENTSO-e, 2013)	9.83	17.29	53.98 (ENTSO-e, 2013)	11.25	558	858
Luxemburg	259 (ENTSO-e, 2013)	0 (ENTSO-e, 2013)	0.10	0.15	0.99 (ENTSO-e, 2013)	0.21	319	491
Montenegro	400 (ENTSO-e, 2013)	280 (ENTSO-e, 2013)	0.30	0.51	0.62 (ENTSO-e, 2013)	0.13	1478	2275

									2013)
Netherlands	740 (ENTSO-e, 2013)	2234 (ENTSO-e, 2013)	1.41	2.68	18.46 (ENTSO-e, 2013)	3.85	234	361	
Poland	7923 (ENTSO-e, 2013)	5354 (ENTSO-e, 2013)	5.85	9.99	22.68 (ENTSO-e, 2013)	4.73	789	1215	
Portugal	3565 (ENTSO-e, 2013)	2434 (ENTSO-e, 2013)	2.64	4.52	8.32 (ENTSO-e, 2013)	1.74	972	1496	
Romania	4796 (ENTSO-e, 2013)	5050 (ENTSO-e, 2013)	4.44	7.87	8.31 (ENTSO-e, 2013)	1.73	1639	2522	
Serbia	2284 (ENTSO-e, 2013)	1713 (ENTSO-e, 2013)	1.77	3.05	6.93 (ENTSO-e, 2013)	1.44	782	1204	
Slovakia	688 (ENTSO-e, 2013)	1644 (ENTSO-e, 2013)	1.10	2.05	4.13 (ENTSO-e, 2013)	0.86	814	1253	
Slovenia	328 (ENTSO-e, 2013)	669 (ENTSO-e, 2013)	0.47	0.86	1.98 (ENTSO-e, 2013)	0.41	719	1107	
Spain	18239 (ENTSO-e, 2013)	20639 (ENTSO-e, 2013)	17.62	31.36	39.64 (ENTSO-e, 2013)	8.25	1362	2097	
Switzerland	4915 (ENTSO-e, 2013)	1737 (ENTSO-e, 2013)	2.83	4.61	7.94 (ENTSO-e, 2013)	1.66	1093	1682	
<b>Other European countries</b>									
Albania	1128 (Board, 2008)	120 (Board, 2008)	0.51	0.78	1.20 (Board, 2008)	0.25	1305	2009	
Armenia	164 (Institute, 2016)	1320 (Institute, 2016)	0.73	1.42	1.20 (Bank, 2011)	0.25	1852	2850	
					1.05 (United States Agency for International Development, 2013)				
Azerbaijan	1226 (DOE, 2004)	1655 (DOE, 2004)	1.32	2.38	6.78 (Yakushau, 2010)	0.22	3833	5900	
Belarus	2281 (Yakushau, 2010)	4502 (Yakushau, 2010)	3.16	5.85		1.41	1428	2199	
Cyprus	7678 (Kontos, 2015)	7678 (Kontos, 2015)	6.91	12.19	0.81 (Kontos, 2015)	0.17	26256*	40416*	
Denmark	3400 (EnergiNetDK, 2014)	3400 (EnergiNetDK, 2014)	3.06	5.4	6.20 (Bach, 2014)	1.29	1511	2327	
Estonia	158 (CIGRE, 2014)	1702 (CIGRE, 2014)	0.91	1.8	1.59 (CIGRE, 2014)	0.33	1764	2716	
Finland	2300 (CIGRE, 2011)	4500 (CIGRE, 2011)	3.17	5.86	14.80 (CIGRE, 2011)	3.08	656	1010	
Georgia	1596 (JSC Georgian State Electrosystem, 2014)	303 (JSC Georgian State Electrosystem, 2014)	0.79	1.23	1.85 (Georgian State Electrosystem, 2014)	0.39	1305	2009	

Great Britain	2014) 6342 (CIGRE, 2014)	2014) 12122 (CIGRE, 2014)	8.60	15.87	56.00 (CIGRE, 2014) 9.89 (Commission, 2014)	11.67	470	724
Greece	8393 (CIGRE, 2015)	2785 (CIGRE, 2015)	4.75	7.68	2.06	1470	2263	
Iceland	859 (CIGRE, 2016)	0 (CIGRE, 2016)	0.34	0.5	2.33 (CIGRE, 2016)	0.49	452	695
Ireland	2000 (CIGRE, 2015)	450 (CIGRE, 2015)	1.03	1.62	5.09 (CIGRE, 2015)	1.06	617	949
Kosovo	353 (Energy, 2004)	181 (Energy, 2004)	0.23	0.39	0.89 (OFFICE, 2005) 1.37 (ENTSO-e, 2012)	0.18	801	1233
Latvia	0 (tīkls, 2014)	1381 (tīkls, 2014)	0.69	1.39	0.29	1546	2380	
Liechtenstein	NA	NA	NA	NA	NA	NA	NA	
Lithuania	0 (Litgrid, 2016)	1761 (Litgrid, 2016)	0.88	1.77	1.69 (Comission)	0.35	1599	2462
Macedonia	0 (CIGRE, 2014)	529 (CIGRE, 2014)	0.26	0.53	1.51 (CIGRE, 2014) 0.44 (timesofmalta, 2015)	0.31	537	827
Malta	8 (Enemalta)	0 (Enemalta)	0.00	0	0.09	22	34	
Moldova	532 (Moldova, 2013)	203 (Moldova, 2013)	0.31	0.51	0.95 (Moldova, 2013)	0.20	1017	1566
Norway	4850 (CIGRE, 2013)	2810 (CIGRE, 2013)	3.35	5.65	24.18 (CIGRE, 2013) 80.32 <sup>#</sup> (International Energy Agency, 2005)	5.04	424	652
Russia until Ural mountains	0 (Federal Grid Company, 2015)	72324 (Federal Grid Company, 2015)	36.16	72.69	16.73	1379	2122	
Sweden	4000 (CIGRE, 2014)	11000 (CIGRE, 2014)	7.10	13.38	23.40 (CIGRE, 2014)	4.88	929	1430
Turkey	85 (CIGRE, 2014)	17747 (CIGRE, 2014)	8.91	17.89	41.00 (CIGRE, 2014) 31.86 (Liudmyla, 2013)	8.54	665	1024
Ukraine	3976 (Liudmyla, 2013)	4934 (Liudmyla, 2013)	4.06	7.27	6.64	390	600	
<b>Middle East</b>								
Bahrain	350 (Bahrain Electricity and Water Authority, 2015)	0 (Bahrain Electricity and Water Authority, 2015)	0.14	0.2	2.88 (Bahrain Electricity and Water Authority, 2015)	0.60	149	229
Djibouti	NA	NA	NA	NA	NA	NA	NA	
Iran	28478 (Monfared, et al., 2013)	17438 (Monfared, et al., 2013)	20.11	34.1	50.18 (CIGRE, 2015) 11.00 (Iraq - MINISTRY OF ELECTRICITY, 2010)	10.45	1227	1889
Iraq	13746 (Iraq - MINISTRY OF ELECTRICITY, 2010)	3723 (Iraq - MINISTRY OF ELECTRICITY, 2010)	7.36	11.74	2.29	2049	3154	
Israel	4579 (CIGRE, 2016)	741 (CIGRE, 2016)	2.20	3.41	11.50 (CIGRE, 2016)	2.40	586	903
Jordan	3522 (NEPCO, 2013)	924 (NEPCO, 2013)	1.87	2.98	2.98 (NEPCO, 2013)	0.62	1926	2964

Kuwait	4014 (Alsayegh, 2008)	854 (Alsayegh, 2008)	2.03	3.19	9.00 (KISR, 2014)	1.88	692	1065
Lebanon	290 (Liban, 2014)	0 (Liban, 2014)	0.12	0.17	1.94 (UNDP, 2004)	0.40	183	282
Oman	2837 (Abdalla, et al., 2009)	686 (Abdalla, et al., 2009)	1.48	2.34	2.77 (Abdalla, et al., 2009)	0.58	1632	2512
Palestine	NA	NA	NA	NA	NA	NA	NA	NA
Qatar	550 (INMR, 2014)	287 (INMR, 2014)	0.36	0.61	6.80 (2016)	1.42	164	252
Saudi Arabia	13489 (Company, 2015)	13489 (Company, 2015)	12.14	21.41	62.26 (Company, 2015)	12.97	597	919
Syria	5785 (Syria, 2011)	1409 (Syria, 2011)	3.02	4.78	7.22 (Syria, 2011)	1.50	1280	1970
United Arab Emirates	437 (Afridi, et al., 2012)	875 (Afridi, et al., 2012)	0.61	1.13	17.74 (UNESCWA, 2011)	3.70	106	163
Yemen	1161 (Al-Shibani, 2013)	0 (Al-Shibani, 2013)	0.46	0.68	0.68 (UNESCWA, 2000)	0.14	2098	3229
<b>North Africa</b>								
Algeria	13390 (CIGRE, 2014)	2872 (CIGRE, 2014)	6.79	10.68	11.19 (CIGRE, 2014)	2.33	1859	2862
Egypt	17570 (Company, 2014)	3060 (Company, 2014)	8.56	13.3	28.02 (Company, 2014)	5.84	935	1440
Libya	13677 (Electric Power System of Libya and its Future, 2010)	442 (Electric Power System of Libya and its Future, 2010)	5.69	8.4	4.76 (Electric Power System of Libya and its Future, 2010)	0.99	3665	5642
Morocco	9220 (Laâbi, 2014)	1753 (Laâbi, 2014)	4.56	7.13	5.60 (Funds, 2014)	1.17	2496	3842
Tunisia	0 (Energetici, 2013)	2792 (Energetici, 2013)	1.40	2.81	3.35 (Energypedia, 2012)	0.70	1275	1963

Cost: 400.000 €<sub>2015</sub>/km (220 kV), 500.000 €<sub>2015</sub>/km (380kV); Assumed capacity for power kilometres: 0.582 GW/km (220 kV), 1.005 GW/km (380 kV). This is based on the assumption of using a double bundle 240/40 (Al/St) with a load of 60%. \*Very high, due to many installed transmission lines and relative low load. Grid expansion cost may be 10 times lower in Cyprus reaching the scale of other countries. # Estimated from the country values with 56.6% of whole country electricity production (International Energy Agency, 2005).  $c_{cb,grid\ trans}$  OHL is a result of the reduction of  $c_{grid\ trans}$  OHL of 35% and for  $c_{cb,grid\ trans}$  UGC a reduction of 52% of  $c_{grid\ trans}$  UGC (calibration result of the case study in Germany).



## 10.3 Chapter 4 – Scenario analysis

### 10.3.1 3 Step: CSP-HVDC, CSP, NUC, CCS sensitivity scenarios

As additional results of the CSP-HVDC and CSP cost bandwidths, the technological configuration bandwidths are shown in Figure 53 by the solar multiple, in Figure 57 by the solar field capacity, in Figure 54 by the thermal energy storage, in Figure 55 by the electrical net generation and in Figure 56 by the electricity generation by co-firing. These results depend on the used cost sensitivities and show the difference between scenarios with 0 (first row of the figures – a,b) and 16 g CO<sub>2</sub>/kWh<sub>demand</sub> (second row of the figures – b,c) neglecting and including CCS (third row of the figures – e,f). The results show that high CO<sub>2</sub> emission and the inclusion of CCS leads to lower CSP configuration values.

The results of sensitivity analysis show in Figure 53 the bandwidths of the solar multiple in the analysed regions with boxplots. In the left column the CSP-HVDC technology and in the right column the CSP technology is described.

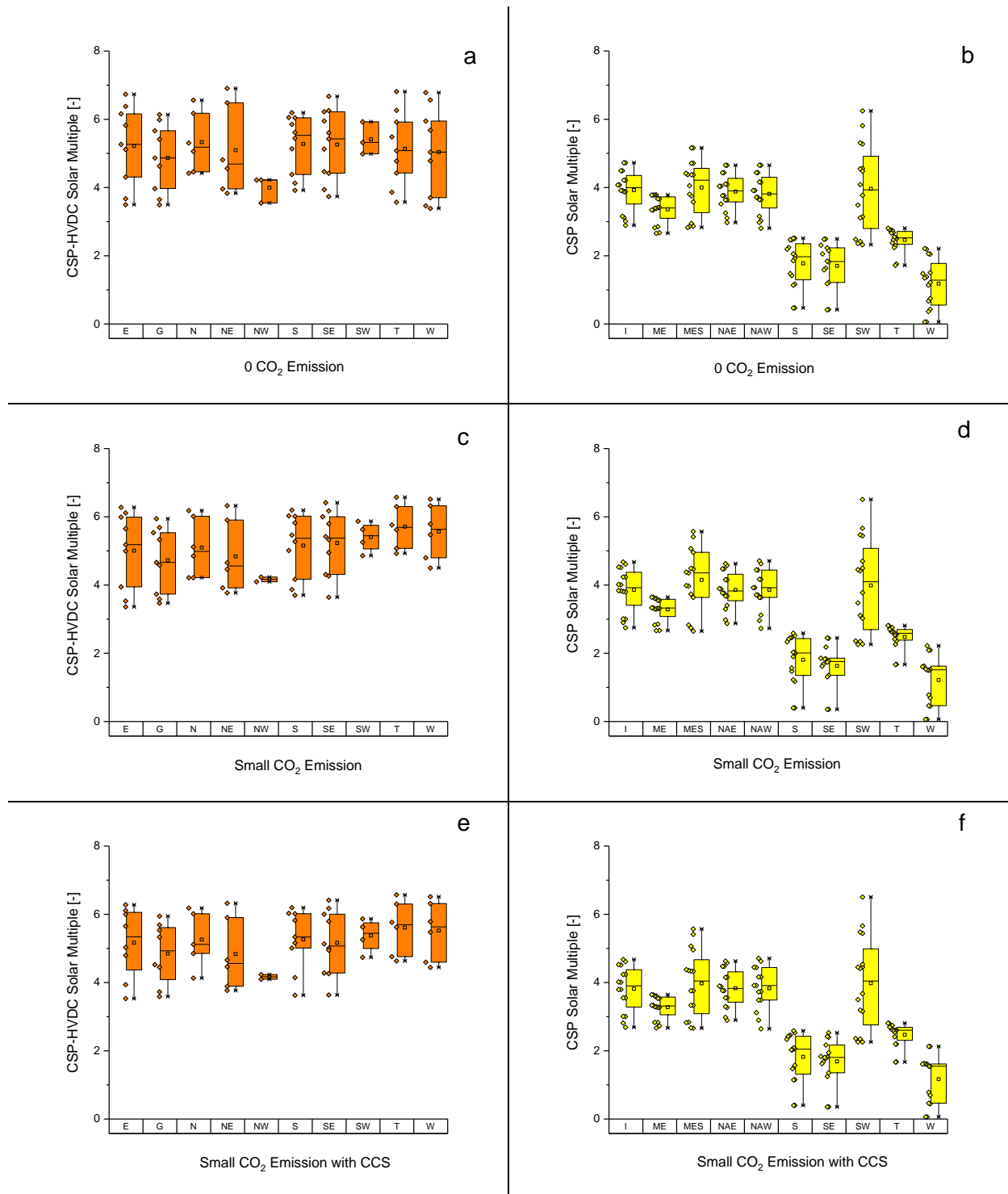


Figure 53: Solar Multiple

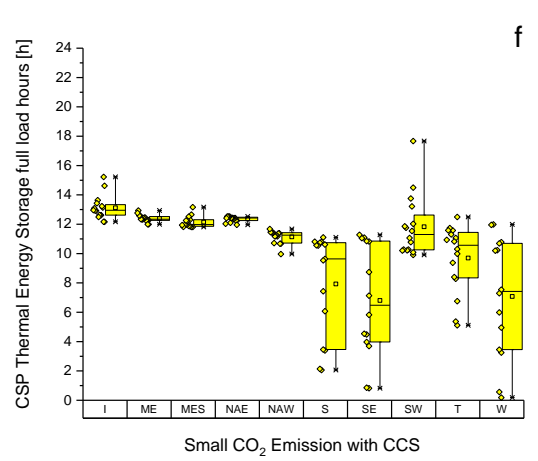
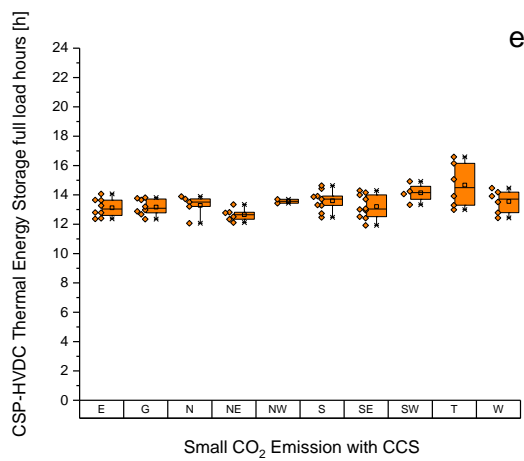
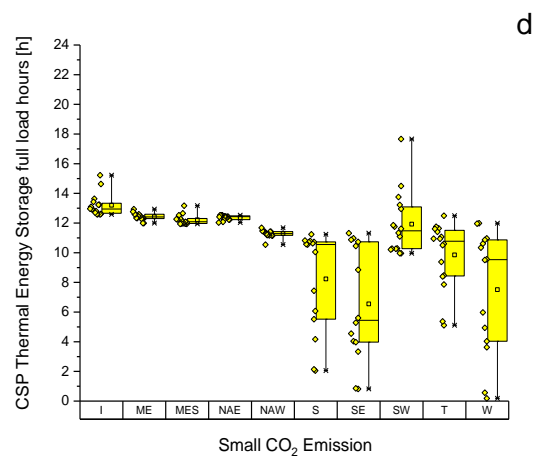
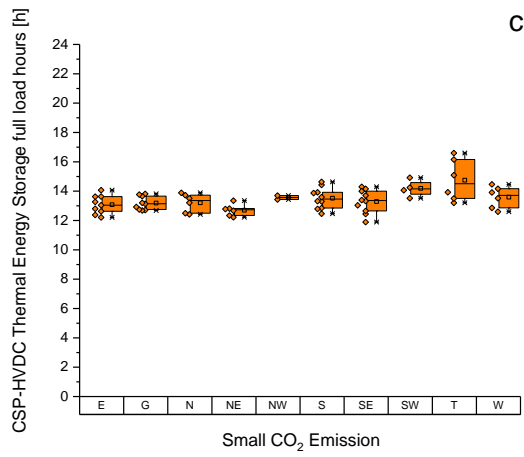
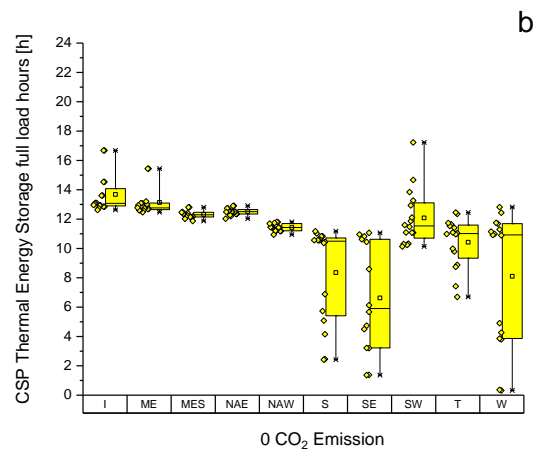
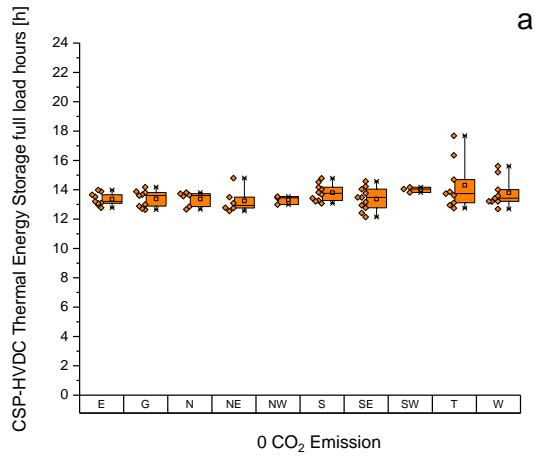


Figure 54: Thermal energy storage full load hours

Figure 55 shows the net electricity generation [TWh<sub>el</sub>] from CSP-HVDC and CSP. In the MENA region (regions I, ME, MES, NAE and NAW) the net electricity generation is relative high due to a high share of CSP. Also the use of the thermal energy storage in Figure 54 is high compared to other regions in MENA.

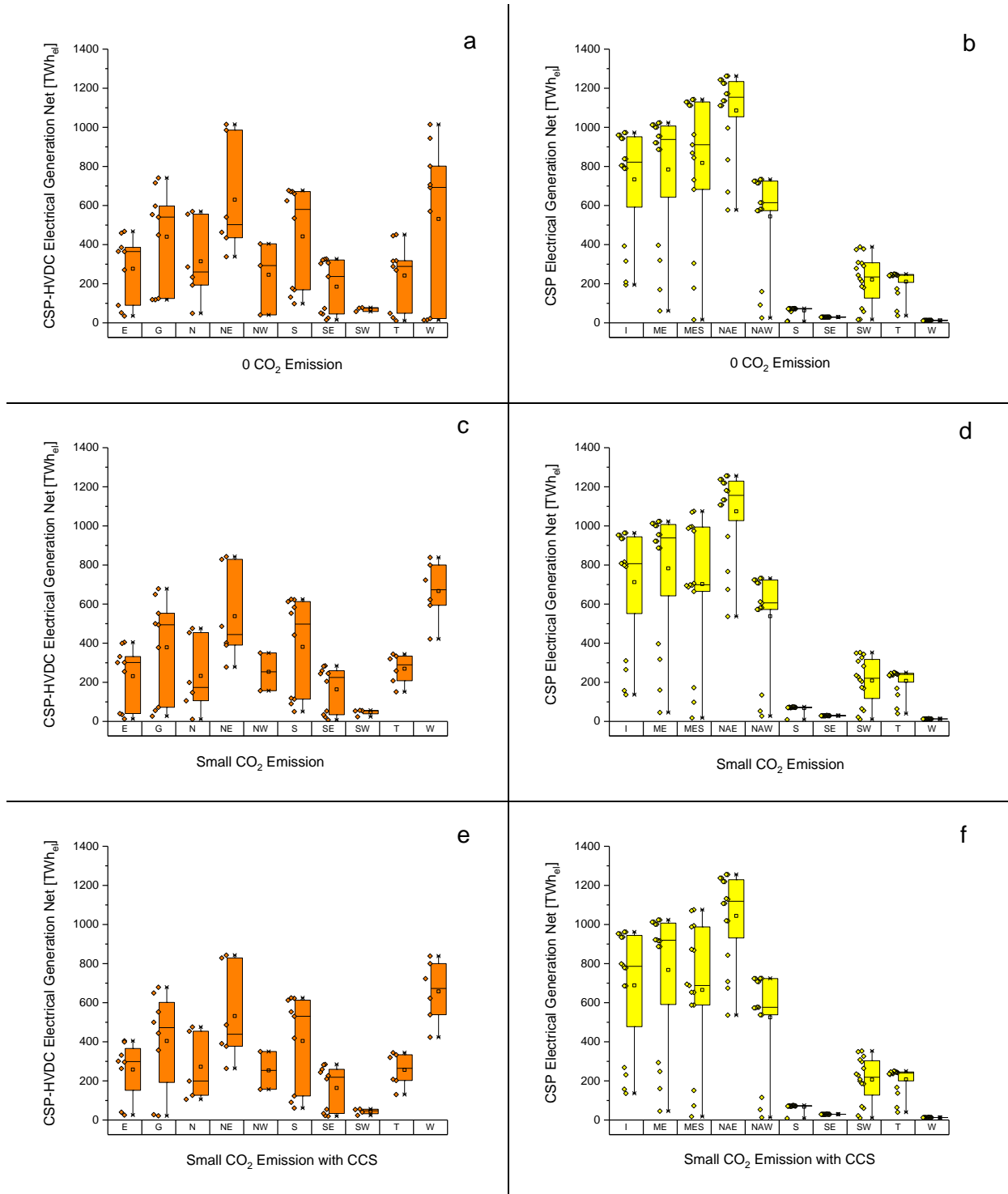


Figure 55: Electrical generation net of the CSP plant without transmission losses.

Figure 56 shows the co-firing with natural gas of the CSP-HVDC and CSP technologies. It can be seen in Figure 56d and f that the electricity generation using co-firing compared to the net electrical generation is low (comparison of Figure 56 and Figure 55). However, some regions have a higher absolute co-firing value. This is not a result of different demand but a consequence of an hourly misfit of renewable energies and the demand curve. The integration of CCS technologies (here CSP has no CCS possibility) leads to a higher co-firing. Thus, it is more efficient to use the co-firing of CSP when CCS is integrated.

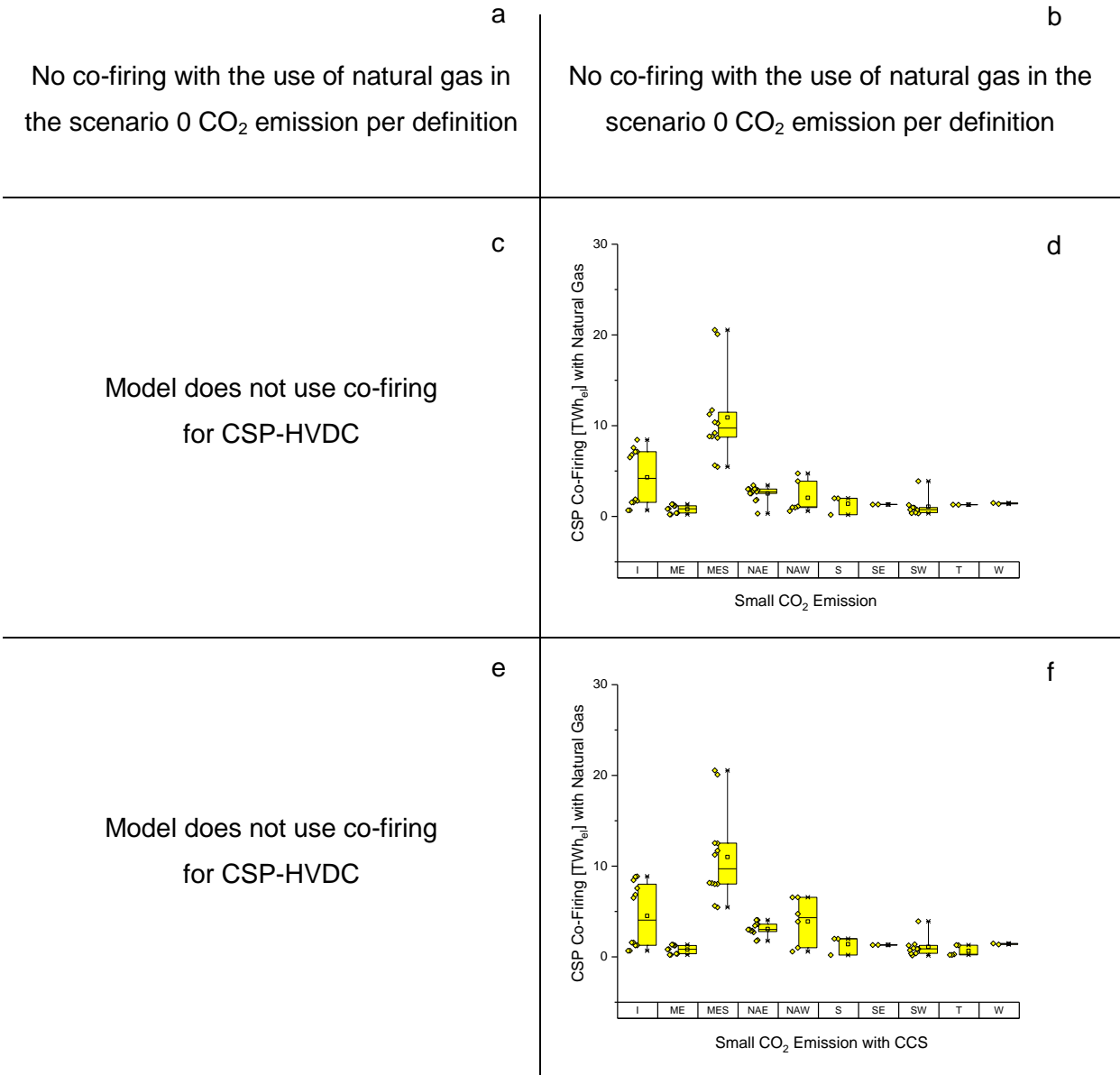


Figure 56: Co-firing with natural gas

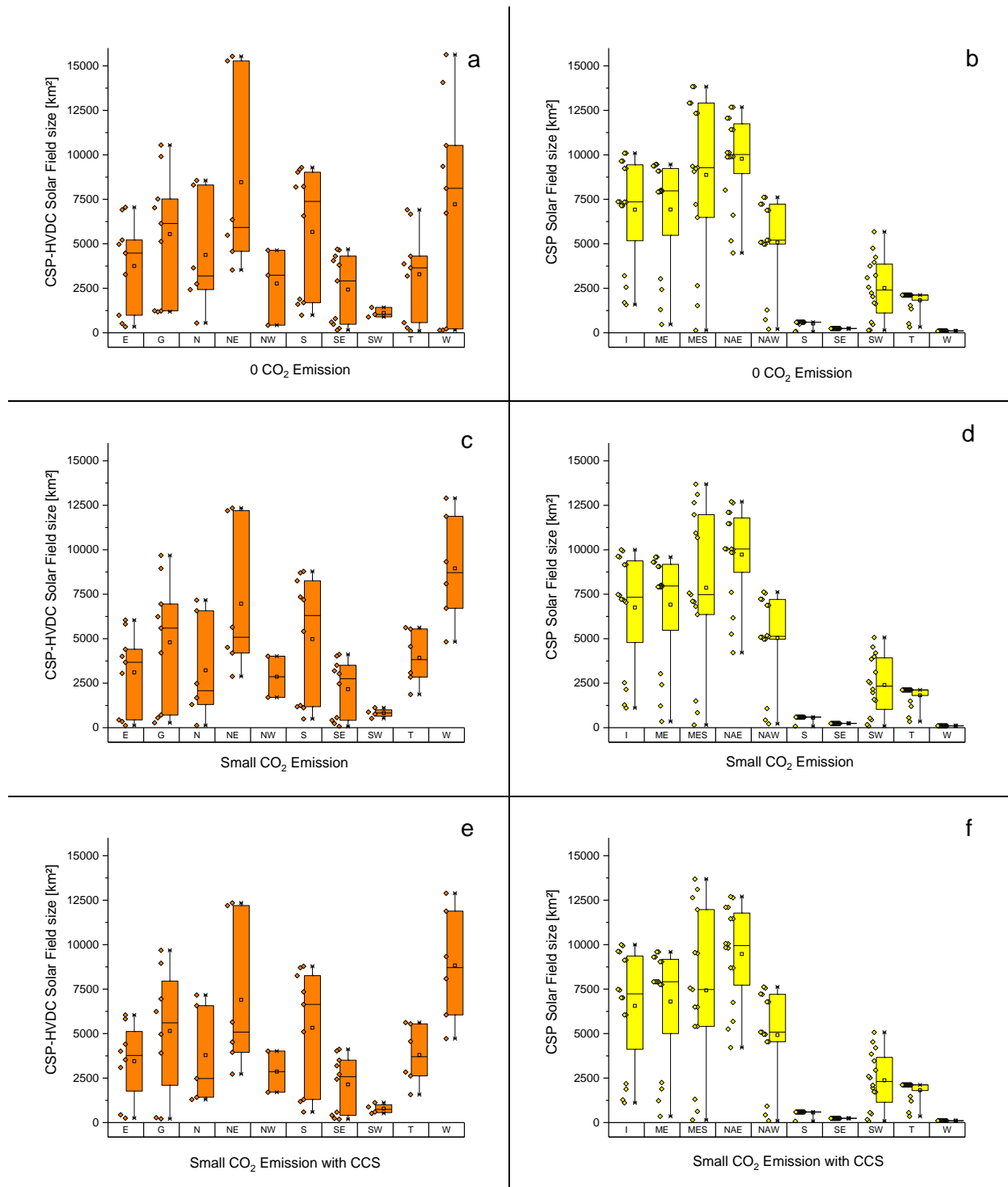


Figure 57: Solar field size – possible bandwidths of demand for land of CSP-HVDC and CSP

### 10.3.2 4 Step: direct comparison of CSP-HVDC, CSP, NUC, CCS with same exogenous capacity

The regional exogenous capacity in Table 42 is based on the power block capacity of CSP-HVDC and CSP. It is assumed that CSP-HVDC is integrated with other renewable dispatchable energies to achieve an energy mix of about 50% dispatchable energy share due to its low cost uncertainty value (see Figure 17f). The solar multiple is approximated based on the scenarios analysing the empirical probability (see Figure 53). The capacity of CSP in the MENA countries is considered with a higher value due to its higher integration probability (see Figure 25 and Figure 26).

Table 42: Regional exogenous capacity [MW] and solar multiple comparing technologies

Model region	CSP- HVDC	SM CSP- HVDC	CSP	SM CSP	Nuclear	CCGT CCS	Coal CCS
G	40000	4	0	0	40000	40000	40000
N	6000	4	0	0	6000	6000	6000
E	18000	4	0	0	18000	18000	18000
S	20000	4	5000	2	20000	20000	20000
W	60000	4	1000	2	60000	60000	60000
NW	60000	4	0	0	60000	60000	60000
NE	38000	4	0	0	38000	38000	38000
SE	5000	4	2000	2	5000	5000	5000
NAE	0	0	150000	4	150000	150000	150000
NAW	0	0	80000	4	80000	80000	80000
SW	3000	4	4000	3	7000	7000	7000
T	50000	4	5000	3	55000	55000	55000
MES	0	0	150000	4	150000	150000	150000
I	0	0	120000	4	120000	120000	120000
ME	0	0	120000	4	120000	120000	120000

### 10.3.3 5 Step: exogenous scenarios handmade

In the last step for the scenario analysis exogenous capacities and parameters are used which are shown in Table 43 to Table 47.

Table 43: Exogenous capacities of CSP components

Model region	CSP-HVDC				CSP			
	Power block [MW]	SM [-]	Solar field [MW <sub>thermal</sub> ]	Thermal energy storage [MWh]	Power block [MW]	SM [-]	Solar field [MW <sub>thermal</sub> ]	Thermal energy storage [MWh]
G	40000	4.1	442213	1358331	0	0.0	0	0
N	6000	4.2	68506	191930	0	0.0	0	0
E	18000	3.5	171956	583796	0	0.0	0	0
S	28403	4.5	344970	980940	13409	2.9	104658	393059
W	60000	3.7	600805	2004039	1000	3.2	8737	28763
NW	60000	3.2	521139	1694940	0	0.0	0	0
NE	42562	3.9	453565	1429071	0	0.0	0	0
SE	9589	4.1	106843	311523	5834	2.7	41890	178021
NAE	0	0.0	0	0	162324	3.8	1668897	5449808
NAW	0	0.0	0	0	81748	4.0	875069	2602720
SW	3000	3.6	29007	97916	22264	3.0	179087	620259
T	50000	3.2	432586	1502329	7754	3.3	69768	238819
MES	0	0.0	0	0	150000	3.2	1287473	4728312
I	0	0.0	0	0	122061	3.8	1266472	4256975
ME	0	0.0	0	0	140242	3.4	1274001	4808231



Table 44: Exogenous capacities of power plants [ $MW_{el}$ ]

Model region	Photo-voltaic	Wind Onshore	Wind Offshore	Hydro Run Off River	Biomass	Geo-thermal	Gas turbine
G	70000	70000	28000	4377	19000	4042	102500
N	50000	20000	8000	39326	33073	255	72400
E	50000	45000	30000	4504	17000	2500	57250
S	70000	60000	15000	31924	22500	2500	95000
W	120000	90000	25000	13943	32000	2112	138100
NW	70000	90000	10000	3507	5500	4711	138900
NE	120000	85000	18000	32448	60000	1800	91000
SE	35000	30000	15000	21721	12000	1069	44800
NAE	50000	15000	0	3033	1300	1800	48700
NAW	40000	20000	2000	1724	6000	1300	37200
SW	50000	30000	10000	8560	10000	3000	46950
T	50000	30000	0	14611	15000	13778	99700
MES	60000	0	0	3313	1300	0	44232
I	60000	0	0	1044	4000	1092	43900
ME	65000	0	0	0	300	10000	62800

Table 45: Exogenous capacities of hydro reservoir and pump storage plants [ $MW_{el}$ ]

Model region	Hydro reservoir turbine	Hydro reservoir pump	Hydro reservoir storage [ $MWh$ ]	Import Hydro reservoir turbine	Import Hydro reservoir pump	Import Hydro reservoir storage [ $MWh$ ]	Pump storage	Pump storage - storage [ $MWh$ ]
G	430	5284	430000	6153	18672	6153000	15875	127000
N	25813	25813	25813000	0	0	0	4781	38248
E	963	9953	963000	3748	10075	3748000	3500	28000
S	16500	23470	16500000	0	0	0	20014	160112
W	11660	46909	11660000	0	0	0	7743	61944
NW	328	5933	328000	7308	37220	7308000	3853	30824
NE	0	0	0	0	0	0	2612	20896
SE	8330	13814	8330000	0	0	0	4149	33192
NAE	0	0	0	0	0	0	0	0
NAW	0	0	0	0	0	0	932	7456
SW	12999	18980	12999000	0	0	0	19588	156704
T	679	13994	679000	0	0	0	571	4568
MES	0	0	0	0	0	0	0	0
I	0	0	0	0	0	0	0	0
ME	0	0	0	0	0	0	0	0

Table 46: Exogenous link capacities

Link according model regions	HVDC link capacity [GW]	380kV link capacity [GW]
G_N	2820	0
G_E	0	5367
G_S	0	7990
G_W	0	11045
G_NW	3450	0
N_NE	0	3196
N_E	3330	0
N_NW	3615	0
NE_E	0	3538
NE_SE	0	3347
NE_T	0	5206
NE_I	0	6402
NW_W	3555	0
NW_SW	3285	0
W_S	0	8603
W_NAW	10980	0
W_SW	0	2593
SW_NAW	0	10693
S_E	0	3065
S_SE	0	3226
S_NAE	9405	0
S_NAW	11115	0
SE_T	0	5156
SE_MES	7965	0
SE_NAE	9465	0
NAE_NAW	0	17356
NAE_T	11325	0
NAE_MES	0	14140
NAE_ME	10305	0
MES_I	0	11025
MES_ME	8805	0
MES_T	0	9829
I_T	0	8201
I_ME	7185	0
E_SE	0	3477

Table 47: Used parameters for distribution and transmission grid inside a model region

<b>Model region</b>	<b>Start of grid expansion in distribution grid [% of peak load]</b>	<b>Distribution grid cost per fluc feed-in [€/kW]</b>	<b>Start of grid expansion in transmission grid [% of peak load]</b>	<b>Transmission grid cost per fluc feed-in [€/kW]</b>
G	60.5%	375	25%	584
N	60.5%	375	25%	801
E	60.5%	375	25%	824
S	60.5%	375	25%	647
W	60.5%	375	25%	582
NW	60.5%	375	25%	481
NE	60.5%	375	25%	1149
SE	60.5%	375	25%	1253
NAE	60.5%	375	25%	1331
NAW	60.5%	375	25%	1939
SW	60.5%	375	25%	1294
T	60.5%	375	25%	1159
MES	60.5%	375	25%	1288
I	60.5%	375	25%	1227
ME	60.5%	375	25%	517

### 10.3.4 Regional power kilometre

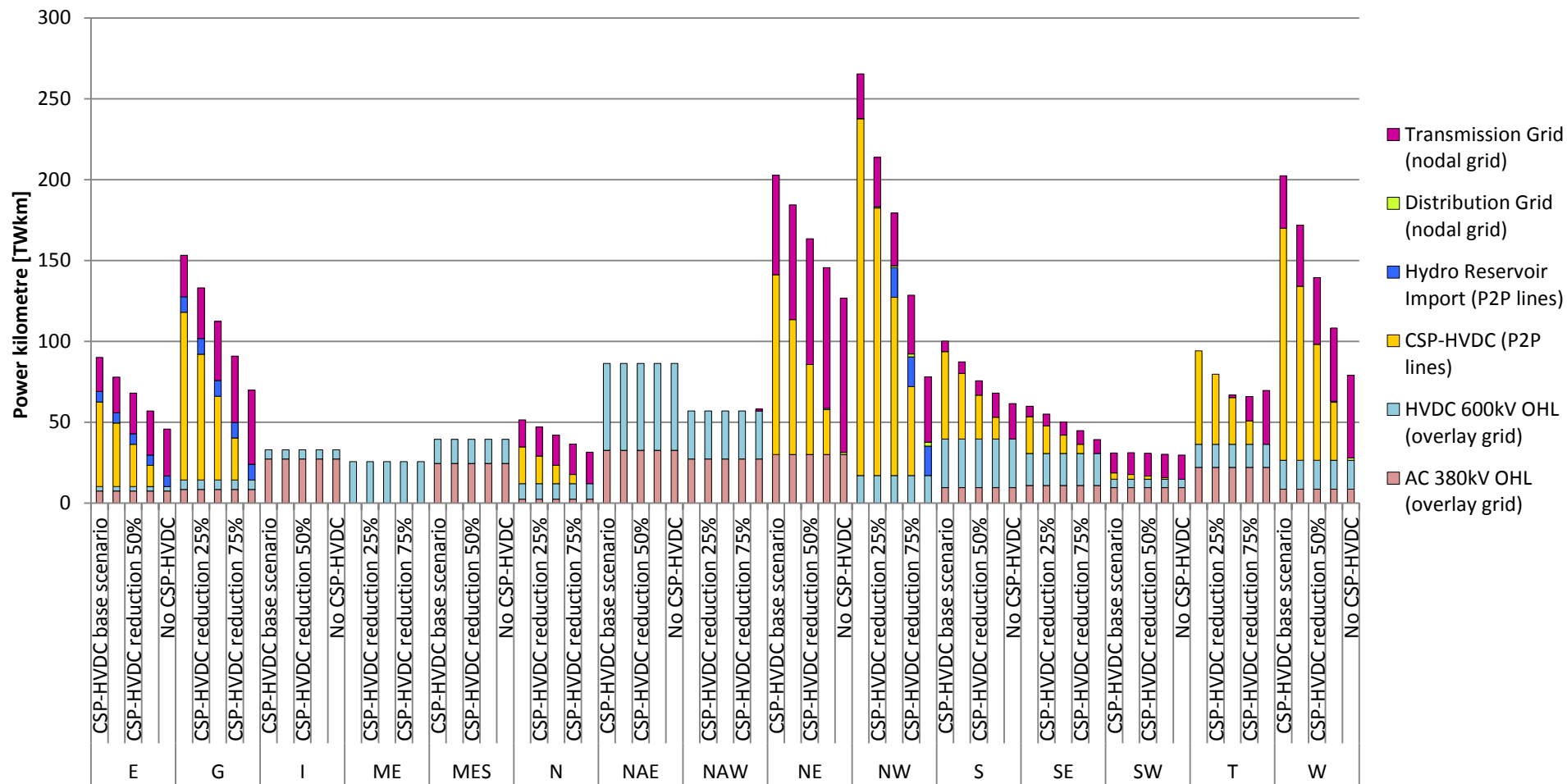


Figure 58: Regional power kilometre of the modelling framework in section 5.1.5.

Optimization of power km of nodal grid and hydro reservoir import P2P. Power kilometre of overlay grid and CSP-HVDC P2P are fixed.

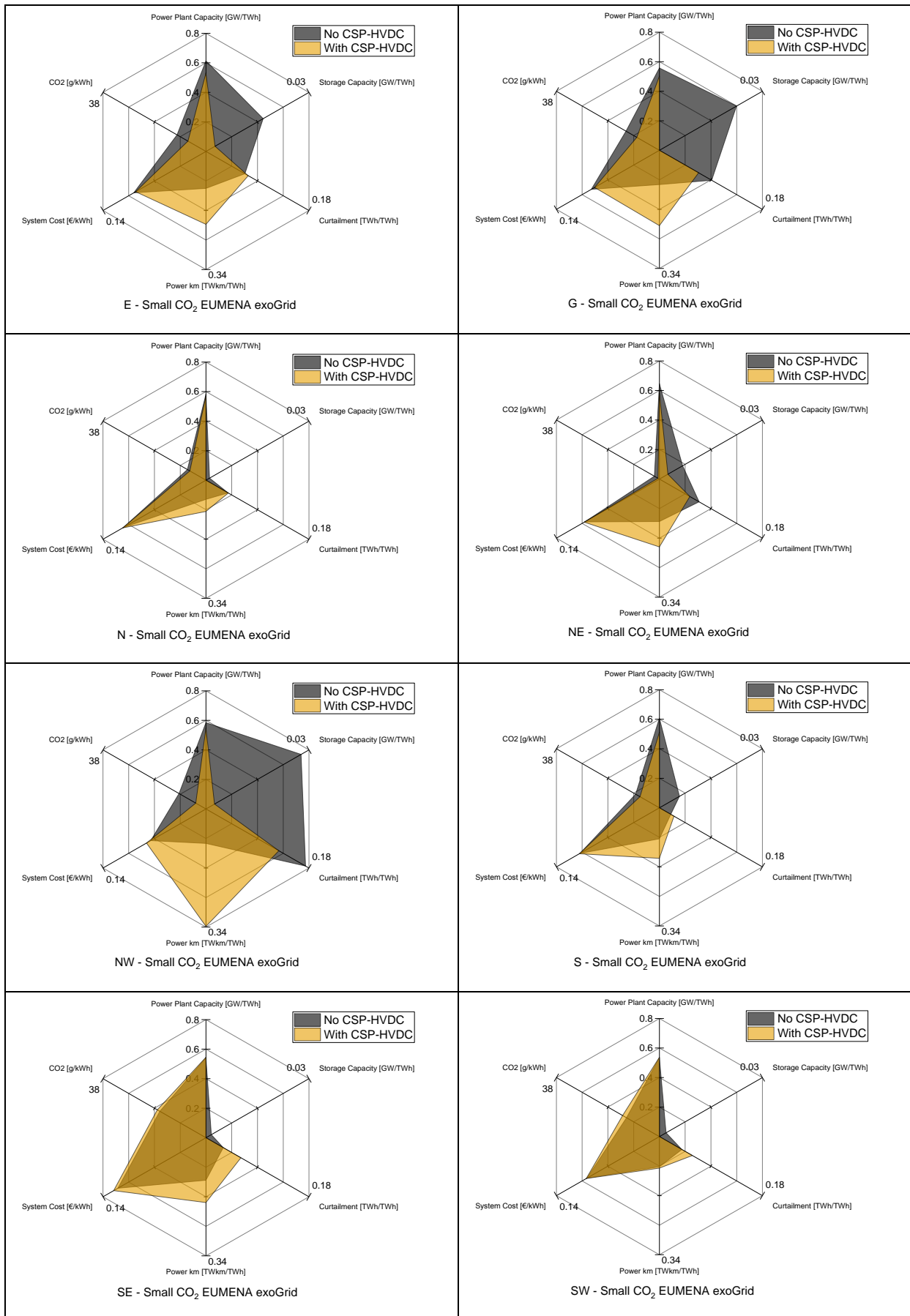
### 10.3.5 Model region radar charts as results of the scenario comparison without and with CSP-HVDC

In Figure 59 to Figure 62 the regionalized results are displayed in radar charts. The regions can be compared to each other with the same scale of evaluation criteria. Figure 59 shows the maximum difference between an exclusion of CSP-HVDC (grey charts) and an inclusion with a relative high share of CSP-HVDC (orange charts). The regions with the highest difference of those charts show a high impact of CSP-HVDC. As a consequence a congruence of the grey and orange chart shows no impact of this technology. The model regions **E**, **G**, **NW**, **T** and **W** exhibit the highest difference and have therefore the highest impact including CSP-HVDC.

A steady reduction of CSP-HVDC capacity from Figure 59 to Figure 62 leads to a shift of evaluation criteria in the model regions. This allows for each region to assess a suitable share of CSP-HVDC. The major effect reducing the share of CSP-HVDC in the majority of regions is a reduction of power kilometre which leads to an increase of electrical storage capacity and electrical curtailment. Another effect is that the increase of the specific CO<sub>2</sub> value in the majority of EU regions increases when the share of CSP-HVDC is reduced. In MENA regions this effect is vice versa. As mentioned in the main text, the integration of CSP-HVDC in EU allows the MENA regions to be more efficient in the use of gas than the EU which leads to some higher CO<sub>2</sub> emission in MENA. This effect is a result of the CO<sub>2</sub> limit for the whole EUMENA region which leads to an optimal use of CO<sub>2</sub> in its sub-regions.

Explanation of system cost in the regionalized radar charts:

The system cost can be considered as an indicator for regional cost. System cost is always based on the whole examination area. Thus, the information of system cost in a region is not exact. For example a power plant built in one region can supply another region but the cost of the power plant is assigned to the region where the power plant is placed. Therefore the made mistake of regional system depends strongly on the modelling framework. Here the scenario is built using a regional expansion of power plants at first in a model with isolated regions. Therefore the power plants can only supply their home region. In a later step the regions are interconnected. The made mistake is therefore small because the model does not build power plants predominantly for the supply of other regions. Another reason why regional system cost is applicable is that in a high renewable energy scenario the share of capital cost of power plants in system cost is high. O&M cost may change in an interconnected system but their influence is rather low.



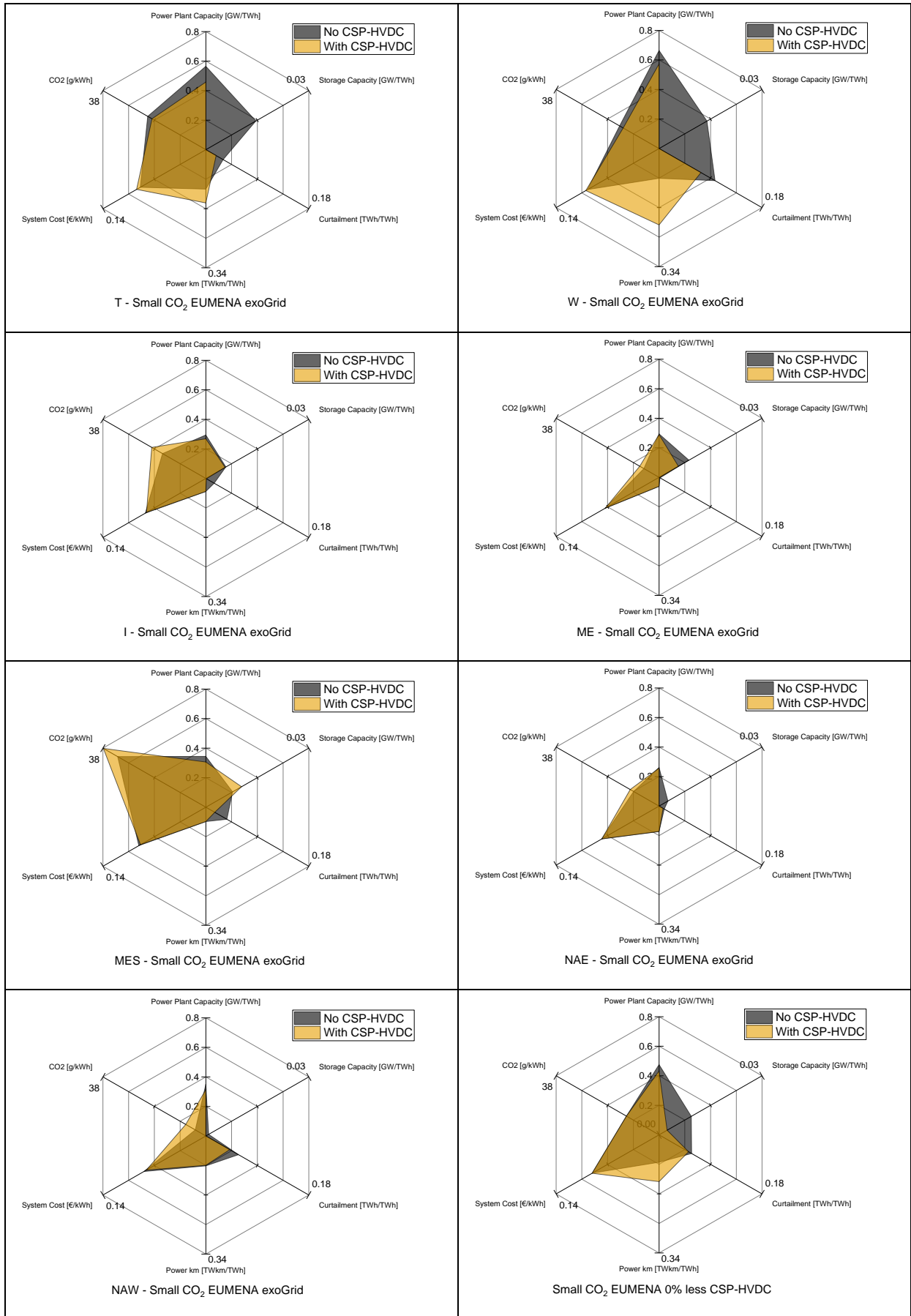
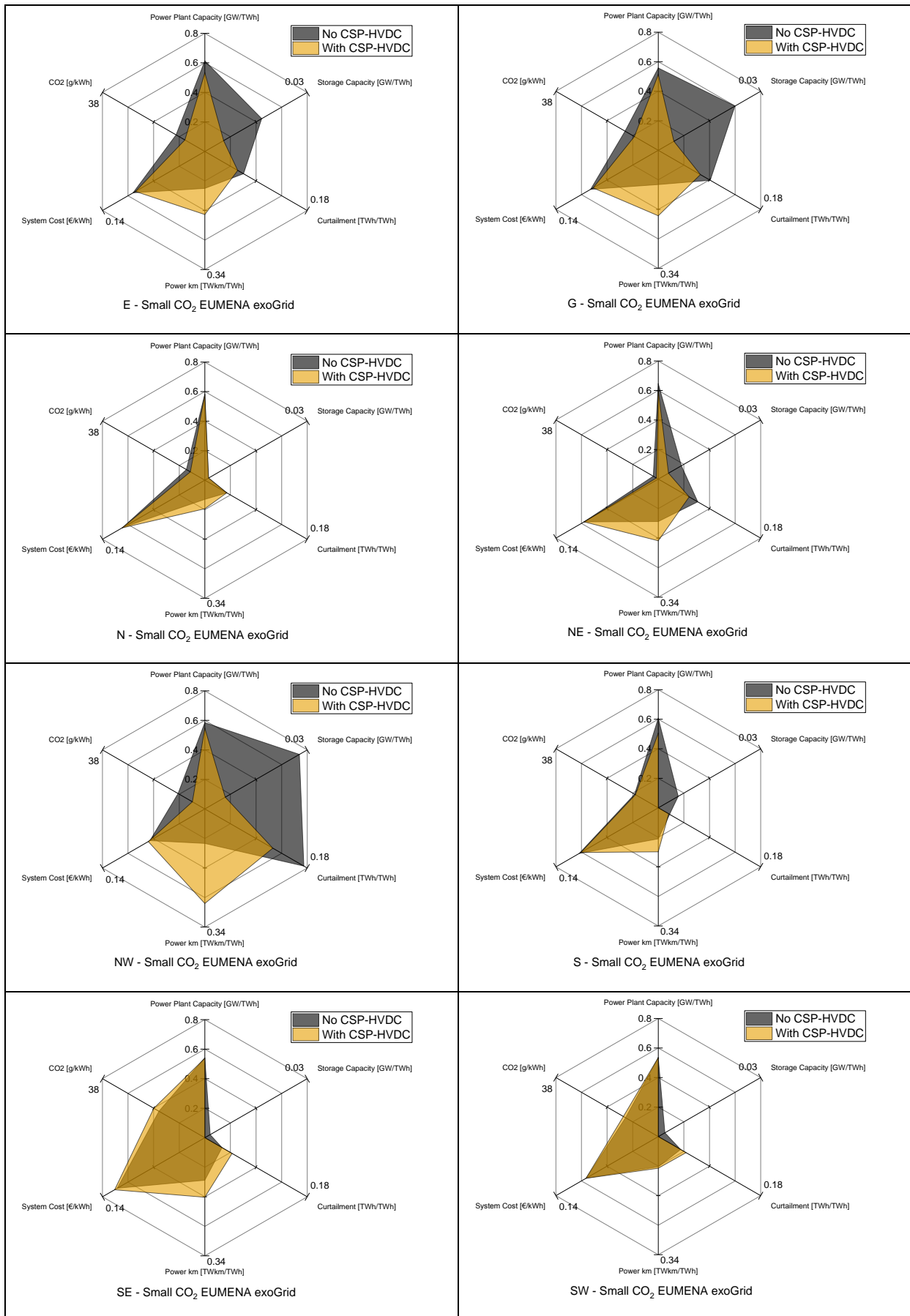


Figure 59: Scenario with maximum set CSP-HVDC capacity (CSP-HVDC base scenario)





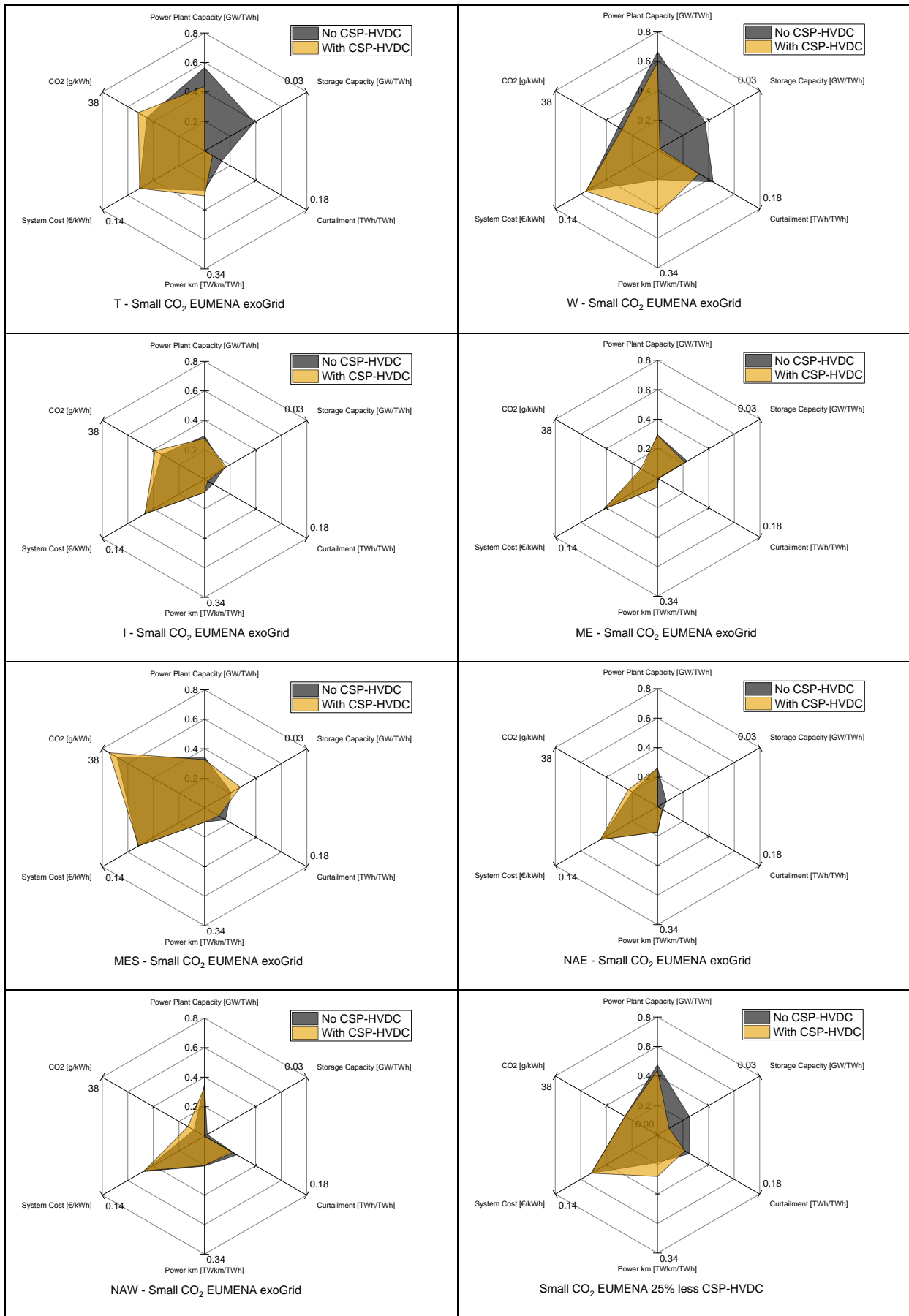
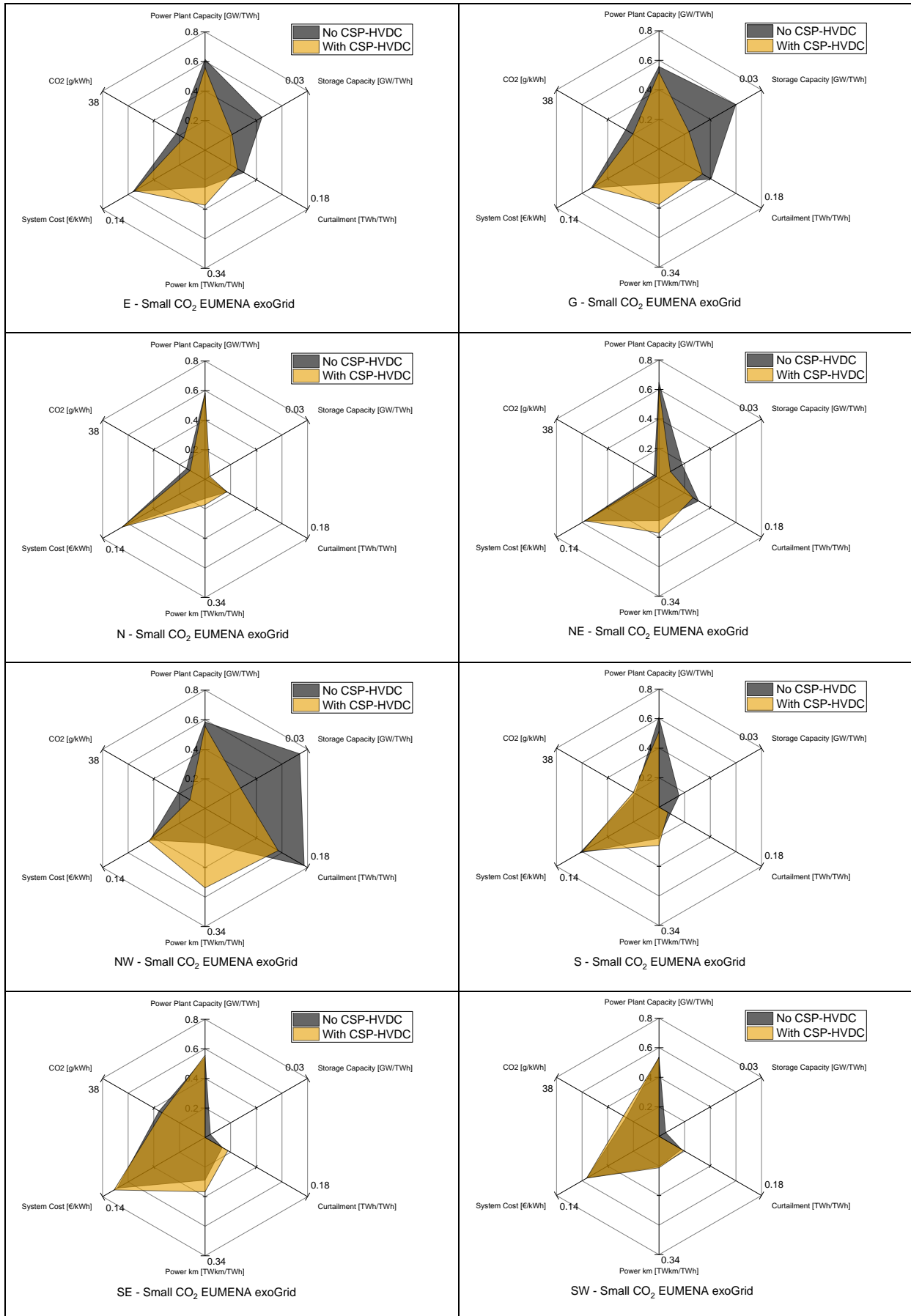


Figure 60: Scenario with 25% reduction of CSP-HVDC capacity (-25% CSP-HVDC)



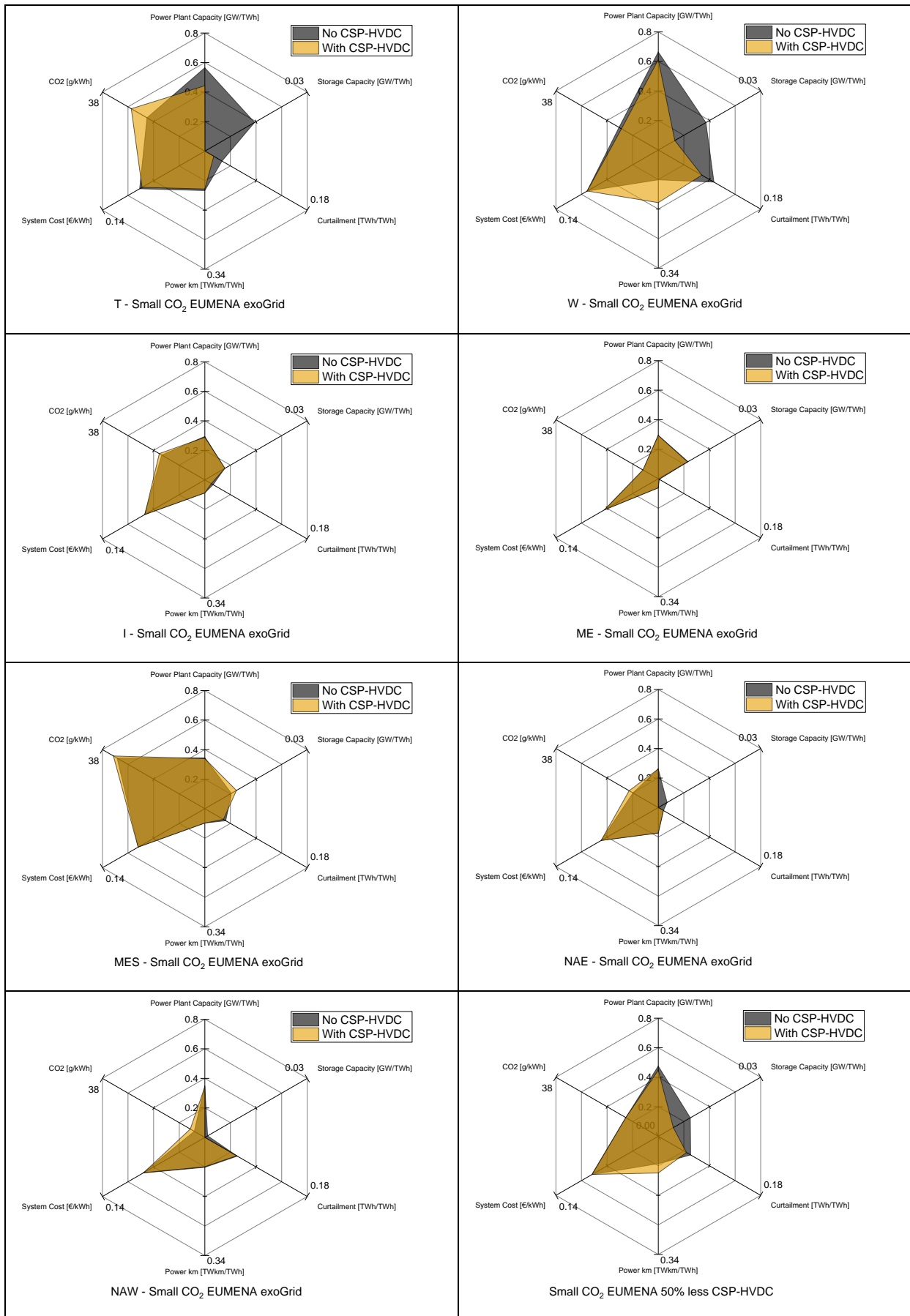
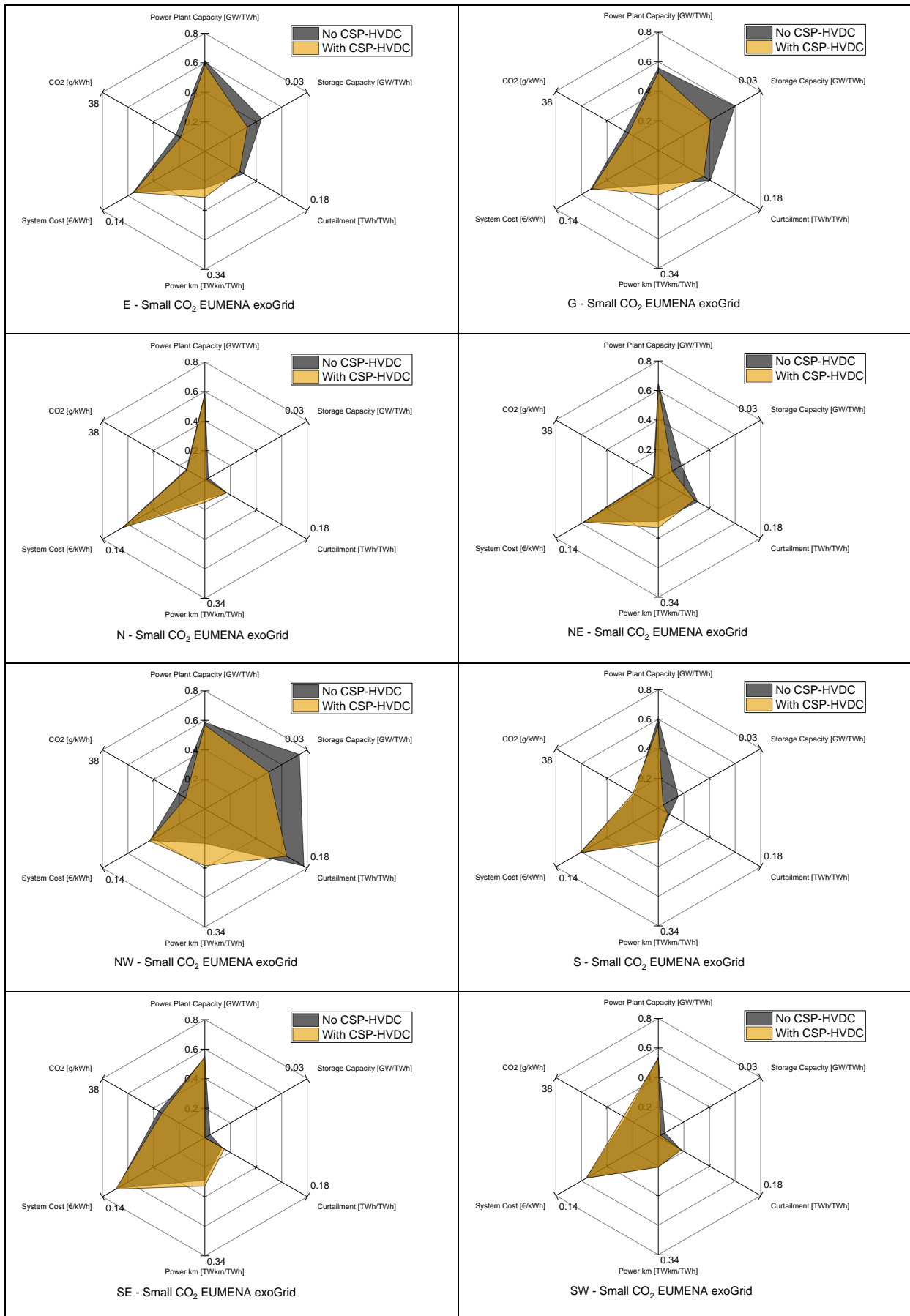


Figure 61: Scenario with 50% reduction of CSP-HVDC capacity (-50% CSP-HVDC)



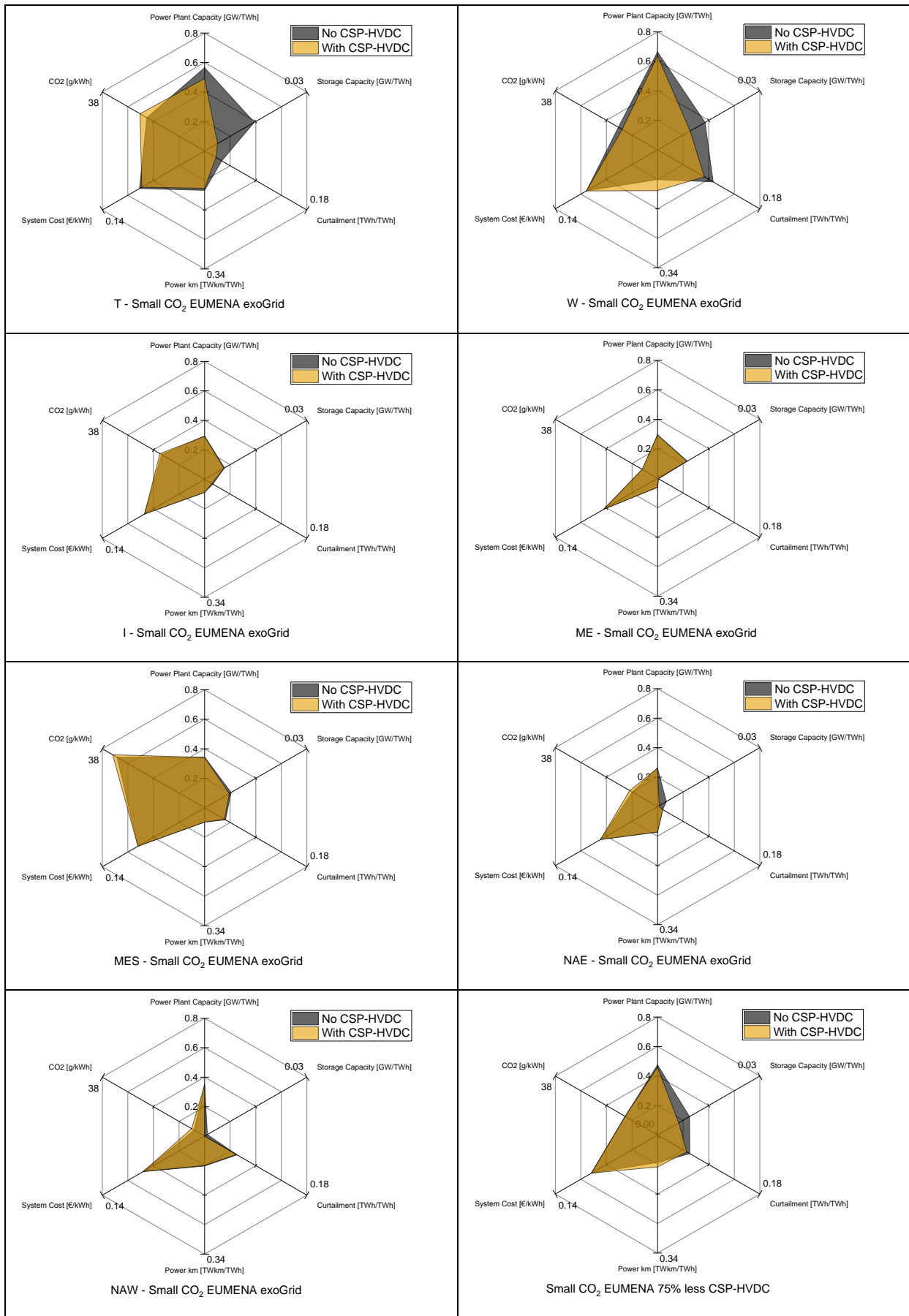


Figure 62: Scenario with 75% reduction of CSP-HVDC capacity (-75% CSP-HVDC)

## 11 CV

**Denis Hess****Personal information**

Birth date and place 25 of March 1988 in Stuttgart, Germany

**Professional experience**

10/2013 – 09/2017 Scientific staff and PhD student at DLR in energy system modelling  
 09/2009 – 09/2013 Research assistant at the German Aero Space Centre (DLR) at the Institute of Engineering Thermodynamics

**Education and teaching**

04/2015 – 10/2015 Co-lecturer at the University of Stuttgart in technical and sociological research of renewable energy systems  
 07/2013 Dipl.-Ing. degree in environmental engineering University of Stuttgart  
 06/2007 Abitur, Stuttgart

**Award and scholarship**

04/2014 Award from the Association of German Engineers (VDI-GEU)  
 01/2008 – 07/2013 Scholarship for the promotion of young talents of the Federal Ministry of Education and Research (BMBF) – StipendiumPlus

**Review activity**

Since 03/2017 Scientific journals: Applied Energy, Energy Research & Social Science, Renewable and Sustainable Energy Reviews, Solar Energy

**Hobbies and volunteer commitment**

- Power and endurance sports, bicycling, archery sports
- Educational journeys in Europe and beyond, foreign languages
- Member of the electoral board during European, federal and regional elections